ASSESSING SITE PERFORMANCE OF LARGE MINE WATER CHILLING MACHINES USING REFRIGERANT-CIRCUIT MEASUREMENTS AND MACHINE MODELLING

Michael Bailey-McEwan

A thesis submitted to the Faculty of Engineering, University of the Witwatersrand, Johannesburg, in fulfilment of the requirements for the degree of Doctor of Philosophy

Johannesburg, 1998

DECLARATION

I declare that this thesis is my own unaided work. It is being submitted for the degree of Doctor of Philosophy in the University of the Witwatersrand, Johannesburg. It has not been submitted before for any degree or examination in any other University.

All information in the thesis has been obtained by me whilst employed by the Chamber of Mines of South Africa.

M. Bailey-McEwan

Michael Bailey-McEwan

this 20 th day of February 1998

---oOo---

ABSTRACT

This thesis contributes to accurate, practicable techniques of ascertaining and assessing site performance of large refrigerating machines chilling water for cooling deep South African mines. It applies to all vapour-compression machines cooling fluids in steady, continuous processes.

To assess whether a water chilling machine is performing satisfactorily, both its actual performance, and the corresponding normal or optimal performance of which it is capable, must be ascertained. Both requirements present difficulties on site. In particular, the traditional "heat balance" method of verifying the apparent performance obtained from measurements in the water circuits does *not* prove that such performance is accurate. The calibration of typical site instrumentation is not assured, so an "acceptable" heat imbalance may conceal large but similar errors - which thus also balance out - in the apparent constituents of the heat balance.

Three methods of independently ascertaining actual performance, so verifying apparent performance, are presented. The first is an enhanced method, applicable to custom-built machines as well as conventional ones, of ascertaining the efficiency of the actual refrigerating process from measurements in the refrigerant circuit. This detects errors concealed in an "acceptable" heat balance. Where some refrigerant-circuit measurements are unavailable, an inexact version of this method still indicates the relative likelihood of the apparent performance being acceptably accurate. The third method, where these two are inadequate, is ascertaining actual performance using available measurements and fundamental machine modelling.

Such modelling is also the most versatile method of predicting corresponding normal or optimal performance. A computer program

simulating complete mine water chilling installations is used here. Actual performance can then be meaningfully assessed and appropriate remedial action justified, as shown in seven case studies. An outcome for conventional water chilling machines with a centrifugal compressor is that keeping heat exchangers clean may prejudice efficiency under part-duties if a machine has been designed for optimum efficiency at full duty. An alternative control philosophy of maximising the machine load may then yield better performance.

If these techniques are included in an automated system of fault diagnosis, they will be of most use to burdened mine staff, who are generally not refrigeration experts.

To my lovely honey wife, Margaret, a pearl among pearls

To my parents, Ronald and Pamela Bailey-McEwan;
my mother-in-law, Lorna Dixie;
and the memory of my father-in-law, Vincent Edward Dixie (1920-1994)

To my beloved children, Dawn and Gordon

ACKNOWLEDGEMENTS

This thesis arises from work carried out as part of the research programme of the Research Organisation of the Chamber of Mines of South Africa. The kind permission of the Chamber to use the material of that work, and the experimental data gathered in the course thereof, is gratefully acknowledged.

During the period of that work, the Directors of the Environmental Engineering division of the Chamber's Research Organisation were Professor T.J. Sheer (now of the University of the Witwatersrand), Dr. S.J. Bluhm (now of Bluhm Burton Engineering (Pty) Ltd) and Dr. D.G. Wymer. The author is grateful to these former Directors for their support and encouragement. Sincere tribute is also paid to Mr. R.D.C. Shone, a now-retired colleague, whose ardent and meticulous interest in thermodynamics bolstered the author's own interest.

Special thanks are due to Dr. J.M. Stewart, Mining Consultant of the Chamber, for generously permitting the author to take long periods of annual and accumulative leave in order to write this thesis.

The author is greatly indebted to his supervisor, Professor I.M. MacLeod, Department of Electrical Engineering, University of the Witwatersrand for his constant interest and patient, helpful encouragement during the years of completing this thesis on a part-time basis.

PREFACE

The author's interest in large refrigerating machines chilling water for cooling deep South African mines dates from 1974, when as a junior engineer on a South African gold mine, he participated in the repair and recommissioning of two such machines. Later, when employed by the Research Organisation of the Chamber of Mines of South Africa, he and a co-worker developed an interactive computer program named CHILLER to predict the performance of complete water chilling installations on mines. This thesis makes extensive use of that program.

Once this program was released in 1987, South African mines were assisted in putting it to use, mainly through two- or three-day courses in refrigeration practice for mine personnel, conducted by the author through the Education Services department of the Chamber.

From 1980 to 1995, whilst employed by the Chamber, the author provided a consultancy service to mines in checking performance of, and diagnosing faults in, large water chilling and ice-making machines. The techniques in the thesis for ascertaining and assessing the site performance of water chilling machines were developed to address the difficulties encountered in this consultancy service. Since 1993, these techniques have been incorporated into the abovementioned short courses for mine personnel, and have been implemented on several South African mines.

CONTENTS

CONTENTS (continued)

CONTENTS (continued)

CONTENTS (continued)

CONTENTS (continued)

CONTENTS (continued)

CONTENTS (continued)

CONTENTS (continued)

LIST OF FIGURES

LIST OF FIGURES (continued)

LIST OF FIGURES (continued)

LIST OF FIGURES (continued)

LIST OF FIGURES (continued)

LIST OF TABLES

LIST OF TABLES (continued)

LIST OF TABLES (continued)

LIST OF TABLES (continued)

NOMENCLATURE

Symbols

a	cross-sectional area	m^2
A	surface area	m^2
c	specific heat	kJ/kg.K
C	a constant	
COP	coefficient of performance	
d	internal diameter	mm
D	diameter	m
E	energy	kJ
f	multiplying factor for electrical kilowatt-hour meter	
F	Fanning friction factor *or* a factor	
F'	correction factor for LMTD for crossflow heat-exchanger configuration	
g	gravitational constant	9,81 m/s^2
Gr	Grashof number	
H	manometric head	m
h	specific enthalpy	kJ/kg
h'	heat transfer coefficient	$W/m^2.K$
I	current in three-phase balanced electrical load	A
k	thermal conductivity	W/r
K	friction coefficient for fittings in pipe	
L	length	m
LMTD	logarithmic-mean temperature difference	deg. C
m	mass flow-rate	kg/s
n	relative error *or* index of compression	
N	amount (of items, quantities, etc.)	

NOMENCLATURE - Symbols (continued)

Nu	Nusselt number	
P	pressure	kPa
Pr	Prandtl number	
Q	heat flow-rate	kW(R)
q	mechanical power expended non-usefully due to thermo-dynamic irreversibilities and appearing as heat flow	kW(R)
r	radius	m
R	ratio of quantities	
R	thermal resistance	°C/W
Re	Reynolds number	
S	entropy	kJ/K
S'	time rate of entropy increase	kJ/(K.s)
s	specific entropy	kJ/(kg.K)
T	absolute temperature	K
t	temperature	°C
U	circumferential speed	m/s
UA	thermal conductance	kW(R)/°C
V	volume	m^3
V	voltage in 3-phase balanced electrical load	V
$\dot{V}$	volumetric flow-rate	m^3/s
v	specific volume	m^3/kg
W	mechanical or electrical power	kW
x	fraction of liquid in a two-phase refrigerant flow	
y	wall thickness of tube	m
Y	ratio of temperature rise of cold fluid in a heat exchanger to difference in inlet temperatures of hot and cold fluids	
Z	ratio of temperature changes of hot and cold fluids in a heat exchanger	

NOMENCLATURE - Symbols (continued)

z	a variable quantity	
β	angle between tip of impeller blade and tangent to outer circumference of impeller	radians
β	coefficient of thermal expansion of a liquid	1/°C
ε	relative heat imbalance	
η	efficiency	
φ	phase angle in 3-phase balanced electrical load	radians
Θ	function of multiple variables	
μ	absolute viscosity	Pa.s
μ	work coefficient of centrifugal compressor stage	
Π	built-in pressure ratio of screw compressor	
ρ	density	kg/m^3
σ	surface tension	N/m
τ	time	s
υ	velocity	m/s
φ	built-in volume ratio of screw compressor	
ϕ	phase shift in electrical instrument transformers	radians
ϕ	flow coefficient of centrifugal compressor stage	
ψ	opening of inlet guide vanes in a centrifugal compressor stage	degrees(°)
ψ	head coefficient of centrifugal compressor stage	
ω	angular velocity	radians/s

NOMENCLATURE (continued)

Subscripts

alt	alternate
aux	auxiliary
b	bubble
c	confirming value
(cfl)	fluid being chilled or cooled
(cw)	chilled water
C	condenser
"C1"	unflooded portion of bottom pass of tubes in a shell-and-tube condenser
"C2"	the other (non-bottom) passes of tubes in a shell-and-tube condenser
[C]	pertaining to condenser
CB	condenser block of generalised water chilling machine
[CB]	pertaining to condenser block of generalised water chilling machine
{Car}	of Carnot cycle
des	design value
eq	equivalent
E	evaporator
[E]	pertaining to evaporator
EB	evaporator block of generalised water chilling machine
[EB]	pertaining to evaporator block of generalised water chilling machine
EC	economiser
EX	expansion valve
f	film of liquid condensate on a surface
(fl)	fluid

NOMENCLATURE - Subscripts (continued)

⟨f⟩	*saturated* refrigerant liquid
⟨g⟩	*saturated* refrigerant vapour
(hfl)	heat-removing fluid
(hw)	heat-removing water
HG	hot gas bypass valve
i	inlet *or* internal
it	current transformer
JB	condenser block *and* vapour-compression block of generalised machine, considered jointly
[JB]	pertaining to these blocks considered jointly
{Lor}	of Lorenz cycle
LI	liquid injection valve
LR	liquid receiver
ℓ	liquid
M	complete water chilling machine
Ms	surroundings outside the thermodynamic boundary of a complete water chilling machine
{Ms}	*from* surroundings of complete water chilling machine
m	electrical energy meter
[*merid*]	meridional
n	ordinal number (of item, quantity, etc.)
o	outlet *or* outside
OC	oil cooler of compressor
{OC}	*from* oil cooler
OP	oil pump of compressor
P	compressor
p	apparent value *or* at constant pressure

NOMENCLATURE - Subscripts (continued)

pa	pass of tubes in a shell-and-tube heat exchanger
pipe	of piping
pol	polytropic
press	of pressure
r	radial
(r)	refrigerant
[r]	pertaining to refrigerant
[*rel*]	relative
R	of ratio
s	isentropic
(s)	surroundings outside a thermodynamic boundary
sat	saturated state
sf	surface
SC	subcooler
"SC1"	flooded portion of bottom pass of tubes in a shell-and-tube condenser
SD	liquid surge drum
[*tng*]	tangential
T	tube
VCB	vapour-compression block of water chilling machine
{VCB}	*from* vapour-compression block
[VCB]	pertaining to vapour-compression block
v	vapour
vt	voltage transformer
wpl	water chilling plant
(w)	water
[*w*]	pertaining to water

GLOSSARY OF TERMS

Apparent value	a measured quantity of uncertain accuracy; *or* a quantity derived from one or more such measured quantities
Characteristic quantity	derived measure of quality of performance
COP	coefficient of performance: the measure of the thermodynamic efficiency of a refrigerating cycle
Duty	load and lift, considered together, of a refrigerating machine
Fault	an undesirable value of a state variable or process parameter within a machine
Fault signature	a set of deviations, suggesting a fault, from normal values of characteristic quantities, state variables or process parameters
Fault symptom	a set of deviations, suggesting a fault, from normal values of measurable quantities or elementary derivations therefrom
Heat-rejection fluid	a fluid passing through a refrigerating installation or any plant thereof - such as a water chilling plant - into which such installation or plant rejects heat
HVAC	Heating, Ventilating and Air-Conditioning
Lift	the difference between the mean temperature of heat extraction from a fluid being cooled and the mean temperature of discard of this heat into a heat-rejection fluid
Load	the rate of heat removal from, or addition to, a stream of fluid being cooled or heated
Model	the set of equations expressing the behaviour of a system
Operating conditions	the set of prevailing inputs, state variables and process parameters of a process
Operating regime	the prevailing inputs and the control philosophy of a process
SAR	South African Rands (currency)
Shortfall in performance	unacceptable discrepancy between an actual and the corresponding normal or optimal measure of performance
Survey	routine check of site performance

1. INTRODUCTION

1.1 General Introduction

More than 1 300 megawatts of refrigerating capacity, abbreviated as MW(R), are installed on deep South African gold mines to maintain their underground workings at acceptable temperatures (CSIR, South Africa, 1994). Virtually all of this capacity is developed by over 300 large water chilling machines, with capacities from 0,7 MW(R) to over 10 MW(R), in centralised installations. It is essential to minimise both breakdowns and shortfalls in performance of these machines. Not only may the costs of consequent losses in production be very considerable, but more importantly, working conditions may become unsafe. In the present climate of falling ore grades and rising working costs (Chamber of Mines of South Africa, 1997 : 23-25), the incentives to achieve optimally reliable and cost-effective operation of these machines become ever stronger.

The proper, objective basis for assessing whether a water chilling machine is operating at satisfactory or optimal cost-effectiveness is the discrepancy between its actual performance and the corresponding normal or optimal performance of which it is capable. It is thus necessary to accurately ascertain both the actual performance attained, and the corresponding normal or optimal performance - under the same or an alternative operating regime[1] - which should be attained. Both of these requirements present difficulties on South African mines. In checking actual performance, the harsh conditions typically prevailing, especially in mine water circuits, make the accuracy of infrequently calibrated, site-fitted instrumentation uncertain. Normal or optimal performance is generally specified only for full-duty, design conditions. Such performance for other operating conditions and regimes - which may vary considerably from the original, design ones - is seldom specified.

---

[1] Operating regime: the inputs to, and the control philosophy of, a machine.

This thesis addresses both of these requirements in assessing site performance of large water chilling machines. First, it contributes to accurate ascertainment of actual performance. It submits an enhanced, more accurate method of independently ascertaining the actual efficiency of a machine through confirming measurements in its refrigerant circuit. Thus the *apparent* machine performance, indicated by the measurements in its water circuits, may be verified for accuracy, and erroneous such measurements may be identified. Where insufficient confirming measurements are available for this enhanced method to precisely ascertain actual performance, two further options are submitted. An inexact form of the method may be able to indicate a range where actual performance must lie, and does indicate the relative likelihood of the apparent performance being acceptably accurate. In addition, fundamental, computer-based machine models may be used to independently ascertain actual performance and so verify apparent performance.

Second, the thesis contributes to accurate ascertainment of corresponding normal or optimal performance. It submits the use of the same fundamental, computer-based machine models to predict such performance under identical or alternative operating regimes. It thus illustrates how actual performance is properly assessed, abnormalities within the machine identified, and those abnormalities constituting faults diagnosed.

These techniques have been developed to enable mine ventilation and engineering personnel to more quickly and reliably assess, maintain and remedy the performance of the large water chilling machines upon which the underground workforce in deep South African mines is so dependent. Moreover, the techniques are applicable to all sectors of industry employing vapour-compression refrigerating machines which cool fluids in steady, continuous processes.

In this chapter, the background to and reasons for undertaking the work are furnished; the objectives and contributions of the work are stated; and the content of the thesis is summarised.

1.2 Background

Well-established, internationally-accepted standards (ISO, 1968; ASHRAE, 1978, 1995; BSI, 1989; ARI, 1992) and draft standards (ISO, 1992, 1994) exist for ascertaining the performance of water chilling machines under pre-specified conditions by testing. Direct measures of performance, such as cooling capacity and efficiency, are calculated from direct measurements of the relevant quantities, such as water flow-rates, water temperatures, and input power. These direct, or principal, measurements are collectively termed the *primary* or *principal test*. Almost all of these standards also specify a simultaneous *confirming test*, consisting of measurements of additional quantities from which confirming values of the same measures of performance can be calculated indirectly. If the direct and indirect measures of performance agree to within the limits specified by the standards, the direct measures of performance are accepted as the actual machine performance.

These standards require testing conditions to be maintained within very close tolerances: for example, four standards require inlet and outlet temperatures of the water being chilled to be maintained to within ±0,3°C of specification. They also require all instruments to be of high accuracy, substantiated by calibration before and after the test. When checking site performance, though, these requirements are unattainable. In general, operating conditions cannot be maintained within such tolerances, and are liable to vary over time. Therefore, all required quantities have to be measured as simultaneously as possible. This is most conveniently achieved by an automated data-logging system, but many installations do not have such a system, and it is thus necessary to rely upon periodic manual measurements.

Moreover, the available fitted instrumentation - which is generally of sub-standard class of accuracy and infrequently calibrated - must be used in checking site performance, except where it can be supplemented with portable instrumentation of better accuracy (for example, calibrated thermometers). All fitted instruments are subject to systematic error developing over time, due to both internal drift and the detrimental effect of their operating enviro .ent. This is especially so with water flow meters of the invasive type (orifices, pitot tubes, etc.) in mine water circuits. The water being chilled, and the water removing heat from the machine, may carry high concentrations of dissolved and suspended solids, and hence be abrasive and either corrosive or scaling. Hence, even if installed correctly, the accuracy of invasive flow sensors is liable to worsen with time unless they *and their upstream and downstream piping* are regularly maintained to specification. Often, therefore, the only site measurements known to be reliable are those of water and refrigerant temperatures made with portable, regularly calibrated thermometers.

Even though many requirements of the above standards are thus unattainable when checking site performance, these standards remain the authoritative guide to ascertaining actual performance, and are thus followed as closely as possible. In particular, in checking site performance, the need for a simultaneous *confirming* check is essential in view of the acc 'racy of fitted water flow meters not being assured for the above reasons. This confirming check customarily takes the form of an overall energy balance, termed a "heat balance". Current practice is to deem site measurements acceptably accurate if the computed heat balance - this being appropriately termed the heat *im*balance - is within "acceptable" limits, specified as ±5 per cent (Burrows, 1982).

The motivation for the work of this thesis was threefold. First, how sound was the basis for setting these limits of acceptability at ±5 per cent? More importantly, did an "acceptable" heat imbalance guarantee acceptable accuracy of site measurements? The author had experienced two cases

where this had not been so. Second, where "acceptable" heat imbalances were not achieved, and it was thus obvious that one or more measurements were erroneous, was there a practicable, accurate, convincing method of identifying such measurements - and better still, of ascertaining the actual values of the erroneously indicated quantities?

Third, diurnal and seasonal influences and the unpredictable nature of mining may cause actual operating conditions to vary considerably from original design conditions, which are generally the only ones for which the manufacturer specifies normal or optimal performance at the time of ordering. Therefore, once actual performance had been accurately ascertained, how could corresponding normal or optimal performance be practicably obtained to compare this with and thus assess it properly?

1.3 Objectives of the Study

Wage costs exceed 40 per cent of total working costs on South African gold mines (Chamber of Mines of South Africa, 1997 : 16,30). It remains vitally necessary, therefore, to improve staff productivity, as unit wage costs drop when such improvements surpass wage increases. With mine staff thus facing increasing workloads, it is important to continually investigate ways of performing tasks more effectively and efficiently.

To timeously provide qualified mine personnel with the two sets of information necessary to properly assess actual performance, diagnose faults and take remedial action, the objectives were, therefore, improved techniques of quickly, accurately and convincingly -

(a) ascertaining actual performance of water chilling machines, and

(b) predicting normal or optimal performance under identical or even alternative operating regimes, thus having valid yardsticks to compare actual performance with.

1.4 Summary of the Thesis

Chapter 2 provides a broad background to this work, describing South African mine cooling practice, and mine fluid cooling and ice-making installations. For fluid cooling installations, the concepts of load, lift, duty and efficiency - this being termed *coefficient of performance* (COP) - are defined. Apart from newly emerging technologies for especially deep mines, centralised fluid cooling installations using vapour-compression refrigerating machines to chill water are likely to remain the dominant technology.

Chapter 3 provides the specific background to the work, focusing on the large water chilling machines employed in mine fluid cooling installations. The energy balances and the *refrigerant-circuit COP* (the COP determined independently from measurements in the refrigerant circuit) for a generalised water chilling machine are first defined. The two classes of machines employed in South African mines - conventional, packaged machines employing a single- or multi-stage centrifugal compressor, and custom-built machines employing one or more screw compressors - are then reviewed. The components of these machines, and how they influence machine performance at full- and part-duties, are described. If a machine is to be efficient throughout its range of duties, all of its components - especially its compressors - must maintain their efficiency throughout this range.

Chapter 4 explains the problems in detecting unsatisfactory performance of water chilling machines. On the ascertainment of actual performance, it critically reviews the requirements of the authoritative standards for testing water chilling machines; the extent to which these requirements are attainable in routine checks of site performance; and current practice and shortcomings in such checks on South African mines. *The main shortcoming is that an "acceptable" heat imbalance is not a guarantee of acceptably accurate measurements in such checks, because calibration of*

all measuring instruments is not assured. Therefore, such a heat imbalance may be concealing large, *similar* errors in the apparent constituents of the heat balance, because such errors also balance out. On the obtainment of corresponding normal or optimal performance, Chapter 4 concludes that prediction thereof by fundamental machine modelling is the most versatile and thus preferable option here, although simplified modelling, empirically attuned, may be more practicable for custom-built machines. Three desirable improvements to current practice in ascertaining and assessing machine performance are identified.

Chapter 5 provides the first such desirable improvement. This comprises enhanced, more conclusive methods of independently ascertaining actual performance, so verifying apparent performance and identifying unacceptable errors in the principal measurements. The chapter first presents the *enhanced Thorp method* of doing this wherever the refrigerant-circuit COP can be precisely determined *and* at least one apparent constituent of the heat balance[2] is independently known to be acceptably accurate. Next, for use where unavailability of key measurements prevents this COP from being precisely determined, the *inexact Thorp method* is presented. This can indicate a range where this COP must lie, and does indicate the relative likelihood of the apparent constituents of the heat balance being acceptably accurate. Where the heat imbalance is significant, this inexact method can thus identify unacceptable measurement errors in most cases. Where the heat imbalance is small, however, it cannot prove the absence of such errors, and so cannot verify that apparent performance is accurate. Finally, therefore, the chapter presents the use of fundamental, computer-based machine models to verify apparent performance where the enhanced Thorp method does not suffice.

---

[2] The apparent constituents of the heat balance are the apparent water chilling load, the apparent heat-rejection load, and the apparent input power.

Chapter 6 provides the second desirable improvement to current practice: a practicable method of accurately predicting corresponding normal or optimal performance to compare actual performance with. It presents the use of the same machine models - incorporated in the CHILLER computer program specifically developed by the author and a co-worker for use in South African mines - to predict normal or optimal performance under identical or alternative operating regimes. Once this is done, it illustrates, through some case studies of the previous chapter, how actual performance is assessed; how abnormalities in the machine are hence detected; and how those abnormalities constituting faults are diagnosed by manual reasoning. An outcome for conventional water chilling machines is that keeping heat exchangers clean may prejudice efficiency under part-duties if a machine has been designed for optimum efficiency at full duty. An alternative control philosophy of maximising the machine load may then yield better performance.

The third desirable improvement to current practice is automated diagnosis of faults causing unacceptable shortfalls in performance. The thesis does not contribute here. However, Chapter 7 critically analyses pertinent literature in fault diagnosis and the automation thereof, shows where the contributions of the thesis are of value therein, and suggests where further work is required. Reliable, automated techniques of fault diagnosis will certainly aid burdened mine staff, who have to speedily identify and rectify faults, yet are unlikely to be refrigeration experts.

Chapter 8 reviews the contributions of the thesis, critically assesses the work and its limitations, and suggests where further work is needed

1.5 Contributions

The first contribution in this work is that Thorp's original method (Thorp, 1974) of verifying the apparent performance of water chilling machines has been extended and placed on a firm theoretical and implementational basis. It is shown that an "acceptable" heat imbalance *does not*

guarantee that apparent performance is acceptably accurate. The *enhanced Thorp method* presented ascertains actual performance independently and accurately, and clearly indicates the degree of accuracy of the apparent performance, together with the reasons. Where this enhanced method cannot be used due to unavailability of required measurements, the *inexact Thorp method* presented does indicate the relative likelihood of the apparent performance being acceptably accurate, and can still signal and identify unacceptable measurement errors when the heat imbalance is significant.

The second contribution is that the fundamental models of water chilling machines in the CHILLER computer program developed by the author and a co-worker (Bailey-McEwan and Penman, 1987) - and an extension to one such model - have been used to independently ascertain actual performance, and so verify apparent performance, of conventional machines where the enhanced Thorp method does not suffice. If sufficient measurable inputs and outputs, such as water and refrigerant temperatures, are accurately known, such models, which make use of detailed machine specifications, can be solved for the unknown or uncertain inputs, outputs and internal quantities needing to be ascertained or verified.

The third contribution is that the same machine models have been used to predict normal and optimal performance of conventional machines, for the purpose of assessing actual performance. The use of machine modelling for this purpose is not original; however, this is the first such use within the South African mining industry of a fundamentally-based, rigorous model of a conventional machine, which models each stage of a multi-stage centrifugal compressor separately, and thus the interactions between these stages. The detailed information and insight yielded by such a model enables better-founded assessment of actual performance and diagnosis of faults in such machines.

2. REFRIGERATING INSTALLATIONS ON SOUTH AFRICAN MINES

This chapter provides the broad background to the thesis. It describes the need for, and tasks of, mine fluid cooling installations, and the duties thus imposed on the water chilling plants within these installations.

The need for refrigeration in South African mines is explained and South African mine cooling practice outlined. The chapter then introduces the concept of the general *mine fluid cooling installation* producing chilled water, cooled air or both for underground use. The thermodynamic operating principles of this general installation are reviewed and the various classes of actual installations on South African mines briefly described. The duties of installations on surface are more affected by diurnal and seasonal weather patterns, and hence vary more, than those of installations situated underground.

A few mines have adopted ice-making installations on surface as an alternative means of providing cooling; the chapter summarises developments here. In closing, it notes that developments in future refrigerating installations for deeper mines will be governed by the need for more cost-effective methods of transporting heat out of the workings.

2.1 The Need for Cooling in South African Mines

The South African gold mining industry employs over 340 000 people, of whom over 210 000 work underground (Chamber of Mines of South Africa, 1997). The weighted mean rockbreaking depth for South African gold mines is 1,8 kilometres (CSIR, South Africa, 1994). Temperatures in the working places would be unacceptably high for these people if the mining industry had not developed techniques for controlling the underground thermal environment.

Extensive research has shown that essentially all the metabolic heat generated by people working in hot underground environments is

dissipated from the body by the evaporation of sweat (Stewart, 1982a). Sweat evaporation rate is governed by the wet-bulb temperature of the air and the air velocity. Air velocities in confined underground working places are low, so it is usual to aim at conditions that will be safe even in still air. Hence the wet-bulb temperature is the major factor in evaluating the underground thermal environment in the conditions found in South African gold mines. Fully acclimatised men can carry out hard work at wet-bulb temperatures as high as 31,7°C, but it is desirable to limit the maximum wet-bulb temperature to 27,5°C, where fit men can undertake all mining tasks in still air with no danger to their health and without the need for acclimatisation (Stewart, 1982b). "The present climate in deep mines can thus be seen as a balance between what can be achieved by engineering the thermal environment and what can be achieved by adapting man to that environment." (Burton et al., 1986)

High temperatures in deep mines are caused by two major factors: heat transfer from the surrounding rock and autocompression[1] of the downcast ventilating air. Fundamentally, two strategies are used in controlling the underground thermal environment. The first and obvious one, where emphasis should lie, is reduction of heat flows, at their sources, into the workings (Ramsden et al., 1988). This can be done directly by, for example, insulation of intake airways (Ramsden, 1990; Ramsden et al., 1988) but far greater reductions are achieved as a complementary goal by techniques to optimise mining layouts and methods. Such techniques include backfilling, increasing the face advance rate, hydropower and recirculation of ventilating air (Ramsden et al., 1988). The need to keep reduction of heat loads as the primary strategy has been well expressed by Gundersen (1991):

---

[1] That is, conversion of potential energy into enthalpy as any fluid descends through the Earth's gravitational field.

> "Only recently... with the advent of backfill and especially hydropower, have we seen synergistic benefits of integrating technologies for cooling and mining which, on their own, may not have been feasible. *While more efficient refrigeration systems continue to be developed, these will only reduce the cost of cooling, not so much the quantity.* More significant savings in ventilation and cooling will result from designing mining methods and layouts with reduced heat loads and shorter air routes."

Notwithstanding all efforts to reduce heat loads, though, underground working places require cooling either when all practicable means of reducing heat loads are inadequate, or when the available, uncooled ventilating air is incapable of ensuring acceptable temperatures. Thus, in deep gold mines, the second, complementary strategy of cooling the workings always remains essential (Ramsden et al., 1988). Better stated thermodynamically, the second strategy is to remove heat that manifests itself in the workings. This heat is the sum of that flowing from the rock; that due to autocompression; and that due to artificial sources - machinery, explosives, people, etc. (Hemp, 1982). According to the First Law of Thermodynamics, the available means (excluding chemical means) of removing this heat are to either transform it into useful work which leaves the workings, or absorb it in fluid streams passing steadily or unsteadily through the workings. To make the first alternative possible, the Second Law of Thermodynamics requires an available heat sink at a sufficiently lower temperature. No such heat sink exists, so the fluids circulating through the working places - water and ventilating air - provide the only means of removing heat from the mine (Hemp, 1982). This means that the heat has to be transported from underground to surface, where it can finally be rejected into the atmosphere.

The functions of a mine cooling system, therefore, utilising the fluids circulating through the mine, are to absorb the required amounts of heat

from the workings, transport this heat from underground to surface, and reject it there.

2.2 South African Mine Cooling Practice

At this point, it is useful to employ Gundersen's concept of a mine consisting of a *transport zone* and a *mining zone* (Gundersen, 1991). The transport zone extends from surface to the top working level; the mining zone from the top level down. The functions of a mine cooling system can then be stated with greater clarity as:

- to absorb the required amounts of heat from the mining zone;
- to transport this heat through the transport zone to surface; and
- to reject this heat on surface.

In the first instance, the normal fluid flows of ventilating air and water which are necessary for mining operations can be used for all three functions. If these flows are insufficient, additional flows of the same or other media can be introduced. Additional flows of chilled water are commonly used, for example.

The key considerations in designing mine cooling systems are the most cost-effective way to perform the above three functions, and the extent to which additional fluids or media are required for this purpose. Obviously, many elements of a mine cooling system are also elements of other systems (the ventilating system, water pumping system, etc.)

From 1977 to 1990, the capacity of installed refrigeration plant in South African gold mines increased rapidly from 400 MW(R) to 1 200 MW(R) (Ramsden and Baker-Duly, 1991). The increase in capacity up to 1993 is depicted in Figure 2.1.

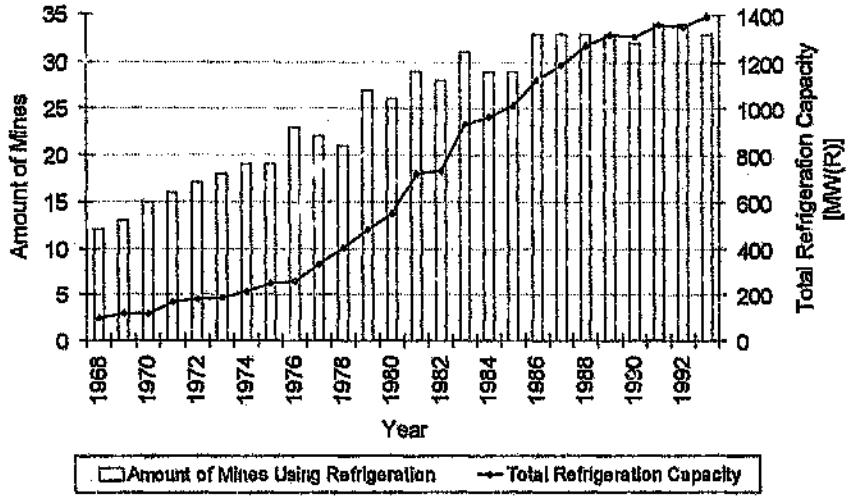

Figure 2.1 Installed Refrigeration Capacity On South African Gold Mines (CSIR, South Africa, 1994)

Chilled water is a very convenient and readily available medium for cooling, as water is used in mines for various operations anyway, and water-chilling equipment is readily available commercially. Air cooling is readily accomplished with chilled water through closed- or open-circuit air-to-water heat exchangers. Also, cooling capacity can be stored in the form of reservoirs of chilled water. For this reason, almost all cooling in South African mines is accomplished through chilled water.

The two main options for distributing cooling are:

- service water chilling, that is, chilling the water used in mining operations, mainly dust suppression and rock drilling. This removes heat from the rock, and to a lesser extent from the air (Stroh, 1982);
- cooling the ventilating air.

In the 1970s, the mines developed a progressive three-phase strategy for distributing cooling, using these two options, as follows (van der Walt and Whillier, 1978).

(1) In the first phase, the service water is chilled. Presently, approximately 29 per cent of cooling in South African gold mines is distributed through the service water (CSIR, South Africa, 1994). However, the quantity of service water used in a working place obviously has an upper limit; so there is a corresponding limit to the amount of cooling possible through chilled service water. For a deep mine, where the cooling requirements are large, cooling distributed through normal mine service water may be 10 per cent or less (Ramsden and Baker-Duly, 1991).

(2) Where the amount of cooling provided by chilled service water is insufficient, such as in deeper mines due to the autocompression of the ventilating air, direct air cooling is carried out in large bulk air coolers positioned either on surface or underground (Ramsden and Bluhm, 1984; Stroh, 1982).

(3) In the third phase, when the heat pick-up by the ventilating air is such that it is necessary to re-cool it during its passage through the workings (Ramsden et al., 1988), this air is re-cooled in small quantities at convenient locations wherever its wet-bulb temperature approaches the maximum permitted value.

Not all South African mines follow this three-phase strategy, but it has been used extensively. It is worth noting that not all cooled air reaches the working places it is intended for. Some is lost due to poor air control at the working places and short-circuiting of cooled air through available leakage paths such as old worked-out areas.

Obviously, the fluids or media which are intended to absorb heat from the workings in the mining zone must be supplied at temperatures low enough to do so. Mine refrigerating installations perform this function. A *mine refrigerating installation* is defined as that part of a mine cooling system which supplies chilled media, according to demand, for cooling in the mining zone.

2.3 The General Mine Fluid Cooling Installation

Currently, almost all South African mine refrigerating installations supply chilled water (as service water or for subsequent air cooling in air-to-water heat exchangers in the mining zone), cooled air, or both. Such installations are thus termed *fluid cooling installations.*

Chilled water supplied by such installations, after being used in the mining zone, is generally returned for re-chilling after filtering and chemical treatment. The inevitable losses of water within the mining and transport zones are replenished with a make-up supply. Installations which cool air in bulk almost always use chilled water to do this[2] in large, open-circuit counterflow heat exchangers termed *direct-contact bulk air coolers.*

Figure 2.2 depicts the general form of a fluid cooling installation, consisting of:

- *reservoirs* for the entering water to be chilled and the chilled water to be delivered. Other reservoirs for water at intermediate temperatures may also be present;
- a direct-contact *bulk air cooling plant,* if cooled air is to be supplied;
- a *water chilling plant* (heat pumping plant), consisting of one or more vapour-compression water chilling machines. One or more *heat-removing water streams,* shown in the figure, transport the heat leaving this plant to the heat rejection plant, now described;
- a *heat rejection plant,* consisting of one or more wet cooling towers.[3] This plant accepts heat from the heat-removing water streams and rejects this into the available heat-rejection fluid, which is almost

---

[2] The rare exception is where refrigerant is used to cool this air directly in air-to-refrigerant heat exchangers.

[3] In the rare case of the heat rejection plant consisting of evaporative condensers instead of wet cooling towers, the heat-removing streams are of refrigerant, not water.

always air. Sometimes, as shown, the water to be chilled also passes through the heat rejection plant before entering the water chilling plant. This is worthwhile when, as for many installations on surface, the initial temperature of this water is significantly higher than the wet-bulb temperature of the available heat-rejection air. As described later, the first step of chilling this water can then be performed directly.

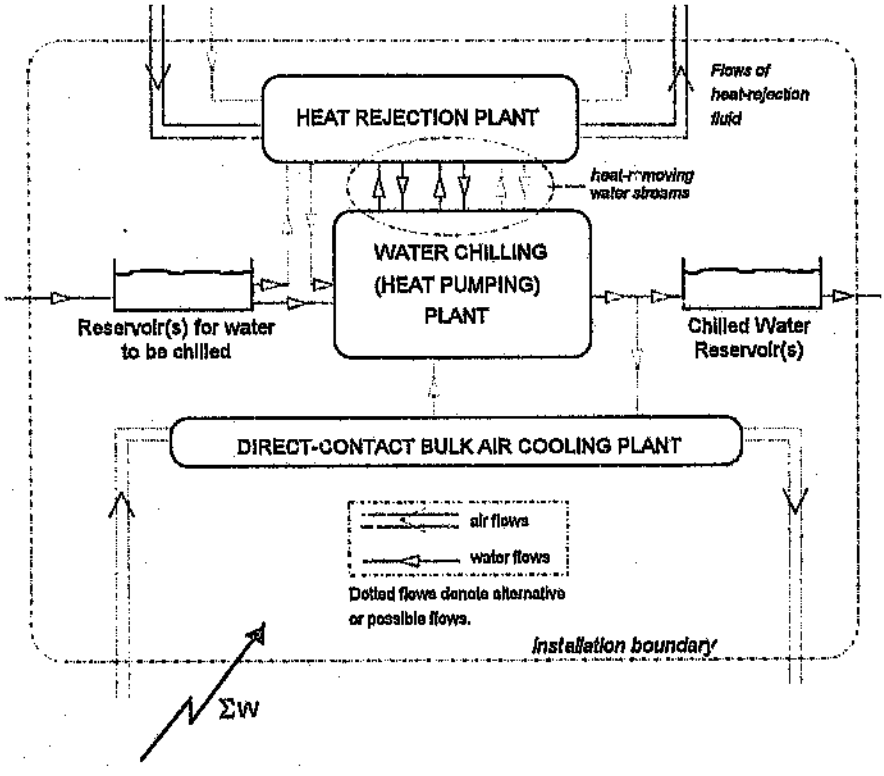

Figure 2.2 General Mine Fluid Cooling Installation

2.3.1 Thermodynamic Functions

The three inseparable thermodynamic functions of a fluid cooling installation are to extract heat from the water or air being cooled; lift this heat to a higher temperature than that of the available heat-rejection fluid; and then reject it into this fluid. The function of extracting heat is quantified by the cooling demand; those of lifting and rejecting this heat

are quantified by the mass flow-rates and properties of the fluid(s) being cooled and th heat-rejection fluid. Some or all of these quantities may vary diurnally and seasonally.

The water reservoirs seldom have capacities exceeding one or two days' use of chilled water; they are provided to smooth or buffer diurnal and shorter-term variations. The installation can thus perform its heat extraction function non-simultaneously with the daily and hourly cooling demand pattern. However, no similar reservoirs are provided in the heat-removing water circuits between the water chilling and heat rejection plants,[4] so these circuits can only smooth or buffer variations of the order of minutes in the heat rejection function. All longer-term variations in the heat extraction and rejection functions must be accommodated by the water chilling and heat rejection plants. At the installation design stage, this is a major consideration in specifying the components of these plants and their interconnections.

2.3.2 Overall Energy Balance

The total mechanical power input required for the installation to perform its three functions of heat extraction, lifting and rejection is shown as $\sum W$ in Figure 2.2. As no energy leaves the installation apart from that in the fluid streams, *all this power input to the installation is transformed into heat which is additional to that extracted from the fluids being chilled, and which has to be rejected along with that heat into the heat-rejection fluid.*

Let the heat flow entering the installation via the heat-rejection fluid be $\sum Q_{(hf)}$ and that entering via the fluid(s) being cooled by $\sum Q_{(cf)}$. Let the net heat flow into the external surfaces of all components of the installation from its surroundings be $\sum Q_{(s)}$. Over a time interval $(\tau_2 - \tau_1)$

---

[4] As the flow-rates in the heat-removing water circuits are generally higher than in the chilled water circuit, the sizes of reservoirs thus required for significant smoothing are generally deemed uneconomic.

long enough for no net storage or release of energy within the installation, the First Law of Thermodynamics stipulates that the sum of the heat $\int_{\tau_1}^{\tau_2}\sum Q_{(hf)}\cdot d\tau$ entering the installation via the heat-rejection fluid; the heat $\int_{\tau_1}^{\tau_2}\sum Q_{(cf)}\cdot d\tau$ entering via all fluids bein cooled; the net heat $\int_{\tau_1}^{\tau_2}\sum Q_{(s)}\cdot d\tau$ entering into the external surfaces of the installation from its surroundings; and the total mechanical work input $\int_{\tau_1}^{\tau_2}\sum W\,d\tau$ must be zero. This is the overall energy balance:

$$\int_{\tau_1}^{\tau_2}\sum Q_{(hf)}\cdot d\tau+\int_{\tau_1}^{\tau_2}\sum Q_{(cf)}\cdot d\tau+\int_{\tau_1}^{\tau_2}\sum Q_{(s)}\cdot d\tau+\int_{\tau_1}^{\tau_2}\sum W\,d\tau=0 \qquad (2\text{-}1)$$

2.3.3 Coefficient of Performance (COP)

The efficiency of any refrigerating installation is measured, like that of a heat engine, by the ratio of the useful effect produced to the means used to produce it. Here, the useful effect is $\int_{\tau_1}^{\tau_2}\sum Q_{(cf)}\cdot d\tau$ and the means used are $\int_{\tau_1}^{\tau_2}\sum W\,d\tau$. The efficiency expressed by their ratio, because it is generally greater than unity, is termed the *coefficient of performance*, abbreviated to COP:

$$COP\equiv\int_{\tau_1}^{\tau_2}\sum Q_{(cf)}\cdot d\tau\Big/\int_{\tau_1}^{\tau_2}\sum W\,d\tau \qquad (2\text{-}2)$$

2.3.4 The Water Chilling Plant

The water chilling plant within the fluid cooling installation comprises one or more water chilling machines and their interconnections. Similarly to its installation, this plant must perform three thermodynamic functions:

- extract the required *load* of heat from the water being chilled;
- *lift* this heat from the temperatures of extraction to the *temperatures of discard*, i.e. those temperatures at which it can be transferred into the heat-removing water streams;
- discard this heat into the heat-removing water streams circulating through the heat rejection plant.

However, unlike its installation, the plant must perform these functions simultaneously, as it has no reservoirs of any significance. Recalling that the water chilling plant is in essence a heat pumping plant, its duty consists of pumping the heat *load* through the *lift* between the mean temperatures of extraction and discard. Its *duty* is thus defined as this heat load and lift considered together.

Overall Energy Balance

The overall energy balance for the water chilling plant is similar to (2-1). As the plant performs all its thermodynamic functions simultaneously, though, *flow-rates* of heat and work must also balance. Let $\sum Q_{(cw)wpl}$ denote the total heat flow into the plant from the water being chilled; $\sum Q_{(hr)wpl}$ the total heat flow into the plant via the heat-removing fluid streams; $\sum Q_{(s)wpl}$ the net heat flow into the external surfaces of the plant from its surroundings; and $\sum W_{wpl}$ the total mechanical power input required for the plant to perform its three thermodynamic functions. The overall energy balance is then

$$\sum Q_{(cw)wpl} + \sum Q_{(hw)wpl} + \sum Q_{(s)wpl} + \sum W_{wpl} = 0 \qquad (2\text{-}3)$$

Actual and Ideal Coefficients of Performance (COP)

Similarly to (2-2), the actual COP is the ratio of the useful cooling produced to the input power required to produce it:

$$COP_{wpl} \equiv \sum Q_{(cw)wpl} / \sum W_{wpl} \qquad (2\text{-}4)$$

To assess how good this actual COP is, it has to be compared with the ideal, maximum possible COP under the same conditions. For a water chilling plant which extracts heat from a stream of water *(cw)* being chilled and thus dropping in temperature, and which discards heat into a stream of heat-removing water *(hw)* which thus rises in temperature, it can be shown (see, for example, Gosney, 1982 : 41-43) that the ideal, maximum possible COP is the *Lorenz COP*, $COP_{(Lor)}$:

$$COP_{(Lor),wpl} \equiv \frac{\overline{\overline{T}}_{(cw)wpl}}{\overline{\overline{T}}_{(hw)wpl} - \overline{\overline{T}}_{(cw)wpl}} \qquad (2\text{-}5a)$$

where $\overline{\overline{T}}_{(cw)wpl}$ and $\overline{\overline{T}}_{(hw)wpl}$ are the logarithmic-mean absolute temperatures of the chilled and heat-removing water streams respectively:

$$\begin{aligned} \overline{\overline{T}}_{(cw)wpl} &\equiv \left(T_{(cw)wpl,o} - T_{(cw)wpl,i}\right) / \ln\left(T_{(cw)wpl,o} / T_{(cw)wpl,i}\right) \\ \overline{\overline{T}}_{(hw)wpl} &\equiv \left(T_{(hw)wpl,o} - T_{(hw)wpl,i}\right) / \ln\left(T_{(hw)wpl,o} / T_{(hw)wpl,i}\right) \end{aligned} \qquad (2\text{-}5b)$$

and the water chilling plant is thermodynamically ideal; extracting, lifting and discarding heat reversibly, with the temperatures of extraction and discard *identical to, and following,* the changing temperatures of the chilled and heat-removing water streams, respectively, within the plant. This is equivalent to chilling the water in an infinite amount of infinitesimal steps.

Of course, the Lorenz COP is not attainable in practice, but does show what can be aimed at. By way of example, in a plant on one South African gold mine designed to chill water from 14,5°C to 4°C, and designed to raise its heat-removing water from 22°C to 27,14°C, the Lorenz COP is 18,4. The specified COP of this plant under these design conditions is 6,48 - only 35 per cent of the Lorenz COP! As will be seen in Section 3.1.3 of Chapter 3, the main reason is that this plant chills water in only one step, with the single temperatures of extraction and discard thus lower and higher, respectively, than the outlet temperatures of the chilled and heat-removing water streams.

An important point emerges from the denominator of the Lorenz COP in (2-5a). $\left(\overline{T}_{(hw)wpl} - \overline{T}_{(cw)wpl}\right)$ is the average temperature lift through which the ideal water chilling plant pumps its heat. The ideal COP, therefore, decreases as this lift increases, and the same holds for the actual COP and its lift (the difference between the mean temperatures of discard and extraction). Other things being equal, the greater the lift, the greater the power input required to provide the same water chilling load, and the less the COP.

2.4 Fluid Cooling Installations on South African Mines

2.4.1 Scattered Installations

Fluid cooling installations can be situated either on surface, or underground in the transport or mining zones. Where small amounts of cooling are required to cater for "hot spots" (Stroh, 1982), or where limited heat rejection facilities prevent use of refrigerating installations of conventional size (Thorp and Bluhm, 1986), local, non-centralised installations are employed underground in the mining zone. The cooling capacities of these small installations range from 250 kW(R)[5] to even

---

[5] kW(R): kilowatts of refrigerating, i.e. heat-removing, capacity.

3 500 kW(R). They generally reject heat into a stream of return ventilating air - that is, air which has passed through the workings and is leaving the mine through a return airway to an upcast shaft and hence to surface. They have the advantages of low capital cost and high positional efficiency;[6] but they have to be moved reasonably frequently as the locations of the "hot spots" change, and heat rejection is often limited by a lack of return air. There is a tendency, therefore, to move away from scattered installations except where very low capacities are involved (Stroh, 1982).

2.4.2 Centralised Installations

In most cases, it is convenient and more cost-effective to have centralised installations serving districts of mines. Siting of a centralised installation is governed by the task that the installation has to perform (supply of chilled water, cooled air, or both, and the demand patterns thereof); the availability of fluids to reject the heat into; the need to minimise costs of transporting the heat through the transport zone (principally, by minimising mass flow-rates of additional media required for this purpose); and the particular circumstances of its mine.

Centralised underground installations are mostly in the mining zone; it is convenient to locate them close to the shaft system because heat can be rejected into the nearby main streams of return ventilating air passing into upcast shafts. Nevertheless, the available quantities and heat-absorbing capacity of this return air are limited, thus limiting the capacities of underground installations. Moreover, the coefficients of performance (COPs) of the water chilling plants in these installations are limited by the high temperature of this return air.[7] However, underground installations

---

[6] That is, they are close to the workings they serve, so that minimum cooling is lost between the installation and these workings.

[7] And thus the high lift (difference between temperatures of discard and extraction) imposed on these water chilling plants.

do have the advantage of being relatively near the workings, so minimum power is required to transport chilled water to the workings and back (Stroh and Kourelos, 1990; Ramsden et al., 1988). Feasibility studies of underground installations rejecting heat into the water being pumped out of the mine, rather than into return air, have been conducted (Stroh and Kourelos, 1990).

Installations on surface have no size or capacity limitations. The COPs of their water chilling plants are far better, because heat can be rejected into relatively cool ambient air on surface (Ramsden et al., 1988). Also, where service water is being chilled, the warm service water arriving from underground for chilling is typically at temperatures in the neighbourhood of 28°C. This temperature is considerably higher than that of the ambient air, so, as previously mentioned, it is worthwhile to pass this water through the heat-rejection equipment first. This water is therefore first passed through one or more *pre-cooling towers* (Stroh, 1982). In summer, when wet-bulb temperatures on surface in South African gold mining regions are 17°C to 18°C on average, this water can thus be cooled to approximately 20°C before entering the water chilling plant. This first step of cooling the service water is virtually "free".

In the colder seasons of the year, these pre-cooling towers assume a greater proportion of the service water cooling load, as illustrated in Figure 2.3. In winter, when wet-bulb temperatures are lowest, pre-cooling towers can provide 40 per cent more cooling than in summer, so some machines in the water chilling plant need not operate, thus facilitating planned maintenance (Baker-Duly, Ramsden and MacKay, 1993).

Installations have been evaluated in which maximum use is made of the lower night-time temperatures (Bluhm and Lancaster, 1987). In these cases a large pre-cooling tower is installed which can cool all the water from underground in the six to eight coolest hours of night-time; the water chilling plant also operates at maximum flow-rates then. Most cooling is

thus carried out during periods of off-peak power tariff. However, substantial water reservoirs are required on surface and underground to achieve the greatest power savings, so the decision whether to use less expensive night-time power must be made on economic grounds (Baker-Duly, Ramsden and MacKay, 1993).

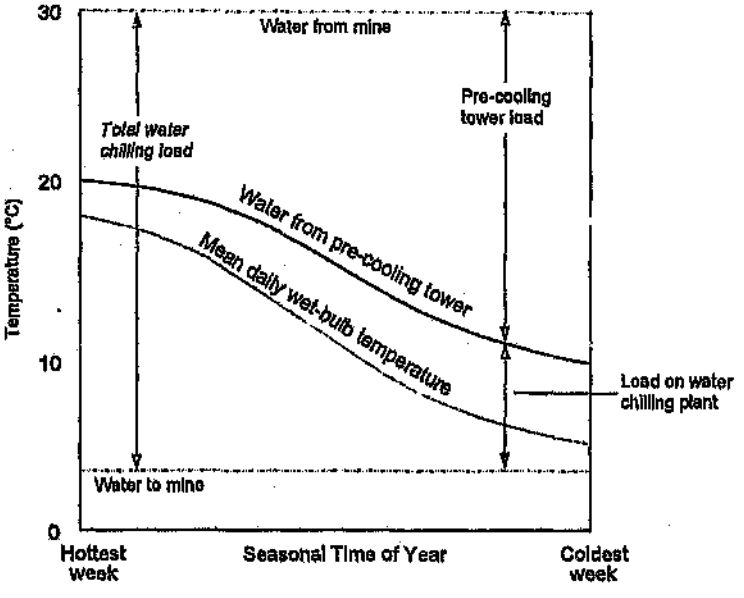

Figure 2.3 Variation of Pre-Cooling Tower Load with Ambient Wet-Bulb Temperature

A severe disadvantage of a surface installation is that considerable pumping power is required for circulating water between it and the underground workings. Although this disadvantage can be alleviated by passing the water through energy-recovery turbines on its way underground, it cannot be eliminated completely, and is still severe as mining depths increase (Stroh and Kourelos, 1990).

The three principal factors economically justifying fluid cooling installations on surface are (a) the use of pre-cooling towers as the first step in chilling service water; (b) the greater COP of the water chilling

plant; and (c) the development of energy-recovery systems to minimise the power required to circulate water between surface and the mining zone. Two additional factors are the escalating costs of establishing and maintaining underground plant (including underground excavations required), and the re-introduction of bulk downcast air cooling systems on surface on some mines (Stroh, 1982).

Classes of Centralised Installations

The various classes of centralised installations on South African mines are now briefly described, with emphasis on the nature of the duty (load and lift) imposed on the water chilling plant. Load can be smoothed or controlled; as mentioned above, wherever water reservoirs are present in the chilled water circuit, the installation can extract heat non-simultaneously with the daily or hourly cooling demand pattern. The installation's control philosophy can exploit this in various ways, ranging from simply smoothing the load on the water chilling plant to predicting the cooling demand and operating the water chilling plant and chilled water reservoir to meet this predicted demand with minimum energy consumption (Middleton, 1984).

Lift imposed on the water chilling plant, however, is neither smoothed nor controlled. As mentioned previously in Section 2.3.1, the heat-removing water circuits between the water chilling and heat rejection plants have no reservoirs of significance, so any diurnal variations in flow-rate and properties of the heat-rejection fluid directly affect the heat rejection function of the installation. Corresponding diurnal variations of temperature in the heat-removing water circuits result. Any such variations in turn directly affect the mean temperatures of discard and hence the lift in the water chilling plant, because this lift is the difference between the mean temperatures of extraction and discard. Therefore, even though the water chilling load may be smoothed or controlled, the lift will still vary hourly and daily if there are any such variations in flow-rate

or properties of the heat-rejection fluid circulating between the water chilling and heat rejection plants. Therefore, for installations on surface, where the heat-rejection fluid is ambient air varying hourly and daily in temperature, corresponding variations of lift in the water chilling plant always occur.

Surface Installation for Bulk Air Cooling

This class of installation is depicted schematically in Figure 2.4. Its task is to cool a large volumetric flow-rate of ventilating air entering a downcast shaft on its way underground. The chilled water leaving the water chilling plant cools this air by direct contact in the open-circuit bulk air cooling plant, and then returns to the machines for re-chilling.

This class of installation has no reservoirs in its chilled water circuit.[8] The cooling load, being entirely dependent on ambient weather conditions, is subject to major diurnal and seasonal variations. The machines in the water chilling plant have to be sized for the peak load and lift, but also have to accommodate the minimum values of these. Oddly, typical control systems attempt to maintain the temperature of the chilled water leaving the machines - and not the wet-bulb temperature of the air leaving the bulk air cooling plant, which appears more logical - at a preset value. Typical temperatures for mid-summer conditions during the hot part of the day are given in the figure.

The wet-bulb temperature of the ambient air directly affects the mean temperatures of both the chilled and heat-removing water streams, and so is the dominant influence on the duty of the water chilling plant. As this wet-bulb temperature reduces from its peak, the load and lift also reduce, and vice versa. Therefore, as diurnal and seasonal ambient temperatures

[8] Except for the water sump in the direct-contact bulk air cooling plant, which provides smoothing of the order of minutes.

reduce from their peaks, both the diurnal and seasonal duties of the water chilling plant are ones of *reducing load, reducing lift.*

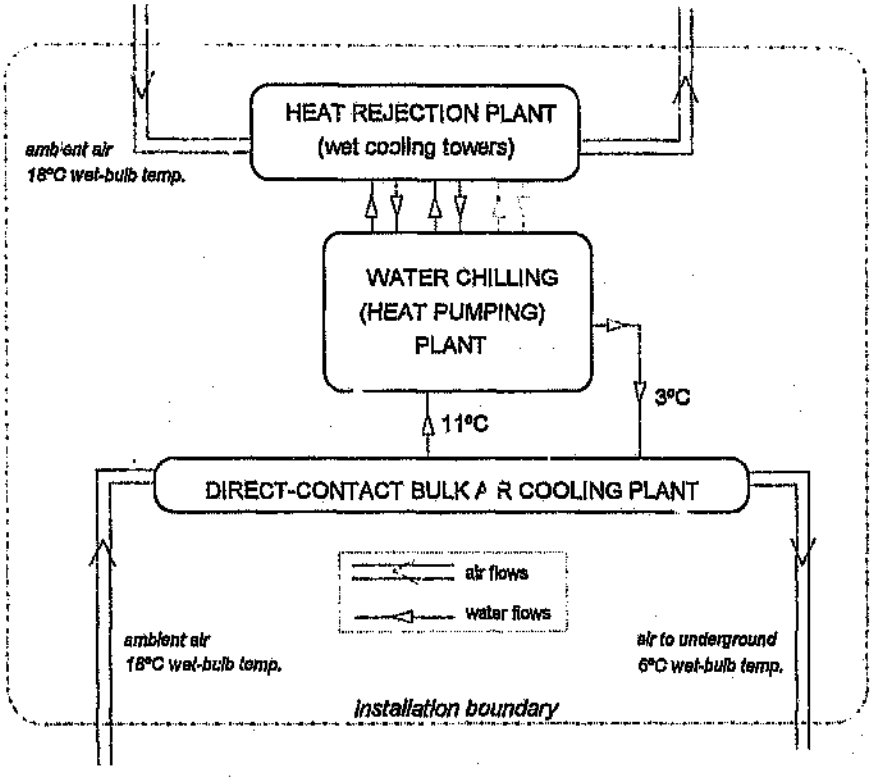

Figure 2.4 Surface Installation for Bulk Air Cooling[9]

Underground Installation for Bulk Air Cooling

In principle, this class of installation is no different from that of Figure 2.4, and has the same components. In detail, it differs in the following aspects:

---

[9] In rare cases, as mentioned in a previous footnote, refrigerant is used to cool this air directly in air-to-refrigerant heat exchangers. No water is then chilled, so the water chilling and direct-contact bulk air cooling plants in Figure 2.4 are replaced by a *bulk air cooling plant*. However, such bulk air cooling plants (and the refrigerating machines within them) experience exactly the same diurnal and seasonal duties as are now described for the water chilling plants normally present in such surface installations.

(a) its water chilling plant may serve two or more direct-contact bulk air coolers in different areas of the mine;

(b) the inlet and outlet wet-bulb temperatures of the air being cooled are in the region of 25°C and 15°C respectively (see, for example, Stroh, 1982 : 673,676);

(c) its heat rejection plant comprises vertical cooling towers or horizontal spray chambers whose heat-rejection fluid is a limited flow-rate of return ventilating air proceeding to upcast shafts. On entering the heat rejection plant, the wet-bulb temperature of this air ranges between 28°C and 40°C, depending on the amount of heat it has absorbed beforehand;

(d) diurnal variations in ambient weather on surface have relatively little effect, diminishing further with increasing depth, on properties of both the air being cooled and the heat-rejection air. This is due to the damping effect of heat absorbed by these air streams during their passage through the mine before entering the installation. Longer-term variations due to seasonal weather changes on surface will still be experienced, but in mitigated form for the same reason.

As diurnal and seasonal ambient temperatures reduce from their peaks, therefore, the diurnal duty of the water chilling plant in such an underground installation is one of substantially *constant load, constant lift;* its seasonal duty is one of reducing load, reducing lift, but less so than for a surface installation.

Surface Installation for Service Water Chilling

Figure 2.5 depicts this class of installation. Its task is to chill warm water pumped out of the mine so that this water may be returned underground as service water for drilling, dust suppression, etc. The temperature of the warm service water arriving from underground is significantly higher than the ambient wet-bulb temperature; so, as mentioned previously, one

or more pre-cooling towers (which form part of the heat re' tion plant) perform the first step of cooling. The water then passes ough the machines for chilling, and thence into the chilled water reservoir. Water is drawn from the chilled water reservoir to underground as demanded.

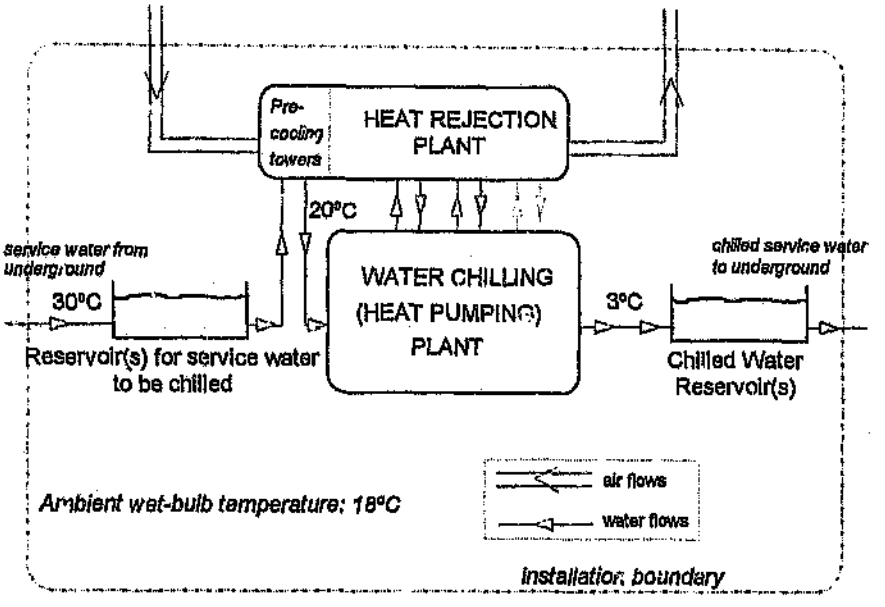

Figure 2.5 Surface Installation for Service Water Chilling

As documented by Middleton (1984), service water demand patterns are highly variable, with significant unpredictability. Current practice is to size the warm and chilled water reservoirs to smooth the load on the pre-cooling towers and water chilling plant as much as possible. These towers, and the machines in this plant, can therefore be sized for the *average* diurnal load in mid-summer. Typical temperatures for mid-summer conditions during the hot part of the day are given in the figure. The cool water leaving the pre-cooling towers will fluctuate in temperature according to the time of day. The control system of the water chilling plant must, none the less, maintain the chilled water delivery temperature at the desired value.

Here, there are two major influences on the duty of the water chilling plant. The first is the wet-bulb temperature of the ambient air; this, as before, directly affects the mean temperature of the heat-removing water streams, but now also that of the chilled water stream (through its influence on the pre-cooling tower performance; see Figure 2.3). Thus it directly affects both load and lift. The second major influence is the mass flow-rate of the chilled water stream passing through the plant; this is varied by the installation's control system to smooth the load on the plant.[10] Therefore, the diurnal duty on the water chilling plant is one of *mostly constant load,*[11] *reducing lift;* the seasonal duty remains one of reducing load, reducing lift.

Underground Installation for Service Water Chilling

Again, there is no difference in principle between such an installation situated underground and that of Figure 2.5. Differing aspects of detail are:

- as for all underground installations, daily and hourly variations in ambient weather on surface have little effect on properties of the heat-rejection air; this air is again limited in available flow-rate, and is at a wet-bulb temperature of between 28°C and 40°C;
- pre-cooling towers are inapplicable and not used; the warm service water proceeds directly to the water chilling plant.

Therefore, the diurnal duty on the water chilling plant is one of mostly constant load, but *constant lift;* the seasonal duty remains one of reducing load, reducing lift, but less so than for a surface installation.

---

[10] Alternatively, as proposed by Middleton (1984), a more advanced control strategy can be used to predict the cooling demand and operate the water chilling plant and the chilled water reservoir to meet this with minimum energy consumption. The diurnal water chilling plant duty is then *controlled load, reducing lift.* Middleton has shown that water chilling machines can be smaller when this control strategy is used.

[11] To the extent that the design and the control system of the installation permit smoothing the load in the face of the varying service water demand.

Surface Installation for Bulk Air Cooling and Service Water Chilling

Figure 2.6 depicts the installation of this class; it is essentially a combination of Figures 2.4 and 2.5.

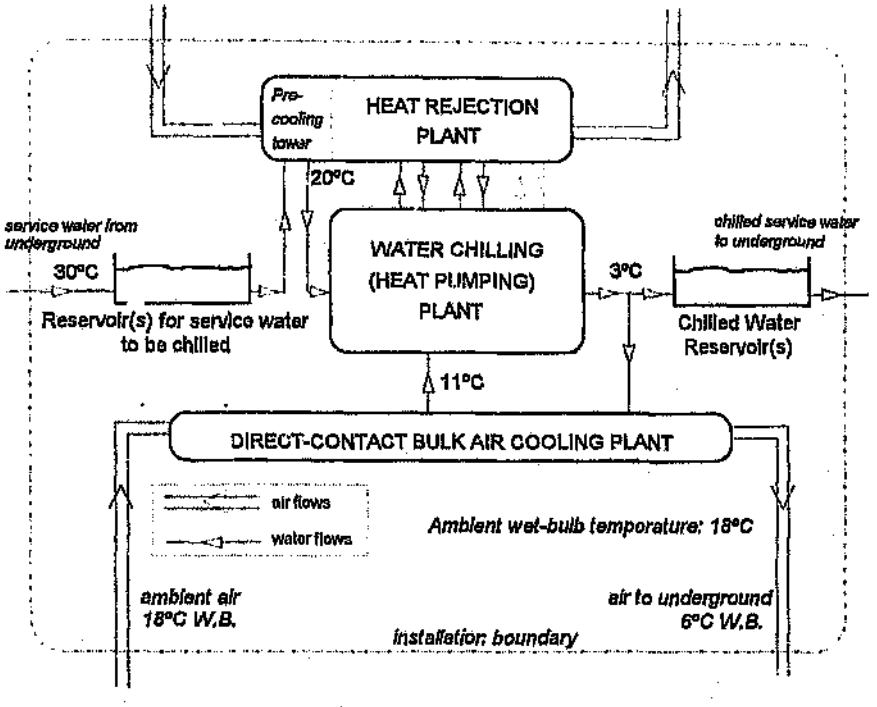

Figure 2.6 Surface Installation for Bulk Air Cooling and Service Water Chilling

During the night, both the pre-cooling tower and the direct-contact bulk air cooling plant deliver cooler water to the water chilling plant, which can thus deliver more water to the chilled water reservoir. At night, therefore, the water chilling plant can be kept operating at maximum capacity to stockpile chilled water in this reservoir. During the day, this stockpile provides for the difference between the generally higher service water demand and the much-reduced delivery into the chilled water reservoir. In this combined task, it is thus possible to present a virtually constant

load to the water chilling plant for almost nine months of the year.[12] Again, this enables the machines in this plant to be sized for the average duty in mid-summer. This system of "thermal stockpiling" is a modified version of the "thermal storage" system of Jansen van Vuuren (1983).

A further reason for stockpiling chilled water at night is that constraints on maximum electrical demand sometimes force installations to partially shut down during the main shift of the day, the typical peak demand period.

The diurnal duty on the water chilling plant is therefore one of *constant load, reducing lift;* the seasonal duty remains one of reducing load, reducing lift.

Underground Installation for Bulk Air Cooling and Service Water Chilling

The principal difference of such an installation from its surface counterpart is that pre-cooling towers are inapplicable and not used. The tasks of the previous two classes of underground installations are simply additive, so diurnal and seasonal duties on the water chilling plant remain ones of mostly constant load, constant lift and reducing load, reducing lift respectively.

Underground Installation Chilling Water for Distributed Air Cooling in Workings

This class of installation is depicted in Figure 2.7. Outside the installation, the chilled water delivered is circulated to networks of closed- or open-type air-to-water heat exchangers in the mining zone, and then returned to the installation for re-chilling.

As for other underground installations, diurnal variations in ambient weather on surface have relatively little effect on properties of both the air being cooled and the heat-rejection air. This class of underground

---

[12] During the 3 months of winter, it is not necessary to operate the bulk air cooling plant.

installation, though, may experience considerable variations in diurnal load *through the influence of another installation in the same shaft system*. For example, the use of chilled service water, supplied from a surface installation, during the day can materially reduce the temperature of the air entering air coolers served by an underground installation, and hence the load on the latter installation (Patterson, 1984). If such load variations occur, the diurnal duty of the water chilling plant is one of varying load, constant lift; if not, this duty is one of constant load, constant lift.

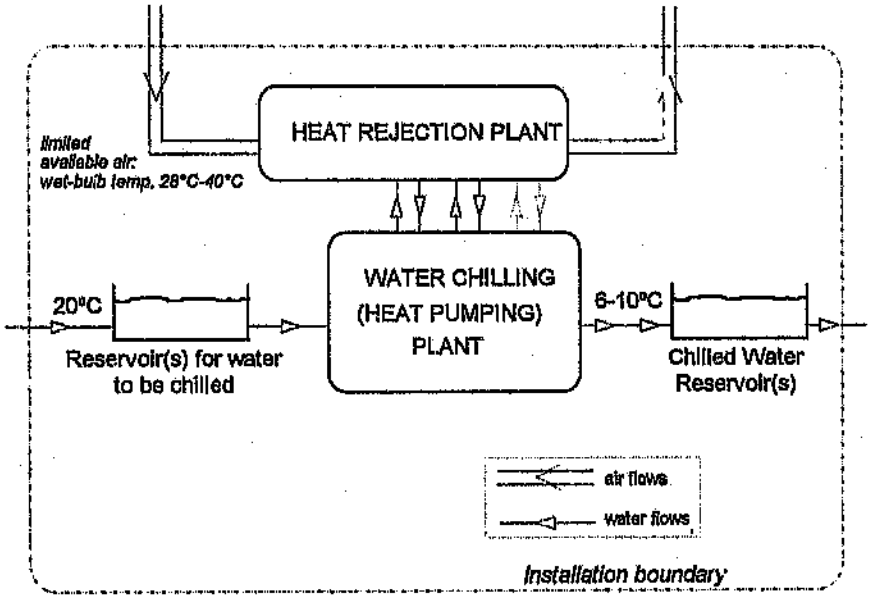

Figure 2.7 Underground Installation Chilling Water for Distributed Air Cooling in Workings

Also, the load on this installation is liable to vary in step fashion over months as air coolers distributed within the working areas are taken into and out of service during the course of mining. Apart from such relatively unpredictable load variations, the seasonal duty of the water chilling plant, as for other underground installations, remains one of reducing load, reducing lift.

Duties Imposed on Water Chilling Plants: Summary

Table 2.1 below summarises the variation of load and lift on water chilling plants in centralised mine fluid cooling installations as diurnal and seasonal ambient temperatures reduce from their peaks.

In sum, for water chilling plants on surface, diurnal lifts are always reducing; diurnal loads are constant if the installation smoothes them, and reducing otherwise. For underground water chilling plants, diurnal lifts are constant, and so are loads unless another installation affects them. Seasonal duty on all water chilling plants is one of reducing load, reducing lift, although less so for underground installations.

Table 2.1 Nature of Duties Imposed on ater Chilling Plants in Centralised Installations

DUTY ON WATER CHILLING PLANT	SURFACE		UNDERGROUND	
	Load	Lift	Load	Lift
Diurnal Duty				
Load unsmoothed:				
Bulk air cooling installation	Reducing	Reducing	Sub-stantially constant	Constant
Distr. air cooling underground	not applicable	-	Constant	Constant
Distr. air cooling underground if affected by other installation	not applicable	-	Varying	Constant
Load smoothed:				
Service water chilling	Mostly constant	Reducing	Mostly constant	Constant
Combined bulk air cooling & service water chilling	Constant	Reducing	Constant	Constant
Seasonal Duty	Reducing	Reducing	Reducing	Reducing

Water chilling plants can accommodate these changes in duty in two ways: either by regulating the capacities of their operating water chilling machine(s), or altering the amount of operating machines. The water chilling machines in these plants, particularly in installations on surface, may thus operate at off-design or part-duties for considerable portions of

their daily or yearly operating periods. Water chilling machines, and the capacity-regulating devices they use to accommodate off-design duties, are the subject of Chapter 3.

2.5 Ice-making Installations on South African Mines

Because of its latent heat of fusion, ice has a cooling capacity of between four and five times that of chilled water (Sheer et al., 1984). Therefore, if ice, instead of chilled water, is produced in a refrigerating installation on surface and transported underground to provide the required cooling by melting, the flow-rate of water required to transport heat through the transport zone is reduced by the same factor. A technical and economic study (Sheer et al., 1984) has shown that, despite the higher costs of making ice compared with chilling water, ice cooling systems can generally become more economical than "conventional" chilled water systems at depths greater than about 3 000 m.

Ice can be produced in various forms, including pure particulate ice, and ice-water mixtures (slurry ice) in various concentrations (Stroh and Kourelos, 1990). Pure particulate ice (100 per cent ice) results in minimum mass flow-rate through the transport zone; two South African mines have surface installations producing particulate ice (Middleton and Muller, 1986; Klostermann, 1994). On the other hand, a major benefit of slurry ice stems from its capacity to desalinate mine water to a high degree (Shone, 1989). The process of making slurry ice is also more efficient (Shone, 1989; Shone and Sheer, 1988) but conveying of ice-slurries presents certain problems which are not completely solved yet (Ramsden and Lloyd, 1992). However, tests on a pilot plant at one mine have been sufficiently encouraging for a cooling system using slurry ice to be proposed for a new shaft (Ramsden and Lloyd, 1992).

2.6 The Future

As reserves are mined out, it will be necessary for mines to increase their mean working depths, which will lead to greater heat loads and hence increased cooling requirements. This, together with other factors, will result in mine cooling costs increasing at a rate far greater than general mining costs (Ramsden, 1990). There is therefore a pressing need for research and development into new mine cooling systems - more specifically, into more cost-effective methods for transport of heat from the mining zone through the transport zone to surface (Ramsden, 1990). The reason is that as mines become deeper, the proportion of the capital and running expenditure of mine cooling systems due to this transport of heat becomes larger, and eventually dominates.

Mines of the future may require refrigerating installations of 100 MW(R) or more in capacity. The resulting sheer magnitude of water quantities and associated equipment will prohibit the widespread use of chilled water in transporting, and possibly even some reticulation systems for *distributing*, such large quantities of cooling (Ramsden, 1990). Notwithstanding the advantages of surface fluid cooling installations and energy-recovery or conserving equipment in chilled water transport systems, the capital and running expenditure required to circulate large flow-rates of water through the transport zone become prohibitive, as does the large space required by the piping in the shaft (Stroh and Kourelos, 1990).

Alternative media for heat transport systems are therefore being sought. The advantages of ice in this regard have already been outlined. The use of ammonia for this purpose is a recent, novel concept. Here, a vapour-compression refrigeration system extends from surface through the transport zone to the mining zone, with the refrigerant (ammonia) thus also serving as the fluid transporting heat through the transport zone. As

the latent heat of vaporisation of ammonia is very large,[13] mass flow-rates of ammonia are correspondingly small. Hence considerable economic advantages accrue, provided that such systems can be made safe. An installation has been designed in detail for one mine (Napier and Patterson, 1992). However, the use of ammonia underground is highly controversial, and there is some doubt about the overall viability of such systems once all the necessary safety features have been incorporated. The technique has not actually been implemented on any South African mine so far.

Air-cycle refrigeration for deep mines has also been investigated. In such a system, air would be compressed on surface, piped underground, and expanded through a turbine in the mining zone to produce cooled air. In general, though, it appears that such systems are only more cost-effective in comparison to chilled water systems at depths below 3 500 m (del Castillo, 1987); the deepest workings of some South African mines have reached this depth (CSIR, South Africa, 1994).

Thus for both existing mines and new mines which are not especially deep (see, for example, Rose and Bluhm, 1994), centralised fluid cooling installations using vapour-compression refrigerating machines to chill water are likely to remain the adopted technology.

---

[13] 1 261 kJ/kg at 0°C (IIR, 1981).

3. WATER CHILLING MACHINES EMPLOYED IN MINE FLUID COOLING INSTALLATIONS

This chapter provides the specific background to the thesis. It describes the water chilling machines within the water chilling plants of mine fluid cooling installations.

The chapter outlines the fundamental concepts and thermodynamic principles of the basic vapour-compression refrigerating cycle and machine. It then introduces real machines on mines by means of the *generalised vapour-compression water chilling machine*. The additional components and fluid flows existing in real machines are thereby highlighted, and their effects incorporated into the overall energy balance and COP of this generalised machine. The concept of the *refrigerant-circuit COP* and its use in verifying the "apparent COP" determined conventionally is also introduced.

Turning to classes of machines on mines, the chapter first reviews conventional packaged water chilling machines with a single- or multi-stage centrifugal compressor. The components of such machines, especially centrifugal compressors, are examined in some detail. Custom-built water chilling machines with one or more screw compressors are next reviewed and their components, notably screw compressors, are similarly examined. The overall energy balances and refrigerant-circuit COPs of these machines, which are needed later, are given. The chapter concludes with brief remarks on how the behavioural interdependence of machine components influences machine performance at full and part-duties.

3.1 Vapour-Compression Refrigerating Machines

Refrigerating cycles pump thermal energy from a region of low temperature to one of higher temperature. Vapour-compression and absorption refrigerating cycles are the two most common methods of such

thermal energy pumping. All water chilling machines on South African mines employ the vapour-compression refrigerating cycle. Any reasonably volatile substance which is liquid at the low temperature desired can be used as a refrigerant in such a cycle.

3.1.1 Refrigerant Pressure-Enthalpy Diagram

The thermodynamic state of any pure substance in equilibrium is defined if two independent thermodynamic properties are known. The two independent properties of pressure and enthalpy conveniently indicate the thermodynamic states of the refrigerant in a vapour-compression cycle on a *pressure-enthalpy diagram* as in Figure 3.1.

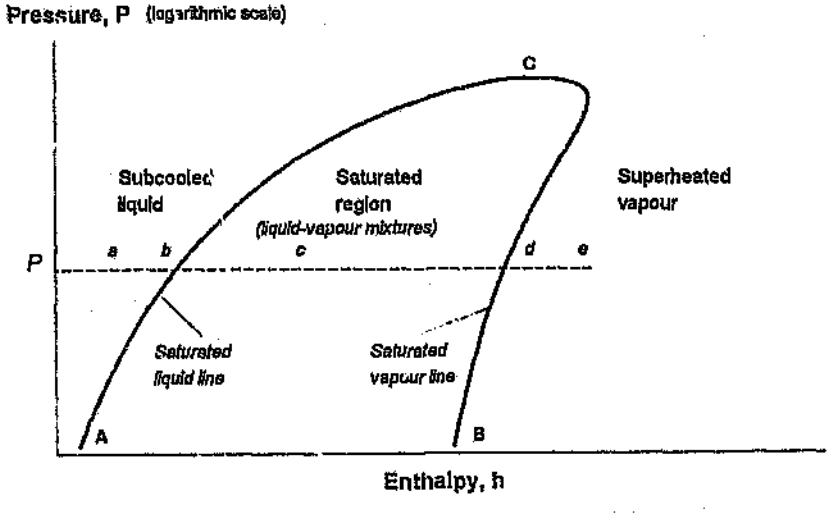

Figure 3.1 Pressure-Enthalpy Diagram for a Refrigerant

At any given pressure, there is only one corresponding temperature at which the refrigerant will evaporate from liquid to vapour or condense from vapour to liquid. This is known as the *saturation temperature* for the given pressure. The *saturated liquid line* AC in Figure 3.1 indicates those pressures and corresponding enthalpies where the refrigerant exists entirely as liquid at the saturation temperature corresponding to its pressure. The *saturated vapour line* BC similarly indicates those

pressures and corresponding enthalpies where the refrigerant exists entirely as *vapour* at the saturation temperature corresponding to its pressure. At the *critical point* C, the distinction between liquid and vapour vanishes.

The possible states of the refrigerant at a given, constant pressure *P* are illustrated by the dashed line *a-b-c-d-e* in the figure. At *a*, the refrigerant is in the liquid state, but its temperature is lower than the saturation temperature for the pressure *P*. Its state is therefore called *subcooled liquid*. At *b*, the refrigerant liquid is at the saturation temperature, and thus saturated; any further increase in enthalpy will cause at least some liquid to evaporate into vapour, *but the temperature will remain at the saturation temperature*. At the enthalpy of *c*, the refrigerant is partly liquid and partly vapour, remaining at the saturation temperature. At *d*, the refrigerant is entirely vapour, but still at the saturation temperature. At the enthalpy of *e*, the temperature of the vapour has risen above the saturation temperature, and the state is thus called *superheated vapour*.

In sum, the area ACB in Figure 3.1, labelled **"saturated region"**, is where refrigerant liquid and vapour can exist together in various proportions. Within this region, pressure and temperature are interdependent. To the left of this area (in the direction of lower enthalpy) is the **subcooled liquid region**, where the refrigerant can exist as liquid only. Liquid which is on the boundary of the saturated region is termed *saturated liquid*. To the right of the saturated region (in the direction of higher enthalpy) is the **superheated vapour region**, where the refrigerant can exist as vapour only. Vapour on the boundary of the saturated region is termed *saturated vapour*.

3.1.2 Ideal (Completely Reversible) Water Chilling Machine

As stated in Chapter 2, the water chilling plant in a mine fluid cooling installation consists of one or more water chilling machines and their

interconnections. Consider one water chilling machine within such a plant, as shown in Figure 3.2, chilling a water stream *(cw)* from absolute temperatures $T_{(cw)i}$ to $T_{(cw)o}$, and discarding heat into a heat-removing water stream *(hw)* which thus rises in temperature from $T_{(hw)i}$ to $T_{(hw)o}$.

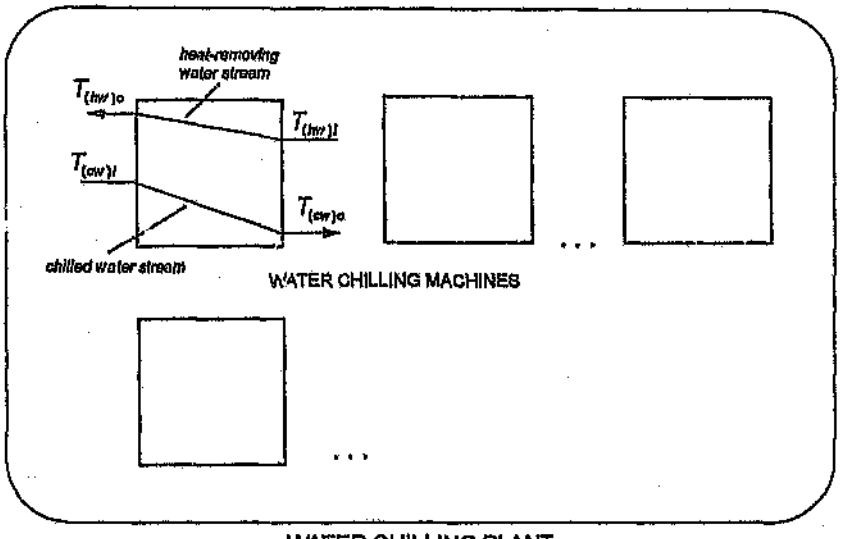

Figure 3.2 Water Chilling Machines within Water Chilling Plant

As for the ideal water chilling plant considered in Section 2.3.4, Chapter 2, if this water chilling machine is thermodynamically ideal, extracting, lifting and discarding heat reversibly, with the temperatures of extraction and discard equal to, and following, the changing temperatures of the chilled and heat-removing water streams respectively, its COP is the Lorenz COP, given by, analogously to (2-5a),

$$COP_{(Lor)} = \frac{\overline{T}_{(cw)}}{\overline{T}_{(hw)} - \overline{T}_{(cw)}} \qquad (3\text{-}1)$$

where $\overline{T}_{(cw)}$ and $\overline{T}_{(hw)}$ are the logarithmic-mean temperatures of the chilled and heat-removing water streams respectively.

3.1.3 Semi-Ideal (Internally Reversible) Water Chilling Machine

In any real vapour-compression water chilling machine, heat exchangers are used to transfer heat from the chilled water stream to the refrigerant, and from the refrigerant to the heat-removing water stream. Such heat exchangers must be of finite size, so these heat transfers between the internal refrigerant circuit and the external water streams have to take place across finite temperature differences and are thus thermodynamically irreversible. Therefore, even if all internal processes within the refrigerant circuit are ideal, and the machine can thus lift heat reversibly, it can neither extract nor discard heat reversibly. Such a semi-ideal machine is termed an *internally* reversible machine.

Moreover, the refrigerant used is a pure substance and, as explained later, it gains heat from and loses heat to these water streams by evaporating and condensing, respectively, in these heat exchangers (which are thus termed the *evaporator* and *condenser)* at essentially constant pressure. Since temperature and pressure are interdependent in the saturated region, as noted previously, these evaporating and condensing processes also occur at essentially constant temperature. Because these heat-transfer processes occur at essentially constant temperature, the maximum possible COP attainable by a semi-ideal, internally reversible machine is the *Carnot COP*, in which the refrigerant passes through a reversed Carnot cycle as shown in the temperature-entropy diagram of Figure 3.3.

In this well-known reversed Carnot cycle (see, for example, Rogers and Mayhew, 1967 : 254,255), refrigerant vapour is compressed at constant entropy, that is isentropically, from a low pressure and temperature (state 1 in the figure) to a higher pressure and temperature (state 2). It then

passes through a condenser, where it condenses at constant pressure and temperature $T_{(r)C}$ to state 3. The refrigerant is then expanded isentropically to its original pressure (state 4), and finally evaporated at constant pressure and temperature $T_{(r)E}$ to state 1. The corresponding Carnot COP is

$$COP_{(Car)} = \frac{T_{(r)E}}{T_{(r)C} - T_{(r)E}} \qquad (3\text{-}2)$$

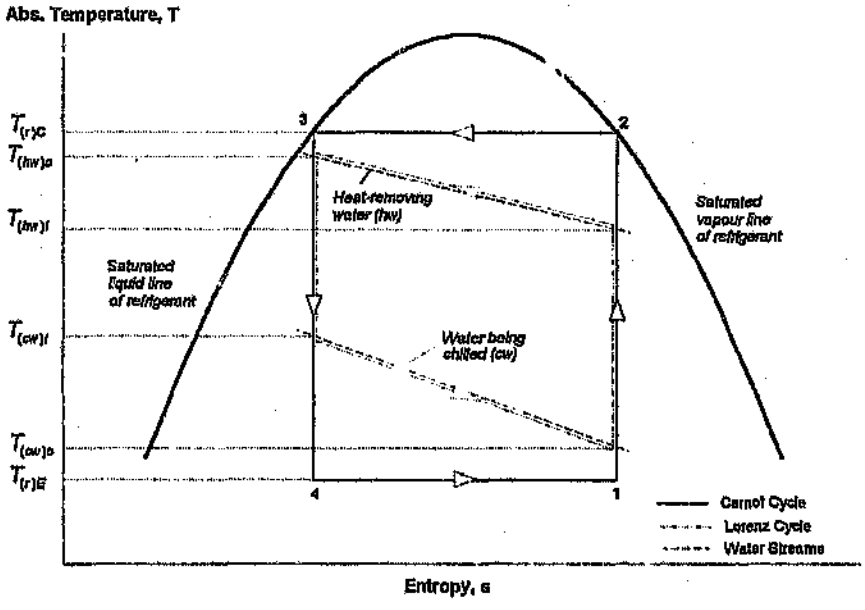

Figure 3.3 Ideal Lorenz and Carnot Cycles of Vapour-Compression Water Chilling Machine

Figure 3.3 also shows the completely ideal Lorenz cycle, where the refrigerant is also compressed and expanded isentropically, but in passing through the evaporator and condenser, follows the changing temperatures of the water streams exactly. Due to the finite temperature differences prevailing in the real evaporator and condenser, $T_{(r)E}$ is less than $T_{(cw)o}$ and thus considerably less than the logarithmic-mean

temperature $\overline{T}_{(cw)}$ of the chilled water stream. Similarly, $T_{(r)c}$ is greater than $T_{(hw)o}$ and thus considerably greater than $\overline{T}_{(hw)}$. Therefore, the semi-ideal Carnot COP is considerably lower than the completely ideal Lorenz COP.

By way of example, the water chilling plant cited in Section 2.3.4, Chapter 2 comprises four identical water chilling machines connected in parallel. Water is thus chilled in one step; so, as for the whole plant, each machine is designed to chill water from 14,5°C to 4°C, and to raise its heat-removing water from 22°C to 27,14°C; its Lorenz COP is thus 18,4. For each machine, though, the design evaporating and condensing refrigerant temperatures are 0,04°C and 30,96°C respectively, so from (3-2), its Carnot COP is 8,84 - only 48 per cent of the Lorenz COP!

3.1.4 Basic, Real Refrigerating Cycle and Machine

The basic, real vapour-compression refrigerating cycle and corresponding machine can now be reviewed. These are thoroughly described in textbooks; see, for example, Gosney (1982). Figure 3.4 illustrates the refrigerant circuit and the pressure-enthalpy diagram of the basic cycle. The refrigerant circuit consists of an evaporator, compressor, condenser and expansion valve. The figure also shows the thermodynamic boundary of this refrigerant circuit, across which flows of heat Q and work W occur, defined as positive if flowing into the refrigerant circuit.

Under conditions of steady flow, the refrigerant leaves the evaporator at point 1 as a low-pressure saturated vapour at saturation temperature $t_{(r)E}$ and enters the compressor, where it is compressed adiabatically with mechanical power input W_P to a high-pressure, high-temperature superheated vapour. At point 2, this vapour leaves the compressor and enters the condenser, where a heat flow Q_C leaves it as it is first de-superheated and then condensed at constant pressure.

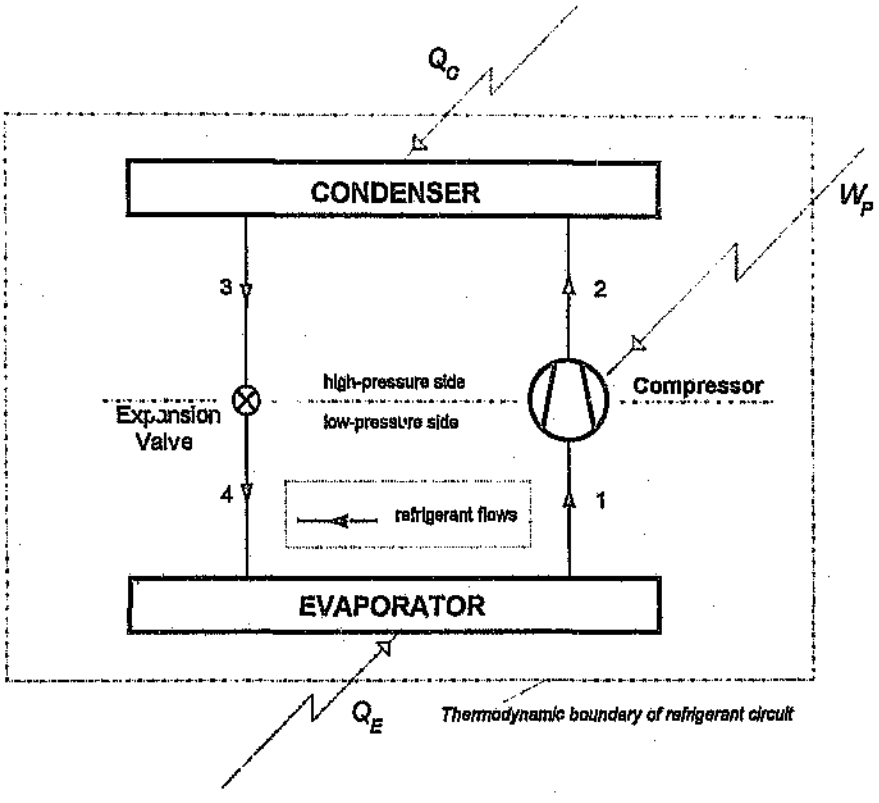

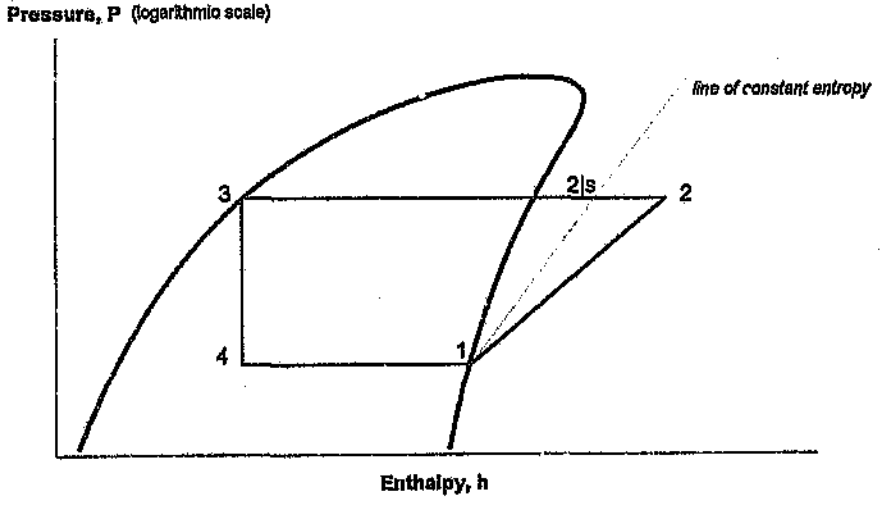

Figure 3.4 Basic Vapour-Compression Refrigerating Machine and Cycle

At point 3, the refrigerant leaves the condenser as a high-pressure saturated liquid at temperature $t_{(r)C}$ and enters the expansion valve, where it is reduced to a lower pressure. Some of the liquid therefore flashes into vapour.[1] At point 4, the refrigerant thus leaves the expansion valve as a low-pressure, low-temperature mixture of mostly liquid and some vapour, termed the "flash vapour" or "flash gas". This mixture enters the evaporator, where an incoming heat flow Q_E evaporates the liquid at constant pressure to the saturated vapour state at point 1.

This real machine is neither externally nor internally ideal. It departs from even the reversed Carnot cycle of Figure 3.3 because of internal thermodynamic irreversibilities in its refrigerant circuit. First, the expansion valve reduces refrigerant pressure by deliberately introducing friction into the refrigerant flow, so the expansion process through this valve is not isentropic, and is inherently irreversible. Second, the real adiabatic compression process is never perfectly isentropic. Third, in the condenser, the desuperheating of the refrigerant vapour before it condenses constitutes heat transfer across a greater temperature difference, and thus greater irreversibility. All these contribute to reducing the actual COP below the Carnot COP (see, for example, Rogers and Mayhew, 1967 : 256-259). On the other hand, modifications such as multi-stage compression with interstage economising can be made to the refrigerant circuit to reduce these irreversibilities and hence improve the actual COP. This modification is incorporated into the machines with a multi-stage centrifugal compressor reviewed in Section 3.2.7 below.

By applying the well-known steady flow energy equation to each component in Figure 3.4, the following relations are obtained:

---

[1] This is because the refrigerant entering the expansion valve is saturated liquid, i.e. liquid at its boiling point at the condensing pressure. As the pressure is reduced in the expansion valve, the refrigerant can no longer exist in equilibrium as entirely liquid and must partially boil into vapour.

$$\begin{aligned} &\text{Compressor:} && W_P = m_{(r)}(h_2 - h_1) \\ &\text{Condenser:} && Q_C = m_{(r)}(h_3 - h_2) \\ &\text{Expansion valve:} && h_4 = h_3 \\ &\text{Evaporator:} && Q_E = m_{(r)}(h_1 - h_4) \end{aligned} \qquad (3\text{-}3)$$

where h_n is refrigerant enthalpy at the subscripted point n in the circuit, and $m_{(r)}$ is the circulating mass flow-rate of refrigerant therein.[2] The overall energy balance for the system is

$$Q_E + W_P + Q_C = 0 \qquad (3\text{-}4)$$

It is important to note that Q_E and W_P, being energy flows into the machine, are positive; Q_C, being an energy flow out of the machine, is negative. Thus (3-4) means that the heat Q_C rejected by the refrigerant in the condenser must equal the sum of the heat Q_E absorbed in the evaporator and the work W_P of compression.

Design and Off-Design Duty

From the point of view of its refrigerant circuit, the duty of the basic water chilling machine consists of pumping the heat load Q_E through the lift between the temperatures of extraction $t_{(r)E}$ and discard $t_{(r)C}$. A machine is performing at its *full* or *design duty* when both load and lift are at design values. All other values of load and lift constitute *off-design duties*, which are termed *part-duties* if load, lift or both are below design values.

---

[2] In applying the steady-flow energy equation, kinetic and potential energy terms are omitted. These terms are numerically insignificant, as refrigerant flow velocities are kept low to avoid fluid friction and undesirable pressure losses, and variations in height within a vapour-compression refrigerating system are usually small.

Coefficient of Performance (COP)

The COP, being the ratio of the useful effect produced to the means used to produce it, is

$$COP \equiv \frac{\text{refrigerating load}}{\text{net work input}} \equiv \frac{Q_E}{W} \tag{3-5a}$$

and so, from (3-3)

$$COP = \frac{h_1 - h_4}{h_2 - h_1} \tag{3-5b}$$

The enthalpy rise $h_1 - h_4$ through the evaporator is known as the *refrigerating effect.*

Compressor Isentropic Efficiency

The static pressure rise resulting from a compressor's work input or, conversely, the amount of work required to produce a given pressure rise, depends on the efficiency of the compressor and the thermodynamic properties of the refrigerant. For an adiabatic compression process, the work input required is minimum if the compression is isentropic. Therefore, actual compression is often compared to an isentropic process (ASHRAE, 1992 : 35.27). An isentropic compression process would result in the state of the refrigerant at the compressor outlet being at point 2|s, instead of point 2, on the pressure-enthalpy diagram in Figure 3.4. The reversible work required by an isentropic compression between states 1 and 2|s is known as the *isentropic work* $W|_s$, measured by the enthalpy difference between these two points:

$$W|_s = h_{2|s} - h_1$$

The irreversible work done by the actual compressor is, from (3-3):

$$W = h_2 - h_1$$

The ratio of isentropic work to actual work is the *isentropic efficiency* η_{is} of compression:

$$\eta_{is} \equiv \frac{W|_s}{h_2 - h_1} = \frac{h_{2s} - h_1}{h_2 - h_1} \qquad (3\text{-}6)$$

The isentropic efficiency of a compressor at it's design duty (which generally corresponds to full capacity) ranges from approximately 0,60 to 0,88, generally increasing with compressor size (ASHRAE, 1992). At part-duties, the isentropic efficiency is generally below the full-duty value, the fall-off depending on the internal geometry of the compressor and the efficiency of its capacity-regulating device.

Refrigerants

As stated earlier, any reasonably volatile substance which is liquid at the low temperature desired can be used as a refrigerant. Apart from the desirability of maximally favourable thermodynamic and thermophysical properties, though, the choice in reality is limited by factors such as cost, toxicity, flammability, chemical stability, and compatibility with compressor oil and materials in the machine.

Briefly, the ideal refrigerant will have high a latent heat of vaporisation, to minimise its mass flow-rate in the refrigerant circuit; a high vapour density to minimise displacement and hence size of positive-displacement compressors; a low liquid density to minimise pressure drops in refrigerant liquid piping and to fill the liquid-containing parts of the machine with the minimum mass of refrigerant; and high liquid and vapour thermal conductivities to minimise resistance to heat transfer in the evaporator and condenser. Table 3.1 below lists such properties of

refrigerants commonly used in large vapour-compression water chilling machines, at a saturation temperature of 0°C.

Table 3.1 Properties of Refrigerants at Saturation Temperature of 0°C (IIR, 1981; ASHRAE, 1993)

	Latent heat of vaporisation, kJ/kg	Density, kg/m³		Thermal conductivity, W/m.K	
		Liquid	Vapour	Liquid	Vapour
Ammonia	1 261,1	638,6	3,46	0,5390	0,0223
Halocarbon refrigerants:					
Refrigerant 11	188,9	1 534,3	2,48	0,0945	not given
Refrigerant 123	179,7	1 523,7	2,25	0,0839	not given
Refrigerant 12	151,5	1 396,9	18,04	0,0783	0,0083
Refrigerant 22	205,4	1 284,8	21,21	0,1001	0,0094
Refrigerant 134a	198,8	1 293,3	14,44	0,0934	0,0118

Except for vapour density, ammonia is thus clearly superior to the halocarbon refrigerants. Its latent heat is an order of magnitude higher than those of the halocarbon refrigerants, so the required mass flow-rate is an order of magnitude lower. Despite its low vapour density, therefore, it can be used in positive-displacement compressors of practicable sizes, which Refrigerants 11 and 123 cannot. The low vapour density of ammonia also means, though, that it does not readily lend itself to use in centrifugal compressors; required impeller tip speeds are too high unless multiple stages are employed (Gosney, 1982). Ammonia's major disadvantage is its toxicity, which is the main reason why halocarbon refrigerants are used in the vast majority of mine fluid cooling installations.

3.1.5 Generalised Vapour-Compression Water Chilling Machine

The refrigerant circuits of the large-capacity water chilling machines in mine fluid cooling installations are considerably more complex than that of Figure 3.4. A generalised vapour-compression water chilling machine, which may be defined as all components within a refrigerant circuit

constructed for water chilling, is illustrated conceptually in Figure 3.5 below. This consists of a *condenser block*, an *evaporator block*, and a *vapour-compression block* between them.

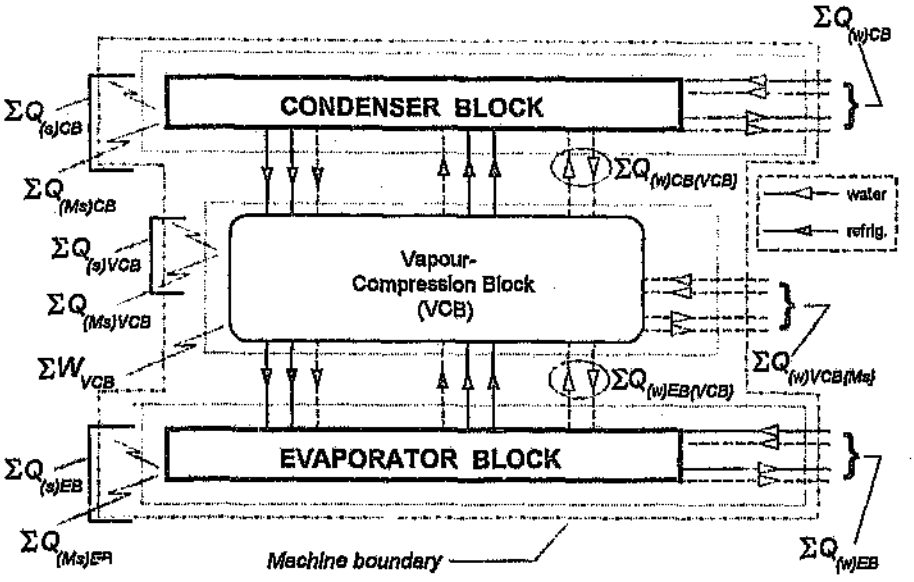

Figure 3.5 Generalised Water Chilling Machine

These blocks are shown enclosed by dotted envelopes, representing the thermodynamic boundaries across which all mass and energy flows take place. These thermodynamic boundaries are defined as crossing all entering and leaving flows of fluid (refrigerant, water, etc.) *at the points where temperature and other thermodynamic properties of these fluid flows are measured.*

The outer envelope in Figure 3.5 represents the similar thermodynamic boundary of the complete machine *(machine boundary)*. As in Figure 3.4, flows of heat across thermodynamic boundaries are denoted by Q, and of mechanical work by W. These flows are defined as positive when entering the machine or a component thereof.

The refrigerant circuit consists of the vapour-compression block, the evaporator and condenser blocks, and the interconnecting refrigerant piping. The vapour-compression block may contain any amount of refrigerant compressors, expansion valves, vessels, heat exchangers and other components. All refrigerant flows between the evaporator and condenser blocks pass through the vapour-compression block. The condenser and evaporator blocks may contain any amount of heat exchangers and other components, interconnected in any way in the refrigerant circuit and their water circuits. Any amounts of water flows may enter and leave these blocks.

Flows of energy across the *machine* boundary are as follows. $\sum Q_{(w)EB}$ denotes the net heat flow entering the evaporator block via all its entering and leaving water flows crossing the machine boundary. $\sum Q_{(w)CB}$ denotes the corresponding heat flow entering the condenser block, and $\sum Q_{(w)VCB(Ms)}$ [3] that entering the vapour-compression block. $\sum W_{VCB}$ denotes the total mechanical power input to this block. $\sum Q_{(Ms)EB}$, $\sum Q_{(Ms)CB}$ and $\sum Q_{(Ms)VCB}$ denote the net heat flow from the *machine* surroundings entering the external surfaces of the evaporator, condenser and vapour-compression blocks respectively.

Within the machine boundary, $\sum Q_{(s)EB}$, $\sum Q_{(s)CB}$ and $\sum Q_{(s)VCB}$ denote the net heat flow entering the external surfaces of the evaporator, condenser and vapour-compression blocks from the surroundings *of these blocks.* As shown in the figure, $\sum Q_{(s)EB}$ thus comprises $\sum Q_{(Ms)EB}$

---

[3] The suffix *{Ms}*, denoting *machine* surroundings, is to emphasise that this term denotes heat flow across the *machine* boundary via water flows to and from the vapour-compression block. Strictly, of course, $\sum Q_{(w)EB}$ and $\sum Q_{(w)CB}$ should also be written $\sum Q_{(w)EB(Ms)}$ and $\sum Q_{(w)CB(Ms)}$; but since these terms are normally understood to mean water-borne heat flow across the machine boundary, *{Ms}* in their subscripts is omitted for brevity. The same applies to $\sum W_{VCB}$.

and the additional heat flow originating from *within* the machine boundary. The same holds for $\sum Q_{(s)VCB}$ and $\sum Q_{(s)CB}$.

Within the machine boundary, as also shown, some water flows may pass between the vapour-compression block and the evaporator and condenser blocks. Such flows may be, for example, to and from oil-to-water compressor oil coolers. The net heat flows into the evaporator and condenser blocks resulting from all such water flows are denoted by $\sum Q_{(w)EB(VCB)}$ and $\sum Q_{(w)CB(VCB)}$ respectively.

For this generalised water chilling machine, the relations for the energy balance and COP are readily extended from (3-4) and (3-5) respectively.

Overall Energy Balance

The overall energy balance for the complete machine is

$$\left(\sum Q_{(w)EB} + \sum Q_{(Ms)EB}\right) + \sum W_{VCB} + \left(\sum Q_{(w)VCB(Ms)} + \sum Q_{(Ms)VCB}\right) + \left(\sum Q_{(w)CB} + \sum Q_{(Ms)CB}\right) = 0 \qquad (3\text{-}7a)$$

If the net heat flow $\sum Q_{(Ms)}$ from the machine surroundings into the external surfaces of all machine components is defined as

$$\sum Q_{(Ms)} \equiv \sum Q_{(Ms)EB} + \sum Q_{(Ms)VCB} + \sum Q_{(Ms)CB} \qquad (3\text{-}7b)$$

then the overall energy balance for the generalised machine becom

$$\sum Q_{(w)EB} + \sum W_{VCB} + \sum Q_{(w)VCB(Ms)} + \sum Q_{(w)CB} + \sum Q_{(Ms)} = 0 \qquad (3\text{-}7c)$$

The three terms on the right-hand side of (3-7b) will at least partially cancel. This is because, in reality, $\sum Q_{(Ms)EB}$ will be positive (the external surfaces of the evaporator(s) in the evaporator block will be cooler than the machine surroundings) whereas $\sum Q_{(Ms)VCB}$ and $\sum Q_{(Ms)CB}$ will be

negative (the external surfaces here will mostly be hotter than the machine surroundings). This cancellation effect will contribute to the likelihood that $\sum Q_{(Ms)}$ is negligible compared to the sum of the other terms in (3-7c). If it is indeed so negligible, then the overall energy balance simplifies to

$$\sum Q_{(w)EB} + \sum W_{VCB} + \sum Q_{(w)VCB(Ms)} + \sum Q_{(w)CB} \cong 0 \qquad (3\text{-}7d)$$

Even this simplified overall energy balance for the generalised machine differs from (3-4), that for the basic machine, in one key aspect: the effect, represented by $\sum Q_{(w)VCB(Ms)}$, of any water flows passing through the vapour-compression block and crossing the *machine* boundary must be taken into account.

Energy Balances for Individual Blocks

Energy balances for individual blocks of the generalised machine are needed to calculate its COP and other quantities. The energy balance for the condenser block is

$$\sum Q_{(w)CB} + \sum Q_{(r)CB} + \sum Q_{(w)CB(VCB)} + \sum Q_{(s)CB} = 0 \qquad (3\text{-}8a)$$

where $\sum Q_{(r)CB}$ denotes the net heat flow entering the condenser block via all the refrigerant flows passing into and out of it. If $\sum Q_{(r)CB} \equiv \sum m_{(r)CB} h_{(r)CB}$, the sum of the products of all refrigerant mass flows $m_{(r)CB}$ entering the condenser block and their corresponding enthalpies $h_{(r)CB}$,

$$\sum Q_{(w)CB} + \sum m_{(r)CB} h_{(r)CB} + \sum Q_{(w)CB(VCB)} + \sum Q_{(s)CB} = 0 \qquad (3\text{-}8b)$$

Similarly, the energy balance for the evaporator block is

$$\sum Q_{(w)EB} + \sum m_{(r)EB} h_{(r)EB} + \sum Q_{(w)EB(VCB)} + \sum Q_{(s)EB} = 0 \qquad (3\text{-}9)$$

and that for the vapour-compression block is

$$\sum W_{VCB} + \sum m_{(r)VCB} h_{(r)VCB} - \sum Q_{(w)EB(VCB)} - \sum Q_{(w)CB(VCB)} + \sum Q_{(w)VCB(Ms)} + \sum Q_{(s)VCB} = 0 \qquad (3\text{-}10)$$

In reality, only one of the terms $\sum Q_{(w)EB(VCB)}$, $\sum Q_{(w)CB(VCB)}$ and $\sum Q_{(w)VCB(Ms)}$ is likely to be non-zero.[4] Formulae (3-8b) through (3-10) simplify accordingly.

Coefficient of Performance (COP) and Refrigerant-Circuit COP

The COP for this generalised machine, being the ratio of the useful cooling produced to the power input required to produce it, is

$$COP \equiv \frac{\sum Q_{(w)EB}}{\sum W_{VCB}} \qquad (3\text{-}11a)$$

Using the energy balances of (3-9) and (3-10), the COP can also be expressed as follows:

$$COP = \frac{-\sum m_{(r)EB} h_{(r)EB} - \sum Q_{(w)EB(VCB)} - \sum Q_{(s)EB}}{\left(\begin{array}{c} -\sum m_{(r)VCB} h_{(r)VCB} + \sum Q_{(w)EB(VCB)} + \sum Q_{(w)CB(VCB)} \\ -\sum Q_{(w)VCB(Ms)} - \sum Q_{(s)VCB} \end{array} \right)} \qquad (3\text{-}11b)$$

Compared to the net energy flows $\sum m_{(r)EB} h_{EB}$ and $\sum m_{(r)VCB} h_{(r)VCB}$ into the refrigerant circuit, the other heat loads in (3-11b) are small, and in many cases negligible. These net energy flows into the refrigerant circuit therefore dominate in the numerator and denominator. If all other terms

---

[4] Because the water flows through the vapour-compression block normally serve compressor oil coolers and all are likely to come from the same source - either the evaporator block, or the condenser block, or a source outside the machine boundary.

are neglected, then (3-11b) reduces to a function of refrigerant mass flows and corresponding enthalpies, and is termed the *refrigerant-circuit COP, $COP_{(r)}$*:

$$COP_{(r)} \equiv \frac{-\sum m_{(r)EB} h_{(r)EB}}{-\sum m_{(r)VCB} h_{(r)VCB}} \qquad (3\text{-}11c)$$

If the other terms in (3-11b) are indeed negligible in comparison to $\sum m_{(r)EB} h_{(r)EB}$ and $\sum m_{(r)VCB} h_{(r)VCB}$ respectively, *the refrigerant-circuit COP is an excellent approximation to the actual COP*, defined by (3-11a).[5] Moreover, (3-11a) and (3-11c) are independent ways of determining COP, as they involve no common quantities. In measuring the performance of water chilling machines, therefore, the refrigerant-circuit COP determined by (3-11c) can be used to verify the "apparent COP" customarily determined by (3-11a). Because of this, the refrigerant-circuit COP is of great importance in the work to follow. It is the basis of the "Thorp method", described in Chapter 4 and developed further in Chapter 5, of verifying the site performance of water chilling machines, obtained in the first instance from water-circuit measurements.

3.1.6 Classes of Large-Capacity Water Chilling Machines Used on Mines

Large-capacity vapour-compression water chilling machines used on mines are of two broad classes: conventional, packaged machines with a centrifugal compressor, or custom-built machines with one or more screw compressors. These two types of compressors employ the dynamic and positive-displacement principles of compression respectively. The type of compressor employed is a key factor in determining the other components

---

[5] Where the refrigerant-circuit COP is not a satisfactory approximation to the actual COP, it can be corrected to make it so, as described in Chapter 5.

employed in a water chilling machine, and the design and arrangement of its refrigerant circuit.

Positive-displacement compressors, such as reciprocating and screw compressors, increase the pressure of vapour by reducing the volume of internal chambers through work applied to the compressor's mechanism. Aside from volumetric efficiency effects, the intake volume is independent of the pressure rise. Dynamic compressors, such as centrifugal and axial compressors, increase the pressure of vapour by continuous transfer of angular momentum from the rotating member to the vapour, followed by a conversion of this momentum into a pressure rise. Pressure rise and flow-rate are interdependent, their relationship being expressed through a characteristic performance curve (ASHRAE, 1992).

Water chilling machines employing centrifugal compressors are almost exclusively of the packaged type, built as an integral unit for air-conditioning applications, and employing one compressor, one evaporator and one condenser in the refrigerant circuit. Screw compressors can also be employed in such packaged machines, but they are most often used in custom-built machines employing multiple compressors, evaporators and condensers. Conventional packaged machines employing a centrifugal compressor will be reviewed first, and then custom-built machines employing screw compressors.

3.2 Conventional Packaged Machines with a Centrifugal Compressor

Centrifugal compressors are used extensively for air-conditioning and industrial refrigeration applications. They are well suited for this purpose because of their ability to produce high pressure ratios. Because their flows are continuous, these machines, like all dynamic compressors, have greater volumetric capacities, size for size, than do positive-displacement compressors (ASHRAE, 1992). For a very wide range of flows, centrifugal compressors have considerable advantages: they are small, robust,

relatively simple, very reliable, and in many cases cheaper and more efficient than other types (Casey and Marty, 1986).

3.2.1 Packaged Machines with a Single-Stage Centrifugal Compressor

The simplest form of packaged water chilling machine - that with a single-stage centrifugal compressor - is illustrated schematically in Figures 3.6 and 3.6a.

The evaporator block consists of a single, horizontal shell-and-tube evaporator, with the water being chilled flowing through the tubes. The condenser block similarly consists of a single, horizontal shell-and-tube condenser, with the heat-removing water flowing through the tubes. As shown, this condenser may incorporate a subcooler, to cool the condensed refrigerant liquid below its saturation temperature. The benefit of a subcooler is that the refrigerating effect is increased without any increase in the work of compression (see, for example, Gosney, 1982).

The vapour-compression block consists of the single-stage centrifugal compressor (with its oil cooler), the expansion valve, and a hot gas bypass valve. This latter valve only opens at low part-duties when the centrifugal compressor would otherwise surge, as explained later.

The compressor oil cooler can be an oil-to-water type as in Figure 3.6, or an oil-to-refrigerant type as in Figure 3.6a.

As for the generalised machine of Figure 3.5, the evaporator, condenser and vapour-compression block are shown enclosed by their dotted thermodynamic boundaries, which are again defined as crossing all entering and leaving fluid flows *at the points where temperature and other thermodynamic properties of these fluid flows are measured.* This is important from the point of view of the compressor oil cooler. If this is an oil-to-water type, Figure 3.6 shows it obtaining its water:

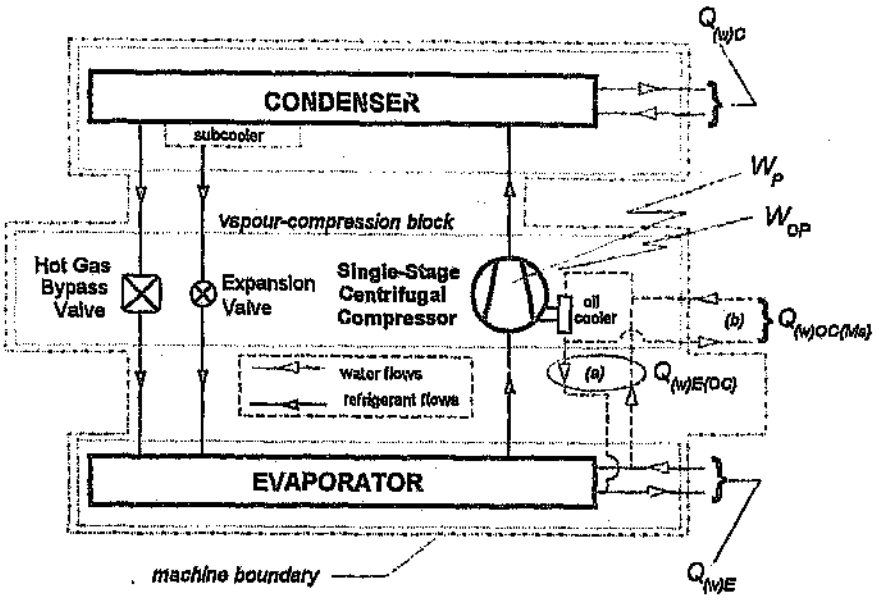

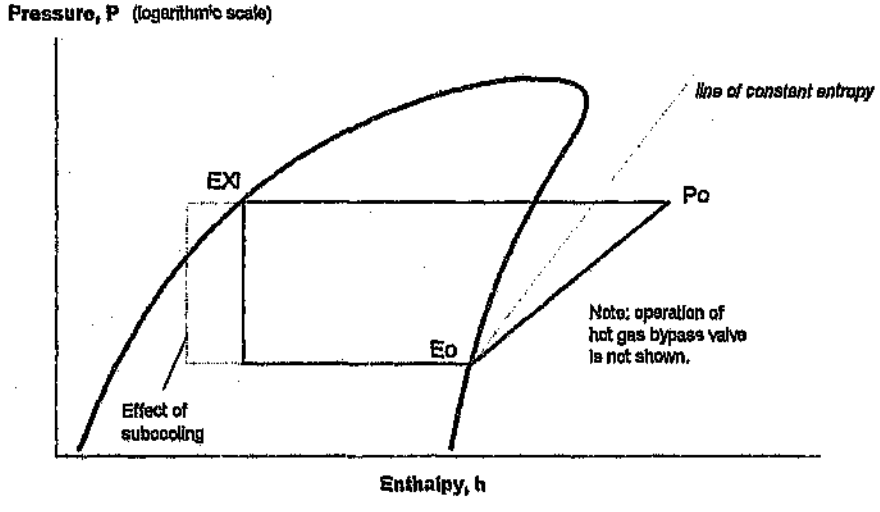

Figure 3.6 Packaged Water Chilling Machine with Single-Stage Centrifugal Compressor: Oil Cooling by Water

(a) either from the evaporator water lines *within the evaporator's thermodynamic boundary,*[6] in which case the oil cooling load is represented by $Q_{(w)E\{OC\}}$ (following the nomenclature for the generalised machine, except that the subscript *{VCB}* is replaced by the more specific *{OC}*, denoting the oil cooler). Of course, the oil cooler could also obtain its water from the condenser water lines, in which case the oil cooling load would be represented by $Q_{(w)C\{OC\}}$;

(b) or from outside the machine boundary, in which case the oil cooling load is represented by $Q_{(w)OC\{MB\}}$.

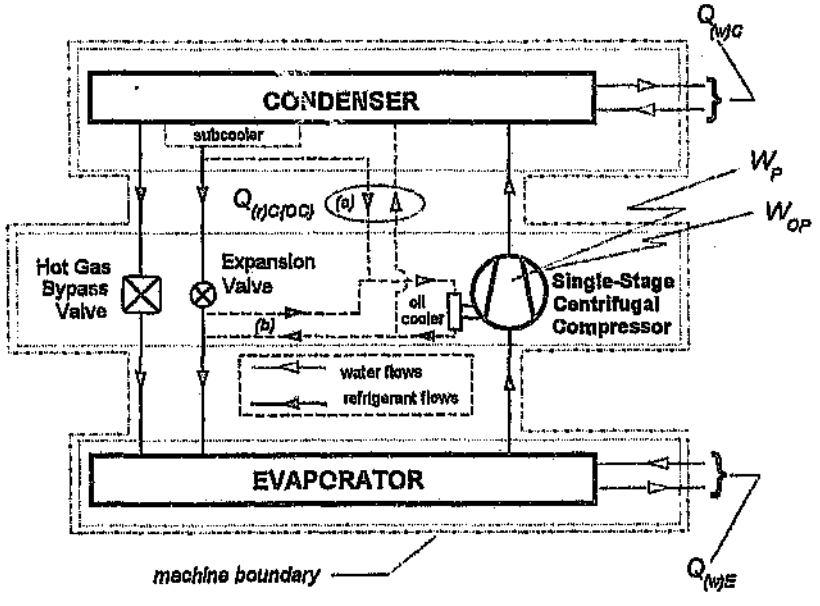

Figure 3.6a Packaged Water Chilling Machine with Single-Stage Centrifugal Compressor: Oil Cooling by Refrigerant

On the other hand, if the oil cooler is an oil-to-refrigerant type, Figure 3.6a shows two customary ways of it obtaining its refrigerant:

---

[6] That is, *between* the evaporator and the points where the temperatures of the water entering and leaving the evaporator are measured.

(a) either from a branch connection in the line from the condenser to the expansion valve, and returning this refrigerant in a separate line to the condenser. The thermosyphon effect circulates refrigerant through the oil cooler. The oil cooling load is represented by $Q_{(r)C(OC)}$. Of course, the oil cooler could also obtain its refrigerant from the evaporator in a similar way, in which case the oil cooling load would be represented by $Q_{(r)E(OC)}$;

(b) or from a branch connection in the line from the expansion valve to the evaporator, and returning this refrigerant into the same line.

Overall Energy Balance

A single water stream passes through the evaporator, and a corresponding single heat flow $Q_{(w)E}$ passes from this stream into the evaporator. The condenser also has a single heat-removing water stream passing through it, and the corresponding heat flow is $Q_{(w)C}$ (which is negative, as this heat is passing from the condenser into the water). The mechanical power inputs to the vapour-compression block are those to the compressor, W_P, and to its oil pump, W_{OP}. From (3-7d), the overall energy balance of this machine is accordingly

$$Q_{(w)E} + W_P + W_{OP} + Q_{(w)OC(Ms)} + Q_{(w)C} \cong 0 \qquad (3\text{-}12)$$

As for the generalised machine, therefore, the effect, represented by $Q_{(w)OC(Ms)}$, of any oil-to water compressor oil coolers transferring heat outside the machine boundary must be taken into account.

Coefficient of Performance

The COP for this single-stage machine is, from (3-11a),

$$COP = \frac{Q_{(w)E}}{W_P + W_{OP}} \qquad (3\text{-}13a)$$

From (3-11b), as shown in Appendix 1, the COP may be expressed as

$$COP = \frac{m_{(r)EX}(h_{Eo} - h_{EXI}) - m_{(r)HG}(h_{HGI} - h_{Eo}) - Q_{(fl)E(OC)}}{(m_{(r)EX} + m_{(r)HG})(h_{Po} - h_{Eo}) + Q_{(fl)E(OC)} + Q_{(fl)C(OC)} - Q_{(fl)OC(Ms)}} \qquad (3\text{-}13b)$$

where $m_{(r)EX}$ and $m_{(r)HG}$ are the refrigerant mass flows through the expansion and hot gas bypass valves; and h_{Eo}, h_{Po}, h_{EXI} and h_{HGI} are the refrigerant enthalpies at the evaporator outlet, compressor outlet, expansion valve inlet and hot gas bypass valve inlet. $Q_{(fl)E(OC)}$, $Q_{(fl)C(OC)}$ and $Q_{(fl)OC(Ms)}$ are the heat loads borne by the oil cooling fluid - whether this be water or refrigerant - circulating between the oil cooler and the evaporator, condenser or a source outside the machine boundary. Analogously to the generalised machine, only one of these terms, the one corresponding to the cooling fluid circuit of the oil cooler, will be non-zero.

As for the generalised machine, the refrigerant-circuit COP is obtained from (3-13b) by neglecting all terms not involving refrigerant mass flows and enthalpies:

$$COP_{(r)} = \frac{m_{(r)EX}(h_{Eo} - h_{EXI}) - m_{(r)HG}(h_{HGI} - h_{Eo})}{(m_{(r)EX} + m_{(r)HG})(h_{Po} - h_{Eo})}$$

or, dividing numerator and denominator by the main refrigerant flow $m_{(r)EX}$,

$$COP_{(r)} = \frac{(h_{Eo} - h_{EXI}) - \frac{m_{(r)HG}}{m_{(r)EX}} \cdot (h_{HGI} - h_{Eo})}{\left(1 + \frac{m_{(r)HG}}{m_{(r)EX}}\right) \cdot (h_{Po} - h_{Eo})} \qquad (3\text{-}14a)$$

If, as in normal operation, there is no flow through the hot gas bypass valve, then $m_{(r)HG} = 0$ and $COP_{(r)}$ simplifies to

$$COP_{(r)} = \frac{h_{Eo} - h_{EXI}}{h_{Po} - h_{Eo}} \qquad (3\text{-}14b)$$

which is the familiar formula, identical to (3-5), for a single-stage vapour-compression machine. It is a sole function of refrigerant enthalpies, and therefore especially convenient to use, as these enthalpies can normally be determined easily from measurements of pressure and temperature at the appropriate points in the refrigerant circuit.[7] *This formula is only valid, though, when flow through the hot gas bypass valve is zero.* Otherwise, formula (3-14a) applies. Furthermore, the greater the relative magnitude of the oil cooling load - no matter which term $Q_{(fl)E(oc)}$, $Q_{(fl)D(oc)}$ or $Q_{(fl)OC(Mo)}$ represents this load - the more the refrigerant-circuit COP exceeds the actual COP, as seen from (3-13b).[8]

Two important points regarding the refrigerant-circuit COP of this machine therefore emerge.

A. If hot gas is being bypassed, $COP_{(r)}$ is no longer a sole function of refrigerant enthalpies, but also a function of the ratio $m_{(r)HG}/m_{(r)EX}$, as seen from (3-14a). In general, if auxiliary refrigerant flows such as hot gas bypass occur in any machine, the refrigerant-circuit COP will be a function of both refrigerant enthalpies and the ratios of these auxiliary flows to the main refrigerant flow. As discussed in Chapter 5, the refrigerant-circuit COP then cannot be determined

---

[7] Provided that the refrigerant circuit is uncontaminated and in good order, as explained in Chapter 5.

[8] In (3-13b), $Q_{(fl)E(oc)}$ and $Q_{(fl)D(oc)}$ are positive if non-zero, and $Q_{(fl)OC(Mo)}$ is negative if non-zero; so whichever term is non-zero, the effect is to reduce the actual COP.

unless sensors to measure refrigerant flows are fitted, which is seldom the case.

B. Due to the effect of the compressor oil cooler, $COP_{(r)}$ is greater than the actual COP and will thus over-estimate it. Chapter 5 shows how the refrigerant-circuit COP may be corrected for such effects to best reflect the actual COP.

Beginning with the centrifugal compressor itself, the components of this single-stage packaged machine will now be described in detail.

3.2.2 The Centrifugal Compressor

Components of a Single-Stage Centrifugal Compressor

A single-stage centrifugal compressor is illustrated in cross-section in Figure 3.7. It consists of the inlet conduit to the impeller; the rotating impeller itself to transfer energy to the vapour; the diffuser to transform kinetic energy to pressure energy; the return volute; and the mechanical (labyrinth) seals between moving and stationary parts.

The suction flow enters the rotating element, or impeller, in the axial direction and is discharged radially at a higher velocity. This dynamic velocity head is then converted to static head, or pressure, through a diffusion process, which generally begins within the impeller and ends in the radial diffuser and volute outboard of the impeller (ASHRAE, 1992).

The suction vapour generally passes through a set of adjustable inlet guide vanes ("IGV" in the figure), or an external suction damper, before entering the impeller. The vanes or suction damper are used for capacity control, as will be described later. The high-velocity vapour discharging from the impeller enters the radial diffuser, which can be vaned or vaneless. Vaned diffusers are typically used in compressors designed to produce high heads; they decelerate the flow in less distance and with less inefficiency, or loss (Casey and Marty, 1986). These vanes are

generally fixed, but they can be adjustable. Adjustable diffuser vanes can be used for capacity modulation either in lieu of or in conjunction with the inlet guide vanes. The flow can diffuse in the three parts of the diffuser - the vaneless space immediately adjacent to the impeller, the diffuser vanes (where these exist), and the return channel or volute. Hence, in general, the fluid decelerates more in the diffuser than in the impeller (Casey and Marty, 1986).

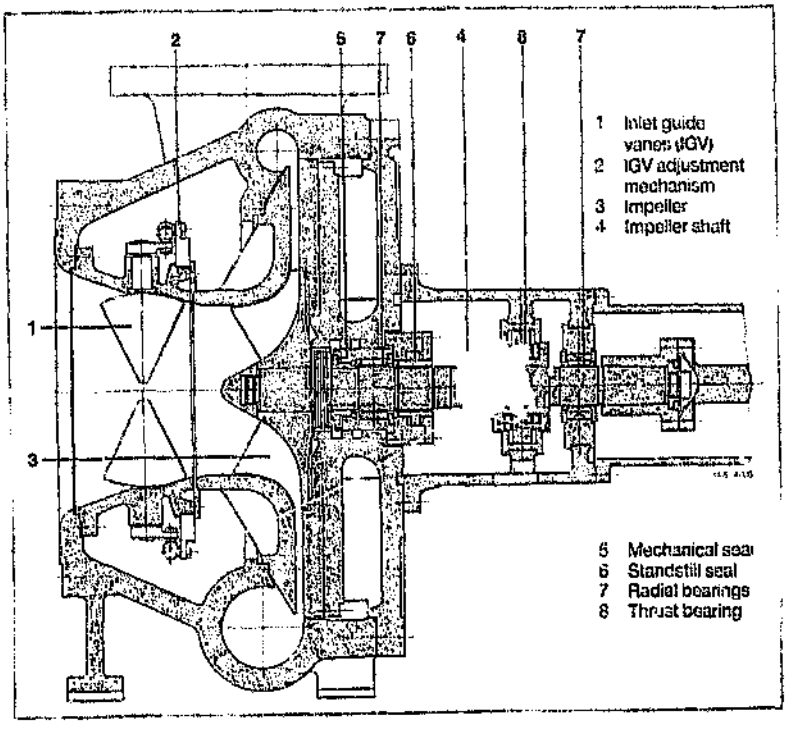

Figure 3.7 Single Stage Centrifugal Compressor[9]

The actual flow process through a centrifugal compressor stage is complex, being three-dimensional, turbulent and unsteady. For many

[9] With acknowledgements to Sulzer Brothers Ltd, Switzerland (Brochure e/25.47.05.40 - X.85-50 of Process Engineering and Refrigeration Division).

practical purposes, however, basic one-dimensional theory is sufficient for obtaining the essential relationships governing the performance of a centrifugal compressor stage (Casey and Marty, 1986).

Basic One-Dimensional Theory

All the energy transfer takes place in the impeller, due to an interchange of angular momentum. The relation between the velocities at the outlet (tip) of the impeller is shown in Figure 3.8. The subscripts 1, 2 and *o* denote the impeller inlet, the impeller outlet and the compressor stage outlet respectively. The fluid leaving the impeller has velocity $v_{[rel]2}$ relative to the impeller, and absolute velocity v_2 resulting from $v_{[rel]2}$ and U_2, the peripheral velocity of the outer circumference of the impeller. The tangential component of v_2 is $v_{[tng]2}$.

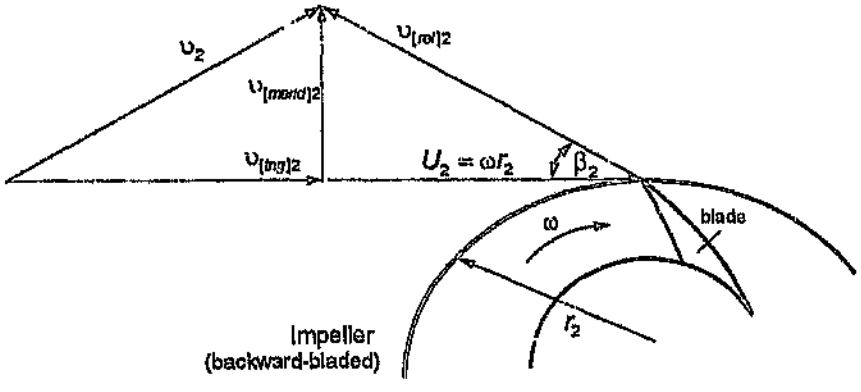

Figure 3.8 Velocity Diagram at Tip of Impeller of Centrifugal Compressor Stage

It is assumed that the fluid approaches the inlet of the impeller purely axially, with no moment of momentum. Hence it follows readily that for a mass flow-rate $m_{(r)}$ of fluid, the power required to turn the impeller is

$W = m_{(r)} v_{[rel]2} U_2$. Denoting the angle between $v_{[rel]2}$ and U_2 as β_2, it is hence shown (see, for example, Gosney, 1982 : 326) that the specific work input per unit mass of fluid, known as the *head* and expressed as enthalpy rise Δh[10] is

$$\frac{W}{m_{(r)}} = \Delta h = U_2\left(U_2 - v_{[merid]2}\cot\beta_2\right) \qquad (3\text{-}15)$$

where $v_{[merid]2}$, shown in Figure 3.8, is the meridional component of v_2.

In reality, as is well known (e.g. Gosney, 1982 : 328), the true fluid angle β is less than β_2, and $v_{[merid]2}$ is not constant over the outlet area of the impeller. (3-15), suitably corrected for these realities, gives the work *absorbed* by the impeller, but does not indicate how much pressure rise is produced. This depends on the inefficiencies present in the machine. In this regard, where the velocities at the stage inlet and outlet are equal, it can also be shown (Casey and Marty, 1986) that the enthalpy rise may be expressed in terms of the absolute velocities v of the vapour at impeller inlet, impeller outlet, and compressor stage outlet, and the velocities $v_{[rel]}$ relative to the impeller at its inlet and outlet:

$$\Delta h = \left\{\left[1-\left(\frac{U_1}{U_2}\right)^2\right]+\left(\frac{v_{[rel]1}}{U_2}\right)^2\left[1-\left(\frac{v_{[rel]2}}{v_{[rel]1}}\right)^2\right]+\left(\frac{v_2}{U_2}\right)^2\left[1-\left(\frac{v_o}{v_2}\right)^2\right]\right\}\Big/2 \qquad (3\text{-}16)$$

The first term in square brackets represents the increase in static pressure due to centrifugal force; this occurs totally without loss (i.e. inefficiency), and accounts for about half the work input in a typical stage. The second term represents the change in relative kinetic energy - that is,

---

[10] Strictly speaking, this is the rise of *stagnation* enthalpy, i.e. the sum of enthalpy and kinetic energy. However, in most compressors the kinetic energies at inlet and outlet are small relative to the enthalpies, and so the head is expressed sufficiently accurately by the difference Δh of static enthalpies.

internal diffusion - in the *impeller* flow passages, where some of the relative velocity is transformed into static pressure. This accounts for about one-fifth of the work input. The third term represents the diffusion in the *diffuser,* and accounts typically for about one-third of the work input (Casey and Marty, 1986).

Impellers may be of the closed or open type (that in Figure 3.7 is the open type), and may have forward-curved, radial, or backward-curved blades, depending on the angle β_2 between the tip of the blade and the tangent to the outlet circumference of the impeller, as shown in Figure 3.9.

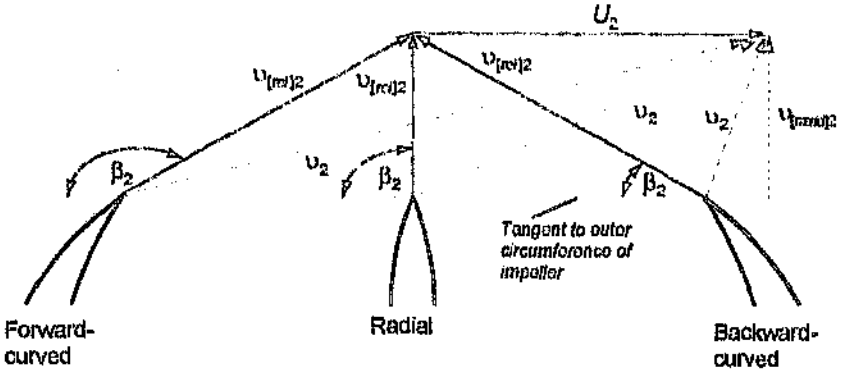

Figure 3.9 Velocity Diagrams of Impellers With Forward-Curved, Radial, And Backward-Curved Blades

In (3-15), the meridional component $v_{[mer]2}$ is proportional to the volume flow-rate through the impeller. The magnitude of the outlet blade angle β_2 therefore influences the head developed. It also influences the general shape of the head-volumetric flow-rate curve. From (3-15), if $\beta_2 = 90°$ (radial blades), $\cot\beta_2 = 0$, and the head is theoretically constant for all flow-rates. When $\beta_2 > 90°$ (forward-curved blades), $\cot\beta_2$ is negative, and the head increases with increasing flow-rates. When $\beta_2 < 90°$,

(backward-curved blades), $\cot\beta_2$ is positive, and the head reduces with increasing flow-rates. The head of (3-15) is then maximum when the flow-rate is zero.

From Figure 3.9 it will be noted that the value of v_2, the absolute velocity of the vapour leaving the impeller, is minimum for backward-curved impeller blades. This means that the least diffusion has to take place in the diffuser, i.e. the diffuser has the minimum task. This is important when considering diffusion losses throughout the range of operation of a compressor. At design conditions, losses in the diffuser are minimised by suiting the shape and angle of the diverging diffuser passages to the design conditions and flow-rate. At all other conditions, the diffusion process is less efficient, resulting in more losses. Where the flow-rate and pressures within the compressor vary widely, as is the case in a water chilling machine with a widely varying duty, it is preferable to achieve the maximum possible static pressure rise in the impeller and rely on diffusion to the minimum. For this reason, centrifugal compressors in water chilling machines generally have backward-curved impeller blades, which impart the minimum net kinetic energy increase and require the least pressure rise in the diffuser (Gosney, 1982), and consequently suffer less from diffusion losses under off-design conditions.

Losses in a Centrifugal Compressor Stage

There are several sources of aerodynamic loss in the impeller and diffuser. A large proportion of the losses are due to friction. Frictional losses are proportional to the square of the mean velocity and inversely proportional to the hydraulic diameter of the flow channels. *Diffusion losses* (losses due to imperfect diffusion) occur in both impeller and diffuser. There is a limit to the deceleration that can take place without the flow becoming unstable, separating, eddying, and hence large losses occurring. To avoid such losses, the relative fluid velocity at the exit of

the impeller cannot be less than about 60 per cent of that at the inlet (Casey and Marty, 1986).

Shock losses are due to entropy increase across the shock waves that form in the impeller and diffuser channels when the inlet velocities approach sonic conditions. The local Mach number at the inlet to the impeller blades, and the blade geometry are the main influences. *Incidence losses* arise at off-design flow conditions, where the direction of the inlet flow is not equal to the inlet angle of the blades in the impeller or diffuser. The resulting deflection of the flow causes both additional diffusion and additional shock losses (Casey and Marty, 1986).

Other losses are not of aerodynamic origin. They include the disc friction of the hub and shroud discs, and leakage losses.

Influence of Losses on Characteristic Curve

These losses modify the ideal relationship of head to volume flow-rate of a centrifugal compressor stage. Shown in Figure 3.10 is how the shock and frictional losses do this for an impeller with backward-curved blades.

The resulting, typical head and efficiency curves for a single-stage centrifugal compressor are shown in Figure 3.11. Peak efficiency obviously occurs at the point of minimum losses, close to where the flow is perfectly matched to the blade angles and profiles of the impeller and diffuser, and there are thus minimum shock and incidence losses. *Peak efficiency thus does not occur at minimum head.* For example, if the volumetric flow-rate reduces below that at peak efficiency, efficiency decreases and net power input *rises* if the rises in power due to the decrease in efficiency and increase in head exceed the fall in power due to the decrease in volumetric flow-rate. This is the underlying reason why machines employing centrifugal compressors sometimes consume more power at low than at moderate part-duties, and hence why there is

sometimes no power saving when their duties reduce below moderate part-duties, as discussed and illustrated in Chapter 6.

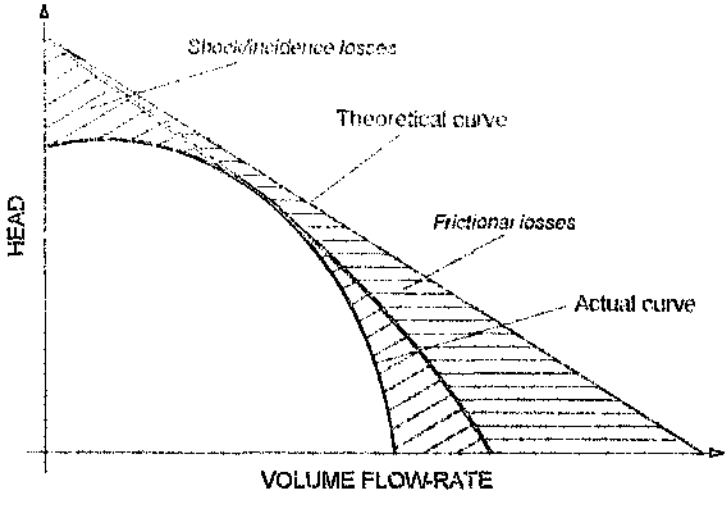

Figure 3.10 Losses In A Centrifugal Compressor Stage with Backward-Curved Impeller Blades (Stepanoff, 1955)

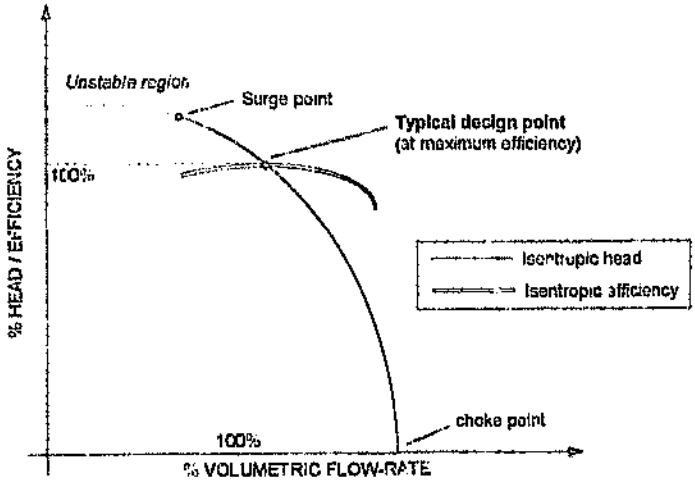

Figure 3.11 Typical Head and Efficiency Curves for Single-Stage Centrifugal Compressor

Strictly, a characteristic curve such as in Figure 3.11, where the coordinates are head and intake volume flow-rate, applies to only one set of conditions at the compressor inlet. This is because the shape of this curve depends not only on compressor construction and speed, but also on the properties of the refrigerant and the *rotational* Reynolds and Mach numbers[11] of refrigerant flow. To provide maximum versatility in predicting compressor performance, compressor designers use generalised correlations based on these rotational numbers and three other non-dimensional parameters: *flow coefficient* ϕ; isentropic or polytropic *head coefficient* ψ; and *work coefficient* μ (ASHRAE, 1992; Gosney, 1982; Casey and Marty, 1986, etc.). These coefficients are given by

$$\phi \equiv m_{(r)} v_i / \left(U_2 D_2^2\right) \qquad \mu \equiv \Delta h / U_2^2$$
$$\psi_{\text{isentropic or polytropic}} \equiv (\text{isentropic or polytropic head}) / U_2^2 \tag{3-17}$$

However, for compressors running at a given speed with the same refrigerant vapour:

- the rotational Reynolds and Mach numbers vary little (Gosney, 1982 : 334), so the generalised characteristics are then plots of μ, ψ and efficiency against ϕ;
- from (3-17), the flow, head and work coefficients above amount to inlet volume flow-rate and head multiplied by constants.

In this thesis, therefore, where the compressors considered always run at the same speed with the same refrigerant vapour, the coordinates of head and volume flow-rate can be and are used because they are more convenient.

---

[11] So called because they are based not on the velocity of the fluid but on that of the

Choke and Surge

The capacity (volumetric flow-rate) of a centrifugal compress
a minimum defined by the *surge point*, and a maximum defin
choke point, both shown in Figure 3.11. Depending on the
compressor, the surge point may occur anywhere between 6
cent of the design flow-rate, and typically at about 120 per c
design head. Choke typically occurs at about 120 per cent
flow-rate. For practical applications, a wide margin between
surge is required (Casey and Marty, 1986).

If the mass flow through a stage is steadily increased, the sp
is eventually reached at some point in the flow passages. N
increase in flow is then possible, and the stage is said to be
Another commonly used term for this phenomenon is stonew
represents the maximum capacity of an impeller (ASHRAE,
Choking can occur anywhere in the flow passages - in the in
impeller, in the rotating impeller passages, or in the diffuser
passages. In compressor stages with well-matched vaned d
choking usually occurs in the diffuser passages (Casey and

If the mass flow through a stage is steadily reduced, the flow
down at some point and become unstable. Two types of ins
occur: surge and rotating stall.

The most serious type of unstable flow is surge. It occurs w
through the stage reduces to the point where the head appr
maximum of which the machine is capable; this is the *surge*
Figure 3.11. The steady flow through the impeller then brea
flow through the stage changes violently at a low frequency,
increased noise and vibration, as it oscillates back and forth
unstable region, around the maximum head, shown in Figur
frequency of surge is mainly a function of the geometry of th
machine (inlet and outlet volume) rather than rotational spee

practical applications, the operating point reaching a horizontal portion of a characteristic curve in any stage of a multi-stage compressor is sufficient to cause surge (Casey and Marty, 1986). Surging can be distinguished from other kinds of noise and vibration by the fact that its flow reversals alternately load and unload the driving motor; motor current varies markedly during surging (ASHRAE, 1992).

The second type of instability, rotating stall, is characterised by small pressure fluctuations, but a steady *mean* mass flow through the machine. "Stall cells" (areas of separated flow) develop around the compressor *stage* annulus, and flow is unsteady here. Stall produces a roaring noise at a frequency determined by the number of stall cells formed and impeller running speed. In contrast to surge, the driver load is steady (ASHRAE, 1992). Stall is different from surge, but a component stalling can change the pressure-rise characteristic of the stage, and trigger surge (Casey and Marty, 1986). There can be various phases in the breakdown of the ideal flow patterns through the compressor before outright surge with its full flow reversal and pressure swings is experienced (Lucas, 1989).

Polytropic and Isentropic Analysis and Efficiency

Compression in a centrifugal compressor stage is effectively adiabatic, as the through-flow of vapour is very large in relation to the areas available for heat transfer. However, the process does require high fluid velocities. High gradients of velocity and shear stresses thus occur at the impeller surfaces, these being the boundaries where energy in the form of work is transferred to the vapour. Not only, therefore, has work to be done against the normal pressure forces in the fluid; considerably extra work has to be done against the internal frictional forces arising from viscous shear in this fluid. Put another way, this extra work is necessary because of the inefficiency of work transfer to the fluid, and constitutes an internal irreversibility. The *polytropic efficiency* η_{pol} of such a compression process is a measure of this extra work required: it is the ratio of the

reversible work input $\int_{P_i}^{P_o} v\,dP$, also known as the *polytropic head*, to the actual enthalpy rise:[12]

$$\eta_{pol} = \frac{1}{h_o - h_i} \cdot \int_{P_i}^{P_o} v\,dP \qquad (3\text{-}18)$$

In contrast to isentropic efficiency, as Casey and Marty (1986) and Gosney (1982) point out, polytropic efficiency is thus a more real and fundamental measure of the efficiency of the centrifugal compression process. It compares the *ideal*, minimum enthalpy rise $\int_{P_i}^{P_o} v\,dP$ (which is the useful work input converted into pressure rise) *in the actual process* to the actual enthalpy rise *in the same actual process*. In contrast, isentropic efficiency compares the actual enthalpy rise in the actual process to an ideal, but *hypothetical, isentropic* process of enthalpy rise $(h_o - h_i)\big|_s$.

Polytropic efficiency thus relates more closely than isentropic efficiency to the actual compression process. The advantage thereof becomes clear when considering the overall efficiency of multi-stage compressors. Where each stage of a multi-stage compressor has the same polytropic efficiency, the entire compressor also has this efficiency. Where each stage has the same isentropic efficiency, though, the isentropic efficiency of the entire compressor is less than that of the stages. This is because the non-useful work input wasted in overcoming losses in each stage causes the specific volume of the fluid to rise, and thus more work input is

---

[12] In thermodynamic performance calculations for centrifugal compressors, the general definition of the polytropic path for a real gas is that on which "the ratio of the reversible work input to the enthalpy rise is constant" (Huntington, 1985 : 872, quoting Schultz, J M, "The Polytropic Analysis of Centrifugal Compressors", ASME Journal of Engineering for Power, Jan. 1962, pp. 69-82). The term "polytropic efficiency" originates from the fact that *for an ideal gas*, such a path is polytropic, i.e. conforming to the relation Pv^n = constant (see, for example, Rogers and Mayhew, 1967 : 448).

necessary in the succeeding stage to produce the required rise in pressure (Gosney, 1982; Casey and Marty, 1985).

The generalised, non-dimensional correlations of compressor performance mentioned earlier are generally more accurate when polytropic, rather than isentropic, coefficients and efficiency are used (see, for example, Gosney, 1982). However, the disadvantage of polytropic efficiency is that $\int_{P_1}^{P_2} v\,dP$ depends not only on the end states, but also on the path of the compression process. The integral can seldom be accurately evaluated, and is generally approximated by assuming that the fluid behaves as an ideal gas. This assumption, even though widely practised, is not strictly correct (Gosney, 1982; Huntington, 1985).[13] On the other hand, isentropic efficiency, in spite of its shortcomings, depends only on the end states of the process and hence can be determined from tabulated thermodynamic properties of refrigerants. In view of:

- the consequent ease of use of isentropic head and efficiency;
- the iteration necessary in calculations involving polytropic head and efficiency to account for the non-ideal behaviour of refrigerants of high molar mass such as the halocarbons (Gosney, 1982 : 341);
- compressor stages always being analysed individually in this thesis, never in combination;

the concepts of isentropic, rather than polytropic, head and efficiency are employed in this thesis, and the non-optimal correlation of performance introduced thereby is acknowledged. The conclusions of the thesis are not affected thereby.

---

[13] Although it works well for refrigerants with simple, light molecules such as ammonia (Gosney, 1982 : 320).

The peak isentropic efficiency of a centrifugal compressor stage varies from about 0,62 to about 0,83, depending on the application (ASHRAE, 1992).

Regulation and Performance under Part-Duty Conditions

The operating point of an unregulated, single compressor stage is confined to its characteristic curve as in Figure 3.11, and this is too inflexible for many process applications, including water chilling. Some capacity-regulating mechanism is needed which will give the compressor wide-ranging ability to operate under off-design conditions. Three methods of regulation are possible: variable speed; or, at constant speed, variable inlet guide vanes or variable diffuser vanes. The choice of the most suitable method of capacity regulation depends on how the required pressure rise and volume flow-rate alter at part-duties.

A comparison of the operating characteristics of a single-stage machine regulated by variable speed, variable inlet guide vanes and variable diffuser vanes is given in Figure 3.12.

Variable-speed regulation allows a compressor to deliver efficiently at outlet pressures less than the design value. Maximum polytropic head, or alternatively pressure rise, that can be developed before surge falls off rapidly with decreasing speed, as seen in Figure 3.12. Volumetric flow-rate varies approximately linearly with speed, and head developed as the square of the speed (Casey and Marty, 1986). For example, a 50 per cent reduction in compressor speed will result in a 50 per cent reduction in volumetric flow-rate; however, the available pressure rise from the compressor will be 25 per cent of its value at full speed. In water chilling applications, such a drastic fall-off of required pressure rise (corresponding to lift) with reducing load is unlikely to be encountered. If the actual pressure rise required under part-duty conditions is greater than the compressor is able to develop at reduced speed, the compressor will surge. Thus, for water chilling applications, variable speed alone is

not a suitable method of regulating compressor capacity. In some water chilling machines on South African mines, though, simple two-step speed variation, in the form of a two-speed gearbox, is used in conjunction with variable inlet guide vanes, discussed immediately below; the lower speed gives better efficiency at lower part-duties (van der Walt, 1979).

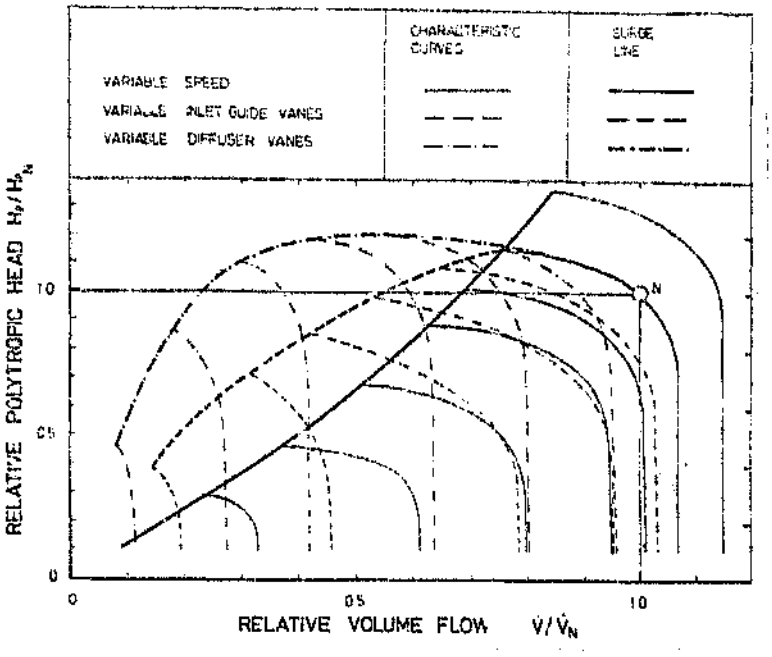

Figure 3.12 Comparison of Operating Characteristics of a Single-Stage Centrifugal Compressor with Variable Speed; Variable Inlet Guide Vanes; and Variable Diffuser Vanes (Casey and Marty, 1986)

Compressors driven at constant speed may be equipped with variable inlet guide vanes. Setting these vanes to pre-rotate the entering flow in the direction of rotation reduces the relative velocity of the fluid at the impeller inlet, and hence the work input to the impeller. Hence a new compressor performance curve, with lower head, results without any change in speed. Controlled positioning of the vanes can be accomplished by pneumatic, electrical, or hydraulic means (ASHRAE, 1992). At low levels of pre-rotation, the guide vanes are very efficient;

they improve the efficiency of the stage by reducing the aerodynamic loading of the impeller. At moderate levels of pre-rotation, the guide vanes introduce significant friction into the fluid flow, and hence the efficiency decreases. At very high levels of pre-rotation, efficiency decreases markedly for the same reason. Variable inlet guide vanes are particularly suitable for machines where required pressure rise decreases with decreasing volumetric flow-rate - that is, for the reducing load, reducing lift type of machine duty. For such applications, they provide a wide control range and very high part-load efficiencies (Casey and Marty, 1986). Variable inlet guide vanes are used in almost all centrifugal machines on South African gold mines, and on all such machines considered in subsequent chapters of this thesis.

A constant-speed machine may also be equipped with variable diffuser vanes. The position of these vanes has no effect on the work input of the impeller; rather, the *matching* between the impeller and the diffuser is altered by the changing inlet angle and throat area of the diffuser vanes. Variable diffuser vanes are particularly suitable for efficient regulation of machines where required pressure rise remains substantially constant with changes in volumetric flow-rate - that is, for the reducing load, constant lift type of machine duty. (As seen in Figure 3.12, the maximum polytropic head that can be developed before surge does not decrease over most of the operating range.) For such duties, a wide operating range is afforded, with some loss in efficiency at part-duty (Casey and Marty, 1986).

Other compressor capacity control methods are movable diffuser walls, impeller throttling sleeves, and combinations of these with variable inlet guide vanes and variable speed (ASHRAE, 1992). Some machines on South African gold mines have both variable inlet guide vanes and variable diffuser vanes. Alternatively, as mentioned above, variable inlet guide vanes may be combined with two-step speed variation.

Where the pressure rise and flow-rate required under part-duty are outside the range achievable by these regulating methods, the only recourse is to artificially increase the flow-rate through the compressor by an amount sufficient to bring the compressor's operating point back into this achievable range. This increase in flow is achieved by opening the *hot gas bypass valve* in Figures 3.6 and 3.6a, which discharges uncondensed, high-pressure vapour to low-pressure conditions, generally into the evaporating liquid refrigerant to cool the gas being bypassed to inlet temperature (Casey and Marty, 1986). This is an energy-wasteful form of capacity regulation, though, as it increases compression work without any increase in refrigerating load, and thus decreases the COP.

Lubrication

Like motors and gears, the bearings and lubrication systems of centrifugal compressors can be internal or external, depending on whether or not they operate in refrigerant atmospheres. Most air-conditioning and refrigerating compressors have internal bearings, as shown in Figure 3.7. The oil pumps are often internal, driven either by an internal motor or the compressor shaft; in the latter case, an auxiliary oil pump is provided for starting and backup service (ASHRAE, 1992).

The oil circuits of most compressors are exposed to the refrigerant vapour being compressed. Most refrigerants, notably the halocarbons, are soluble in lubricating oils, the extent increasing with refrigerant pressure and decreasing with oil temperature. A compressor's oil may typically contain 20 per cent of refrigerant by mass during idle periods[14] and 5 per cent during normal operation. Thus refrigerant will come out of solution, causing the oil to foam, when the compressor is started. To prevent excessive foaming from cavitating the oil pump and thus starving the

[14] This is because the compressor's oil reservoir is generally exposed to suction pressure, which is higher during idle periods than during operation.

bearings, oil heaters are fitted to minimise refrigerant solubility in oil during idle periods (ASHRAE, 1992).

Oil droplets also become entrained in the refrigerant vapour being compressed, and hence pass into the refrigerant circuit and dissolve in the liquid refrigerant. The important effect of this is discussed below, in the section on the flooded shell-and-tube evaporator.

The thrust bearing shown in Figure 3.7 is the most important bearing in a centrifugal compressor. Thrust is present because the pressure behind an impeller exceeds the pressure at its inlet. In multi-stage machines, the thrust due to each impeller adds to the total thrust, unless some impellers are mounted backward. It is customary, unless this is done, to provide a balancing piston on the last impeller, with pressure on the piston thrusting in the opposite direction. Most of the heating in the lubricating oil occurs in the thrust bearing, due to viscous shear in the oil (ASHRAE, 1992).

Oil cooling load is small, typically between 1 and 3 per cent of compressor shaft power. Single or dual oil coolers usually use condenser water, chilled water, refrigerant or air as their cooling medium. Oil-to-water and oil-to-refrigerant models may be built into the compressor. Many oil coolers are mounted externally for easy serviceability (ASHRAE, 1992).

3.2.3 The Shell-and-Tube Evaporator

A diagram of a horizontal shell-and-tube evaporator, with water flowing through the tubes, is given in Figure 3.13 below. The refrigerant vaporises on the outside of the tubes, which are submerged in boiling liquid refrigerant. As noted in Section 3.1.4, the entering refrigerant, having passed through the expansion valve, is a low-temperature mixture of mostly liquid and some vapour; this is usually fed into the bottom of the shell through a distributor to ensure even distribution. As bubbles rise up through the inter-tube spaces, the liquid surrounding the tubes becomes increasingly bubbly (or foamy, if much oil is present).

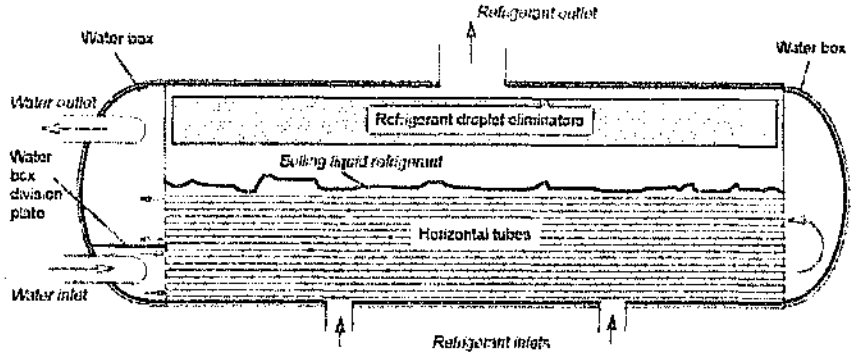

Figure 3.13 Flooded Shell-and-Tube Evaporator

Entrained refrigerant liquid droplets must be separated from the refrigerant vapour before this vapour leaves the evaporator. This is accomplished through a drop-out area between the top row of tubes and the refrigerant outlet, and by special droplet eliminators shown in the figure.

The evaporator in the figure has two passes; that is, water enters at the bottom and travels through the bottom rows of tubes on its first pass along the length of the evaporator. As shown, it then reverses direction and travels through the top rows on its second and final pass. *Division plates* in the water boxes at the ends of the evaporator route the water from pass to pass. The size of tubes, amount of tubes, and amount of passes are generally selected to maintain the water velocity typically between 1 and 3 m/s. Velocities above 3 m/s cause tube erosion and wear if the water contains abrasive or fouling substances.[15] Minimum water velocity is governed by the need to maintain turbulent flow to ensure good heat transfer.

[15] Unless the tubes are of an especially durable material such as titanium, which is the case in some machines.

The external surfaces of the tubes are generally finned or specially formed in other ways to promote boiling of the refrigerant and hence enhance heat transfer thereto.

Refrigerant pressure drop in this type of evaporator is small, as the cross-sectional areas through which the refrigerant flows are large, and refrigerant velocities are low. Hence the refrigerant temperature is virtually constant and is denoted by $t_{(r)E}$. Inlet and outlet water temperatures are denoted by $t_{(w)Ei}$ and $t_{(w)Eo}$ respectively. Heat transfer Q_E in this evaporator can be expressed by the well-known steady-state relationship:

$$Q_E = UA_E \cdot LMTD_E \tag{3-19}$$

where $LMTD_E$ is the logarithmic-mean temperature difference between the water and the refrigerant, and UA_E is the overall thermal conductance of the evaporator. For all heat exchangers, the thermodynamic efficiency of a given heat transfer rate Q is maximised if the finite, mean temperature difference by which this transfer occurs is minimised. However, this requires the UA to be maximised, and since the heat exchanger provides this UA, its cost is increased. There is thus always an economic trade-off between UA and the mean temperature difference. For a shell-and-tube evaporator exchanger where, as here, the refrigerant temperature is assumed constant, the logarithmic-mean temperature difference $LMTD$ is given by

$$LMTD = \frac{\left(t_{(w)o} - t_{(r)}\right) - \left(t_{(w)i} - t_{(r)}\right)}{\ln\left(\frac{t_{(w)o} - t_{(r)}}{t_{(w)i} - t_{(r)}}\right)} = \frac{t_{(w)o} - t_{(w)i}}{\ln\left(\frac{t_{(w)o} - t_{(r)}}{t_{(w)i} - t_{(r)}}\right)} \tag{3-20}$$

and UA by the well-known formula (for example, Burrows, 1982 : 624)

$$\frac{1}{UA} = \frac{1}{h'_{[w]}A_{T[w]}} + \frac{1}{h'_f A_{T[w]}} + \frac{y_T}{k_T \bar{A}_T} + \frac{1}{h'_{[r]}A_{T[r]}} \qquad (3\text{-}21)$$

The four terms on the right-hand side of (3-21) represent the resistances to heat transfer due to the water, water-side fouling, tube material, and refrigerant respectively. $A_{T[w]}$ and $A_{T[r]}$ are the total tube surface areas in contact with the water and refrigerant; $h'_{[w]}$ is the coefficient of heat transfer to or from water by forced convection; $h'_{[r]E}$ is the coefficient of heat transfer to or from the refrigerant; h'_f is the coefficient of heat transfer through the layer of water-side fouling on $A_{T[w]}$; y_T and k_T are the thickness and thermal conductivity of the tubes; and $\bar{A}_T$ is the logarithmic mean of $A_{T[w]}$ and $A_{T[r]}$.

Because of the small refrigerant pressure drop, this type of evaporator is relatively simple to model and analyse.[16] Another advantage is that it acts as its own refrigerant reservoir. Its main disadvantage is its inflexibility; there is no way of enlarging its capacity, even incrementally, except by installing another such evaporator in parallel. Also, the evaporating refrigerant temperature must be greater than 0°C, otherwise there is a risk of ice forming in tubes and bursting them. Generally, therefore, water is not chilled to a temperature lower than 3°C with this type of evaporator.

Water-Side Fouling

Most waters (and mine water is no exception) foul the water-side heat transfer surface. Water-side fouling increases overall resistance to heat transfer; thus either the LMTD must increase to maintain the same heat-transfer rate, or the heat-transfer rate is lowered. Fouling may result from sediment, biological growths, or corrosion products. Scale results from the deposition of chemicals from the water onto the warmer or colder walls

---

[16] Appendix 15 reviews steady-state modelling of this type of evaporator.

of the tubes. Obviously, control of scaling or corrosion by proper water treatment is important. It is also important that the tubes be accessible for mechanical cleaning.

Manufacturers' ratings are based on commercially clean equipment with an allowance for the possibility of water-side fouling. A *fouling factor* (i.e. a fouling allowance) is always incorporated in the design; this is a thermal resistance referenced to the water-side area of the heat-transfer surface. The water-side fouling factor is defined as $1/h_i$ in the second term on the right-hand side of (3-21).

Allowance for a specified fouling factor has a greater than proportionate effect on equipment size. The required increase in surface area means lower water velocity in the tubes. Consequently, the increase in heat-transferring surface required for the same performance is due to both the anticipated fouling resistance and the additional thermal resistance which results from lower water velocity (Starner, 1976). At the design stage, specifying the correct fouling factor to match actual conditions is therefore important. Other things being equal, if the actual fouling factor is higher than the design value, UA_E decreases and so, to maintain a given heat transfer rate, $LMTD_E$ must increase; the COP therefore decreases and power is wasted. Too high a design fouling factor, on the other hand, wastes heat-exchanger material. Moreover, as explained in Chapter 6, if the actual fouling factor is normally lower than the design value, the LMTD is decreased; but if compressor efficiency is also lower at this actual fouling factor, *power is not necessarily saved.*

Dissolved Oil in Refrigerant

As mentioned earlier, wherever the oil circuit of the compressor is exposed to the refrigerant vapour, oil droplets tend to become entrained in this vapour and thus pass into the refrigerant circuit and dissolve in the liquid refrigerant, *most of which is present in the evaporator.*

Unfortunately, dissolved oil affects the thermodynamic and thermophysical properties of the refrigerant, and thus changes it from a well-understood pure substance into a poorly understood solution whose properties may have altered significantly, depending on the oil type and concentration (ASHRAE, 1990; Hughes et al., 1982). What is known is that dissolved oil reduces refrigerating effect, because, for the same pressure, the boiling point of the solution rises and the oil holds a portion of the refrigerant in the liquid phase (Hughes et al., 1982). Other things being equal, to maintain the same refrigerant evaporating temperature (and hence the same LMTD and heat transfer rate), the pressure thus has to be lowered *below* the corresponding saturation pressure of the pure refrigerant. Thus the pressure rise required of the compressor increases, which increases the required power input and decreases the COP. Devices termed *oil eductors* or *rectifiers* are therefore fitted to such evaporators; these are designed to distil sufficient oil out of the refrigerant in the evaporator to maintain the oil concentration therein at a value which does not significantly affect refrigerant properties.

3.2.4 The Shell-and-Tube Condenser

Condensers transfer heat in two steps: sensible cooling in the vapour desuperheating stage and transfer of latent heat in the condensing stage. An additional step of sensible cooling occurs if the condensed refrigerant is subcooled before leaving the condenser. In the horizontal shell-and-tube condenser, the refrigerant condenses outside the tubes, and the heat-removing water circulates through the tubes in a single or multi-pass arrangement. A four-pass shell-and tube condenser is illustrated in Figure 3.14.

Refrigerant vapour enters the shell at the top and condenses on the outside of the tubes. The condensed refrigerant drains off the tubes and collects at the bottom of the shell, whence it drains out. It is important that the condenser be kept drained of condensed liquid; if such liquid

accumulates, it floods the bottom rows of tubes, so decreasing the surface area available for condensing the vapour. The overall thermal conductance of the condenser, and hence its performance, thus decreases.[17] Analogously to the shell-and-tube evaporator, the outside surfaces of the tubes are finned or formed specially to enhance condensation and promote drainage.

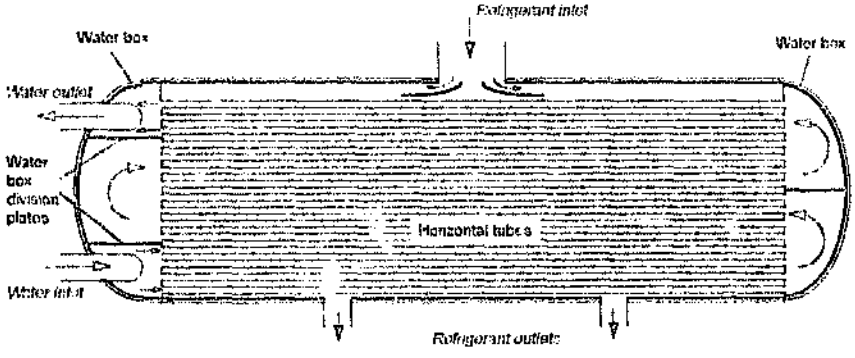

Figure 3.14 Horizontal Shell-and-Tube Condenser

As for the shell-and-tube evaporator, refrigerant pressure drop through this type of condenser is small, so (3-20) and (3-21) for the LMTD and UA apply. For water-side fouling, the same considerations as for the shell-and-tube evaporator apply.

Non-Condensable Gases in Refrigerant

If any non-condensable gases like air or water vapour are present as contaminants in the refrigerant circuit, they accumulate in the condenser, because the expansion valve (reviewed in Section 3.2.6 below) of the machine allows only refrigerant liquid to leave the condenser. Such

[17] For slight flooding, this decrease may not be significant, because there is a partial compensating effect: the bottom rows of tubes subcool the liquid flooding them. An example of this (Case Study A) is analysed in detail in Chapters 5 and 6.

accumulated gases, due to their partial pressure, raise the pressure in the condenser above the saturation pressure corresponding to the temperature at which the refrigerant condenses. They also raise this refrigerant condensing temperature somewhat because they form a heat transfer-resisting film over some of the outside surfaces of the tubes (ASHRAE, 1992). The increased condensing pressure increases the pressure rise required of the compressor, which again increases the required power input and decreases the COP. Hence it is important to keep the level of such non-condensable gases to a minimum. For low-pressure refrigerants such as R11 and R123, where the operating pressure in the evaporator is below atmospheric pressure, even slight inward leaks are a source of such gases; a purge system to continually and automatically expel them is thus essential (ASHRAE, 1992).

3.2.5 Subcoolers

Without special arrangements, a shell-and-tube condenser as in Figure 3.14 provides negligible subcooling of the condensed refrigerant liquid. Where a specific amount of subcooling is required, it may be obtained by submerging the lowest rows of tubes in the condensed liquid, in which case heat is transferred principally by natural convection (ASHRAE, 1992). Subcooling performance can be improved by enclosing these tubes in a separate compartment within the condenser, to obtain the benefits of heat transfer by forced convection. If the condenser is multi-pass, the subcooling tubes should be included in the first pass to gain exposure to the coolest water (ASHRAE, 1992). Alternatively, an altogether separate shell-and-tube subcooler may be used, such as in Figure 3.15 in which the baffle plates achieve counterflow of the refrigerant liquid and water.

Subcooling benefits are achieved at the expense of the additional heat-exchanging surface and refrigerant charge required. An optimum design should be based on these opposing factors (ASHRAE, 1992).

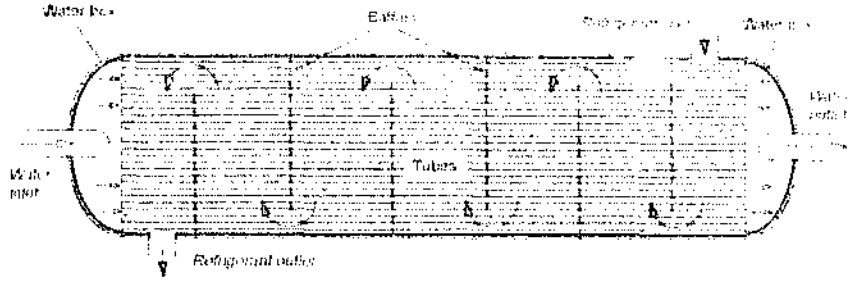

Figure 3.15 Horizontal Shell-and-Tube Subcooler

3.2.6 Expansion Valves

The function of an expansion valve is to automatically drain away all refrigerant liquid from the condenser, as fast as it is generated, and feed this to the evaporator at the required, lower pressure. Expansion devices are most commonly of the float type, controlling the position of a needle valve, as shown in Figure 3.16. Alternatively, sets of orifice plates are used by some manufacturers.

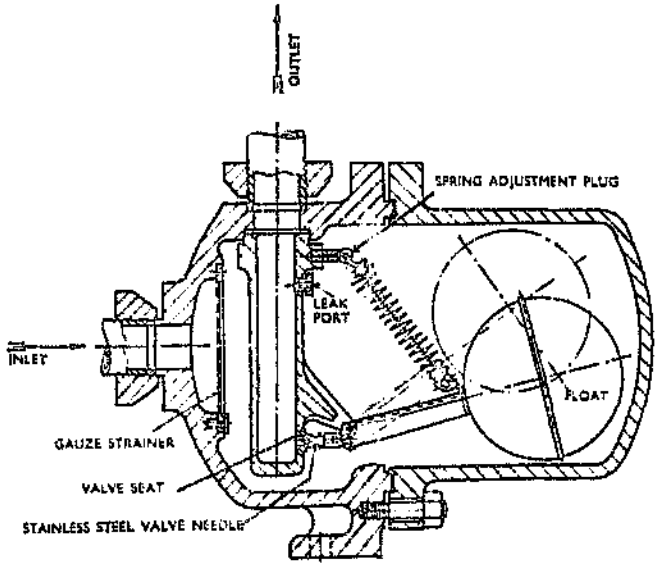

Figure 3.16 Typical Float-Type Expansion Valve

3.2.7 Packaged Machines with a Multi-Stage Centrifugal Compressor

The isentropic head, and hence the pressure rise, through a single centrifugal compressor stage is limited by two factors: the need to maintain high efficiency, and the need to limit impeller tip speed to limit mechanical stresses in the impeller (ASHRAE, 1992; Gosney, 1982; etc.) Where difficulty is thus experienced in achieving the required pressure rise with a single compressor stage, multi-stage compressors can be employed. A multi-stage centrifugal compressor commonly has two or more impellers mounted in the same casing, as shown in Figure 3.17 below.

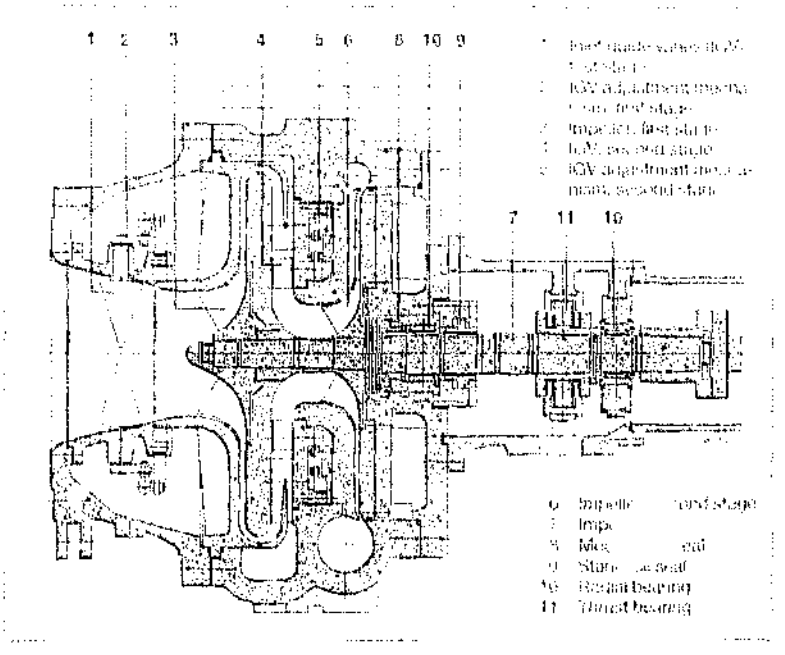

Figure 3.17 Two-Stage Centrifugal Compressor[18]

The amount of stages depends on the pressure ratio required and the type of refrigerant being handled. Variable inlet guide vanes are provided

[18] With acknowledgements to Sulzer Brothers Ltd, Switzerland (Brochure c/25.39.06.40 - XI.84-50 of Process Engineering and Refrigeration Division).

at the inlet to the first compressor stage, and sometimes at the inlets to subsequent stages as well. Side inlets to the second and subsequent stages can be provided to permit auxiliary flows into these stages. These auxiliary flows can be either from side loads (auxiliary refrigerating loads at higher temperatures), or from economisers in multi-stage refrigerating cycles, now described.

Two-Stage Compressor with Economiser

Where a multi-stage centrifugal compressor is employed, advantage may be taken of this by introducing the same amount of stage *expansion* of the refrigerant liquid from condensing to evaporating pressure. The flash vapour generated at each stage of expansion (except the last) is separated from the liquid in special open flash chambers, or *economisers*, and passed into the side inlet of the corresponding compressor stage.

A packaged water chilling machine employing a two-stage centrifugal compressor in this type of cycle is illustrated in Figure 3.18. Here, the two corresponding stages of expansion are implemented by two expansion valves. An economiser is employed to collect the flash vapour generated in the first expansion valve; this vapour is then directed into the side inlet to the second stage of the compressor

As shown a *flash vapour control valve* is sometimes fitted in the line to this side inlet; it is normally fully open. As explained later, its function is to prevent the pressure in the economiser from falling too low on part-duties. The hot gas bypass valve fulfils the same function as for the single-stage machine. Sometimes, a second hot gas bypass valve is fitted between the condenser and the economiser.

The most important advantage of this two-stage cycle is that the flash vapour from the first expansion valve is compressed only from the interstage pressure back to final discharge pressure. This reduces the

irreversibility of the throttling process through the expansion valve (see, for example, Gosney, 1982); there is thus a saving in compression work.

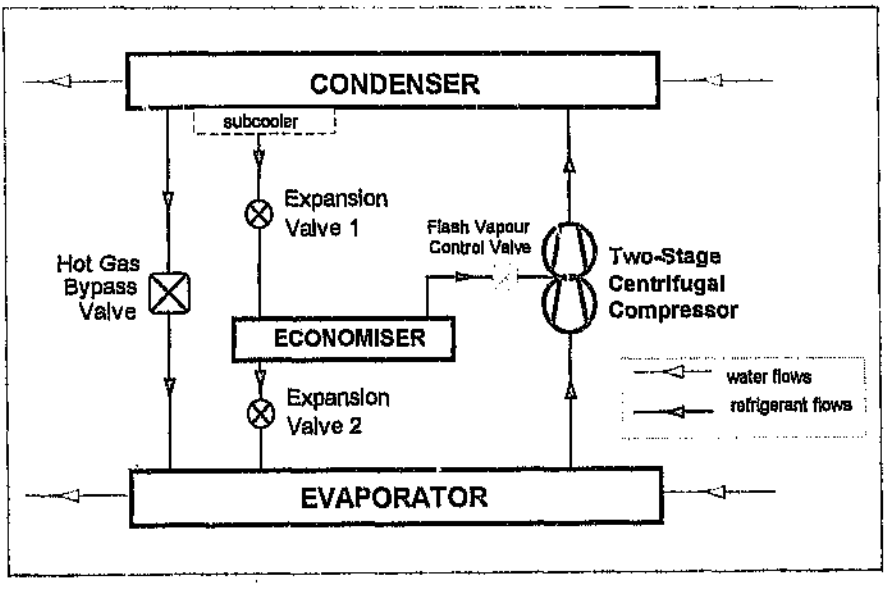

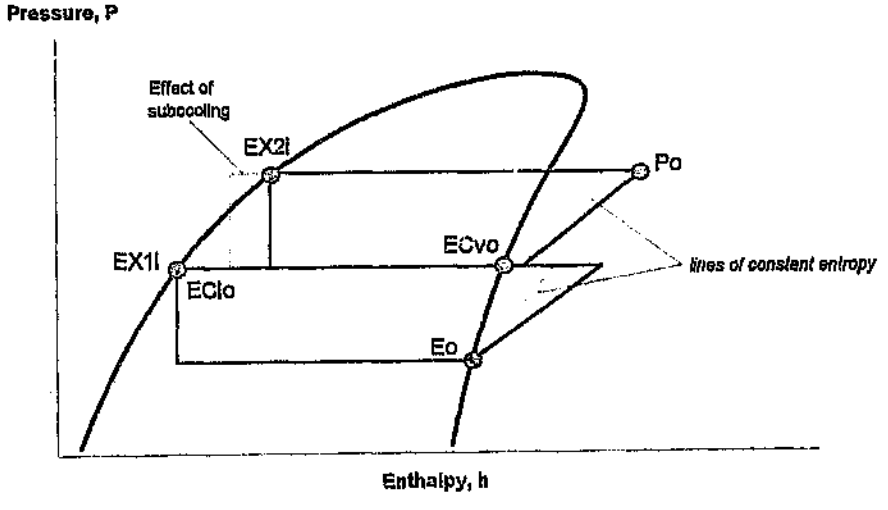

Figure 3.18 Machine with Two-Stage Centrifugal Compressor and Economiser

The amount of flash vapour, expressed as a fraction A of the refrigerant flow-rate through the evaporator, is

$$A = \frac{h_{EX1l} - h_{ECl_o}}{h_{ECv_o} - h_{EX1l}} \tag{3-22a}$$

where h_{ECl_o} and h_{ECv_o} are the enthalpies of the liquid and vapour, respectively, leaving the economiser; and h_{EX1l} is the enthalpy of the liquid entering the first expansion valve (expansion valve 1 in Figure 3.18). The refrigerant-circuit COP, derived from (3-11c) in exactly the same way as for the single-stage machine, is

$$COP_{(r)} = \frac{\left(h_{E_o} - h_{ECl_o}\right) - \dfrac{m_{(r)HG}}{m_{(r)EX2}} \cdot \left(h_{HGl} - h_{E_o}\right)}{\left(h_{P_o} - h_{E_o}\right) \cdot \left(1 + \dfrac{m_{(r)HG}}{m_{(r)EX2}}\right) + A\left(h_{P_o} - h_{ECv_o}\right)} \tag{3-22b}$$

where A is given by (3-22a), and $m_{(r)HG}/m_{(r)EX2}$ is the ratio of mass flow of bypassing hot gas to that through the *second* expansion valve (the final one that feeds the evaporator). If, as is normally the case, there is no flow through the hot gas bypass valve, then $m_{(r)HG} = 0$ and hence $COP_{(r)}$ simplifies to

$$COP_{(r)} = \frac{\left(h_{E_o} - h_{ECl_o}\right)}{\left(h_{P_o} - h_{E_o}\right) + A\left(h_{P_o} - h_{ECv_o}\right)} \tag{3-22c}$$

In most packaged machines with two-stage compressors on South African gold mines, only the first stage of the compressor is regulated, that is, equipped with variable inlet guide vanes. Such compressors may have difficulty in accommodating the reducing load, reducing lift type of part-duty imposed on them in surface installations.

As explained in detail by Shone (1983), the flow and head reduce under this type of part-duty, and one or both compressor stages may thus approach the surge point. In addition, the unregulated second stage develops an increasingly greater share of the reducing head. The interstage pressure between the two compressor stages therefore falls toward evaporating pressure, and the pressure in the economiser in Figure 3.18 does likewise. The difference between economiser and evaporating pressures can thus fall too low for Expansion Valve 2 in the figure to pass liquid refrigerant from the economiser into the evaporator at the required rate. If fitted, therefore, the flash vapour control valve in Figure 3.18 can be partially closed under such duties, raising economiser pressure above interstage pressure and so avoiding this problem. Without such a flash vapour control valve, the only recourse is to bypass hot gas if the machine must operate at such extreme part-duties.

Three-Stage Compressor with Two Economisers

The required temperature lift and thus the pressure rise sometimes justify using three-stage centrifugal compressors, such as in underground installations where refrigerant condensing temperatures may approach 60°C. In such cases, three corresponding stages of expansion and thus two economisers are used, with a resultant further saving in compression work. The refrigerant circuit of such a machine is depicted in Figure A7.1, Appendix 7, and the refrigerant-circuit COP for no hot gas being bypassed is given by (A7-3a) in that appendix.

3.2.8 Arrangements of Conventional Water Chilling Machines within Installations

In installations with conventional packaged water chilling machines, it is undesirable for the water chilling plant to comprise just one machine, as a breakdown means that all refrigerating capacity is lost. Hence two or more machines are generally employed. For logistical reasons, it is preferable that all machines be identical in make, model and capacity.

As mentioned in Chapter 2, water chilling plants can accommodate variations in duty in two ways. They can accommodate:

- minor variations by regulating the capacities of their operating machines, and sharing total duty equally or unequally;
- major variations by altering the amount of operating machines.

The load imposed on the water chilling plant can vary because of variations in incoming water temperature, chilled water flow-rate, or both. How the plant shares its total duty among its machines depends on which of these variations dominate. If it has to alter the amount of operating machines, the question arises of how best to connect these machines in the chilled and heat-removing (condenser) water circuits. The discussion here follows van der Walt (1979).

Variable-Flow Load: Water-Circuit Connections in Parallel

The variation in water chilling load may be primarily due to changes in total water flow-rate, with entering and leaving water temperatures comparatively constant; an example would be an underground installation supplying water for distributed air cooling. Here, the evaporators and condensers of all machines (presumed identical) in the water chilling plant may be connected in parallel in their water circuits, as illustrated in Figure 3.19. As the load on the plant changes, machines can be brought into or out of operation as required.

Variable-Temperature Load: Water-Circuit Connections in Series

On the other hand, the total water flow-rate may remain essentially constant, with the variation in water chilling load being primarily due to changes in entering water temperature; an example would be a surface installation with a pre-cooling tower, supplying chilled service water. Here, the evaporators of the identical water chilling machines can be connected in series, as shown in Figure 3.20.

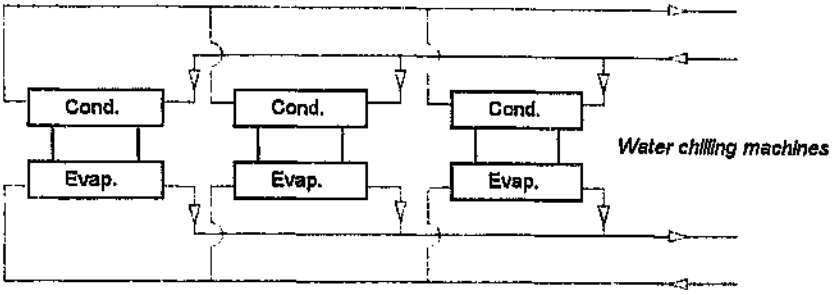

Figure 3.19 Water Chilling Machines with Water-Circuit Connections in Parallel

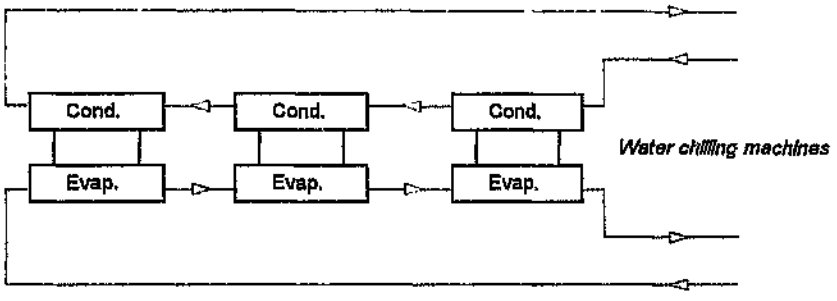

Figure 3.20 Water Chilling Machines with Water-Circuit Connections in Series

Water is thus chilled in two or more steps. As the load on the water chilling plant changes, the entering water temperature will alter, and machines can be brought into or out of operation as required.

In Figure 3.20, there are two reasons for connecting the condensers in series-counterflow, that is with their heat-removing water flow in the opposite direction to the chilled water flow through the evaporators. First, at design duty, the lift (the difference between evaporating and condensing refrigerant temperatures) is approximately the same for each machine. As the machines are identical, this ensures that each machine operates under as nearly identical conditions as possible, and close to its point of optimum efficiency. Second, chilling water in two or more steps by this series-counterflow arrangement is an approximation to the ideal

Lorenz cycle for chilling water, shown in Figure 3.3. Other things being equal, the COP of this water chilling plant is therefore considerably better than if water were chilled in one step only.

The plant control philosophy normally shares minor variations in load unequally between operating machines, regulating the machine performing the final step of chilling to accommodate such variations, but keeping the others at full capacity. If so, the duty of this final machine, or *lag machine* as it is often termed, is different from that of the others, termed *lead machines*. For example, if the duty on the plant is one of reducing load, reducing lift, the duty of the lag machine will also be such, but those of the others will be ones of constant load, reducing lift. As noted previously, if the machines have a two- (or multi-) stage centrifugal compressor with variable inlet guide vanes on the first stage only, the lag machine may therefore not be able to accommodate extreme part-duties of reducing load, reducing lift without closing its flash vapour control valve or bypassing hot gas.

Combined Series and Parallel Connections in Water Circuits

Where the water chilling load varies due to major changes in both total water flow-rate and entering water temperature, such as for a surface installation providing bulk air cooling and service water chilling, the evaporators of the water chilling machines can be connected so that a pair of evaporators in series operate in parallel with another pair of series-connected evaporators, as shown in Figure 3.21.

A major reduction in water flow-rate (such as when the bulk air cooling plant ceases to operate in winter) is accommodated by bringing one such pair of series-connected machines out of operation; a similar reduction in entering water temperature is accommodated by bringing one machine *in each series-connected pair* out of operation. Only one machine operates when there are major reductions in both water flow-rate and entering water temperature.

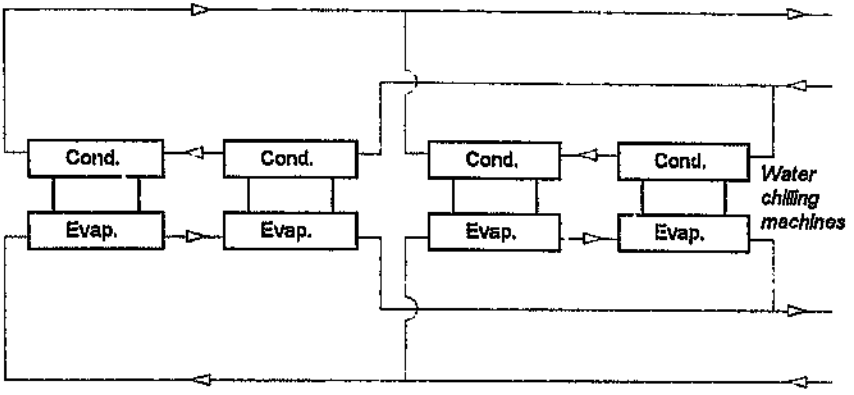

Figure 3.21 Water Chilling Machines with Water-Circuit Connections in Series-Parallel

3.3 Custom-Built Machines with Screw Compressors

As mentioned earlier, the second class of large-capacity water chilling machines on mines is of custom-built machines employing screw compressors. As explained later, these compressors may freely be connected in parallel; this permits greater flexibility in the refrigerant circuit, which may incorporate multiple compressors, evaporators, and condensers connected in series or parallel. Compared to a conventional, packaged machine, the refrigerant circuit is thus more extensive and complex, and the refrigerant charge is accordingly greater. The advantage is that no matter how the heat exchangers are connected in the chilled and heat-removing water circuits - in parallel, series, or series-parallel - *all* heat exchangers can be connected into *one and the same refrigerant circuit*. Hence, as noted for example by Perry (1987b), *all* the heat-transferring area in *all* heat exchangers can be used all the time, thus maximising heat-transferring efficiency, even when not all compressors are required to run. (The heat exchangers in a packaged machine, on the other hand, are rendered inoperative when its compressor stops.) Water chilling plants with custom-built machines

mostly comprise just one such machine, in which case the plant and machine are synonymous.

Most custom-built machines on South African mines are on surface and use ammonia as the refrigerant (which, as mentioned earlier, does not lend itself to use with centrifugal compressors).

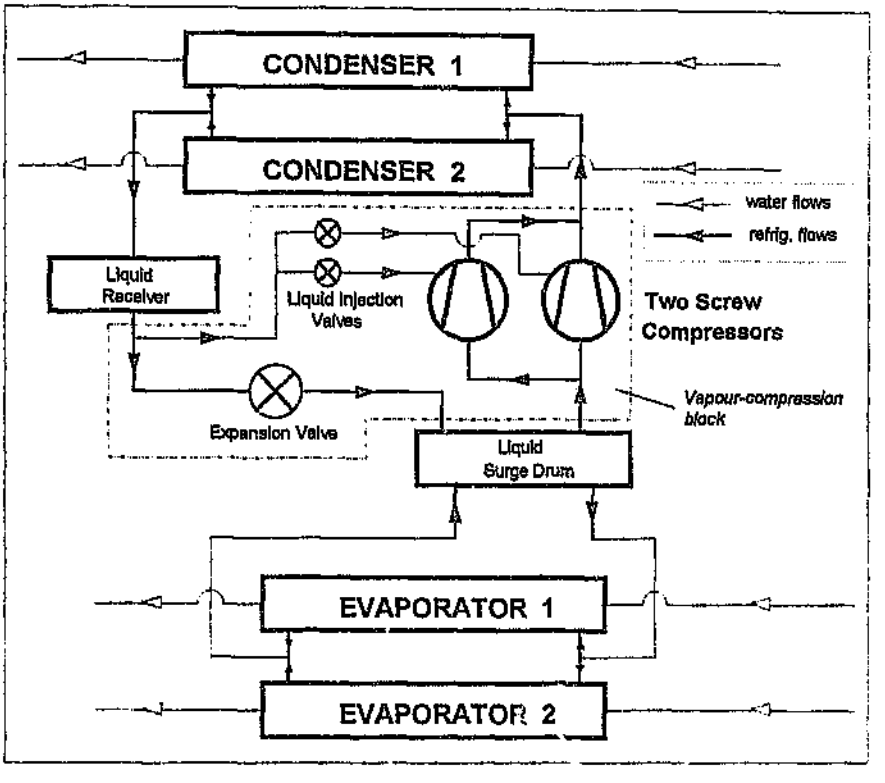

Figure 3.22 Custom-Built Machine: Evaporators and Condensers in Parallel

Figure 3.22 schematically illustrates a custom-built machine using ammonia as the refrigerant. The evaporator block comprises two parallel banks of open plate-type evaporators (described later), connected in parallel in both the water and refrigerant circuits, and supplied with refrigerant liquid from the liquid surge drum shown. The function of this surge drum is also described later. The condenser block comprises two

shell-and-tube condensers, likewise connected in parallel and passing condensed refrigerant liquid to the liquid receiver shown. The vapour-compression block, shown bordered, consists of the expansion valve, the two screw compressors connected in parallel, and two corresponding liquid injection valves; these inject small flows of liquid refrigerant into the compressors to cool their oil, as described later.

The refrigerant-circuit COP of this machine, derived from (3-11c) in exactly the same way as for conventional machines, is

$$COP_{(r)} = \frac{h_{SDo} - h_{LRo}}{\left(h_{(P1+P2)o} - h_{SDo}\right) + \dfrac{m_{(r)LI1} + m_{(r)LI2}}{m_{(r)EX}}\left(h_{(P1+P2)o} - h_{LRo}\right)} \qquad (3\text{-}24)$$

Where, referring to Figure 3.22, h_{SDo} is enthalpy of the refrigerant vapour, generated in the evaporators, at the outlet of the liquid surge drum; $h_{(P1+P2)o}$, that of the refrigerant vapour from both compressor outlets after these flows have merged into a common pipeline; h_{LRo}, that of the liquid refrigerant leaving the condensed liquid receiver; $m_{(r)LI1}$ and $m_{(r)LI2}$, mass flow-rates of liquid injected into the first and second compressor respectively; and $m_{(r)EX}$, mass flow-rate of refrigerant through the expansion valve. The liquid injection into the compressors constitutes an auxiliary refrigerant flow, and so, analogously to conventional machines bypassing hot gas, $COP_{(r)}$ here depends not only upon enthalpies, but upon the ratio of total liquid-injection flow to the main refrigerant flow. This ratio is conveniently termed the *liquid injection ratio.*

Figure 3.23 illustrates an alternative custom-built machine where the evaporators are in series in the water circuit, and each is served by a separate, dedicated screw compressor in the refrigerant circuit. Such a machine is suited to an essentially variable-temperature load. Analogously to the water chilling plant of Figure 3.20, minor changes in

such a load are accommodated by regulating compressor capacity; when the load falls to approximately half the full-duty value, one compressor can be brought out of operation.

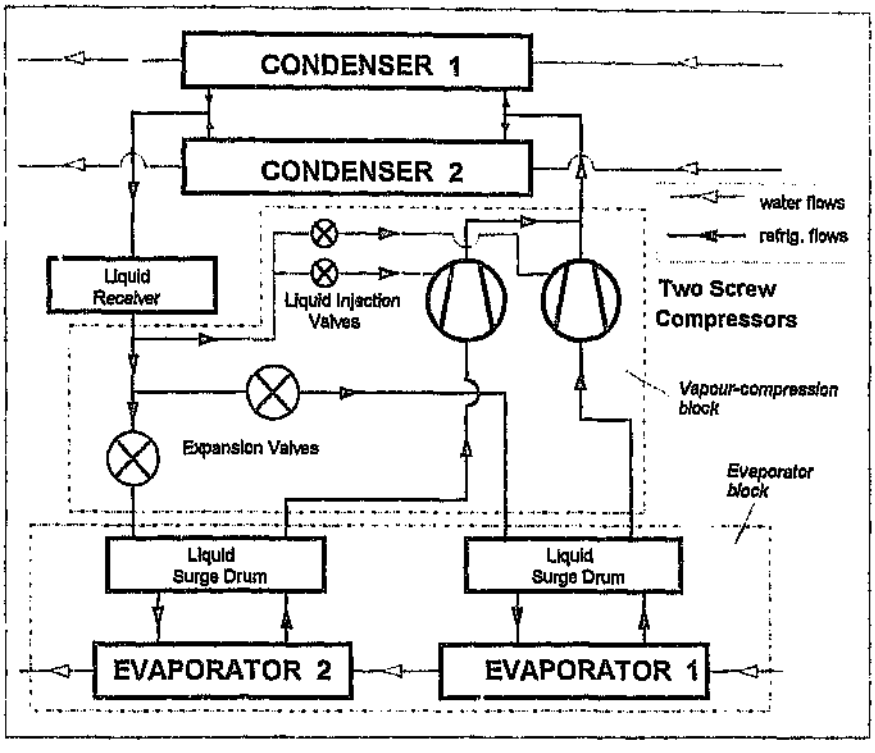

Figure 3.23 Custom-Built Machine: Evaporators in Series, Condensers in Parallel

There is one major difference between this machine and all the machines previously described. As there are two evaporators, and their refrigerant sides are not connected in parallel within the evaporator block (unlike Figure 3.22), *two* refrigerant streams, of differing mass flow-rates and properties, circulate between the evaporator block and the vapour-compression block. Hence the refrigerant-circuit COP, again derived from (3-11b), depends on the ratios of these differing mass flow-rates to their sum, as well as on the ratio of the liquid injected into the compressors to this sum:

$$COP_{(r)} = \frac{h_{[(SD1+SD2)o]} - h_{LRo}}{h_{(P1+P2)o} - h_{[(SD1+SD2)o]} + \frac{m_{(r)LI1} + m_{(r)LI2}}{m_{(r)EX1} + m_{(r)EX2}}\left(h_{(P1+P2)o} - h_{LRo}\right)} \qquad (3\text{-}25a)$$

where the symbols are as for (3-24), except that $m_{(r)EX1}$ and $m_{(r)EX2}$ are the differing refrigerant mass flow-rates through the first and second expansion valves, and

$$h_{[(SD1+SD2)o]} = \frac{m_{(r)EX1}}{m_{(r)EX1} + m_{(r)EX2}} h_{SD1o} + \frac{m_{(r)EX2}}{m_{(r)EX1} + m_{(r)EX2}} h_{SD2o} \qquad (3\text{-}25b)$$

where h_{SD1o} and h_{SD2o} are the enthalpies of the refrigerant vapour, generated in Evaporators 1 and 2, at the outlets of their liquid surge drums.

Finally, Figure 3.24 illustrates a custom-built machine where the evaporators are in series in the water circuit, but in parallel in the refrigerant circuit. Unlike the previous two machines, this machine is installed underground and employs Refrigerant 12. Its oil is not cooled by liquid injection, but by a water-cooled oil cooler supplied with water from outside the machine boundary.

The refrigerant-circuit COP of this machine, derived from (3-11c) in the same way as before, is simply

$$COP_{(r)} = \frac{h_{SDo} - h_{LRo}}{h_{Po} - h_{SDo}} \qquad (3\text{-}26a)$$

but here, $COP_{(r)}$ does *not* reflect actual COP accurately, considerably over-estimating this. As explained below, the oil in screw compressors absorbs a significant amount of the heat of compression, so the oil cooling

load, represented by $Q_{(w)VCB(Ms)}$ in (3-11b), is too large to neglect.[19] Again, Chapter 5 shows how $COP_{(r)}$ may be corrected to reflect actual COP.

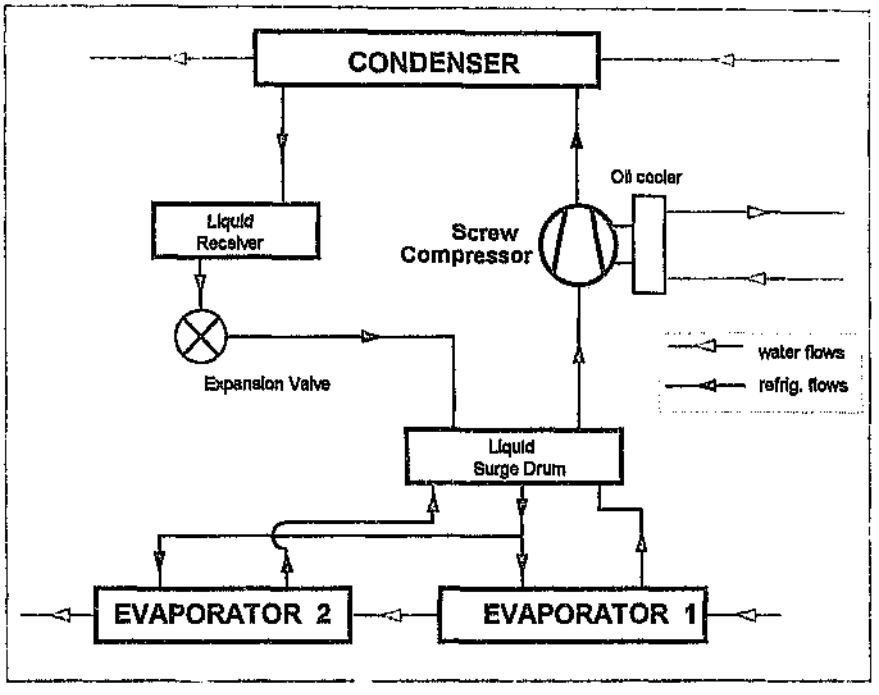

Figure 3.24 Custom-Built Machine: Evaporators in Series in Water Circuit Only

Beginning with the screw compressor, the components of these custom-built machines are now described in some detail.

3.3.1 The Screw Compressor

Large custom-built water chilling machines on South African mines almost exclusively employ twin screw compressors. The twin screw compressor is thus described here.

---

[19] In the machine of Figure 3.24, the design oil cooling load is about 13 per cent of the power input to the compressor; for machines using ammonia, it may be as much as 30 per cent thereof.

Compression Process

Screw compressors employ the positive-displacement principle of compression. A twin screw compressor consists of two intermeshing, helically grooved rotors in a stationary housing with suction and discharge gas ports or openings, as in Figure 3.25. The lobes of the male rotor mesh with corresponding flutes in the female rotor. As the rotors turn, they unmesh on the side facing the suction opening, so gas is drawn through this opening to fill the space between adjacent lobes. When a particular interlobe space along the rotors is filled, the rotor tips bounding this space move past the suction opening (point X in the figure), so sealing this space. As the rotors continue to rotate, they pass point Y in the figure and then begin to re-mesh on the side facing the discharge opening, progressively reducing the space occupied by the gas and thus compressing it. Compression continues until the rotor tips pass point Z, whereupon this interlobe space opens to the discharge opening, and the continued rotation of the rotors expels the gas into this opening.

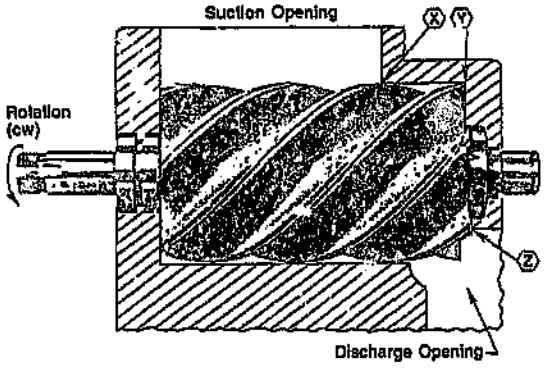

Figure 3.25 Sectional Side View of Twin Screw Compressor (Carrier Corporation, 1981)

During this remeshing process, a fresh charge of gas is drawn through the suction opening on the opposite side. For example, with four male lobes rotating at 3 600 RPM, four interlobe volumes are filled and give 14 400

discharges per minute. Since the intake and discharge processes overlap effectively, the gas flow is smooth and continuous for practical purposes. In screw compressors for refrigeration, the female rotor is normally directly driven by the male rotor on a light oil film provided by oil injection, described further below. Frequently used lobe combinations are 4+6, 5+6, and 5+7 (male + female). Rotor profiles, clearances and other mechanical design features are optimised for specific temperatures, pressures, speeds, and wet (oil-injected) or dry operation (ASHRAE, 1992).

Built-in Volume Ratio

The degree of compression within the interlobe spaces is determined by the location of the suction and discharge ports. The built-in volume ratio φ_i of screw compressors is defined as the ratio of the volume of an interlobe space at the start of the compression process to the volume of the same interlobe space when it first begins to open to the discharge port. The location of the discharge port thus determines this volume ratio. Corresponding to φ_i there is a built-in internal pressure ratio Π_i given by $\Pi_i = \varphi_i^n$, where n is the index of polytropic compression. The value of n depends on the refrigerant being compressed and the conditions of compression (Gosney, 1982).

Only the suction pressure and the built-in volume ratio of the compressor determine the internal pressure achieved before opening to discharge. However, the actual discharge pressure, and the ratio P_o/P_i of the pressures at compressor outlet and inlet, are determined by the condensing and evaporating temperatures in the machine which the compressor serves. Any mismatch between the internal pressure ratio Π_i and the actual pressure ratio P_o/P_i results in under- or over-compression losses and lower efficiency (see, for example, Gosney, 1982 : 74,309). The ratio of the minimum polytropic compression work when the pressure

ratio equals Π_i to that at the prevailing pressure ratio P_o/P_i is called the *built-in efficiency* η_φ, and represents the unavoidable loss when these ratios differ - even were the internal compression process reversible, which it is not. Gosney (1982) shows that η_φ is given by

$$\eta_\varphi = \frac{\left[n/(n-1)\right]\left[(P_o/P_i)^{(n-1)/n} - 1\right]}{\left[n/(n-1)\right]\left[\varphi^{(n-1)/n} - 1\right] + \left[(P_o/P_i) - \varphi^n\right]/\varphi} \qquad (3\text{-}27)$$

Figure 3.26 plots the variation of this built-in efficiency with prevailing pressure ratio P_o/P_i for three values of built-in volume ratio φ_i commonly furnished by manufacturers. The curves peak at $\eta_\varphi = 1$ when $P_o/P_i = \Pi_i$. Once the losses in the *internal* compression process, mechanical losses, etc. are added, these curves become those of isentropic efficiency, with the same basic shape (see, for example, ASHRAE, 1992 : 35.19).

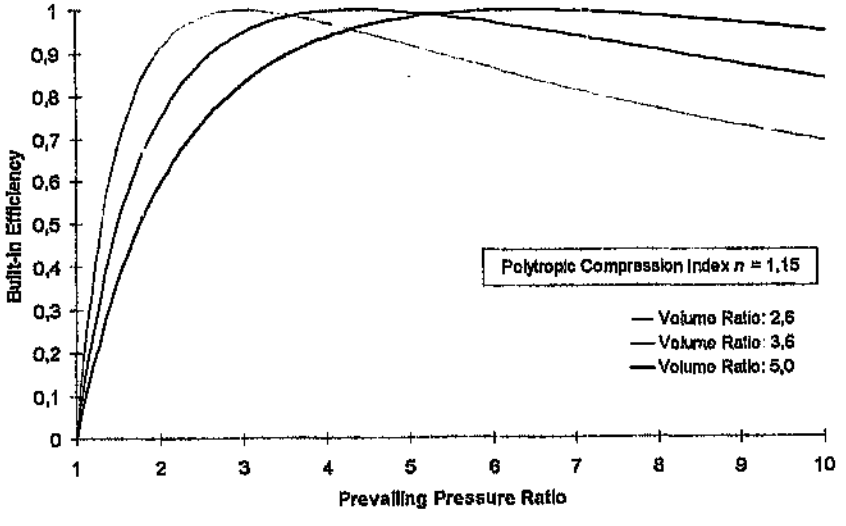

Figure 3.26 Variation of Built-In Efficiency of Screw Compressor with Prevailing Pressure Ratio

Isentropic efficiency of a screw compressor, therefore, depends strongly on the matching between prevailing pressure ratio and built-in internal pressure ratio Π_i. Figure 3.26 shows that the efficiency falls less rapidly from its peak for $P_o/P_i > \Pi_i$ than for the other way round. The built-in volume ratio is thus normally specified so that Π_i is somewhat lower than the most frequently encountered prevailing pressure ratio.

In contrast to isentropic efficiency, the volumetric efficiency of a screw compressor - that is, the ratio of inlet volumetric flow-rate to the rate at which its rotors sweep through the volume of their interlobe spaces - is almost constant, decreasing only slightly with increasing prevailing pressure ratio (ASHRAE, 1992, etc.). This is principally due to increased leakage between the rotors and the casing. Thus a screw compressor is a virtually "constant-volume" machine - it will maintain a virtually constant inlet volumetric flow-rate regardless of the prevailing pressure ratio, mechanical limitations[20] and power rating of its driving motor permitting. Fundamental mathematical models of the screw compression process have been developed. However, as noted by Stosic et al. (1992), the accompanying phenomena such as leakage, oil injection (see later) and heat transfer between gas, rotors and casing cannot easily be represented analytically, and are approached differently in the various models. As these phenomena influence actual performance to a large extent, predicted performance still has to be confirmed by test.

Unlike a centrifugal compressor, a screw compressor cannot surge. Also unlike centrifugal compressors, screw compressors may be freely connected in parallel in refrigerant circuits, as small differences in prevailing pressure ratio (due, for example, to different lengths of suction and discharge piping) will not affect how they share duty.

---

[20] Such as allowable discharge temperature and flexion of the rotors at high pressure ratios.

Usually, in compressors equipped with a capacity-regulating slide valve (see later), the radial discharge port is located in the discharge end of the slide valve. A short slide valve thus gives a low volume ratio, and a long slide valve a higher volume ratio. The difference in length basically locates the discharge port earlier or later in the compression process. Manufacturers customarily make compressors with three or four discharge port locations and thus volume ratios, such as the three in Figure 3.26, that correspond to frequently-encountered operating conditions.

Oil-Flooded Operation

The oil-flooded twin screw compressor is the most common type used in refrigeration and air-conditioning. Oil-flooded compressors generally have oil supplied to the compression area at a volume rate of about 0,25 to 0,5 per cent of the displacement volume. Part of this oil is, of course, used for lubrication of the bearings and the shaft seal. The oil is normally injected into a *closed* interlobe space, through either ports in the movable slide valve or stationary ports in the casing. The oil fulfils three primary purposes: sealing, cooling and lubrication. It also tends to fill any leakage paths around the rotors, thus keeping volumetric efficiency high. Much of the heat of compression is transferred from the gas to the oil, keeping typical discharge temperatures below 90°C, which allows high compression ratios without risk of the oil or refrigerant breaking down. The mass flow-rate of oil injected into the compressor depends primarily on the desired discharge temperature. Oil also protects the rotor contact areas through lubrication (ASHRAE, 1992; Gosney, 1982).

Oil injection is normally achieved by a separate oil pump generating an oil pressure of 200 to 300 kPa over compressor discharge pressure, and absorbing 0,3 to 1,0 per cent of compressor motor power. Sometimes oil is automatically injected without a pump; this is possible due to the pressure difference between the oil reservoir (which is exposed to

discharge pressure) and the reduced pressure in the interlobe spaces during the compression process (ASHRAE, 1992).

Oil Separation and Cooling

Oil injection, of course, requires an oil separator to remove entrained oil from the high-pressure refrigerant vapour leaving the compressor. Separation equipment routinely gives less than 5 ppm of oil in the circulated refrigerant (ASHRAE, 1992). A small proportion of the oil leaving the compressor will be in vapour form; this cannot be mechanically trapped in the oil separator, and thus passes into the refrigerant circuit. Suitable oil recovery devices must therefore be incorporated into the refrigerant circuit to extract this oil and return it to the compressor (ASHRAE, 1990).

Since the oil absorbs a significant amount of the heat of compression in an oil-flooded compression process, it must be cooled to prevent excessively high compressor discharge temperatures. The oil can be cooled in a separate oil cooler, and the cooling medium can be water from the chilled or preferably the condenser water circuit; air; or liquid refrigerant. Where the heat from the oil cooler is rejected separately and independently from that from the condenser, the condenser can be reduced in size by the amount of the oil cooler capacity.

An alternative oil cooling method is by direct injection of liquid into the compression process. The amount of liquid injected is normally controlled to maintain the discharge temperature at a specified value. Some of the injected liquid mixes with the oil and leaks to lower-pressure interlobe spaces, where it tends to raise pressures and reduce the amount of gas that the compressor can draw in. Also, any liquid that has time to absorb heat and change to vapour must be re-compressed to discharge pressure, which increases net power requirement. Compressors designed for such oil cooling have liquid injection ports as late as possible in the compression process to minimise these capacity and power penalties.

Typical penalties are in the 1 to 10 per cent range, depending on the compression ratio (ASHRAE, 1992).

Liquid-injection oil cooling is especially convenient when ammonia is the refrigerant. The mass flow-rate of liquid to achieve the required cooling is small, due to the high latent heat of ammonia (see Table 3.1), and capacity and power penalties are correspondingly small.

Regulation of Capacity

Ideal capacity modulation for a screw compressor should afford continuous modulation down to less than 10 per cent of capacity, and good part-capacity efficiency. Variable compressor speed and variable compressor displacement are the best means of achieving this. With constant-speed drives, variable compressor displacement by means of a slide valve is the most common capacity control method used.

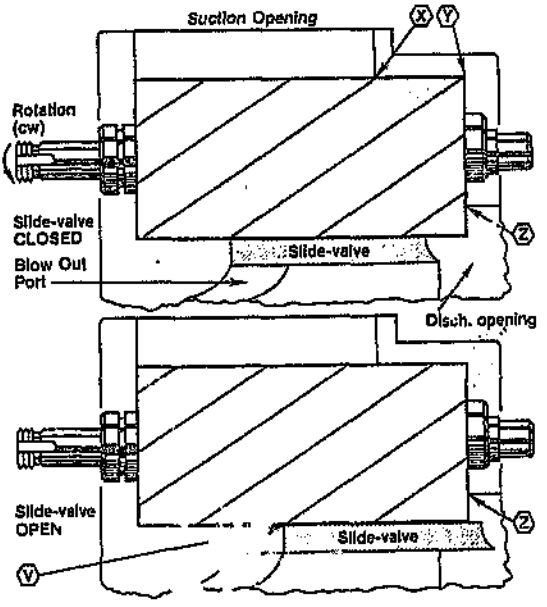

Figure 3.27 Slide Valve Unloading Mechanism (Carrier Corporation, 1981)

Such a valve has a sliding action parallel to the rotor bores, as illustrated in Figure 3.27. Depending on its position, it allows a variable portion of the gas drawn into the interlobe spaces at suction to pass back to the suction area through the *blow-out port* shown. Only when the rotor tips bounding a particular interlobe space move past the point V in the lower diagram of the figure is this space sealed and compression begun. The discharge port in such compressors must consist of an axial part as well as a radial part: this is because the slide valve moves the radial discharge port towards the discharge end of the compressor upon unloading, thus gradually closing it and reducing the *radial* area available for gas discharge (Gosney, 1982). The axial discharge port is designed to achieve a volume ratio giving good part-capacity performance without prejudicing efficient full-capacity performance.

Performance under Part-Duty Conditions

For water chilling applications, prevailing pressure ratios are unlikely to exceed 3, so, as may be seen from Figure 3.26, it is appropriate to select a low built-in volume ratio, typically 2,2 to 2,6. Figure 3.28 shows, for such a screw compressor, the variation of built-in volume ratio and isentropic efficiency with capacity as the slide valve reduces this.

As mentioned earlier, at full capacity, the built-in volume ratio φ_i is the dominant factor determining isentropic efficiency. However, at part-capacity, the internal geometry of the compressor changes and losses other than that due to mismatch of the internal and prevailing pressure ratios become more dominant (Lundberg, 1980).

In Figure 3.28, the graph of isentropic efficiency against capacity is for Refrigerant 22 at a constant pressure ratio of 3; the inlet and outlet pressures are kept constant during capacity reduction. If the pressure ratio is allowed to decrease at part-capacities, a better part-duty efficiency is obtained.

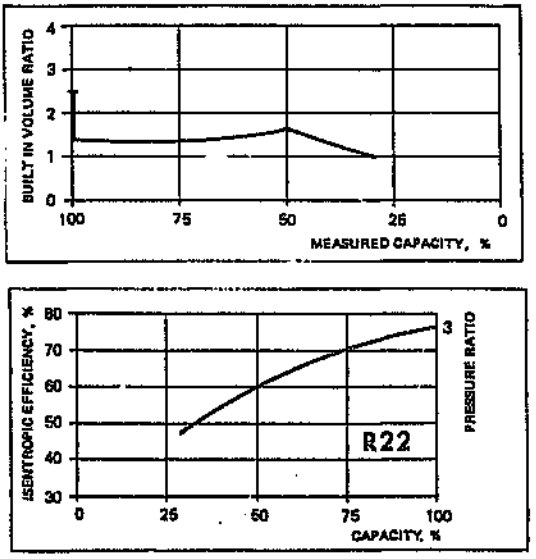

Figure 3.28 Variation of Built-In Volume Ratio and Isentropic Efficiency with Capacity Reduction in a Twin Screw Compressor (Lundberg, 1980)

3.3.2 Evaporators

Open-Plate Evaporators

Plate-type heat exchangers are customarily used with custom-built machines. A diagram of an open-plate type of evaporator, known as a *Baudelot cooler,* and its auxiliary equipment is given in Figure 3.29 below.

This evaporator consists of a number of parallel vertical plates, externally corrugated. The water being chilled is distributed uniformly over the top of these plates, and flows down their outside surfaces by gravity to a collection pan below. The water is chilled by refrigerant evaporating inside these plates. Unlike the shell-and tube evaporator of Section 3.2.3, these plates cannot act as their own refrigerant reservoir,[21] so the

[21] This is because the mass of boiling refrigerant in these plates decreases with increasing load, as vapour then occupies more of their limited internal volume.

auxiliary equipment shown in Figure 3.29 is necessary to perform this function, as now explained.

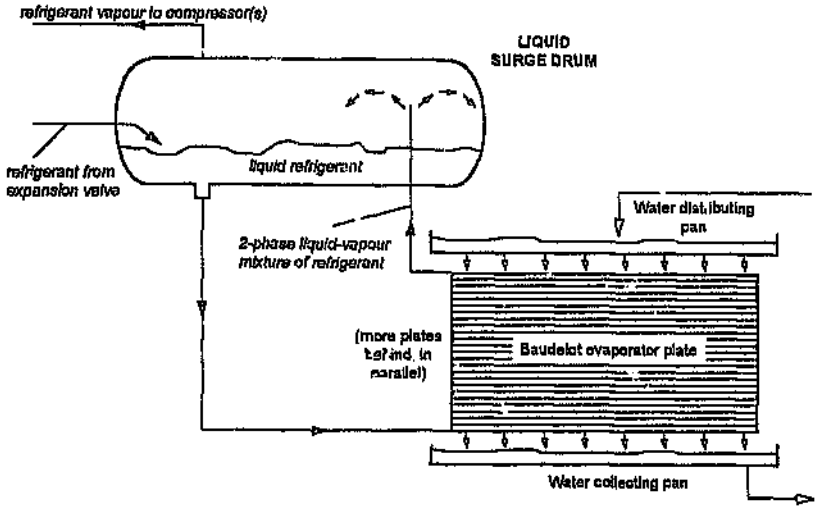

Figure 3.29 Baudelot Open-Plate Evaporator and Auxiliary Equipment

The inlets and outlets of these plates pass into manifolds which are connected into the bottom and top, respectively, of a refrigerant liquid reservoir termed a *surge drum*. The plates are thus fed with liquid refrigerant by gravity from the bottom of this surge drum. This refrigerant boils inside the plates, which have limited internal volume, and thus expel a two-phase mixture of liquid and vapour through their outlets. The difference in density between this leaving two-phase mixture and the entering single-phase liquid provides the necessary driving force to circulate the refrigerant through the plates; this means of circulation is known as the *thermosyphon system*. The mixture of liquid and vapour is returned into the top of the surge drum, where the liquid portion falls out and returns into the main body of liquid therein. The vapour outlet of the surge drum is positioned to ensure that only liquid-free refrigerant vapour passes out of this drum and into the compressor.

The advantages of an open-plate evaporator over the shell-and-tube type are:

- water can be chilled to nearly 0°C, as any ice forming on the plates will not damage them;
- (in theory, if the water does not form a hard scale) the plates are easily cleaned;
- flexibility; capacity can be adjusted by adding or removing individual plates.

The auxiliary equipment needed, consisting of the surge drum, piping, manifolds and water distributing and collecting pans, is considerable, though. Moreover, the arrangement of open plates occupies much more floor area than an equivalent shell-and-tube evaporator.

Closed-Plate Evaporators

Closed-plate heat exchangers, which can be used either as evaporators or as condensers, consist of a stack of corrugated metal plates provided with ports for the passage of the two fluids involved. The plates are fitted with gaskets which seal the channels and direct the two fluids into alternative channels, as seen in Figure 3.30. True counter-current, turbulent flow occurs.

Again, auxiliary equipment, namely a surge drum and a thermosyphon refrigerant-circulating system, as in Figure 3.29 (or refrigerant circulating pumps) is necessary. The advantages of closed-plate evaporators over shell-and-tube ones are:

- they are more compact (apart from the auxiliary equipment);
- it is especially easy to adjust capacity by adding or removing plates to or from the stack;

- very high heat transfer coefficients are obtained, as the swirling motion imparted to the fluid by the channels assures turbulent flow at very low Reynolds numbers of between 10 and 400 (Saunders, 1988);
- as for open-plate evaporators, they can chill water to nearly 0°C.

In addition, unlike open plate evaporators, they can easily be connected in series, as the water flows remain confined in closed circuits.

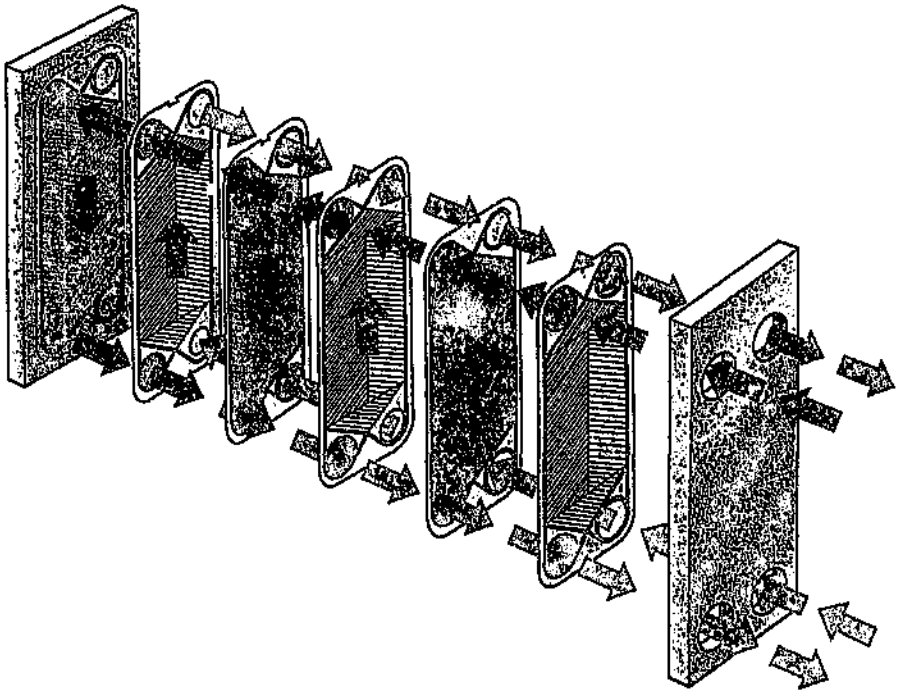

Figure 3.30 Closed-Plate Heat Exchanger[22]

[22] With acknowledgements to Alfa-Laval, Sweden (Brochure PB 67025E, 88-06, "Heat Exchangers in Refrigerant Systems").

3.3.3 Condensers

Custom-built machines can use shell-and-tube condensers, evaporative condensers or closed-plate heat exchangers, as in Figure 3.30, as condensers. Again, auxiliary equipment in the form of a condensed liquid receiver is necessary for such closed-plate condensers, as the plates cannot act as their own refrigerant reservoirs.

3.3.4 Expansion Valves

Expansion valves feeding the cold liquid surge drums in custom-built machines, as in Figures 3.22 and 3.23, generally have the function of maintaining a constant liquid level in these vessels, mainly to ensure adequate refrigerant circulation in thermosyphon systems. Since this liquid level is likely to be very disturbed because of the boiling action in the evaporator, a separate float chamber is provided for the float or other liquid level sensor. This chamber is connected to the evaporator by balance pipes of comparatively small bore, so that a steady level is maintained in this chamber.

3.4 Performance of Machines under Part-Duties

Whether a water chilling machine is of the conventional or custom-built class, there is a complex interdependence between the performances of its components. These components are generally designed for optimal performance at the design duty (full duty) and other conditions specified by the mine, and are matched to each other at this duty. If operating conditions are considerably different, particularly under part-duties, such altered conditions may improve the performance of certain machine components, *but simultaneously worsen that of others*, so machine performance is no longer necessarily optimal. It will be seen in Chapter 6, for example, that for a constant water chilling load, enhancing heat-transferring efficiency of an evaporator by minimising water-side fouling may cause compressor efficiency to deteriorate, and thus actually worsen

the COP! Another example, as already noted, is that a machine with a multi-stage centrifugal compressor with variable inlet guide vanes on its first stage only (termed a "first-stage-regulated" compressor) may have difficulty in accommodating extreme reducing-load, reducing-lift duties, and hence be compelled to bypass hot gas to avoid surge - thus again reducing the COP. Thus, in general, *every* component of a machine must possess good efficiency throughout the range of possible machine duties if the desirable goal of good machine efficiency throughout this range is to be achieved. This applies especially to the compressor(s), whose efficiency should peak at the *most frequently-encountered* operating conditions, which may differ considerably from design full-duty conditions (Gluckman, 1993). If this is not the case, it is better if possible to alter the control philosophy of the water chilling plant to confine the machine to a narrower range of duties where all its components do possess good efficiency. As will be illustrated in Chapter 6, this is likely to mean operating at maximum possible load for conventional machines with multi-stage, "first-stage-regulated" compressors.

4. PROBLEMS IN DETECTING UNSATISFACTORY PERFORMANCE OF WATER CHILLING MACHINES

Fluid cooling installations serving mines must ensure acceptable temperatures for the underground workforce, and hence maintenance of production. Thus they must operate effectively, that is, deliver the specified (and preferably the maximum) flow-rates of chilled water and cooled air at the specified temperatures. As shown in Appendix 2, running costs of fluid cooling installations are not significant in the working costs of the South African gold mining industry as a whole. Far more costly are the penalties of unsatisfactory installation performance and non-availability due to breakdowns. These penalties are, primarily, endangering the health and safety of persons, because temperatures in the workings may exceed the safe limits referred to in Chapter 2; and also losses in production. Hence, from the viewpoint of South African gold mines, *cost*-effective operation of fluid cooling installations tends to be operation under whatever conditions best guarantee maximal effectiveness and full availability. This may or may not correspond to operation at minimum running cost; if it does not, there is little incentive to operate at such minimum cost.

Turning to the water chilling machines - the most complicated components of fluid cooling installations - it follows that there is a need to plainly and unmistakably detect unsatisfactory performance of these machines as early as possible, in order to promptly remedy the cause(s) thereof and minimise the consequential cost of such performance to the mine. To detect unsatisfactory performance of a machine, it is obviously necessary to ascertain its operating conditions, and its actual performance under those conditions. However, ascertaining just actual performance is not enough; it is also necessary to know what its *normal* performance (defined later) would be under the same operating regime, and possibly what its optimal performance would be under the same or an alternative operating

regime. Only by comparing actual performance with this corresponding normal or optimal performance can the extent of unsatisfactory performance be established, and hence the causes - whether within the machine or elsewhere - reliably pinpointed and appropriate remedial action justified. Two quotes from Hemp (1981) draw attention to this:

> "Routine measurements of cooling plant performance must first be analysed... If these measurements indicate that the plant performance is deficient, perhaps because of the poor performance of some of the plant components, it is of some value if an indication can be given of the expected results should the recommended action be taken to improve matters. This action could, for example, be cleaning tubes, or increasing water flow-rates. The expected results can be calculated quite easily by predicting the plant performance under the new conditions."

> "Cooling plant performance prediction... is in fact a necessary part of performance assessment, for it provides a means for predicting the results of any action taken to improve performance."

The procedure of comparing actual performance with the corresponding normal or possibly optimal performance, and evaluating the effectiveness and quality of the actual performance on this basis, is termed *assessing* site performance. *Actual performance cannot be properly assessed without a yardstick to compare it with; this yardstick being at least the corresponding normal performance.*

This chapter critically reviews current practice in ascertaining actual performance, predicting corresponding normal or optimal performance, and hence assessing actual performance. The chapter first reviews the well-established standards for testing water chilling machines, these standards being the authorities on ascertaining actual performance accurately. Almost all of these standards require a simultaneous confirming test to verify the results of the direct or principal test, and the

methods they specify for these confirming tests are critically reviewed. The chapter then examines the extent to which these standards are attainable in routine checks or *surveys* of performance of machines on site. It reviews current practice on South African mines here, principally the confirming checks (corresponding to the confirming tests of the standards) employed to verify the results of the principal check. The deficiencies of these confirming checks are pointed out.

Turning to the prediction of corresponding normal or optimal performance, the chapter reviews the methods available for doing this, and concludes that fundamentally based mathematical modelling, made practicable by computer, is the most reliable and versatile method. The chapter finally summarises where current practice in assessing site performance of machines can be improved, and states where the thesis contributes here.

4.1 Fundamental Concepts and Definitions

In concept, any technical process can be represented as in Figure 4.1 (Isermann, 1982), with the following quantities:

- measurable, time-varying *input variables* or *inputs;*
- measurable, time-varying *output variables* or *outputs,* combined with non-measurable noise from the process (and its controlling and measuring equipment);
- non-measurable *process parameters,* which are either constant or change slowly with the passage of time, and
- measurable and non-measurable, time-varying *state variables.*

For the process in the generalised water chilling machine of Figure 3.5, examples of these quantities are given in Table 4.1.

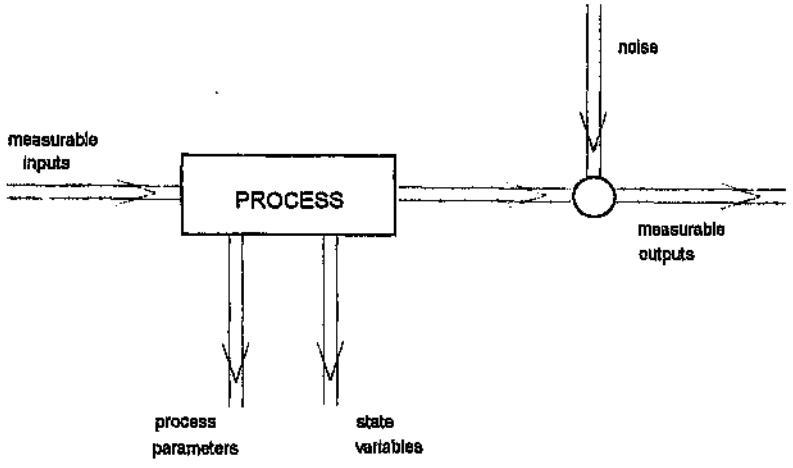

Figure 4.1 Representation of a Process (Isermann, 1982)

Table 4.1 Examples of Process Quantities in Generalised Water Chilling Machine

Process Quantity	Examples in Gen. Water Chilling Machine
Measurable inputs	Mass flow-rates and properties of all fluid streams entering through the machine boundary: e.g. for each entering water stream, mass flow $m_{(w)}$, inlet temperature $t_{(w)i}$, etc. Flows of work entering through the machine boundary.
Measurable outputs	Mass flow-rates and properties of all fluid streams leaving through the machine boundary: e.g. for each leaving water stream, mass flow-rate $m_{(w)}$, outlet temperature $t_{(w)o}$, etc.
Process parameters	Attributes (specifications) of machine components; total mass (termed *charge)* of refrigerant in machine; concentrations of contaminants (water, oil, etc.) in refrigerant charge; water-side fouling factors in evaporator(s) and condenser(s).
State variables	Masses of refrigerant residing in components of machine.

4.1.1 Effectiveness and Quality of Performance

Measures of performance of a water chilling machine, comprising both measurable and derived quantities, fall into two classes. Measures of *effectiveness of performance* are measurable quantities like chilled water flow-rate and outlet temperature, and derived quantities like water chilling

load. Measures of *quality of performance* are measurable quantities like input power, and derived, characteristic quantities like COP.

4.1.2 Normal, Design, Optimal and Satisfactory Performance

The performance of interest in a water chilling machine in a mine fluid cooling installation is the *static* performance; the time constants of the machine components which store mass[1] and energy are of the order of minutes, whereas the inputs generally vary far more slowly over time. Dynamic effects on machine performance are thus usually of relatively short duration[2] and negligible.

Normal performance is static performance when all process parameters and state variables are at their specified design values, regardless of the inputs. *Design performance* is normal performance when the operating regime is at design specification, that is, all inputs are at their specified design values and the control philosophy is at design specification.

Optimal performance is static performance when all measures of effectiveness and quality of performance satisfy specified criteria of optimality. (The process parameters and state variables are *not* constrained to be at their design values.) From the mine's viewpoint, as mentioned above, the criteria of optimality are most likely to be the specified or maximum delivery of chilled water, at the specified or lowest possible temperature, without jeopardising machine effectiveness and availability. Other criteria such as minimum running cost or optimal COP are not likely to be adopted if they conflict with this.

Satisfactory performance is static performance when, for the prevailing operating regime,

---

[1] Here, of liquid refrigerant and oil.

[2] Examples are short-term disturbances due to starting or stopping machines, adjusting regulating devices in step fashion, etc.

(a) the measures of effectiveness of actual performance correspond, within pre-agreed tolerances, to those required - or approach them as closely as the machine's specifications and the achievable limits of its process parameters permit, *and*

(b) the measures of quality of actual performance correspond, within pre-agreed tol nces, to - or are better than - the normal values, that is, the values which would obtain under corresponding normal performance.

4.1.3 Assessment of Performance

Therefore, in order to assess whether actual performance is satisfactory,

1) actual performance must be ascertained with acceptable accuracy; that is, all measurable quantities must be ascertained accurately enough so that the uncertainties in the measures of actual performance are small enough for it to be meaningfully compared with corresponding normal (or optimal) performance; and

2) corresponding normal (or optimal) performance must be either known in advance or predicted, with sufficient accuracy for actual performance to be meaningfully compared with it and so assessed for satisfactoriness.

Where one or both criteria for satisfactory performance are not met, actual performance is unsatisfactory. Some discrepancies between actual and normal measures of performance are then outside the pre-agreed tolerances and fall short of the requirements of the mine, and are thus judged as unacceptable *shortfalls* in performance. Unless these shortfalls are wholly due to an off-design operating regime,[3] the undesirable values

[3] That is, some inputs being at off-design values; the control philosophy not being at design specification; or both of these.

of state variables or process parameters, termed *faults*, partially or wholly causing these shortfalls must then be identified and remedied.

4.2 Ascertaining Actual Performance

4.2.1 Concepts and Definitions

In a routine check or *survey* of site performance of a water chilling machine, the *principal measurements* are those used to directly derive the required measures of performance. The *principal measures of performance* are the measures of effectiveness and quality of performance so derived.

The principal measurements in a routine survey of a generalised water chilling machine (Figure 3.5) are those of flow-rate and inlet and outlet temperatures of the water streams being chilled; and electrical input power to the compressor motors and all auxiliary devices. The principal or *apparent* measures of performance - apparent water chilling load $\sum Q_{(w)EBp}$, apparent mechanical input power $\sum W_{VCBp}$ and apparent COP $\sum Q_{(w)EBp} / \sum W_{VCBp}$ - are derived therefrom. Additional measurements are normally taken for two reasons:

1) to verify the principal measures of performance and hence the principal measurements. Such additional measurements are called *confirming measurements;*

2) to provide more complete information on the process, both in themselves and by enabling non-measurable process parameters or state variables to be estimated if required.

The simultaneous confirming measurements made are of:

- flow-rate and inlet and outlet temperatures of the heat-removing water streams passing through the condenser block; the apparent heat-removing water load $\sum Q_{(w)CBp}$ is derived therefrom;

- refrigerant pressures, temperatures and sometimes flow-rates[4] at all points in the refrigerant circuit which are key points in the refrigerating cycle.[5]

4.2.2 Standards for Testing Performance of Water Chilling Machines

Well-established international standards, referred to below, are the authorities in reliably and accurately ascertaining the performance of water chilling machines. All these standards ascertain performance by *testing* under controlled conditions: that is, measurements are made under conditions artificially held steady, within tight tolerances, for the purpose of ascertaining performance with high accuracy. Also, some operating conditions may be set at specified values. In contrast, when *checking* the operating performance of machines on site, the prevailing conditions are neither altered nor artificially held steady. Isermann (1982) concisely explains this difference between checking and testing:

> "Fault detection in processes can be effected by checking or by testing. When 'checking' is referred to, it is understood that particular actual values during operation are examined to see if they are within a certain tolerance of the normal value... 'Testing' means checking by means of certain artificially introduced test signals, circuits or measurements."

Moreover, when testing a machine according to a standard, all measuring instruments must meet the specifications of that standard and have their calibration certified. On the other hand, routine checks or surveys of performance must rely on the available, infrequently calibrated, site-fitted instruments except where facilities exist for quantities to be measured by more frequently calibrated, portable instruments of better accuracy.

---

[4] As mentioned on page 65, Chapter 3, sensors to measure refrigerant flow-rates are seldom fitted. This will be elaborated upon in Chapter 5.

[5] Other quantities appropriate to the machine, for example oil levels and temperatures in the compressor lubricating oil circuit, are of course also measured.

Nevertheless, as a reference point, it is helpful to examine the provisions of the various established standards for ascertaining the performance of water chilling machines by testing. These standards are:

1) Air-Conditioning and Refrigeration Institute (ARI) Standard 550-92, "Standard for Centrifugal and Rotary Screw Water-Chilling Packages" (ARI, 1992);

2) BS 7120, "British Standard Specification for Rating and Performance of Air to Liquid and Liquid to Liquid Chilling Packages" (BSI, 1989);

3) ASHRAE Standard 30-78, "Methods of Testing Liquid Chilling Packages" (ASHRAE, 1978); and the superseding ANSI/ASHRAE Standard 30-1995, "Method of Testing Liquid-Chilling Packages" (ASHRAE, 1995);

4) ISO Recommendation R916, "Testing of Refrigerating Systems" (ISO, 1968);[6] and

5) two parts of the draft international standard, ISO/DIS 916, intended to replace ISO R916:

    - ISO/DIS 9 3-1, "Refrigeration Systems - Test Methods - Part 1: Testing of Systems for Cooling Liquids and Gases Using a Positive Displacement Compressor" (ISO, 1992);

    - ISO/DIS 916-3, "Refrigeration Systems - Test Methods - Part 3: Testing of Systems for Cooling Liquids and Gases Using a Turbocompressor" (ISO, 1994).

All these standards and draft standards do make the abovementioned principal measurements, and derive net refrigerating capacity, COP, and other principal measures of performance therefrom. The principal

---

[6] And the relevant DIN Standard, DIN 8976 (1972), "Leistungsprüfung von Verdichter-Kältemaschinen", which is identical to ISO R916.

measurements are collectively termed the **principal (or primary) test.** In addition, all standards except BS 7120 (BSI, 1989) require a simultaneous **confirming test,** consisting of additional measurements which are used to derive the required measures of performance independently and indirectly. These indirectly derived measures of performance are then used to verify the corresponding, directly derived ones of the principal test.

Table 4.2 Methods for Confirming Test in Standards

Method for Confirming Test	*Measures of performance indirectly derived using:*
Condenser energy balance method (ISO, 1968; ISO, 1992; 1994; ASHRAE, 1978)	apparent heat-removing water load $\sum Q_{(w)CBp}$; refrigerant-circuit enthalpies; auxiliary heat flow-rates and power inputs
Overall energy balance method (ISO, 1968; ISO, 1992; ASHRAE, 1978, 1995; ARI, 1992)	$\sum Q_{(w)CBp}$; apparent input power $\sum W_{VCBp}$
Refrigerant flow/quantity method (ISO, 1968; ISO, 1992, 1994; ASHRAE, 1978)	refrigerant-circuit enthalpies; refrigerant mass flow-rates
Compressor energy balance method (ISO, 1968)	$\sum W_{VCBp}$; refrigerant-circuit enthalpies; auxiliary heat flow-rates and power inputs

Table 4.2 above lists the prescribed methods for the simultaneous confirming test.[7] These confirming methods are now critically reviewed. Following this, the requirements of these standards on accuracy of measurement, test procedures, process parameters and instrumentation are reviewed.

Methods for Confirming Tests

Condenser energy balance method. This presumes accuracy of measurements in the water circuits of the condenser block and the

[7] In addition to the methods in this table, the ISO/DIS draft standards (ISO, 1992, 1994) include one based on the refrigerant mass or volumetric flow-rate determined from a separate test of the compressor under reference conditions. This method is omitted here because it is generally not suitable for site testing or checking, where varying conditions are encountered.

refrigerant circuit. *Single* refrigerant flows $m_{(r)CB}$ and $m_{(r)EB}$ entering and leaving the condenser and evaporator blocks are assumed. As described in Appendix 3, the method uses the apparent heat-removing water load $\sum Q_{(w)CBp}$ (termed *condenser* water load by the standards), and refrigerant enthalpies derived from pressure and temperature measurements in the refrigerant circuit, to estimate the refrigerant flow-rate $m_{(r)CB}$ through the condenser block:

$$m_{(r)CB} = \frac{\sum Q_{(w)CBp} + \sum Q_{(w)CB(VCB)} + \sum Q_{(s)CB}}{h_{CBo} - h_{CBi}} \qquad (4\text{-}1a)$$

where h_{CBi} and h_{CBo} are the refrigerant enthalpies at the inlet and outlet of the condenser block; and $\sum Q_{(s)CB}$ is the estimated net heat flow entering its external surfaces from its surroundings.

The refrigerant flow-rate $m_{(r)EB}$ through the evaporator block is estimated next. As shown in Appendix 3, this is given by the general relation

$$m_{(r)EB} = m_{(r)CB} \cdot \frac{h_{CBi} - h_{CBo}}{h_{EBo} - h_{EBi}} \cdot \frac{COP_{(r)}}{1 + COP_{(r)}} \qquad (4\text{-}1b)$$

where h_{EBo} and h_{EBi} are the refrigerant enthalpies at the refrigerant outlet and inlet, respectively, of the evaporator block, and $COP_{(r)}$ is the refrigerant-circuit COP of the machine as defined by (3-11c).

Finally, the confirming value of net chilling capacity, $\sum Q_{(w)EBc}$, is given by

$$\sum Q_{(w)EBc} = m_{(r)EB}\left(h_{EBo} - h_{EBi}\right) - \sum Q_{(w)EB(VCB)} - \sum Q_{(s)EB} \qquad (4\text{-}1c)$$

where $\sum Q_{(s)EB}$ is the estimated net heat flow into the external surfaces of the evaporator block from its surroundings.

Overall energy balance method. This presumes accuracy of measurements in the water circuits of the condenser block and of measured input power. Here, (3-7c) is merely rearranged to yield the confirming value of net chilling capacity, $\sum Q_{(w)EBc}$, from the apparent heat-removing water load $\sum Q_{(w)CBp}$ and the input power $\sum W_{VCBp}$ derived from the principal test (ISO, 1968 : 16; ISO, 1992 : 35; ASHRAE, 1978 : 6):

$$\sum Q_{(w)EBc} = -\sum Q_{(w)CBp} - \sum W_{VCBp} - \sum Q_{(w)VCB(Ms)} - \sum Q_{(Ms)} \qquad (4\text{-}2)$$

where $\sum Q_{(Ms)}$ is the net heat flow into the external surfaces of the complete machine from its surroundings.

A modern variant of this method is found in ARI Standard 550-92 (ARI, 1992) and ANSI/ASHRAE Standard 30-1995 (ASHRAE, 1995). Here, using (3-7c), a "per cent heat balance" is calculated, ignoring $\sum Q_{(w)VCB(Ms)}$ and $\sum Q_{(Ms)}$:

$$\%\ \text{heat balance} = \frac{\sum Q_{(w)EBp} + \sum W_{VCBp} + \sum Q_{(w)CBp}}{\sum Q_{(w)CBp}} \times 100 \qquad (4\text{-}3a)$$

For the principal test to be acceptable, this per cent heat balance must be within the following tolerance:

$$\%\ \text{tolerance} = 10{,}5 - 0{,}07(\%FL) + \frac{833{,}3}{DT_{FL}(\%FL)} \qquad (4\text{-}3b)$$

where FL is rated full-duty water chilling load, and DT_{FL} is the *water chilling range* - the difference between inlet and outlet water temperatures in degrees Celsius - at this full load. Figure 4.2 shows that this tolerance thus increases for both decreasing fraction of rated full-duty load and

decreasing water chilling range (when the accuracy of measuring this range must decrease).

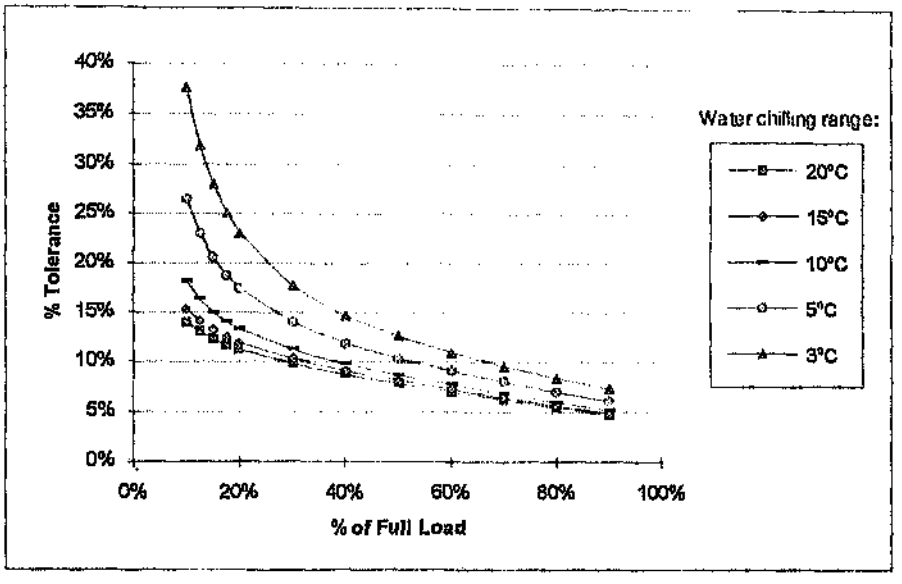

Figure 4.2 ARI Standard 550-92 and ANSI/ASHRAE Standard 30-1995: Tolerances for Heat Balance

Compressor energy balance method. This method involves no water-circuit measurements; it presumes accuracy of refrigerant-circuit measurements and measured input power. Only ISO R916 (ISO, 1968) includes this method; as discussed in Appendix 3, it does so non-explicitly and only for machines with single-stage compressors. However, as shown in Appendix 3, the method is not limited thereto; it is applicable to any vapour-compression block, with single- or multi-stage compressors, provided that *single* refrigerant flows $m_{(r)CB}$ and $m_{(r)EB}$ (as for the condenser energy balance method) enter and leave the condenser and evaporator blocks. The refrigerant flow-rate $m_{(r)EB}$ through the evaporator block is given by, as derived in Appendix 3,

$$m_{(r)EB} = COP_{(r)} \cdot \frac{\left[\begin{array}{l}\sum W_{VCBp} + \sum Q_{(w)VCB(Ms)} \\ -\sum Q_{(w)EB(VCB)} - \sum Q_{(w)CB(VCB)} + \sum Q_{(s)VCB}\end{array}\right]}{h_{EBo} - h_{EBi}} \qquad (4\text{-}4)$$

where $\sum W_{VCBp}$ is the apparent input power and $\sum Q_{(s)VCB}$ is the net heat flow into the external surfaces of the vapour-compression block from its surroundings. $\sum Q_{(w)EBc}$ is then obtained by (4-1c).

Refrigerant flow/quantity method. This presumes accuracy of only the refrigerant-circuit measurements. Here, refrigerant flow-rates entering or leaving the evaporator block are measured directly by quantity or flow meters, and, in conjunction with refrigerant enthalpies, used to calculate $\sum Q_{(w)EBo}$ by (4-1c) above. Alternatively, refrigerant flow-rates entering or leaving the *condenser* block are measured and checked for sufficiently close correspondence with calculated values derived from the principal test.

Remarks on Confirming Methods

Condenser and compressor energy balance methods. First, as already noted, these methods assume *single* refrigerant flows entering and leaving the evaporator and condenser blocks of the machine being tested. This assumption is not true for the generalised machine of Figure 3.5, so it is not always true for the water chilling machines subsequently described in Chapter 3. In particular, it is not true for conventional machines *when hot gas is being bypassed or any other auxiliary refrigerant flows occur.* Neither is it true for the custom-built machine of Figure 3.23,[8] for example. The condenser and compressor energy balance methods are thus not universally applicable unless extended to

[8] Here, each evaporator is served by its own compressor, so two refrigerant streams, of differing mass flow-rates and properties, enter and leave the evaporator block.

cater for multiple refrigerant flows entering and leaving the evaporator and condenser blocks.

Second, as seen from (4-1b) and (4-4), these methods require the refrigerant-circuit COP $COP_{(r)}$, and hence all the measurements in the refrigerant circuit needed to calculate this. Some such measurements must be of refrigerant mass flow-rates where $COP_{(r)}$ depends on these[9] in addition to enthalpies. As is clear from formulae (3-24) through (3-26) for the custom-built machines discussed in Chapter 3, the amount of measurements needed to calculate refrigerant-circuit COP increases with the complexity of the refrigerant circuit. *Only where all such measurements can be made can the condenser and compressor energy balance methods be used.*

Finally, these methods presume accuracy of measurements in the refrigerant circuit. Fortunately, accurate measurements are generally easier to assure here than in the water circuits, because the refrigerant circuit is a closed circuit, and thus less subject to detrimental processes caused by continuously infiltrating contaminants.

Condenser and overall energy balance methods. These methods presume accuracy of measurements in the water circuits of the condenser block. As seen later, it is thus unwise to use them for routine surveys of machine performance, where accuracy of some such measurements, particularly of water flows, may not be assured.

---

[9] More precisely, $COP_{(r)}$ depends on *ratios* of auxiliary to main refrigerant flow-rates, as noted in Chapter 3, page 64. See, for example, (3-24) for the custom-built machine of Figure 3.22. Where the refrigerant flow-rates needed to evaluate such ratios are the same as those required by the refrigerant flow/quantity method, it is of course simpler to use the latter method directly.

Accuracy Requirements for Principal Measurements

All the aforementioned standards require that the instrumentation used must be of specified accuracy and be calibrated both before and after the test. The principal measurements must be of the accuracies given in Table 4.3 below. Here, it is important to note the difference in philosophy between ISO R916 (ISO, 1968) and the other standards. The others explicitly specify allowable uncertainties for the individual principal measurements. ISO R916 does not do this; instead, it specifies allowable uncertainties *in the final results* (that is, in measures of performance), and leaves the instrument accuracy to be selected accordingly.

Table 4.3 Accuracies Required by Standards for Principal Measurements

Quantity	ISO R916	ISO/DIS 916 and BS 7520	ASHRAE 30 and ARI 550
Water flows	-	±1%	±1% within range of flows measured
Temperatures to determine heat flow to/from water circuits	to achieve uncertainty of ±7% in chilling capacity	±0,1°C	±0,08°C[10]
Electrical power/energy input	to achieve uncertainty of ±5% in measurement of power absorbed	±1% of measured value	±0,5% of reading

For all standards except ISO R916, the uncertainties accordingly achieved in the directly derived water chilling capacity are calculated per Appendix 4 and depicted in Figure 4.3. As seen, accuracies of ±5 per cent or better in water chilling capacity can be achieved provided that water chilling range is 3°C or more. At a water chilling range of 5°C or more, accuracies of ±3 per cent or better can be achieved. These accuracies are, of course, far better than those required by ISO R916. ISO R916 states, though, that its recommended accuracies apply to

[10] For ASHRAE 30-78 (1978). The superseding ANSI/ASHRAE 30-1995 (1995) refers to ANSI/ASHRAE Standard 41.1-1986 for the required accuracy.

"normal industrial tests". As will be seen later, this standard is the only one attainable in routine surveys of performance of machines.

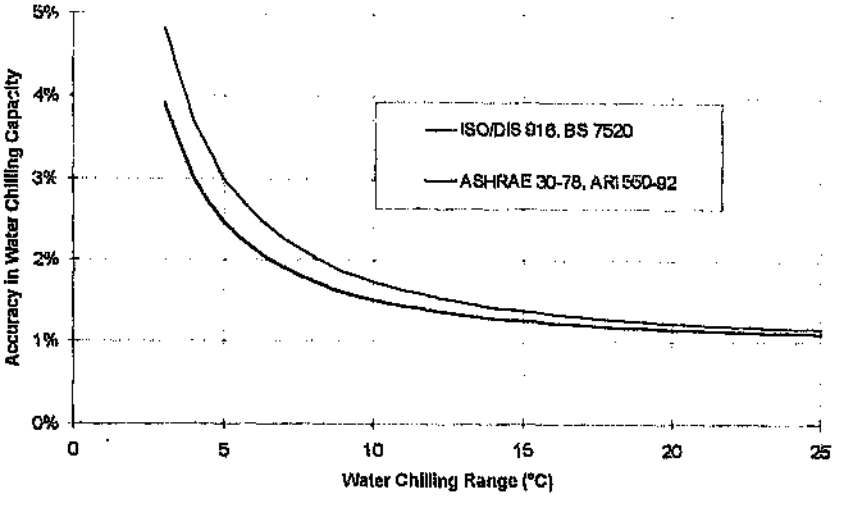

Figure 4.3 Accuracies in Water Chilling Capacity Yielded by Standards

Stipulated Test Procedures, Process Parameters and Instrumentation

ISO R916 (ISO, 1968) and the ISO/DIS draft standards (ISO, 1992, 1994) require the water chilling range to be at least 3°C. The ISO/DIS draft standards likewise require that the heat-removing (condenser) water must rise in temperature by at least 3°C.

Process parameters. All standards require the refrigerant charge to be correct, non-condensable gases to be removed, and the content of compressor lubricating oil in the liquid refrigerant not to be excessive.

Positioning of instruments: refrigerant circuit. Where both pressure and temperature of refrigerant are to be measured, the standards require these measurements to be made at the same point (cross-section).

Positioning of instruments: water circuits. To ensure that net (i.e. useful) water chilling capacity is measured, the ASHRAE and ARI standards (ASHRAE, 1978, 1995; ARI, 1992) stipulate that if chilled water is used to cool the compressor motor or for some other incidental functional use (e.g. cooling the compressor oil), then temperature and flow-rate of chilled water must be measured at points *beyond* (i.e. further from the evaporator than) such take-offs and returns, as illustrated in Figure 4.4.

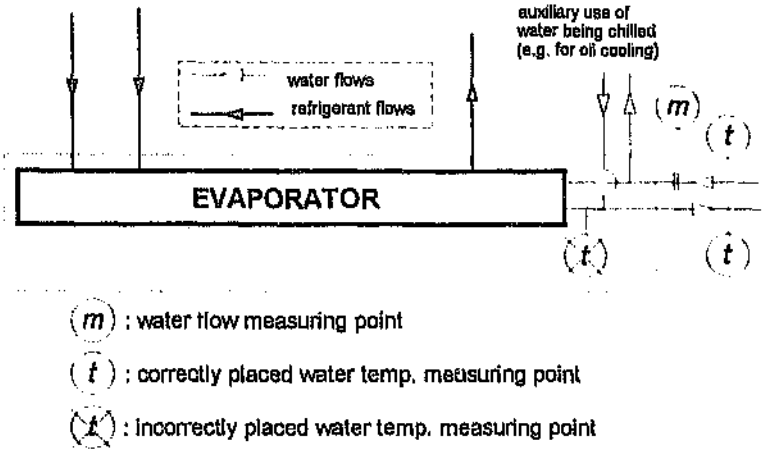

Figure 4.4 Positioning of Temperature and Flow-Rate Measuring Points in Chilled Water Circuit to Measure Net Chilling Capacity

ASHRAE Standard 30-78 and ARI Standard 550-92 also stipulate that if condenser water is used to cool the compressor motor or for some other incidental functional use (e.g. cooling the compressor oil), then temperature and flow-rate of condenser water must be measured at points *ahead of* (i.e. closer to the condenser than) such take-offs and returns, so that the measured heat load reflects gross condenser heat rejection. This is illustrated in Figure 4.5. ASHRAE 30-78 presumably stipulates this to

ensure accuracy in the confirming test by the condenser energy balance method.[11,12]

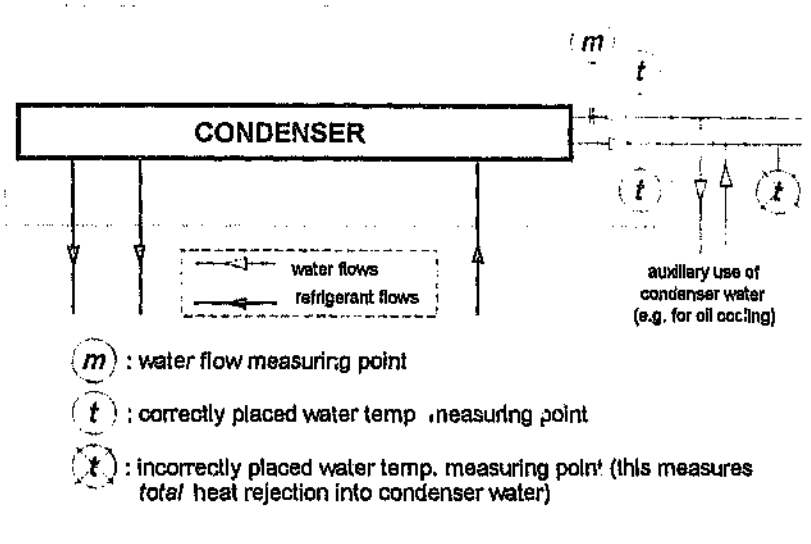

Figure 4.5 Positioning of Temperature and Flow-Rate Measuring Points in Condenser Water Circuit to Measure Gross Condenser Heat Rejection

Accuracy of confirming measurements. The standards require accuracies of confirming measurements to be as in Table 4.4 below.

Steadiness of conditions during test. The standards limit deviations from specified values of certain quantities as in Table 4.5 below.

---

[11] If the water flow-rate and temperature measuring points are beyond such take-offs and returns, the auxiliary water flows passing through these take-offs and returns pass through the condenser's thermodynamic boundary. In applying the condenser energy balance method, the net heat load due to such auxiliary water flows must then be taken into account as $\sum Q_{(w)CB(VCB)}$ in (A3-2), Appendix 3.

[12] It is not clear why ARI 550-92 makes this stipulation, because it prescribes only the overall energy balance method as the confirming test. ANSI/ASHRAE 30-1995 also prescribes only this method, which is presumably why it stipulates the opposite - namely that temperature and flow-rate of condenser water must be measured at points *beyond* such take-offs and returns, so that the measured heat load reflects "gross heat rejection" - i.e. *total* heat rejection into the condenser water.

Table 4.4 Accuracies Required by Standards for Confirming Measurements

Quantity	ISO R916	ISO/DIS 916	BS 7520	ASHRAE 30[13] and ARI 550
Temperatures *(apart from water-circuit temperatures)*	graduations must permit reading to ±0,5°C	±0,3 K	±0,1°C	±0,08°C
Condensing and evaporating refrigerant pressures	to permit calculating corresponding temperatures to ±0,5°C	±1% for abs. suction pressure; ±2% for other abs. pressures	-	to permit determining saturation temp. to within ±0,14°C
Other refrigerant pressures	-		-	

Table 4.5 Deviations Allowed by Standards from Specified Values of Quantities

Quantity	ISO R916	ISO/DIS 916[14]	BS 7520	ASHRAE 30 and ARI 550
Inlet and outlet chilled water temperatures	maximum permissible deviations should be laid down	outlet: ±0,2 K	±0,3°C	±0,28°C (ASHR. 30-78) ±0,3°C (ASHR. 30-1995) ±0,3°C (ARI)
Chilled water temp. range	-	±0,2 K	-	±0,28°C or ±0,3°C (ASHR.)
Heat-removing (condenser) water temperatures		inlet: ±0,3 K		
Heat-removing (condenser) water temp. range	-	±0,2 K	-	-
Water flow-rates	-	±2%	-	±5%
Electrical supply	-	Voltage: ±3% Current, frequency: ±1%	Voltage: ±2%	ARI only: Voltage: ±10%; Freq.: ±1%

[13] For ASHRAE 30-78 (1978). The superseding ANSI/ASHRAE 30-1995 (1995) refers to ANSI/ASHRAE Standards 41.1-1986 and 41.3-1989 for the required accuracies of temperature and pressure measurements respectively.

[14] "Greater deviations", the limits of which are unspecified, are allowed provided that the difference of the refrigerating capacities obtained by the principal and the confirming tests does not exceed 15% (ISO/DIS 916-1) or 10% (ISO/DIS 916-3) of that obtained by the principal test. This criterion is of dubious validity, though; it is likely to be very difficult to evaluate what proportions of such percentage differences are due to instrument error as opposed to dynamic effects caused by such "greater deviations".

Amount of, and interval between, successive test readings. Stipulations here are as in Table 4.6.

Table 4.6 Stipulations of Standards for Test Readings

Quantity	ISO R916	ISO/DIS 916	BS 7520	ASHRAE 30 and ARI 550
Sets of readings necessary for calculation of performance	at least 10	at least 5	7 consecutive sets within tolerated deviations of Table 4.5	at least 3 consecutive sets within limits of Table 4.5
Interval between successive sets of readings	max. 20 min.	at least 15 min.	10 min.	≥ 10 min. (ASHR. 30-78) ~5 min. (ASHR. 30-1995; ARI)

4.2.3 Checking Site Performance of Water Chilling Machines

The stipulated test procedures and instrumentation required by these standards are now compared to the available facilities and feasible procedures for the routine checks or surveys of machines on site. It is quickly seen that it is very difficult to attain the requirements of these standards, except for ISO R916 (ISO, 1968), in such surveys.

Process Parameters

Proper maintenance of the machine will ensure that the refrigerant circuit is in good order, and that the stipulations on page 135 for its process parameters are thus met. Such maintenance, though, is often lacking.

Steadiness of Conditions during Surveys

As mentioned above, operating conditions are not artificially held constant for the purpose of *checking* performance, and in general do vary. Electrical voltage and frequency, and thus compressor speed, are generally well-behaved. However, the stipulations for steadiness of the other quantities, particularly temperatures, in Table 4.5 will not be met except for most underground installations, which operate under virtually

constant diurnal duty, as recalled from Table 2.1. For all other installations, diurnal variations in load and lift are liable to cause water temperatures, temperature ranges, or flow-rates to vary more widely than the standards permit.

This means that measurements have to be taken quickly and simultaneously, which requires many observers unless fitted instrumentation records measurements automatically. Often, sufficient observers are not available, as noted by Anderson and Dieckert (1990):

> "Often, simultaneous temperature, flow and power measurements could not be taken manually. Done manually, simultaneous measurements required one person per gauge plus one to do calculations."

Also, rarely is there enough time during routine surveys to meet the stipulations of Table 4.6; if manual measurements are necessary, it is normally attempted to take at least three consecutive sets of simultaneous measurements at 5-minute intervals.

Instrumentation Fitted to Machines on Site

Attention is next turned to the normally available instrumentation compared to that required by the standards as listed in Tables 4.3 and 4.4. Fitted instrumentation, of course, is for two purposes: monitoring and control. Often, one instrument performs both functions. Particularly in conventional machines, the minimum amount of instrumentation is provided in the refrigerant circuit, unless more and better-quality instrumentation is specified when ordering. Site-fitted instrumentation is often calibrated only quarterly or during annual shutdowns. Departures from the requirements of the standards are as follows.

Positioning of instruments: refrigerant circuit. Seldom are measuring points for refrigerant pressure and temperature fitted at the same cross-

section where both are to be measured. Thermowells to measure temperatures at key points in the refrigerant circuit are generally fitted; but as they are usually meant to give only an approximate indication for monitoring purposes, they are not always mounted in the best position to give the accurate readings required by the standards. Refrigerant pressure measuring points are generally provided for only evaporating and condensing pressures, and sometimes for economiser pressures and compressor suction and discharge pressures.

Positioning of instruments: water circuits. Temperature measuring points in the chilled water circuit are sometimes placed in the positions shown as incorrect . . Figure 4.4 and Figure 4.5. Unfortunately, the standards give no guidance on how to accommodate this possibility. If the evaporator outlet water temperature measuring point is positioned incorrectly, this means that gross, not net, water chilling capacity is measured. If the conde .ser outlet water temperature measuring point is positioned "incorrectly", *total* heat rejection into the condenser water is measured - i.e. that of auxiliary components (such as oil coolers) *plus* that of the condenser. This ensures the accuracy of a confirming check by the overall energy balance method, but can cause serious error in such a check by the condenser energy balance method.[15]

Water circuits: instruments measuring temperatures. Fitted temperature-measuring instrumentation in the chilled and condenser water circuits consists of indicators connected to sensors mounted in thermowells in the water piping. These thermowells should be installed correctly.[16] The sensors may be thermocouples, thermistors or platinum-resistance types;

---

[15] Unless such auxiliary heat loads are taken into account; see footnote 11 on page 137.

[16] To ensure that the measured temperatures are the average bulk stream temperatures. In brief, such thermowells should be of low thermal conductivity, and extend into the piping for approximately two-thirds of its diameter. When installed for measuring outlet water temperatures of the evaporator and condenser, they should be situated sufficiently downstream of pipe fittings to guard against stratification (York Division, Borg-Warner Corporation, 1971).

indicators are analogue or digital. Resolution to lower than 0,1°C is not always provided, and if not, these thermometers cannot provide the accuracies required by ISO/DIS 916, ASHRAE 30-78 and 30-1995, and ARI 550-92. Extra thermowells are generally provided to enable observers conducting manual surveys to use their own portable, calibrated temperature-measuring instruments. Such portable instruments may be of the abovementioned types or be mercury-in-glass thermometers calibrated for partial immersion, in either case desirably having resolutions of 0,01°C and accuracies of no worse than ±0,05°C after calibration.

Water circuits: instruments measuring flow-rates. Fitted water flow-rate sensors in the water circuits are mostly of the invasive type (orifices or sometimes pitot tubes) generating a differential pressure. Difficulties with such water flow-rate sensors are well known, but deserve brief recapitulation. As noted by Anderson and Dieckert (1990), "Water flows proved to be the most difficult, expensive and critical to measure in the field."

As is well known (see, for example, Brain and Scott, 1982), the mass flow-rate of liquid $m_{(\ell)}$ through an orifice is given by

$$m_{(\ell)} = Ca_2\sqrt{2\rho_{(\ell)1}\left(\Delta P_{(\ell)}\right)} \qquad (4\text{-}5)$$

where C is the coefficient of discharge of the orifice; a_2 is the cross-sectional area of the orifice; $\rho_{(\ell)1}$ is the liquid density at the orifice inlet; and $\Delta P_{(\ell)}$ is the pressure differential across the orifice. The performance characteristics of flow-measuring orifices are well established, and if they are manufactured, installed and used to a standard such as ISO 5167, they can be used, uncalibrated, to measure flow-rates to within an uncertainty of ±2 per cent (Brain and Scott, 1982). However, their accuracy is dependent on:

accurate measurement of pressure differential;

(ii) accurate knowledge of the coefficient of discharge; a minimum uncertainty of ±0,6 per cent exists here (Brain and Scott, 1982);

(iii) maintenance of critical meter dimensions in service, especially smoothness of the upstream face and sharpness of the inlet edge. Even very slight rounding of the inlet edge can cause significant changes in the discharge coefficient (Brain and Scott, 1982). For the same reason, care must be taken to avoid even slight corrosion, wear or fouling during service;

(iv) proper location of the meter with respect to other flow-disturbing elements in the system (performance is affected markedly by changes in upstream pipework configurations).

Orifice plates for mine use are generally of stainless steel to minimise corrosion; but as mine water typically contains suspended solids (Pulles, 1992), orifice plates suffer wear in service. Also, their rangeability is low, being less than 4 to 1 in most cases. This is because at a quarter of the flow, it can readily be seen from (4-5) that the pressure differential drops to 6,25 per cent of that at full flow.

With respect to (iv) above, orifice meters are not always installed per standard recommendations (sometimes it is difficult to do this in tightly confined spaces, particularly underground), and are sometimes installed incorrectly (the wrong way round, for example). As untreated or inadequately treated mine waters are liable to cause either corrosion or scaling (Pulles, 1992), orifice plates and their upstream piping are also subject to these. Often orifice plates are serviced, but their upstream and downstream piping is not, and thus remains corroded or scaled and continues to disturb the flow pattern.

Refrigerant circuit: instruments measuring temperatures. The same remarks apply as for instruments measuring temperatures in the water circuits. Accurate temperature measurements are needed if accurate refrigerant enthalpies are to be determined therefrom.[17]

Refrigerant circuit: instruments measuring pressures. Pressure gauges are almost always of the bourdon tube type. The graduations on these gauges are usually no finer than in Table 4.7 below.

Table 4.7 Graduations on Typical Site Pressure Gauges Fitted to Water Chilling Machines

Refrigerant	Graduations on Pressure Gauges	
	Evaporator Side (lower operating pressure)	*Condenser Side (higher operating pressure)*
R11, R123	2 kPag (0,5 psig, or 0 inch of mercury vacuum[18])	7 kPag (1 psig)
R12, R22, R134a, ammonia	10 kPag (1 psig)	20 kPag (5 psig)

Even if such gauges were perfectly accurate, it can be shown from tabulated refrigerant properties (for example, IIR, 1981) that, with such graduations, saturation temperatures corresponding to indicated pressure cannot be determined to an accuracy of better than between ±1°C and ±0,6°C in the range of refrigerant pressures encountered in mine water chilling machines.[19]

Electric power measurements. Integrating watt-hour meters measuring the electrical energy input to compressor driving motors are typically of

---

[17] And more importantly, if accurate quantities dependent on such enthalpies are to be derived. The relative magnitudes of the partial derivatives in Table A12.1, Appendix 12 are an example of the sensitivity of refrigerant-circuit COP to refrigerant temperatures.

[18] Operating pressures on the low-pressure side of machines employing Refrigerants 11 or 123 are below atmospheric pressure.

[19] This range corresponds to saturation temperatures of between 0°C and 60°C (the latter being the condensing temperature encountered in some underground installations).

Class 2 accuracy. This means that their accuracy will be ±2 per cent, as long as motor power factor is above 0,5. For lower power factors, accuracy worsens (BSI, 1979).

Table 4.8 Accuracy of Measurement Required by Standards and Available on Site

Quantity	Accuracy of Measurement		
	Required by ISO R916	*Required by Other Standards*	*Typically Available on Site*
Water flows	-	±1%	±2% at best; worse regardless at lower-than-design flows
Temperatures to determine heat flow to or from water circuits	to achieve uncertainty of ±7% in chilling capacity	±0,08°C to ±0,1°C	±0,1°C or better with portable instruments
Electrical power/energy input	to achieve uncertainty of ±5% in measurement of power absorbed	±0,5% to ±1%	≥±2%; worse at motor power factors < 0,5
Temperatures apart from water-circuit temperatures	graduations must permit reading to ±0,5°C	±0,08°C to ±0,5°C	±0,1°C or better with portable instruments
Condensing and evaporating refrigerant pressures	to permit calculating corresp. temperatures to ±0,5°C	• ±1% for abs. suction pressures; ±2% for other abs. pressures • to permit calculating corresp. saturation temperatures to between ±0,14°C and ±0,5°C	• ±2% of full-scale deflection • permits calculating sat. temperatures to between ±1°C and ±0,6°C
Other refrigerant pressures	-	to permit calculating corresp. saturation temperatures to ±0,14°C	as above

Standards Attainable in Site Surveys

Table 4.8 summarises the requirements of the aforementioned standards compared to the accuracy of measurement typically available on site. It is clear from this table that ISO R916 (ISO, 1968) is the only standard attainable in routine site surveys of performance. ISO R916 does require

refrigerant pressure gauges of higher quality than customarily fitted, but this is easily achieved. It does not require accuracies in measuring water flow and electrical energy input which are beyond the capabilities of customary site-fitted instruments. This is because it simply specifies that the accuracies of principal measurements must be such that the determination of chilling capacity therefrom is accurate to within ±7 per cent.

The accuracy in measuring water temperatures which will satisfy this requirement of ISO R916 is calculated in Appendix 4 and plotted in Figure 4.6 below for assumed uncertainties in water flow measurement of ±2%, ±5% and ±6%. So, for instance, if water flow-rate measurement uncertainty is ±5 per cent, and water chilling range is 5°C, the required accuracy of each water temperature measurement is ±0,17°C or better.

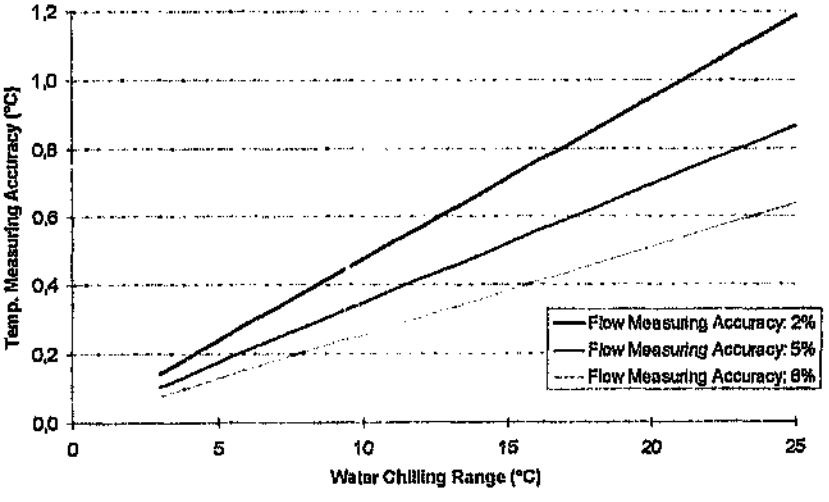

Figure 4.6 Required Temperature Measuring Accuracy for Uncertainty of ±7% (ISO R916 Requirement) in Calculated Water Chilling Capacity

According to Figure 4.6, if the water chilling range is at least 5°C and the accuracy of flow measurement is no worse than ±6 per cent, the overall

uncertainty of ±7 per cent specified by ISO R916 for water chilling capacity can be attained with a temperature measuring accuracy of ±0,1°C, which is attainable with portable, calibrated instruments.

There is a further reason why ISO R916 (ISO, 1968) is the only standard attainable in routine surveys of performance. As recalled from Table 4.2, it is the only one including the compressor energy balance method for the confirming test. *Unless refrigerant flow meters are installed - which is seldom the case - this method is the best, in principle, for the confirming check in routine surveys.* This is because with infrequently calibrated site-fitted instrumentation, measurements of water flow-rates are most liable to error, as most fitted water-flow sensors are invasive types, which are subject to wear, corrosion and fouling under the arduous conditions typically prevailing in mine water circuits. As the apparent heat-removing water load $\sum Q_{(w)cap}$ may be seriously in error for this reason, it is unwise to use the first two confirming methods in Table 4.2 - the condenser and the overall energy balance methods - as the confirming check. In contrast to these first two methods, the compressor energy balance method requires no water-circuit measurements. It requires that of input power, and all measurements in the refrigerant circuit necessary to obtain the refrigerant-circuit COP $COP_{(r)}$. As noted earlier, the accuracy of measurements in the refrigerant circuit is more assured, because this closed circuit is not subject to the fouling and other detrimental processes affecting water circuits. ISO R916, though, only applies the compressor energy balance method to a machine with a single-stage compressor (see Appendix 3), so this method must be extended to conventional machines with a multi-stage compressor, and to custom-built machines. The enhanced Thorp method, presented in Chapter 5, amounts to such an extension most often.

The other confirming method in Table 4.2 - the refrigerant flow/quantity method - also requires no water-circuit measurements, but requires one or

more refrigerant flow meters, which are almost never fitted.[20] It is therefore concluded that instrumentation normally fitted on site does not permit attaining the requirements of any standard except ISO R916 (ISO, 1968). Interestingly, a field testing manual published by a machine manufacturer (York Division, Borg-Warner Corporation, 1971) relaxes the requirements of the ASHRAE and ARI standards[21] in much the same way as ISO R916.[22]

In parenthesis, it is strange that ISO R916 (ISO, 1968) is the only standard to specify the compressor energy balance method, and then only for single-stage machines. The reason is most probably threefold. First, as remarked earlier on page 133, the amount of measurements needed to calculate refrigerant-circuit COP increases with the complexity of the refrigerant circuit. Second if some such measurements are of refrigerant mass flow-rates, it is simpler to use the refrigerant flow/quantity confirming method.[23] Third, including the compressor energy balance method may simply have been deemed unnecessary in the other standards, on the grounds that the other confirming methods adequately cater for all but unusual, rare cases of testing.[24]

Finally, from the remarks on confirming methods on page 132, it is worth emphasising that the standards do not provide adequate confirming

---

[20] If such meters are fitted, this method can of course be used for the confirming check. Fannin and Hundy (1987) review suitable types of such flow meters and give guidance on their installation. Accuracy of most flow meters deteriorates as flow reduces, so the accuracy of this method reduces commensurately.

[21] Obviously, earlier versions of these standards.

[22] For example, by specifying an overall uncertainty of ±5% in water chilling capacity, but leaving the accuracy of the water flow meter unspecified (although it specifies the ASME Power Test Code in the construction of the measuring orifice).

[23] See footnote 9 on page 133.

[24] It is arguable, of course, that it is unrealistic to expect standards to specify confirming methods catering for rare modes of operation in conventional machines, such as hot gas bypass; or to specify confirming methods for custom-built machines, of which there are endless variants. The primary purpose of the standards is to lay down methods for testing well-known designs of machines, such as conventional machines, to verify attainment of specified full- and part-duty performance under conditions agreed to contractually between manufacturer and user.

methods for surveying *site* performance of machines. First, accuracy of site-fitted instruments, particularly water flow meters, is not assured, so neither is the reliability of the overall energy balance method. This is elaborated upon in the next section and in Chapter 5. Second, the condenser and compressor energy balance methods require extension to cater for *multiple* refrigerant flows entering and leaving the evaporator and condenser blocks. The enhanced Thorp method, presented in Chapter 5, represents the best that can be done here in the absence of meters to measure such flows.

4.2.4 Current Confirming Methods on South African Mines

Attention is now turned to the confirming methods currently employed in routine surveys of performance of water chilling machines at South African mines.

The Heat Imbalance

The overall energy balance for the generalised water chilling machine, from (3-7c), is

$$\sum Q_{(w)EB} + \sum W_{VCB} + \sum Q_{(w)VCB(Ms)} + \sum Q_{(w)CB} + \sum Q_{(Ms)} = 0 \qquad (4\text{-}6)$$

The major constituents of this overall energy balance (customarily termed "heat balance") are evaporator block water load $\sum Q_{(w)EB}$, input power $\sum W_{VCB}$ and condenser block water load $\sum Q_{(w)CB}$. The relative heat *imbalance* ε yielded by the *apparent* values $\sum Q_{(w)EBp}$, $\sum W_{VCBp}$ and $\sum Q_{(w)CBp}$ of these major constituents, derived from the performance survey, is computed:

$$\varepsilon = \frac{\sum Q_{(w)EBp} + \sum W_{VCBp} + \sum Q_{(w)CBp}}{\sum Q_{(w)CBp}} \qquad (4\text{-}7)$$

If ε is within the limits of ±5 per cent (following earlier versions of the abovementioned ARI and ASHRAE standards), the principal measurements are taken to be acceptably accurate (Burrows, 1982).

The same practice of accepting the principal measurements on the basis of a small heat imbalance, commonly termed a "close" heat balance, is followed elsewhere in the world. All the aforementioned standards except BS 7120 (BSI, 1989) specify the overall energy balance as one confirming method. A field testing manual of a major manufacturer (York Division, Borg-Warner Corporation, 1971) specifies a heat balance check, including the effect of the compressor oil cooler. Authors of recent articles on field testing of refrigerating machines (Anderson and Dieckert, 1990; Perry, 1987a; Scrine, 1987) all accept a heat balance within certain limits as the criterion by which data can be accepted with confidence and as statistically legitimate.

It can be concluded, therefore, that accepted practice throughout the world is to rely on a sufficiently close, or "acceptable" heat balance as the criterion for accepting the principal measurements as sufficiently accurate. All the aforementioned standards and the above references, though, specify that all measuring instruments, including water flow meters, must be calibrated. As already emphasised, site-fitted instrumentation on water chilling machines at mines is seldom or infrequently calibrated; and *where the calibration of instruments is not assured, an "acceptable" heat imbalance, by itself, is not a guarantee of acceptably accurate principal measurements.*

The reason, as shown in Section 5.1.2, Chapter 5, is that an "acceptable" heat imbalance is necessary *but not sufficient* for acceptably accurate principal measurements. If the relative errors in all apparent constituents of the heat balance - particularly the evaporator and condenser block loads - are similar, then these errors, whether large or small, will also balance each other, yielding a small heat imbalance which may give an

entirely false impression of accuracy. An "unacceptable" heat imbalance does indicate that at least one apparent constituent of the heat balance is unacceptably in error, *but the converse is not true where calibration of site-fitted instruments, including water flow meters, is not assured.*

The Thorp Method for Conventional Machines

If the heat imbalance ε of (4-7) obtained from a performance survey is outside the limits of ±5 per cent, it is judged unacceptable and as indicating unacceptable errors in one or more of the apparent major constituents $\sum Q_{(w)EBp}$, $\sum W_{VCBp}$ and $\sum Q_{(w)CBp}$ of the heat balance (Burrows, 1982). In such an event, the South African mining industry commonly employs a confirming method known as the *Thorp method* (Thorp, 1974) to attempt to identify the most erroneous apparent constituent. For reasons explained later, this method is confined to conventional packaged machines, which have one evaporator, one condenser and one single- or multi-stage centrifugal compressor. The major constituents of the heat balance in conventional machines are thus simply $Q_{(w)E}$, W_{VCP} and $Q_{(w)C}$; their apparent values obtained from a survey are denoted by Q_{Ep}, W_{VCPp} and Q_{Cp}, with $_{(w)}$ in the subscripts deleted for brevity.

Accordingly, the energy balance (assuming that the other terms in (4-6) are zero or comparatively negligible) and COP for a conventional water chilling machine are

$$Q_{(w)E} + W_{VCB} + Q_{(w)C} \cong 0 \qquad COP \cong Q_{(w)E}/W_{VCB} \tag{4-8a}$$

The relations below follow directly:

$$\begin{aligned} Q_{(w)E} &= W_{VCB} \cdot COP &&\cong -Q_{(w)C} \cdot COP/(1+COP) \\ W_{VCB} &= Q_{(w)E}/COP &&\cong -Q_{(w)C}/(1+COP) \\ Q_{(w)C} &\cong -W_{VCB}(1+COP) &&\cong -Q_{(w)E}(1+1/COP) \end{aligned} \tag{4-8b}$$

The Thorp method assumes that *one* apparent constituent Q_{Ep}, W_{VCBp} or Q_{Cp} is unacceptably in error. First, using refrigerant tables, it determines the refrigerant enthalpies at all key points in the refrigeration cycle from the confirming measurements of refrigerant pressures and temperatures. Next, it calculates the refrigerant-circuit COP, $COP_{(r)}$, of the machine, using (3-15b) and (3-23c) for machines with a single-stage compressor and a two-stage compressor respectively. (This is the reason for the Thorp method being confined to conventional machines; the refrigerant-circuit COPs given by (3-15b) and (3-23c) are sole functions of refrigerant enthalpies, and so are determinable once these enthalpies are known.) $COP_{(r)}$ is presumed to accurately reflect actual COP; so then, using $COP_{(r)}$ in the relations of (4-8b), "alternate values" of input power and condenser load are calculated from apparent evaporator load Q_{Ep}:

$$W_{VCB[alt]} = Q_{Ep}/COP_{(r)} \qquad Q_{C[alt]} = -Q_{Ep}\left(1+1/COP_{(r)}\right)$$

Using the relations of (4-8b), similar "alternate values" of evaporator and condenser loads, and of evaporator load and input power, are obtained from W_{VCBp} and Q_{Cp} respectively. The apparent and alternate values of all three constituents of the heat balance are finally tabulated as in Table 4.9.

If the refrigerant-circuit COP indeed accurately reflects actual COP, and all three apparent constituents are accurate, the apparent and alternate values in Table 4.9 will agree closely. If one (and only one) apparent constituent is significantly in error, that apparent constituent will produce alternate values of the other two constituents *differing significantly from both the apparent and the other alternate values of these other two constituents.*

Table 4.9 Thorp Method: Tabulation of Apparent and Alternate Constituents of Heat Balance

	Alternate values calculated on the basis of apparent:		
Apparent and alternate values of:	Evaporator load	Input power	Condenser load
Evaporator load	Q_{Ep} *(apparent value)*	$W_{VCBp} \cdot COP_{(r)}$ (alternate value)	$\frac{Q_{Cp} \cdot COP_{(r)}}{1+COP_{(r)}}$ (alternate value)
Input power	$Q_{Ep}/COP_{(r)}$ (alternate value)	W_{VCBp} *(apparent value)*	$Q_{Cp}/\left(1+COP_{(r)}\right)$ (alternate value)
Condenser load	$Q_{Ep}\left(1+1/COP_{(r)}\right)$ (alternate value)	$W_{VCBp}\left(1+COP_{(r)}\right)$ (alternate value)	Q_{Cp} *(apparent value)*

Thorp's own example (Thorp, 1974), where an "unacceptable" heat imbalance of -7,4% occurred, is reproduced in Table 4.10. Here, the apparent condenser load produced alternate values of evaporator load and input power which were 8 per cent above *both* their apparent *and* their other alternate values (see the shaded column in the table). Moreover, the two alternate values of condenser load agreed with each other (see the shaded row in the table). It was therefore concluded that the apparent condenser load was most likely to be unacceptably in error.

Cases can arise, though, where there is no acceptable agreement between apparent and alternate values of any constituent. This obviously means that more than one apparent constituent is significantly in error; but it cannot be concluded from the tabulation alone which two, or possibly all three, are most likely to be so. Such an example, where the heat imbalance was +23,2%, is given in Table 4.11 below; this is from the survey of the lag machine of Case Study C, Section 5.2.6, Chapter 5.

Finally, cases can occur where the Thorp method draws the wrong conclusion. An example where the heat imbalance of +5,4% was just outside the "acceptable" limits of ±5% is given in Table 4.12 below; this is from the survey of the machine of Case Study B, Section 5.2.4, Chapter 5.

Table 4.10 Thorp Method: Example 1 (Thorp, 1974)

Heat imbalance: -7,4%	*Alternate values calculated on the basis of apparent:*		
Apparent and alternate values of:	Evaporator load	Input power	Condenser load
Evaporator load, kW(R)	1 497 *(apparent value)*	1 500 (alternate value: 0,2% above app. value)	1 617 (alternate value; 8% above app. value)
Input power, kW	372 (alternate value: 0,3% below app. value)	373 *(apparent value)*	403 (alternate value: 8% above app. value)
Condenser load, kW(R)	-1 869 (alternate value: 7% below app. value)	-1 873 (alternate value: 7% below app. value)	-2 020 *(apparent value)*

Table 4.11 Thorp Method: Example 2 (Bailey-McEwan, 1991)

Heat imbalance: +23,2%	*Alternate values calculated on the basis of apparent:*		
Apparent and alternate values of:	Evaporator load	Input power	Condenser load
Evaporator load, kW(R)	2 748 *(apparent value)*	3 447 (alternate value: 25% above app. value)	3 769 (alternate value; 37% above app. value)
Input power, kW	728 (alternate value: 20% below app. value)	914 *(apparent value)*	999 (alternate value: 9% above app. value)
Condenser load, kW(R)	-3 476 (alternate value: 27% below app. value)	-4 362 (alternate value: 9% below app. value)	-4 768 *(apparent value)*

Table 4.12 Thorp Method: Example 3 (Bailey-McEwan, 1990)

Heat imbalance: 5,4%	*Alternate values calculated on the basis of apparent:*		
Apparent and alternate values of:	Evaporator load	Input power	Condenser load
Evaporator load, kW(R)	3 222,6 *(apparent value)*	2 715,6 (alternate value: 16% below app. value)	3 301,3 (alternate value; 2% above app. value)
Input power, kW	779,9 (alternate value: 19% above app. value)	657,2 *(apparent value)*	798,9 (alternate value: 22% above app. value)
Condenser load, kW(R)	- , 002,5 (alternate value: 2% below app. value)	-3 372,8 (alternate value: 18% below app. value)	-4 100,2 *(apparent value)*

Here, apparent input power produced the alternate values of the other two constituents (shown by the shading) differing most from their apparent values. The other alternate and the apparent values of these other two constituents agreed within 2 per cent. Here, the Thorp method would thus conclude that apparent compressor input power is most likely to be unacceptably in error. *Such a conclusion would be completely wrong;* as shown in the discussion of this case in Chapter 5, *apparent input power was in fact accurate,* while apparent evaporator and condenser load were unacceptably erroneous by similar, large percentages: +19% and +21% respectively. These similar errors in the apparent loads, therefore:

- produced alternate values of evaporator and condenser loads which were similarly erroneous and so agreed closely with the erroneous apparent values;
- accounted for the "just unacceptable" heat imbalance of +5,4%; as noted on page 150 and as will be proved in Chapter 5, they virtually cancelled in the computation thereof.

Apart from the possibility of such erroneous conclusions, the Thorp method has another deficiency. The refrigerant-circuit COP calculated by (3-15b) or (3-23c) for a conventional machine with a single- or two-stage centrifugal compressor respectively, may not reflect actual COP adequately for the two reasons noted on pages 64 and 65, Chapter 3. First, it over-estimates actual COP by neglecting the effect of the compressor oil cooler. *Second, (3-15b) and (3-23c) are invalid if auxiliary refrigerant flows, including but not limited to hot gas bypass, are occurring.* For the specific case of hot gas being bypassed, (3-15a) and (3-23b) must be used. Unfortunately, as seen from these latter two relations, refrigerant-circuit COP then depends on the mass flow ratio of bypassing hot gas to liquid refrigerant entering the expansion valve feeding the evaporator, and this mass flow ratio is normally not measured and thus not available.

4.2.5 Desirable Improvements to Current Confirming Methods

The deficiencies of the confirming methods currently employed in routine surveys of performance of water chilling machines on South African gold mines can be summarised as follows.

1. *Heat imbalance within ±5%.* In routine surveys of performance, calibration of site-fitted instruments is not assured, so a heat imbalance within ±5% is *not* a guarantee of acceptably accurate measurements. As already noted and as will be proved in Chapter 5, large but similar errors in, for example, evaporator and condenser block water loads can be present, and such errors will go undetected.

2. *Heat imbalance outside ±5%; conventional machines with no auxiliary refrigerant flows.* First, the refrigerant-circuit COP may be significantly over-estimated because the effect of the compressor oil cooler is neglected. Second, where more than one apparent constituent of the heat balance is unacceptably in error, the Thorp method may either yield no definite conclusion (e.g. Table 4.11) or, where two apparent constituents have similar relative errors, falsely imply that the third such constituent is most in error (e.g. Table 4.12).

3. *Heat imbalance outside ±5%: conventional machines with auxiliary refrigerant flows, and custom-built machines.* The Thorp method cannot be used in these cases, as facilities are generally not available to measure all quantities required to determine refrigerant-circuit COP. The only way of identifying the erroneous apparent constituents is then to check all site-fitted measuring instruments.

It is clear, therefore, that these current confirming methods are unsatisfactory when it is recalled that the whole purpose of a performance survey is to ascertain site performance accurately. The confirming method employed in such a survey should yield independent measures of

performance; conclusively verify whether apparent performance is acceptably accurate or not; and also identify any unacceptably erroneous measurements, or at least give strong indications of such identities. Moreover, it should perform these functions for all classes of water chilling machines, conventional or custom-built, under all their modes of operation. An alternative confirming method that fulfils these functions as completely as possible is therefore needed for site performance surveys, taking the realities encountered therein, such as limitations of site-fitted instrumentation, into account.

Section 4.2.4 above concludes that site-fitted instrumentation does not permit routine performance surveys to attain the requirements of any standard except ISO R916 (ISO, 1968), and that the compressor energy balance method, included in this standard alone, is the confirming method best suited in principle to such surveys. It therefore seems natural to extend this confirming method, which ISO R916 only specifies for machines with a single stage of compression, to all classes of machines on mines in all their operating modes.

The enhanced Thorp method, presented in Chapter 5, does this and more. It produces a confirming value of COP and compares this with the apparent COPs. This confirming COP is the refrigerant-circuit one, $COP_{(r)}$, *but corrected to reflect actual COP as accurately as possible.* Then, if any apparent constituent of the heat balance is independently known to be acceptably accurate, that constituent and the corrected refrigerant-circuit COP can be used to calculate confirming values of the other two constituents, so verifying apparent performance. If that constituent is apparent input power, which it most often is,[25] the enhanced Thorp method amounts to a generalised compressor energy balance

---

[25] Generally, apparent input power is more likely to be acceptably accurate than apparent evaporator or condenser block loads. This is because, as mentioned previously, water flow meters of the invasive type are subject to the detrimental processes affecting mine water circuits.

method.[26] Where $COP_{(r)}$ is a function of not just refrigerant enthalpies, but also of other quantities, such as refrigerant flow-rates - and these other quantities are not measured - an indication of the relative likelihood of unacceptable errors in the apparent performance can still be obtained.

4.3 Predicting Corresponding Normal Performance

As mentioned at the beginning of this chapter, the actual performance of a machine is properly assessed by comparison with corresponding normal (and possibly optimal) performance, either known beforehand or predicted. This normal or optimal performance must be available timeously, and be as accurate as possible. Subsequent actual performance after any remedial action should then justify such action, hence establishing the credibility and value of assessing performance in this way.

Practicable methods of predicting performance under any possible set of inputs, state variables and process parameters - these being collectively termed *operating conditions* - are therefore needed. It is important to note that in the absence of such methods, corresponding normal or optimal performance is simply not obtained. The only yardstick to compare actual performance with is then quoted full-duty, design performance (or, in rare cases, quoted performance at specified off-design conditions). Such comparison may be valid for installations operating under relatively constant conditions, such as most underground installations (see Table 2.1); but it is not valid where actual operating conditions differ considerably from design (or quoted off-design) values. Actual performance is then liable to be inadequately and superficially assessed, hence possibly permitting unsatisfactory performance to persist, with all the penalties this incurs.

---

[26] However, if that constituent is, for example, apparent condenser block load, the enhanced Thorp method amounts to a generalised *condenser* energy balance method.

4.3.1 Methods of Obtaining Corresponding Normal Performance

Four options are available for obtaining corresponding normal performance:

1) information already available, supplied by the manufacturer, of quoted normal performance for a range of anticipated off-design conditions;

2) predicting normal performance on the basis of extensive, accurately recorded operating data;

3) predicting normal (or optimal) performance by comprehensive, fundamental mathematical modelling;

4) predicting normal performance by simpler fundamental modelling and limited, accurately recorded, key operating data.

Off-Design Performance Quoted by Manufacturer

Upon request, machine manufacturers supply detailed information on performance under design (specified full-duty) conditions, and sometimes for a limited set of user-specified off-design, part-duty conditions. Such supplied information may be quite satisfactory for machines with constant diurnal and slowly varying seasonal duties, such as those in most underground installations. Where the duty of a machine varies widely, though, a limited set of user-specified conditions may not adequately represent all possible actual conditions encountered, so comprehensive information on performance over the full range of expected off-design conditions is required. Manufacturers are reluctant to supply such comprehensive information; apart from the considerable extra work involved, it amounts to revealing the complete performance characteristics of their compressors, which they understandably deem to be proprietary information.

Moreover, substantial, permanent changes in machine duty can occur due to the unpredictable nature of mining. Examples are a change to a ventilation district resulting in less heat-rejection air being available for the cooling towers of an underground installation; an installation being modified; or machines being moved to another installation with a different duty, as can happen particularly with underground installations as mining areas are exhausted and new areas opened up.

For both these reasons, it is unlikely that information supplied by manufacturers will adequately represent normal performance under all conditions to be encountered.

Predicting Normal Performance from Past Operating Data

The second option is to build up an accurate, extensive historical base of operating data under fault-free conditions, and use this to develop a regression model to predict normal performance.

Grimmelius et al. (1995) report a comprehensive effort in this regard. They used 8 000 sets of measured data under fault-free conditions in developing a nine-coefficient linear regression model of a custom-built water chilling machine with two reciprocating compressors. Inputs were inlet water temperatures of the evaporator and condenser.[27] The outputs of outlet water temperatures, refrigerant-circuit pressures and temperatures, and compressor driving motor currents were predicted with correlation coefficients exceeding 0,94. Chapter 7 reviews this work in more detail, as well as that of Pape et al. (1991) in predicting normal power demand of a conventional water chilling machine by linear regression.

The option of regression modelling, though, has serious drawbacks in mining applications. The historical data base must embrace the full range

---

[27] Water flow-rates were always constant and thus omitted.

of expected off-design conditions. If significant seasonal variations in duty occur, such a base requires years to build up, and because its data must be of fault-free operation, a continuously high standard of instrument and machine maintenance is required that may be difficult to sustain. Also, such a data base must be built up for each machine in an installation, except where identical machines have identical duties.[28]

Moreover, regression models are not necessarily valid for operating conditions outside the range of their data base. Such conditions may arise when, for example, the aforementioned substantial, permanent changes in machine duty occur due to the unpredictable nature of mining. Finally, regression models are based purely on measured input and output variables and so do not, in themselves, yield values of important non-measurable process parameters (e.g. water-side fouling factors) and state variables. To estimate these, mathematical models are needed in any case.

Predicting Normal Performance by Comprehensive Fundamental Modelling

If a water chilling machine is comprehensively modelled on a fundamental level, its specifications and the well-known principles of thermodynamics, fluid mechanics and heat transfer provide enough information to predict its performance for any given set of inputs, process parameters and state variables.

The advantages of such modelling are that it can be used to predict optimal, not just normal, performance, because the process parameters and state variables of the model can be adjusted. Once a fundamental model of a water chilling machine is developed, it can be used for

---

[28] In reality, the performances of even such machines will differ at least slightly. Machine components are only "identical" within the limits of manufacturing tolerances, and some operating conditions (for example, water-side fouling factors) will inevitably differ somewhat.

machines with different specifications and of different makes. It can also be used to predict performance under substantial, permanent changes in duty. A well-developed, comprehensive fundamental model is thus versatile, unlike a regression model, which is specific to a particular machine. Finally, such modelling is of great aid in fault diagnosis, because it can estimate the *actual* values of important, non-measurable process parameters and state variables. Here, the necessity for accurate fundamental modelling is well expressed by Isermann (1982): "As the goal is not only to detect but to diagnose process faults, the process models should express as closely as possible the physical laws which govern the process behaviour." Comprehensive fundamental modelling, if it can be made practicable, is thus the most desirable option.

Predicting Normal Performance by Simpler, Empirically Attuned Fundamental Modelling

However, comprehensive fundamental modelling may not be the most practicable option. As elaborated upon in the next section, such models are impracticable if not in the form of computer software. In addition, fundamental models of some machine components, especially compressors, may be unavailable, inadequately developed or proprietary. In such cases, the question arises of whether a simpler fundamental model, empirically attuned on the basis of minimum data accurately recorded over the machine's entire operating range, will suffice to predict corresponding normal performance.

Gordon and Ng (1994, 1995) and Gordon, Ng and Chua (1995) have developed such a simpler, empirically attuned model - based on fundamental thermodynamic and heat-exchanger theory - of a machine with a single evaporator, condenser and compressor as in Figure 3.4. Appendix 5 summarises the basis and development of this model. The key simplifying assumption is that the internal thermodynamic

irreversibilities[29] are dominant: that is, the external irreversibilities of heat transfer through the condenser and evaporator cause small rates of work "loss" (i.e. work expended non-usefully) compared to those due to the internal irreversibilities. Gordon and Ng (1994, 1995) show, as summarised in Appendix 5, that this assumption is valid for commercially available machines using reciprocating and centrifugal compressors for which data have been reported.

The simplest version of Gordon and Ng's model applies when the variations in inlet condenser water temperature $T_{(w)Ci}$ and outlet evaporator water temperature $T_{(w)Eo}$ are small compared to the variation in evaporator load Q_E. The *temperature-independent* model, which predicts a straight-line relationship between $1/COP$ and $1/Q_E$, results:

$$\frac{1}{COP} \cong C_0 + \frac{C_1}{Q_E} \qquad (4\text{-}9a)$$

where $C_0 \equiv -1 + T_{(w)Ci}/T_{(w)Eo}$ (plus an additional term if possible evaporator or condenser water-side fouling is taken into account; see Appendix 5) and $C_1 \equiv \left(q_{l\text{-}p.side} T_{(w)Ci}/T_{(w)Eo} + q_{h\text{-}p.side}\right)$. $q_{l\text{-}p.side}$ and $q_{h\text{-}p.side}$ are the rates of work "loss" due to the internal irreversibilities in the low-pressure (evaporator) side and high-pressure (condenser) side of the machine's refrigerant circuit. C_1, the slope of the straight-line relationship, thus characterises the internal irreversibilities of a particular machine.

On the other hand, $T_{(w)Ci}$ and $T_{(w)Eo}$ may vary appreciably as well as Q_E (as for instance with water chilling machines in surface installations). As

---

[29] These being throttling through the expansion valve; non-isentropic compression; fluid friction; and heat leaks.

summarised in Appendix 5, Gordon and Ng (1994, 1995) derive a *temperature-dependent* model for such cases:

$$\frac{1}{COP} \cong -1 + \frac{T_{(w)Cl}}{T_{(w)Eo}} + \frac{-C_0 + C_1 T_{(w)Cl} - C_2\left(T_{(w)Cl} / T_{(w)Eo}\right)}{Q_E} \qquad (4\text{-}9b)$$

where the constants C_0, C_1 and C_2 characterise the internal irreversibilities of a particular machine.

The appropriate model, (4-9a) or (4-9b), is attuned to a particular machine by determining the constants C through regression analyses of sets of accurately recorded values of $T_{(w)Cl}$, $T_{(w)Eo}$, Q_E and COP over the machine's entire operating range (Gordon and Ng, 1994, 1995). The attuned model can then be used to predict COP. Phelan, Brandemuehl and Krarti (1997) have successfully used these temperature-independent and -dependent models to predict COP, and hence electrical power and energy demand, of conventional machines with a centrifugal compressor. Their results indicate that accurate predictions are obtainable with relatively small data sets, provided that these span the entire operating range.

Whether in the form of (4-9a) or (4-9b), this relatively simple, empirically attuned thermodynamic model of a water chilling machine does not predict water chilling load, but requires it as an input; has only one output, COP; and yields no refrigerant quantities as outputs. Nevertheless, it appears to offer two considerable advantages. The first is simplicity and ability to predict the performance quantities of immediate practical and economic relevance - COP and hence input power. For predicting just these normal quantities of performance, this model may be preferable to a detailed, fundamental model - especially for custom-built machines, which are more complicated than conventional machines to model fundamentally in detail. The second advantage, as elaborated upon in Chapter 7, is ability to

detect the presence of any fault causing significant changes in rates of work "loss" due to irreversibilities.

The disadvantages of the model for the purposes of this thesis are explained in Appendix 5 and summarised as follows. First, as for regression models, (4-9a) or (4-9b) may not be valid outside the range of the operating data for which the model has been attuned. Second, if the model is to be used to predict normal performance, the operating data used to attune it must be independently verified as representing normal performance. Third, the model cannot generally be directly used to predict *optimal* performance. Finally, the model requires modification, although this does not appear difficult in principle, to make it applicable to the generalised machine of Figure 3.5, and hence to the large-capacity water chilling machines considered in this thesis. Because of these disadvantages, this model is not pursued further, although its advantages are acknowledged where appropriate. The option of comprehensive fundamental modelling is pursued.

4.3.2 Mathematical Modelling of Performance of Water Chilling Machines

Referring to Isermann's representation of a process (Figure 4.1), the static performance of a water chilling machine is uniquely determined by the following quantities:

- *measurable inputs.* These are flow-rates and inlet temperatures of all water streams crossing the machine boundary; and settings of capacity-regulating devices of compressors.

- *process parameters.* These are of three classes:

  - *fluid properties:* properties of water, oil and refrigerant;

  - *time-invariant machine specifications,* comprising the physical attributes of evaporators, condensers, compressors and other

components; and characteristic performance specifications of compressors, expansion valves, hot gas bypass valves, etc. Some specifications may be known and others not (like proprietary compressor performance specifications); and

- *unknown, not directly measurable quantities, changing very slowly with the passage of time,* like water-side fouling factors of evaporator and condenser; extent of contamination of refrigerant by oil or non-condensable gas, etc.

- *state variables* (such as masses of liquid refrigerant residing in machine components); for static operating conditions, these will not vary with time.

There are three difficulties impeding attempts to make fundamental mathematical modelling of performance under off-design conditions practicable. The first is that the calculations involved in so predicting the performance of a machine are complex, iterative and tedious, and thus impracticable without the aid of a computer (Hemp, 1981; Hemp et al., 1986; Bailey-McEwan and Penman, 1987, etc.).

The second is that it is seldom sufficient to predict the performance of just the machine of interest in isolation. Referring to Figure 2.2, the interactions between the water chilling, heat rejection and other plants in a mine fluid cooling installation (and internal interactions between the various components in each of these plants) may well necessitate that the performances of *all significantly interacting components,* which may well mean all components in the whole installation, have to be predicted simultaneously.

Finally, the third and most serious difficulty, already briefly mentioned, is that machine manufacturers generally do not release the detailed performance specifications - for example, characteristic curves - of their centrifugal or screw compressors, which they regard, understandably, as

proprietary information. The off-design performance of a machine employing a centrifugal compressor is sensitive to the precise characteristic behaviour of its compressor - particularly for multi-stage compressors where only the first stage has variable inlet guide vanes to regulate capacity (Shone, 1983). The same holds for machines with slide valve-regulated screw compressors. As mentioned in Chapter 3, such compressors have more complicated internal geometry at part-capacities, and losses other than that due to built-in volume ratio are more dominant (Lundberg, 1980). It is therefore difficult, in the absence of detailed, accurate compressor performance specifications, to accurately predict machine performance under off-design conditions.

Detailed, fundamental, computer-based models of water chilling machines reported in the open literature are next reviewed, and the extent to which they address these difficulties is examined. The use of the CHILLER computer program, simulating complete mine water chilling installations, in the work of this thesis is then justified on the basis of this review.

4.3.3 Computer-Based Models for Predicting Water Chilling Machine Performance

Conventional Machines with a Centrifugal Compressor

Computer programs have been developed to predict static performance of conventional, packaged water chilling machines for any user-specified set of operating conditions. Programs developed within the South African mining industry are those of Hemp (1981) and Bailey-McEwan and Penman (1987). Programs developed elsewhere include those of Chi (1979), Braun et al. (1987), Jackson, Chen and Hwang (1987), Wong and Wang (1989), van Houte and van den Bulck (1994), and larger programs designed to simulate complete HVAC systems (e.g. the DOE2 program used by Beyene et al., 1994). In the quest to achieve accurate performance prediction in the absence of characteristic curves from

manufacturers of centrifugal compressors, different approaches have been adopted.

Braun et al. (1987) have adopted a fundamental approach based on polytropic analysis. For each compressor stage, the impeller blade angle β_2 (see Figure 3.8), outlet flow area and "reference polytropic efficiency"[30] must be known. Compressor stage performance is then predicted using (3-15) - expressed non-dimensionally in terms of the flow and work coefficients of (3-17) - and published, generalised correlations, representing well-designed centrifugal compressors, of polytropic efficiency and work coefficient for actual flow coefficient and rotational Mach and Reynolds numbers. These rotational numbers depend on the properties of the refrigerant employed. Modelling centrifugal compressor stage performance in this fundamental way is naturally the most versatile approach, inherently able to model the effect of impeller dimensions, impeller speed and refrigerant employed. Unfortunately, Braun et al. (1987) developed their model for a variable-speed centrifugal compressor, so it does not model the effect of variable inlet guide vanes in regulating a compressor driven at constant speed.

Most other models are based on isentropic rather than polytropic analysis. The reason, as discussed in Chapter 3, is that in spite of its shortcomings, isentropic efficiency depends only on the end states of the process and hence can be determined from tabulated thermodynamic properties of refrigerants. Jackson, Chen and Hwang (1987) have predicted the performance of a single-stage, variable-speed compressor from a "compressor map" giving refrigerant mass flow-rate and isentropic efficiency as functions of the rotational Mach number, flow coefficient and isentropic head coefficient. Unfortunately, they neither provide nor indicate the source of this compressor map; it is thus unlikely to be in the

---

[30] The peak polytropic efficiency associated with a reference rotational Mach number of 1,1. As noted by Braun et al., it is typically between 0,80 and 0,85.

open literature. This model, like the previous one, has no facility for modelling a constant-speed compressor regulated by variable inlet guide vanes.

Chi (1979) has modelled a constant-speed, single-stage compressor regulated by variable inlet guide vanes. In the absence of performance curves from the manufacturer, he used an earlier (1972) version of the map of ASHRAE (1992 : 35.31) of typical performance of a centrifugal compressor with various settings of variable inlet guide vanes. The condenser of the machine was connected to a cooling tower, also modelled. Brief mention is made of use of the model to simulate two such machines connected either in series or in parallel.[31]

Wong and Wang (1989) have modelled a packaged water chilling machine, also coupled to a cooling tower, with a constant-speed, two-stage centrifugal compressor. These authors again used an earlier (1983) version of the map of ASHRAE (1992 : 35.31) of typical compressor performance with various settings of variable inlet guide vanes. Because the compressor had guide vanes on both stages, the economiser temperature was assumed to always be the mean of the evaporating and condensing temperatures.

Another approach is to estimate the characteristic curves of a centrifugal compressor from operating data. Van Houte and van den Bulck (1994) have used this approach in modelling a machine with a single-stage centrifugal compressor regulated by variable inlet guide vanes. Unfortunately, their brief section on modelling the machine[32] merely states

---

[31] That is, the water sides of the evaporators of the two machines are connected in series or parallel; it is not stated how their condensers are connected.

[32] Their paper is mostly concerned with the advantages of the simultaneous equation-solving procedure over the sequential modular procedure in solving the equations describing machine performance. The correlation of compressor performance is based on isentropic analysis, but how it accounts for the setting of the inlet guide vanes is not clear.

that all internal machine parameters - by implication including the compressor characteristic curves - were correlated from measurements during a winter period. Such empirically derived curves, of course, apply only to the compressor they were developed for, and only within the range for which data is available.

If a machine manufacturer provides a limited amount of information on compressor performance, a semi-empirical approach may be adequate for modelling compressors *of that make* on the basis of this information. This is exemplified by Hemp (1981), who modelled a range of conventional machines with a two-stage centrifugal compressor - all from the same manufacturer - as machines with an equivalent single-stage compressor. All compressors had inlet guide vanes on both stages. The modelling was done semi-empirically, using composite curves[33] supplied by the manufacturer, supplemented with data from acceptance tests carried out at the manufacturer's works. This approach worked satisfactorily for this range of machines, which were all in underground installations, and seldom operating under loads much below the full-duty value. Thus the inlet guide vanes were seldom less than fully open. All machines were modelled with their condensers connected to a cooling tower. The program was extended to model a machine whose evaporator was connected to cooling coils; another machine with a combined task of service water chilling and bulk air cooling; and two machines whose evaporators and condensers could be connected in series or parallel.

However, a computer program suitable for the South African mining industry must be as generally applicable to all makes of compressors (and machines) as possible, and must account for -

---

[33] That is, the manufacturer combined the proprietary characteristic curves for the first and second stages of the two-stage compressor into one composite curve representing the characteristic behaviour of the complete compressor - as if it were a single-stage machine.

- many two- and three-stage centrifugal compressors in conventional machines having guide vanes on the first stage only;
- the interactions between the water chilling, the heat rejection and other plants in the installation, and between the components within each of these plants, in simulating static performance. As mentioned previously, this may well necessitate simulating the performance of all significantly interacting components in the installation.

These requirements are met in a versatile, predictive computer program named CHILLER, developed by the Chamber of Mines of South Africa for the South African mining industry (Bailey-McEwan and Penman, 1987). CHILLER models the centrifugal compressor of conventional machines more fundamentally, using artificial compressor curves for *each* compressor stage. The principal features of these artificial curves are specifiable in order to match the curves of each stage of the actual compressor as closely as possible. A full description of the CHILLER program, which can predict the performance of complete, user-specified water chilling installations, is given in Appendix 16. It will be seen in the next two chapters how CHILLER can be used for both verifying actual machine performance and predicting corresponding normal or optimal performance, hence enabling actual performance to be assessed.

In parenthesis, it is worth noting that because of the need for buildings to be energy-efficient, versatile routines simulating packaged water chilling machines are also likely to be included in computer programs for designing and simulating complete HVAC systems in buildings. Beyene et al. (1994) give a limited description of one such program, DOE2. This incorporates characteristic curves for centrifugal (and reciprocating) compressors, supplied by the Lawrence Berkeley Laboratory, University of California, USA. User-defined curves can be used instead if available. DOE2 can simulate machines connected to a cooling tower, as well as machines connected in series or parallel.

Custom-Built Machines with Screw Compressors

Brief remarks will suffice here, as custom-built machines are not modelled in this thesis. Generalised software simulating industrial refrigeration plants, such as that of Cleland and Cleland (1989) seems most appropriate for predicting normal performance of such machines. Cleland and Cleland's software simulates dynamic and static performance of complex systems used in food refrigeration - incorporating screw compressors with continuous unloading[34] - and liquid chillers. It thus is certainly capable of simulating static performance of custom-built water chilling machines. The authors state that this software may have wider application.

Howes (1990, 1992) reports models of custom-built water chilling plants, incorporating multiple screw compressors, in two Australian mines. These models were used in developing optimum control strategies to meet underground cooling demands. However, the screw compressor specifications reported are merely curve fits of the full- and part-capacity performance of particular compressor makes and models, and hence are obviously limited thereto.

4.4 Assessing Performance and Diagnosing Faults

Once both accurately ascertained actual performance and corresponding, predicted normal (or optimal) performance are to hand, the former is assessed for satisfactoriness as described in Section 4.1.3 above. Unless all shortfalls in performance are wholly due to an off-design operating regime, the undesirable values of state variables or process parameters, termed *faults*, partially or wholly causing these shortfalls must then be diagnosed. As noted previously, process parameters and some state variables are not measurable. Those process parameters and non-

---

[34] That is, continuous capacity regulation by slide valve.

measurable state variables constituting faults must be diagnosed either through estimating such parameters and states, or through known symptoms or signatures in measured or derived quantities. This final step of fault diagnosis, which is customarily done manually, is reviewed in Chapter 7. It is highly desirable to automate fault diagnosis, though, in order to optimise rapid, reliable identification of faults so that burdened mine staff, who are not refrigeration experts, may timeously remedy them.

4.5 Desirable Improvements to Current Practice

The desirable improvements to current practice indicated by this chapter can be summarised as follows. The first is an improved confirming method to rapidly and conclusively verify the apparent site performance obtained from principal measurements. The thesis provides this in Chapter 5 in the form of extensions to the Thorp method, termed the *enhanced* and *inexact* Thorp methods. Where these are inadequate to conclusively verify apparent performance, Chapter 5 also illustrates the use of machine modelling to do this.

The second is rapid, accurate prediction of corresponding normal and possibly optimal performance. For this, fundamental, computer-based mathematical modelling is the preferred approach, because of its versatility. In this thesis, the CHILLER computer program and an extension thereto are used, as illustrated in Chapters 5 and 6.

The third is rapid, automated diagnosis of faults causing unacceptable shortfalls in actual performance. The thesis does not contribute here, but, in Chapter 7, reviews reported procedures of fault detection and diagnosis in vapour-compression water chilling machines, and shows where its contributions are of value therein. It suggests that further work is required in determining the minimal set of measurements necessary for unambiguous fault diagnosis, and in detecting unanticipated faults.

5. ASCERTAINING SITE PERFORMANCE OF WATER CHILLING MACHINES

This chapter attempts to provide the first desirable improvement to current practice identified in Chapter 4 - that of a confirming check in performance surveys which yields independent measures of performance; rapidly and conclusively verifies whether the apparent performance is acceptably accurate; and also identifies any unacceptably erroneous measurements, or at least gives strong indications of such identities.

After introducing some fundamental concepts, this chapter, as indicated in Chapter 4, shows that an "acceptable" heat imbalance does not guarantee acceptably accurate principal measurements. It then presents a confirming method which, in principle, meets all the criteria stated above. This is the *enhanced Thorp method,* based on the refrigerant-circuit COP, corrected wherever necessary to accurately reflect the actual COP. Most often, this method amounts to the compressor energy balance method of ISO R916 (ISO, 1968), generalised to all classes of machines in all their operating modes.

The enhanced Thorp method illustrates information in lucid, graphical form. It can verify apparent performance if the refrigerant-circuit COP can be precisely determined and at least one apparent constituent of the heat balance is independently known to be accurate. Where these conditions are not met, an extension termed the *inexact Thorp method* can still indicate the relative likelihood of unacceptable errors in the apparent constituents. Here, however, to finally verify apparent performance, machine model[ling] has to be used.

Illustrative case studies of both the enhanced and inexact Thorp methods are presented. Finally, case studies of the use of machine modelling to verify apparent performance and estimate non-measurable process parameters or state variables possibly constituting faults are presented.

5.1 Fundamental Concepts

5.1.1 The Heat Balance: True and Apparent Constituents

The true values of the net water-borne heat flows across the machine boundary into the evaporator, condenser and vapour-compression blocks, and of the total mechanical power input, appear in the overall energy balance (3-7c) for the generalised machine:

$$\sum Q_{(w)EB} + \sum W_{VCB} + \sum Q_{(w)VCB(Ms)} + \sum Q_{(w)CB} + \sum Q_{(Ms)} = 0$$

As $\sum Q_{(w)VCB(Ms)}$ will almost always in reality comprise heat rejected across the machine boundary from oil-to-water compressor oil coolers or like heat exchangers, it is convenient to define a quantity $\sum Q_{(w)JB}$ jointly representing $\sum Q_{(w)VCB(Ms)}$ and $\sum Q_{(w)CB}$, that is, representing *all* heat rejected via water flows across the machine boundary:

$$\sum Q_{(w)JB} \equiv \sum Q_{(w)VCB(Ms)} + \sum Q_{(w)CB} \qquad (5\text{-}1a)$$

$\sum Q_{(w)JB}$ is termed the *rejection load*. It reduces to the condenser block water load $\sum Q_{(w)CB}$ where $\sum Q_{(w)VCB(Ms)}$ is either zero or negligible in comparison.[1] Using (5-1a), the overall energy balance becomes

$$\sum Q_{(w)EB} + \sum W_{VCB} + \sum Q_{(w)JB} + \sum Q_{(Ms)} = 0 \qquad (5\text{-}1b)$$

or, if $\sum Q_{(Ms)}$ is negligible compared to the sum of the other terms,

$$\sum Q_{(w)EB} + \sum W_{VCB} + \sum Q_{(w)JB} \cong 0 \qquad (5\text{-}1c)$$

---

[1] For screw compressors, oil cooling load can be up to 30 per cent of input power, as noted in Chapter 3. $\sum Q_{(w)VCB(Ms)}$ is thus *not* negligible for machines employing screw compressors with oil-to-water oil coolers whose water streams cross the machine boundary, as in Figure 3.24.

In reality, of course, $\sum Q_{(w)EB}$, $\sum Q_{(w)JB}$ and $\sum W_{VCB}$ - the true values of the major constituents of the energy balance, customarily termed the heat balance - are not known. Only the *apparent* values, derived from the principal and confirming measurements, are available. As in the previous chapter, let these apparent values of evaporator block water load, mechanical input power, and rejection load be denoted by $\sum Q_{EBp}$, $\sum W_{VCBp}$, and $\sum Q_{JBp}$ respectively, with the subscripts $_{(w)}$ deleted for brevity. In general, these apparent values will differ from the true values. Let them be expressed as sums of the corresponding true values and of errors δQ_{EBp}, δW_{VCBp} and δQ_{JBp} respectively:

$$\sum Q_{EBp} \equiv \sum Q_{(w)EB} + \delta Q_{EBp} \qquad \sum W_{VCBp} \equiv \sum W_{VCB} + \delta W_{VCBp}$$
$$\sum Q_{JBp} \equiv \sum Q_{(w)JB} + \delta Q_{JBp} \tag{5-2}$$

As these errors can be positive or negative, the apparent values can be greater or less than their corresponding true values. The *relative* errors n_{EBp}, n_{VCBp} and n_{JBp} in the apparent values are defined as fractions of the true values:

$$n_{EBp} \equiv \frac{\delta Q_{EBp}}{\sum Q_{(w)EB}} \qquad n_{VCBp} \equiv \frac{\delta W_{VCBp}}{\sum W_{VCB}} \qquad n_{JBp} \equiv \frac{\delta Q_{JBp}}{\sum Q_{(w)JB}} \tag{5-3}$$

Substituting the definitions of (5-2) into (5-1c) above and rearranging, the sum of the *apparent* values of the three major constituents of the heat balance is

$$\sum Q_{EBp} + \sum W_{VCBp} + \sum Q_{JBp} \cong \delta Q_{EBp} + \delta W_{VCBp} + \delta Q_{JBp} \tag{5-4}$$

That is, this sum - which is the heat *im*balance - is almost equal to the sum of the *errors* in the apparent values. It must be noted that, as for the true values, $\sum Q_{EBp}$ and $\sum W_{VCBp}$ are positive, and $\sum Q_{JBp}$ is negative.

5.1.2 The Relative Heat Imbalance

The *relative* heat imbalance ε is normally expressed as a fraction of the largest constituent of the heat balance, the rejection load. Dividing both sides of (5-4) by the apparent rejection load,

$$\varepsilon \equiv \frac{\sum Q_{EBp} + \sum W_{VCBp}}{\sum Q_{JBp}} + 1 \cong \frac{\delta Q_{EBp} + \delta W_{VCBp} + \delta Q_{JBp}}{\sum Q_{JBp}} \qquad (5\text{-}5)$$

Unless the errors δQ_{EBp}, δW_{VCBp} and δQ_{JBp} are all positive or all negative, it can readily be seen that they do not have to be small to achieve an "acceptable" relative heat imbalance. If one error is positive and the other two are negative, or vice versa, all that is necessary to achieve an "acceptable" heat imbalance is that they cancel out sufficiently. *Therefore, an "acceptable" heat imbalance, in itself, is no guarantee of acceptably accurate apparent constituents of the heat balance, and hence of acceptably accurate principal measurements.*

Acceptable Limits of Accuracy for Apparent Constituents of Heat Balance

An attempt is now made to lay down soundly based limits for an "acceptable" heat imbalance in routine performance surveys. To do this, it is first necessary to specify limits of acceptable accuracy for the apparent major constituents of the heat balance, namely apparent evaporator block and rejection loads $\sum Q_{EBp}$ and $\sum Q_{JBp}$, and apparent input power $\sum W_{VCBp}$. Chapter 4 concluded that ISO R916 (ISO, 1968) was the only standard attainable in routine surveys of water chilling machines. This standard, as noted in Tables 4.3 and 4.8, requires the following limits of accuracy:

- water chilling capacity (i.e. evaporator block load): ±7%
- absorbed (i.e. input) power: ±5%

It is submitted that these limits ar. realistic for mine conditions, and that it is also realistic to assign limits of accuracy of ±7% to the rejection load.

Unacceptability Confirmation Limits for the Heat Imbalance

Let these limits be assigned to the relative errors defined in (5-3) above - that is, ±7% to n_{EBp} and n_{JBp}, and ±5% to n_{VCBp}. Then what is the worst possible heat imbalance that can result from worst-case combinations of th: se acceptability limits? Recalling from (3-11a) that the COP for the generalised machine is defined as

$$COP \equiv \frac{\sum Q_{(w)EB}}{\sum W_{VCB}} \tag{5-6}$$

it is shown in Appendix 6 that the relative heat imbalance ε of (5-5) can be expressed in terms of the COP, as defined in (5-6), and the relative errors defined in (5-3):

$$\varepsilon \cong \frac{1}{1+n_{JBp}} \cdot \left[\frac{COP \cdot n_{EBp}}{1+COP} - \frac{n_{VCBp}}{1+COP} + n_{JBp} \right] \tag{5-7}$$

As the COP is always positive, ε will be largest in magnitude when the first two relative errors inside the square brackets are positive and the third negative, or vice versa. For the corresponding worst-case combinations of relative errors at their limits of acceptability, Table 5.1 gives the extreme values of relative heat imbalance ε yielded by (5-7) for the range of COPs attained by water chilling machines.

As seen, these values of ε are almost independent of COP. It is safe, therefore, to affirm as follows. If the abovementioned limits of accuracy for apparent evaporator block load, input power and rejection load are adopted, the relative heat imbalance ε must be less than -15%, or greater than +13%, *in order to prove that at least one apparent constituent of the heat balance is unacceptably in error.* (These extreme values of -15%

and +13% are best termed *unacceptability confirmation limits* for the heat imbalance.) On the other hand, if ε lies between these two limits, it is *not* proved that all apparent constituents, and hence principal measurements, are acceptably accurate.[2] Nothing can be concluded without further information (which, as will be seen, the enhanced Thorp method presented below can provide in most cases).

Table 5.1 Extreme Values of Relative Heat Imbalance for Worst-Case Combinations of Acceptable Relative Errors

	Worst-Case Combinations of Acceptable Relative Errors	
	n_{EBp}: +7% n_{VCBp}: +5% n_{JBp}: -7%	n_{EBp}: -7% n_{VCBp}: -5% n_{JBp}: +7%
COP	Relative Heat Imbalance ε (%)	
2	-14,34	+12,46
4	-14,62	+12,71
6	-14,75	+12,81
8	-14,82	+12,88
10	-14,86	+12,91

Interestingly, the current criterion in the South African mining industry is that the heat imbalance denotes unacceptable measurement errors if outside the limits of ±5 per cent (Burrows, 1982). In this case, it can similarly be shown that, for example, n_{EBp} and n_{JBp} must have limits of ±2,5%, and n_{VCBp} limits of ±1,8%. Such limits are unrealistically stringent for routine performance surveys on mines; the aforementioned ones of ISO R916 (ISO, 1968) are preferable.

---

[2] Of course, the closer the heat imbalance is to either unacceptability confirmation limit, the less likely it is that all apparent constituents are acceptable.

5.2 Verifying Apparent Performance by Enhanced Thorp Method

5.2.1 The Enhanced Thorp Method: Procedure

It is assumed that apparent evaporator block load, rejection load and input power have been calculated from the measurements of the performance survey. The proposed procedure - appropriately termed the *enhanced Thorp method* - of verifying these apparent constituents of the heat balance is then as follows.

Relative Heat Imbalance

First, the relative heat imbalance ε is calculated per (5-5) above:

$$\varepsilon = \frac{\sum Q_{EBp} + \sum W_{VCBp}}{\sum Q_{JBp}} + 1 \qquad (5\text{-}8)$$

If ε lies between the unacceptability confirmation limits of -15% and +13%, apparent evaporator load, rejection load, and input power could all be acceptably accurate, *but this is by no means yet proved.* If ε is outside these limits, at least one apparent constituent of the heat balance - and hence at least one measurement - is unacceptably in error.

Apparent Evaporator-Load and Rejection-Load COPs

From (5-1b) and (5-6), the actual COP can be expressed in two ways. Both involve input power. The first involves evaporator block load, and the second, rejection load.

$$COP = \frac{\sum Q_{(w)EB}}{\sum W_{VCB}} \qquad COP = \frac{-\left(\sum Q_{(w)JB} + \sum W_{VCB} + \sum Q_{(Ms)}\right)}{\sum W_{VCB}} \qquad (5\text{-}9a)$$

Both these COPs, being the actual COP, will be identical to each other. If $\sum Q_{(Ms)}$ is negligible compared to $\left(\sum Q_{(w)JB} + \sum W_{VCB}\right)$,

$$COP = \frac{\sum Q_{(w)EB}}{\sum W_{VCB}} \qquad COP \cong \frac{-\left(\sum Q_{(w)JB} + \sum W_{VCB}\right)}{\sum W_{VCB}} \qquad \text{(5-9b)}$$

The corresponding two COPs calculated from the *apparent* loads and input power are termed apparent *evaporator-load* COP, $COP_{[EB]p}$, and apparent *rejection-load* COP, $COP_{[JB]p}$, and are defined as follows.

$$COP_{[EB]p} \equiv \frac{\sum Q_{EBp}}{\sum W_{VCBp}} \qquad COP_{[JB]p} \equiv \frac{-\left(\sum Q_{JBp} + \sum W_{VCBp}\right)}{\sum W_{VCBp}} \qquad \text{(5-9c)}$$

The next step is to calculate these two apparent COPs from the apparent loads $\sum Q_{EBp}$ and $\sum Q_{JBp}$ and the apparent input power $\sum W_{VCBp}$. In general, because of inevitable errors in measurements, these apparent COPs will be equal neither to each other nor to the actual COP.

Refrigerant-Circuit COP

The actual COP of the machine must now be estimated from the independent, confirming measurements taken in the refrigerant circuit. To begin with, the refrigerant-circuit COP, denoted by $COP_{(r)}$, is calculated.

Appendix 7 gives formulae for $COP_{(r)}$ for the key types of conventional, packaged water chilling machines in use on mines. Refrigerant-circuit COPs of custom-built machines vary from case to case; (3-24) through (3-26) in Chapter 3 give $COP_{(r)}$ for the machines illustrated in Figures 3.22 through 3.24. It is first necessary, using tables of refrigerant properties, to determine refrigerant enthalpies at all key points in the refrigerant circuit from the confirming measurements of pressure and temperature taken at these points. These enthalpies are then substituted into the appropriate formula for $COP_{(r)}$.

As seen in Appendix 7, for conventional packaged machines with a single- or multi-stage centrifugal compressor, $COP_{(r)}$ is a function solely of refrigerant enthalpies at key points in the refrigerant circuit, *unless hot gas is being bypassed*.[3] In this case, $COP_{(r)}$ also depends on the ratio of this hot gas flow to the flow through the expansion valve feeding the evaporator. For custom-built machines employing screw compressors, $COP_{(r)}$ likewise also depends on the ratio of any auxiliary refrigerant flows to the main flow.

Correcting Refrigerant-Circuit COP to Reflect Actual COP

It is shown in Appendix 8 that if no water flows pass through the vapour-compression block, and if *all* refrigerant flows passing between blocks are included in the determination of $COP_{(r)}$, this reflects actual COP:

$$COP \cong COP_{(r)} \qquad (5\text{-}10a)$$

However, if water flows do pass through the vapour-compression block (for example, if the compressor oil coolers are oil-to-water heat exchangers), or if certain auxiliary refrigerant flows are excluded in the determination of refrigerant-circuit COP (as may be convenient for auxiliary refrigerant flows passing through oil-to-refrigerant compressor oil coolers), it is necessary to correct the refrigerant-circuit COP for it to accurately reflect the actual COP.

If all water flows passing through the vapour-compression block, or all such auxiliary refrigerant flows, circulate between the vapour-compression and *evaporator* blocks, Appendix 8 shows that actual COP is reflected by

---

[3] Or other auxiliary refrigerant flows occur.

$$COP \cong COP_{(r)}\left(1+R_{[VCB]}\right)+R_{[VCB]}$$

$$\text{where } R_{[VCB]} = -\frac{\sum Q_{(w)EB(VCB)} + \sum Q_{(r.aux)EB(VCB)}}{\sum W_{VCBp}} \qquad (5\text{-}10b)$$

and $\sum Q_{(w)EB(VCB)}$ is the net heat flow into the evaporator block due to all water flows between it and the vapour-compression block. $\sum Q_{(r.aux)EB(VCB)}$ is the net heat flow into the evaporator block due to all auxiliary refrigerant flows *excluded* in the determination of $COP_{(r)}$ and circulating between this block and the vapour-compression block.

On the other hand, if all water flows passing through the vapour-compression block circulate between this block and either the *condenser* block or sources outside the machine boundary - or where all auxiliary refrigerant flows excluded in the determination of $COP_{(r)}$ pass between the vapour-compression and *condenser* blocks - Appendix 8 shows that actual COP is reflected by

$$COP \cong COP_{(r)}\left(1+R_{[VCB]}\right)$$

$$\text{where } R_{[VCB]} = \frac{\sum Q_{(w)VCB(Ms)} - \sum Q_{(w)CB(VCB)} - \sum Q_{(r.aux)CB(VCB)}}{\sum W_{VCBp}} \qquad (5\text{-}10c)$$

and $\sum Q_{(w)VCB(Ms)}$ is the net heat flow into the vapour-compression block due to all water flows between it and sources outside the machine boundary. $\sum Q_{(w)CB(VCB)}$ is the net heat flow into the condenser block due to all water flows between it and the vapour-compression block. $\sum Q_{(r.aux)CB(VCB)}$ is the net heat flow into the condenser block due to all auxiliary refrigerant flows *excluded* in the determination of $COP_{(r)}$ and circulating between this block and the vapour-compression block.

If all terms in the numerators of $R_{[VCB]}$ in (5-10b) and (5-10c) represent heat flows out of the vapour-compression block - as for compressor oil

cooling loads - $R_{[VCB]}$ will always be negative and *so actual COP will always be less than* $COP_{(r)}$. For conventional machines with centrifugal compressors, it is sufficient to determine the applicable numerators of $R_{[VCB]}$ approximately, as oil cooling load is small compared to $\sum W_{VCB}$. For custom-built machines employing screw compressors, though, the applicable numerators of $R_{[VCB]}$ should be determined accurately, as oil cooling load may be as much as one-third of $\sum W_{VCB}$.

Plotting Load Error Lines on the Acceptability Plot

As shown in Appendix 9, the relative errors n_{EBp} and n_{JBp} in the apparent evaporator block and rejection loads can be expressed in terms of the corresponding apparent COP; the actual COP, COP; and the error n_{VCBp} in apparent input power:

$$n_{EBp} = \frac{COP_{[EB]p}\left(1+n_{VCBp}\right)}{COP} - 1 \qquad n_{JBp} = \frac{\left(1+COP_{[JB]p}\right)\left(1+n_{VCBp}\right)}{1+COP} - 1 \quad (5\text{-}11)$$

These relationships are linear functions, and thus particularly easy to plot graphically in the appropriately named *acceptability plot*. The framework for this plot is illustrated in Figure 5.1. The horizontal axis represents the error n_{VCBp} in apparent input power, and the vertical axis the errors n_{EBp} and n_{JBp} in apparent evaporator block and rejection load. The limits of acceptability for these errors are conveniently indicated on this plot by dotted lines, the spans between which are termed *acceptability bands.* These acceptability bands of ±7% for the errors in apparent evaporator block and rejection loads, and ±5% for the error in apparent input power, are shown. The *acceptability window* in the centre of the plot is where these bands intersect.

It is assumed that the probability distributions of the errors in apparent loads and input power are normal with zero means, per the dotted curves

in Figure 5.1. Significant proportions of the areas underneath these sketched normal probability distributions lie outside the acceptability bands, reflecting the experiential fact that errors are often outside these b. . nd hence unacceptable).

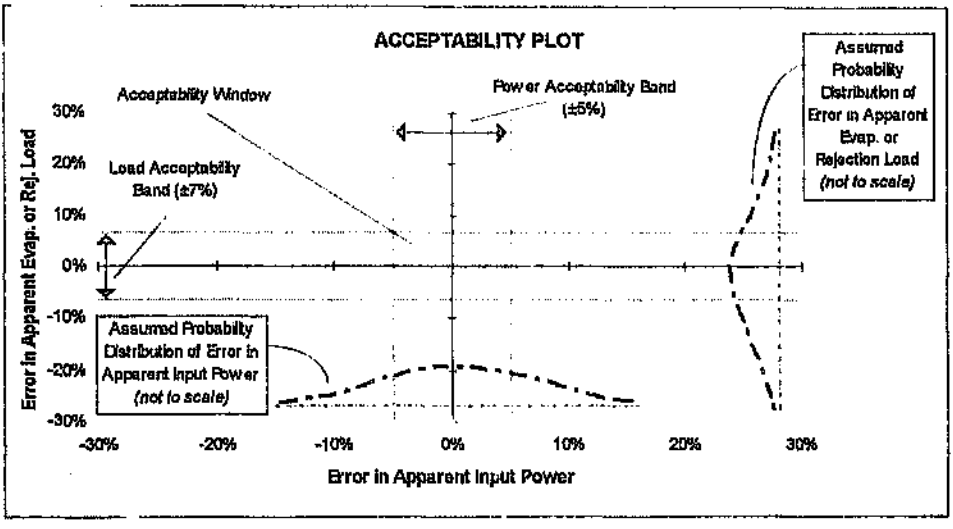

Figure 5.1 Framework for Acceptability Plot

The straight lines resulting from plotting the relationships of (5-11) on the acceptability plot (see Figures 5.2 through 5.7 following for examples) are appropriately termed the *evaporator* and *rejection load error lines.* Substituting (5-11) into (5-7), the relative heat imbalance ε is obtained as

$$\varepsilon = \frac{1+n_{VCBp}}{1+n_{JBp'}} \cdot \frac{COP_{[JB]p} - COP_{[EB]p}}{1+COP} \qquad (5\text{-}12)$$

which shows that ε is proportional to the difference between the two apparent COPs. The closer these two are to each other *(but not necessarily to the actual COP),* the smaller is the heat imbalance, and - from (5-11) - the closer n_{EBp} and n_{JBp} are. So, *the smaller the heat imbalance, the closer are the two load error lines given by (5-11).*

An important consideration is to what extent the inevitable uncertainty in the corrected refrigerant-circuit COP, used for *COP* in (5-11), affects the conclusions drawn from the acceptability plot. It is shown by example in Case Studies A through C presented later that for refrigerant temperature measurements accurate to ±0,2°C, and pressure measurements accurate to ±2 per cent of full scale, the uncertainty in corrected refrigerant-circuit COP was too small to affect these conclusions.

5.2.2 Interpreting Position of Load Error Lines on Acceptability Plot

Examples are now given of typical positions of the load error lines on the acceptability plot, and how these positions are to be interpreted.

Small Heat Imbalance; All Apparent Constituents Likely to be Acceptable

Here, both load error lines will be close together, and will pass through the acceptability window for most or all of its width. In Figure 5.2, the acceptability ranges "J" and "E" denote the ranges of error in apparent input power where the rejection and evaporator load error lines, respectively, are within the load acceptability band, and hence where the apparent rejection and evaporator loads are acceptably accurate. The overlap of these two acceptability ranges is the range of *joint* load acceptability - that is, the range of error in apparent input power where *both* load error lines are within the load acceptability band and thus where both apparent loads are acceptably accurate. This range of joint load acceptability is also indicated in Figure 5.2; as seen, it is entirely within the acceptability window, and spanning most of its width.

Therefore if, for example, apparent input power is independently known to be acceptably accurate - that is, to lie within its acceptability band - the balance of probabilities is that all apparent constituents, and hence all principal measurements, are acceptably accurate. This is the basis for saying that all principal measurements can be declared acceptable. It is easily verified that the same conclusion holds if either apparent

evaporator block load or apparent rejection load is independently known to be acceptably accurate. If the apparent input power is independently known to be acceptably accurate,[4] the enhanced Thorp method amounts to verifying apparent performance by the compressor energy balance method of ISO R916 (ISO, 1968) generalised to all classes of machines in all their operating modes.[5]

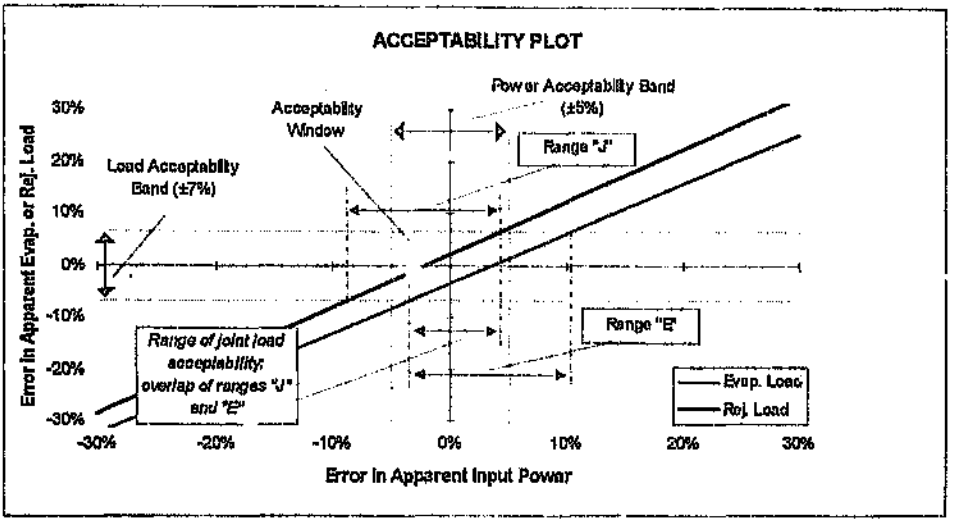

Figure 5.2 Acceptability Plot: Small Heat Imbalance, Acceptability of All Apparent Constituents Likely

The principles illustrated in Figure 5.2 are now stated as follows.

A. An apparent load (evaporator or rejection load) is acceptably accurate for that range of error in apparent input power where the error line of that load is within the load acceptability band (e.g. ranges "E" and "J" in Figure 5.2).

---

[4] As mentioned in Chapter 4, the apparent input power is the apparent constituent of the heat balance most likely to be acceptably accurate, because it is derived from measurements of electrical quantities, which are not subject to the fouling and other detrimental processes occurring in water circuits.

[5] It amounts to this in principle; in reality, all measurements required to precisely determine refrigerant-circuit COP may not be available, as explained later.

B. If the two load error lines are close enough to be within the load acceptability band *for overlapping ranges of error in apparent input power,* both apparent loads (evaporator and rejection load) are acceptably accurate within the range of overlap, termed the *range of joint load acceptability.*

C. If a load error line passes through the acceptability window, apparent input power and the apparent load represented by that line are both acceptably accurate within the range between the intercepts of that line with the window.

D. If a range of joint load acceptability exists and is partly or wholly within the power acceptability band (and thus within the acceptability window), all three apparent constituents of the heat balance are acceptably accurate for that subrange of joint load acceptability within the power acceptability band. This subrange is termed the *range of complete acceptability.* (In Figure 5.2, the entire range of joint load acceptability lies within the power acceptability band, and is therefore the range of complete acceptability.)

E. *All apparent constituents of heat balance acceptable.* All apparent constituents of the heat balance, and hence all principal measurements, can be declared acceptable if:

   E.1 a range of complete acceptability exists; spans more than half of the power acceptability band; and is mostly within the acceptability window; and

   E.2 *any one apparent constituent of the heat balance is independently known to be acceptably accurate;* that is, its error is known to be within its acceptability band. (Otherwise, even if condition E.1 holds, there is no proof that the errors lie within the window; they may be outside it.)

Small Heat Imbalance, but Acceptability of All Apparent Constituents Doubtful

Here, the load error lines will be close together and both will pass through the acceptability window, but at least one line will pass through *less* than half of this window's width. In the example of Figure 5.3, the evaporator load error line does this, just passing through the bottom right-hand corner of the window.

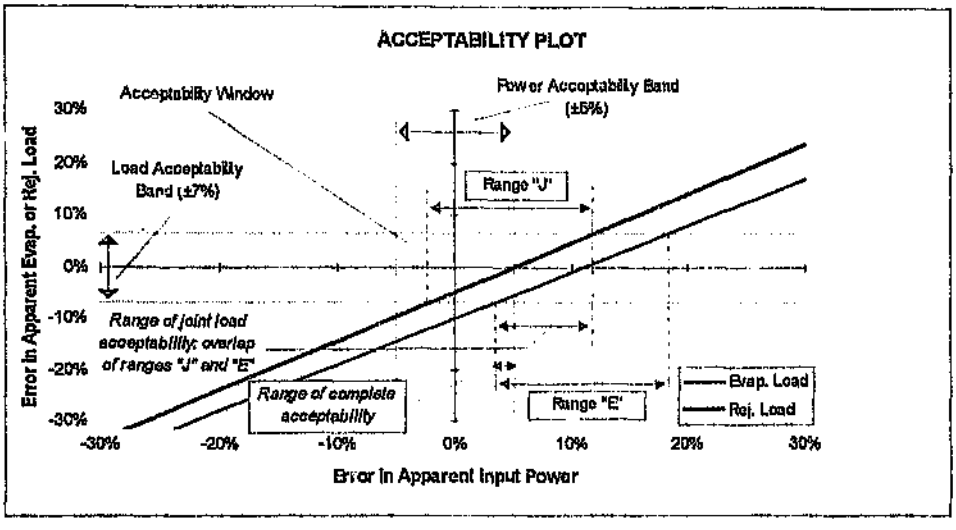

Figure 5.3 Acceptability Plot: Small Heat Imbalance, Acceptability of all Apparent Constituents Doubtful

As in the previous figure, the acceptability ranges "J" and "E" denote where the rejection and evaporator load error lines, respectively, pass through the load acceptability band, and hence where the apparent rejection and evaporator loads are acceptably accurate. The range of joint load acceptability is also indicated; as seen, it is mostly outside the power acceptability band. (As seen, the range of complete acceptability is the minor subrange, within this band, of the range of joint load acceptability.) Therefore, although it is still possible that all apparent constituents of the heat balance are acceptably accurate, it is more likely that:

- if apparent input power is acceptably accurate, then at least one apparent load is unacceptably erroneous (in Figure 5.3, apparent evaporator load is then most likely too low); or

- if apparent evaporator and rejection loads are both acceptably accurate, then apparent input power is unacceptably erroneous (in Figure 5.3, apparent input power is then most likely too high, as the range of joint load acceptability is mostly to the right of the acceptability window).

Small Heat Imbalance, but Acceptability of All Apparent Constituents Impossible

Here, the two load error lines will be close together, but one or both will miss the acceptability window; in the example of Figure 5.4, both lines miss it. The range of joint load acceptability is entirely outside the window. All apparent constituents of the heat balance cannot be acceptable; the alternatives are:

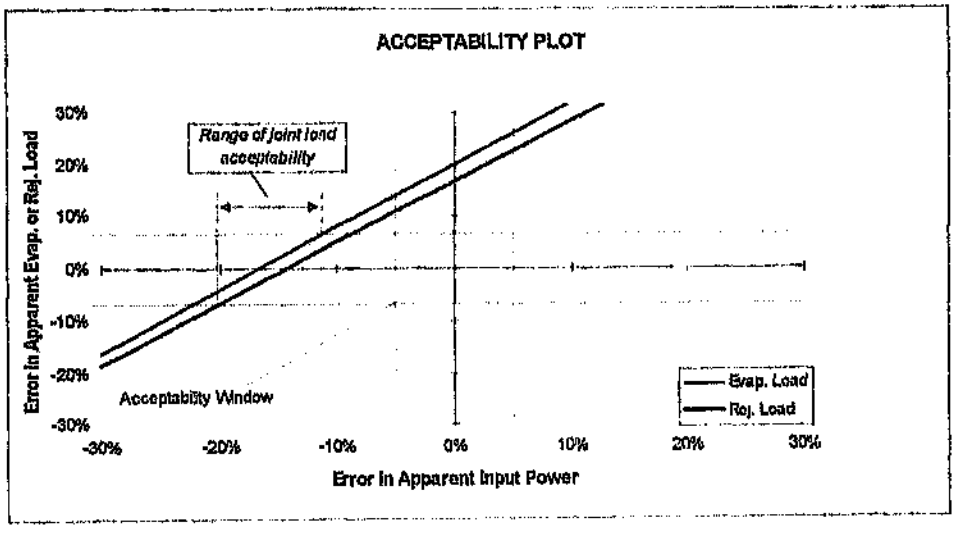

Figure 5.4 Acceptability Plot: Small Heat Imbalance, Acceptability of all Apparent Constituents Impossible

- if apparent input power is acceptably accurate, then *both* apparent loads are unacceptably and similarly erroneous (in Figure 5.4, both apparent loads are then too high); or

- if both apparent loads are acceptably accurate, then apparent input power is unacceptably in error (in Figure 5.4, apparent input power is then too low, as the range of joint load acceptability is entirely to the left of the acceptability window); or

- apparent input power and both apparent loads are *all* unacceptably in error. Although relatively unlikely, this remains a possibility.

The next three examples are of large heat imbalances, where the two load error lines, as shown by (5-12), are thus further apart.

Large Heat Imbalance; Acceptability of Two Apparent Constituents Likely

Here, one load error line will pass through more than half the width of the acceptability window. The other line will be on the opposite side of this window, either passing through significantly less than half its width, or wholly missing it. In the example of Figure 5.5, the other line misses the window. This figure also shows the load acceptability ranges "J" and "E" where the rejection and evaporator load error lines pass through the load acceptability band. *These ranges do not overlap, so there is no range of joint acceptability for the two apparent loads.* Either one or both apparent loads are therefore unacceptably in error. The alternatives are:

- (most likely) if *either* apparent input power, *or* the apparent load whose error line passes through the window is known to be acceptably accurate, then both these apparent constituents are acceptably accurate and the other apparent load is unacceptably in error (in Figure 5.5, apparent input power and evaporator load are then acceptably accurate, and apparent rejection load is unacceptably in error); or

- (less likely) if the apparent load whose error line misses the window (in Figure 5.5, apparent rejection load) is known to be acceptably accurate, then the other two apparent constituents are unacceptably in error (in Figure 5.5, apparent input power and evaporator load are then unacceptably in error); or

- (least likely, but possible) apparent input power and both apparent loads are *all* unacceptably in error.

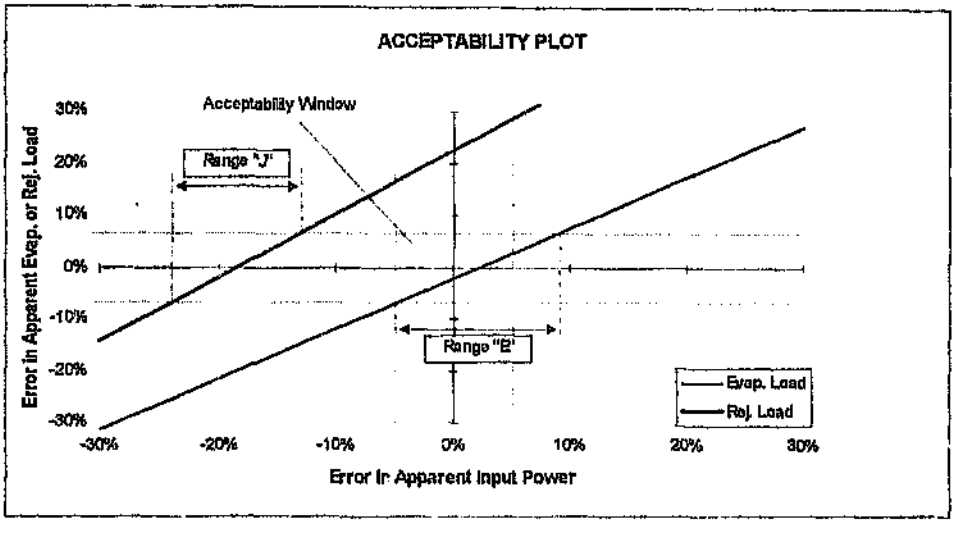

Figure 5.5 Acceptability Plot: Large Heat Imbalance, Acceptability of Two Apparent Constituents Likely

Large Heat Imbalance; Acceptability of Two Apparent Constituents Doubtful

As for the previous case, the load error lines will be on opposite sides of the acceptability window. One line will pass through a quarter or less of the width of the window; the other, on the opposite side, will either do likewise or miss the window. In the example of Figure 5.6, both lines pass through a quarter or less of the width of the window, on opposite sides. As for Figure 5.5, the load acceptability ranges "J" and "E" do not overlap,

so either one or both apparent loads are unacceptably in error. The alternatives are:

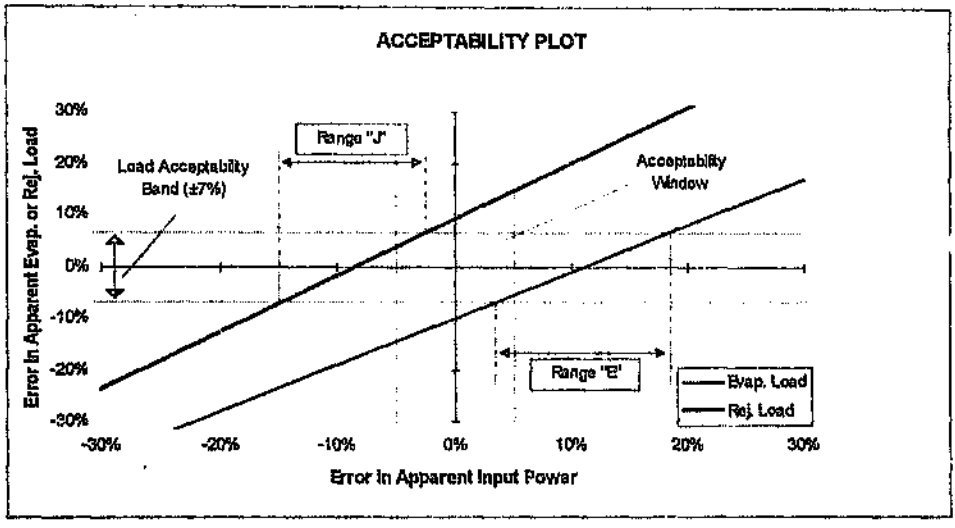

Figure 5.6 Acceptability Plot: Large Heat Imbalance, Acceptability of Two Apparent Constituents Doubtful

- (most likely) only one of the apparent constituents - apparent input power, evaporator load, or rejection load - is acceptably accurate;
- (less likely) apparent input power and the apparent load whose error line passes through the window are acceptably accurate. (If both lines pa s through the window, as in Figure 5.6, apparent input power and either apparent load could be acceptably accurate.);[6]
- (least likely, but possible) apparent input power and both apparent loads are *all* unacceptably in error.

---

[6] This alternative is less likely because the acceptability range(s) of the apparent load(s) whose error lines pass through the window do not extend into the window for more than a quarter of its width, as seen in Figure 5.6; so at least half of the width of the window (the central portion) has no load acceptability range present. Hence, if apparent input power is known to be acceptably accurate, it is more likely that neither apparent load is acceptably accurate.

The additional principle illustrated in Figures 5.4 through 5.6 is now stated as follows.

F. *At least one apparent constituent unacceptable.* If

- both load error lines pass through the acceptability window for *non-overlapping* ranges of error in apparent input power, or
- only one load error line passes through the acceptability window, or
- if the range of joint acceptability of the two apparent loads is entirely outside the power acceptability band,

only two apparent constituents of the heat balance can be acceptably accurate at once. *Hence at least one apparent constituent is unacceptably in error.*

Large Heat Imbalance: Acceptability of Any Two Apparent Constituents Impossible

Here, as in Figure 5.7, both load error lines will miss the acceptability window, but will be on opposite sides of it. It is easily seen that - as for Figure 5.5 - there is no range of joint acceptability for the two apparent loads, so either one or both of these loads are unacceptably erroneous. Furthermore, at least two apparent constituents of the heat balance must be unacceptably in error. The alternatives are:

- if apparent input power is acceptably accurate, then one apparent load (in Figure 5.7, rejection load) is unacceptably, erroneously high and the other (in Figure 5.7, evaporator load) is unacceptably, erroneously low; or
- if one apparent load is acceptably accurate, then both apparent input power and the other apparent load are unacceptably in error. For example, in Figure 5.7, if apparent evaporator load is known to be

acceptably accurate, then both apparent input power and apparent rejection load are unacceptably, erroneously high; or

- apparent input power and both apparent loads are *all* unacceptably in error.

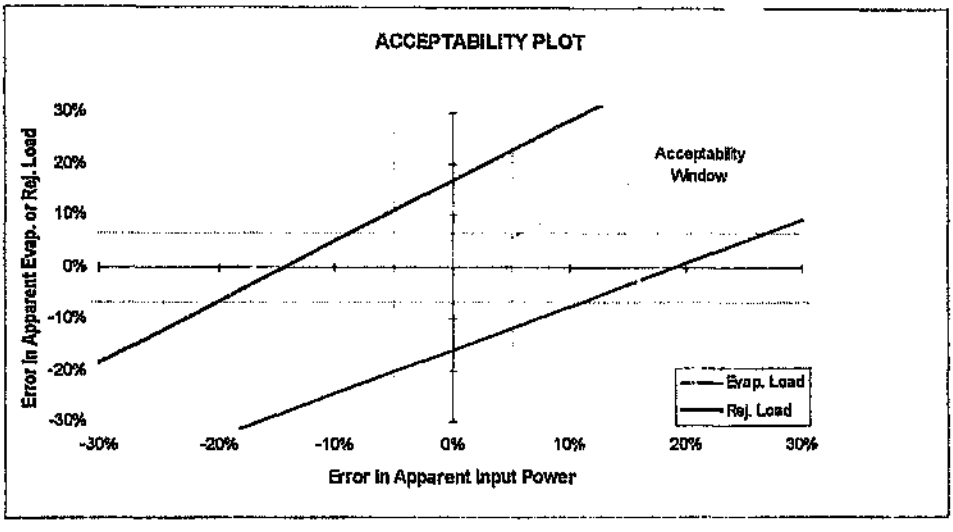

Figure 5.7 Acceptability Plot: Large Heat Imbalance, Acceptability of Two Apparent Constituents Impossible

The additional principle of Figure 5.7 can be stated as follows.

G. *At least two apparent constituents unacceptable.* If no load error line passes through the acceptability window, and there is no range of joint load acceptability, only one apparent constituent of the heat balance can be acceptable at once. *Hence at least two apparent constituents are unacceptably in error.*

The usefulness and convenience of this enhanced Thorp method of verifying apparent site performance of water chilling machines is best made clear through case studies. Those now described were conducted by the author between 1983 and 1994, as the opportunity arose.

Appendix 10 describes the experimental technique employed in the surveys of performance in these case studies.

5.2.3 Case Study A: Acceptable Heat Imbalance, Acceptable Principal Measurements

In the first case study, both the heat imbalance and the principal measurements turned out to be acceptable. The machine surveyed was a large single-stage centrifugal machine, employing Refrigerant 12 and of 7 MW(R) rated capacity, situated on surface. This machine was equipped with a refrigerant subcooler following the condenser, as shown in Figure 5.8 below.

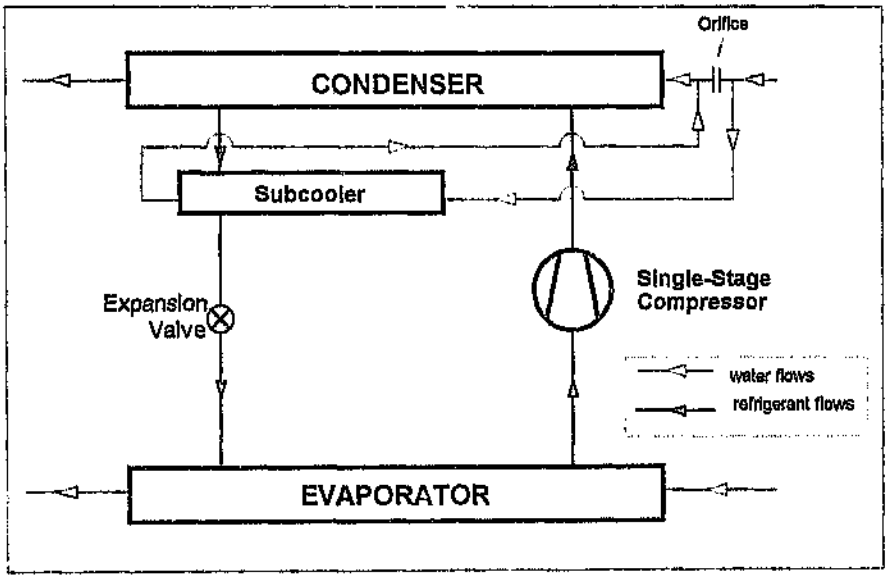

Figure 5.8 Case Study A: Single-Stage Centrifugal Machine with Subcooler

The enhanced Thorp method was applied to verify the principal measurements. The heat imbalance, apparent COPs and corrected refrigerant-circuit COP (the estimate of actual COP) are given in Table 5.2 below. By way of example, the measurements made and the calculations are set out in Appendix 11. The heat imbalance was small, +4,92%, but

as noted above, this was not a guarantee of acceptable principal measurements.

Table 5.2 Case Study A: Verification of Principal Measurements by Enhanced Thorp Method

QUANTITY	UNIT	VALUE
Apparent Evaporator Load	kW(R)	6 362
Apparent Input Power	kW	925
Apparent Condenser and Subcooler Load	kW(R)	-7 665
Heat Imbalance ε	%	+4,92
Apparent Evaporator-Load $COP_{[EB]p}$		6,88
Apparent Rejection-Load $COP_{[JB]p}$		7,29
Refrigerant-Circuit COP $COP_{(r)}$		7,468 ± 0,304
Corrected Refrigerant-Circuit COP		7,186 ± 0,295

The acceptability plot, depicted in Figure 5.9, was then drawn. The last section of Appendix 11 sets out how this was done. The uncertainties in the refrigerant-circuit COP and corrected refrigerant-circuit COP in Table 5.2 were determined as described in Appendix 12, assuming that accuracies of measured refrigerant temperatures and pressures were ±0,2°C and ±2 per cent of full scale respectively.

Examining Figure 5.9, the error lines of evaporator and condenser water loads were close together, as they should have been for a small heat imbalance. Both lines passed through the acceptability window for a common range of error in apparent input power. This range of joint acceptability of between -2 and +5 per cent of error in apparent input power amounted to more than half the width of the power acceptability band. Finally, it is shown in Section A11.2 of Appendix 12 that one

apparent constituent of the heat balance - apparent input power - was acceptably accurate; its uncertainty was ±4 per cent.[7] Criterion E on page 188 was thus met, and so all principal measurements could be declared quite acceptable.

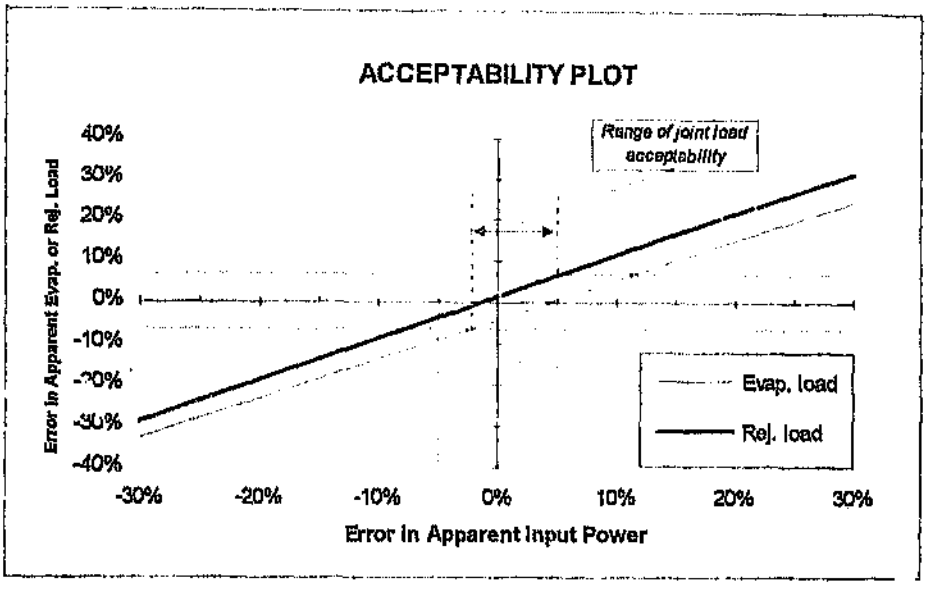

Figure 5.9 Case Study A: Acceptability Plot

The corrected refrigerant-circuit COP, as seen from Table 5.2, had an uncertainty of ±4,1 per cent.[8] Fortunately, the conclusions drawn from the acceptability plot were hardly affected by even this degree of uncertainty. Shown in Figure 5.9a is the acceptability plot if the corrected refrigerant-circuit COP were at its lower limit of uncertainty: (7,186 - 0,295), or 6,890.

---

[7] As noted in Appendix 12, provided that the kilowatt-hour meter measuring electrical energy input to the compressor driving motor was within its Class 2 accuracy limit of ±2 per cent. Electrical power or energy meters can give unacceptably erroneous readings, though, if they are adjusted or connected incorrectly. As for all instruments measuring important quantities, such meters should therefore be checked at specified intervals.

[8] Most of this, as noted in Appendix 12, was due to the uncertainties in the measured refrigerant pressures. If the pressure gauges had been calibrated for accuracies of ±1 per cent of their full scale values, the uncertainty in refrigerant-circuit COP would have shrunk to ±2,3 per cent.

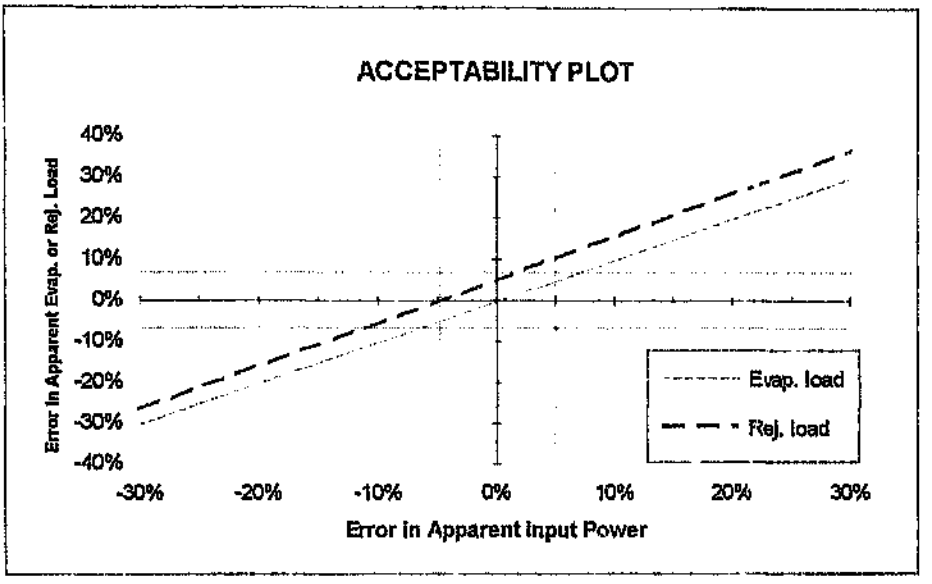

Figure 5.9a Case Study A: Acceptability Plot with Corrected Refrigerant-Circuit COP at its Lower Limit of Uncertainty

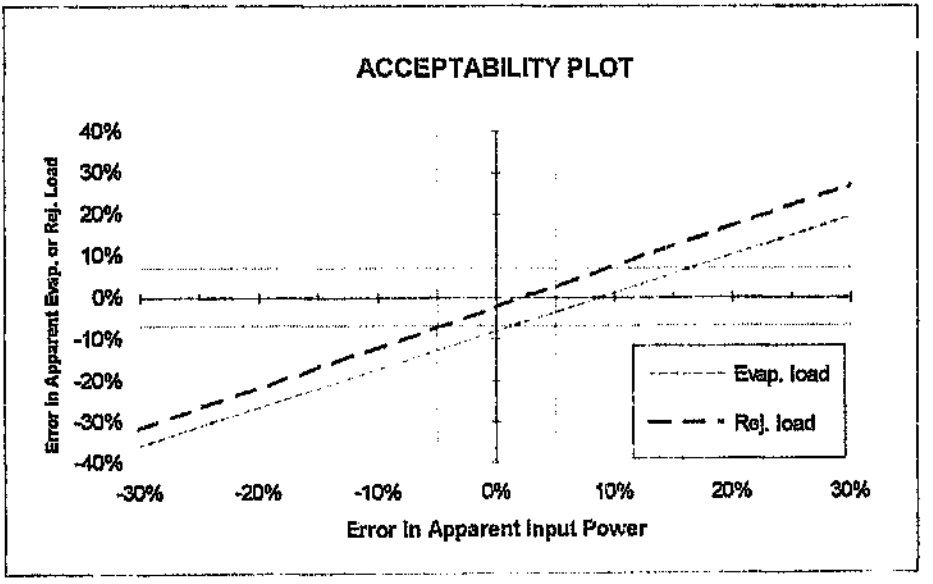

Figure 5.9b Case Study A: Acceptability Plot with Corrected Refrigerant-Circuit COP at its Upper Limit of Uncertainty

It can be seen that the conclusions were not affected; both load error lines still passed through more than half of the acceptability window's width, and the range of joint load acceptability was still mostly inside this window and spanned more than half its width (i.e. the width of the power acceptability band).

For the corrected refrigerant-circuit COP at its upper limit of uncertainty - (7,186 + 0,295), or 7,481 - the conclusions were marginally affected, as shown in Figure 5.9b. Here, the evaporator load error line passed through just less than half of the acceptability window, and the range of joint load acceptability was just less than half of this window's width. However, this was at the extreme upper limit of the uncertainty. The conclusion therefore remained that unless the corrected refrigerant-circuit COP was at the upper limit of its estimated uncertainty, all principal measurements were acceptably accurate.

5.2.4 Case Study B: Acceptable Heat Imbalance, Unacceptable Principal Measurements!

In the next case study, an acceptable heat imbalance concealed grossly unacceptable principal measurements, because of the cancelling effect of large but *similar* errors. This case study was first reported in a previous paper (Bailey-McEwan, 1990) and the application of the enhanced Thorp method reported later (Bailey-McEwan, 1995a). Here, an acceptance test was being carried out on a two-stage centrifugal machine situated underground, employing Refrigerant 11 and of 3 MW(R) rated capacity. Hence, in contrast to all other case studies in this thesis, *testing* with some calibrated instruments[9] was done here, as opposed to *checking* with all instruments uncalibrated except portable thermometers. The refrigerant circuit of this machine is illustrated in Figure 5.10 below.

---

[9] See Section A10.2, Appendix 10 for details.

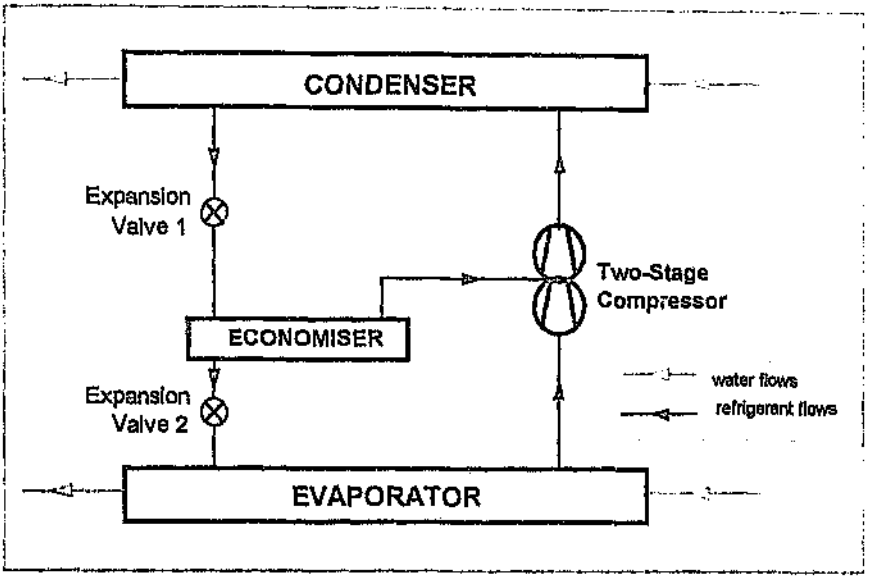

Figure 5.10 Case Study B: Two-Stage Centrifugal Machine

Table 5.3 Case Study B: Verification of Principal Measurements by Enhanced Thorp Method

QUANTITY	UNIT	VALUE
Apparent Evaporator Load	kW(R)	3 222
Apparent Input Power	kW	657
Apparent Rejection Load	kW(R)	-4 100
Heat Imbalance ε	%	+5,38
Apparent $COP_{[EB]p}$		4,90
Apparent $COP_{[JB]p}$		5,24
Refrigerant-Circuit COP		4,115 ± 0,019
Corrected Refrigerant-Circuit COP		3,998 ± 0,030

The quantities calculated by the enhanced Thorp method are given in Table 5.3 above. The heat imbalance was +5,38%, which seemed quite acceptable and small. From Table 5.3, though, it is seen that the corrected refrigerant-circuit COP was markedly lower than both apparent

COPs. The implication of this became clear when the acceptability plot was drawn as in Figure 5.11. The conclusions drawn from this plot were not affected at all by the estimated uncertainty in corrected refrigerant-circuit COP of ±0,74 per cent,[10] determined as for Case Study A.

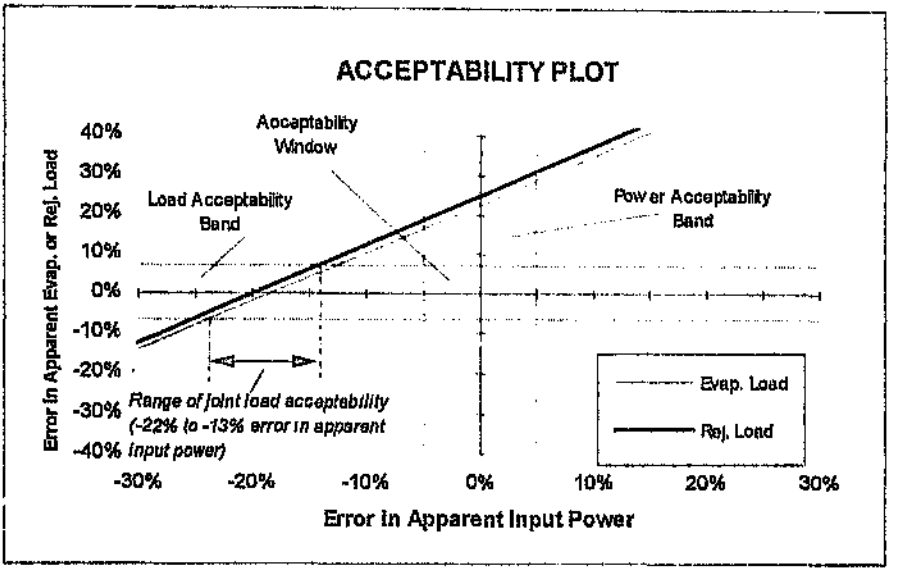

Figure 5.11 Case Study B: Acceptability Plot

In Figure 5.11, the load error lines were remarkably close together, but neither passed through the acceptability window! It was thus impossible for all apparent constituents of the heat balance to be acceptable. However, as annotated on the figure, the range of joint load acceptability was between -22 and -13 per cent of error in apparent input power. Thus the acceptability plot clearly showed the following:

---

[10] This uncertainty was much lower than that of Case Study A because the refrigerant vapour leaving the evaporator was saturated (it was superheated in Case Study A, as noted in Appendix 11), and the refrigerant liquid entering both expansion valves was saturated (the liquid entering the expansion valve in Case Study A was subcooled). The enthalpies of these refrigerant streams were thus functions of refrigerant temperatures only. Because the uncertainty in temperature measurement (±0,2°C) was less than that in pressure measurement, the uncertainty in refrigerant-circuit COP accordingly decreased.

- the errors in apparent evaporator and rejection load were very similar, whatever they were;
- if the apparent loads were both acceptably accurate, apparent input power had to be between -22 and -13 per cent in error;
- alternatively, if apparent input power was acceptably accurate (i.e. if its error was within the power acceptability band), *both apparent loads had to be between +15 and +25 per cent in error.*

As in Case Study A, it could be shown that the error in apparent input power was within ±4 per cent. Thus apparent evaporator and rejection loads were in error by at least +15 and +18 per cent respectively. Because all thermometers had been calibrated, the measured evaporator and condenser water *flow-rates* were in error by these percentages.

The reason for the small heat imbalance was that the relative errors n_{EBp} and n_{JBp} in the apparent water loads were very similar. Therefore, in computing the relative heat imbalance, they almost cancelled out, as can be seen from (5-7) above. However, these load errors were far from zero, a[illegible]ssly unacceptable! This case study strikingly illustrates the conclusion of Section 5.1.2 that an acceptable heat imbalance, by itself, does *not* confirm the accuracy of the principal measurements. The enhanced Thorp method must *always* be used to verify the accuracy of the apparent constituents of the heat balance, and hence that of the principal measurements.

5.2.5 Additional Checks for Machines Sharing Common Water Flows

An additional check for accuracy of measured water *temperatures* or apparent input powers is possible for machines sharing common water flows - such as when evaporators or condensers, or both, are connected in series in their chilled or condenser water circuits, as in Figure 3.20.

Let the evaporators of two conventional machines share a common water flow. Provided that conditions do not change appreciably over the period of taking measurements, *and* that there are negligible errors in measured water temperatures, the only significant error in the two apparent evaporator loads is that arising from measurement of the common water flow. So the relative errors in these two apparent loads will be virtually equal; that is, $n_{EB1p} \cong n_{EB2p}$. If the evaporator load error lines for both these machines are plotted on the same acceptability plot, they will thus coincide *if:*

- all water temperatures are perfectly accurate (thus making $n_{EB1p} = n_{EB2p}$); *and*
- the errors in apparent input powers of both machines are identical (i.e. $n_{VCB1p} = n_{VCB2p}$).

The extent to which these error lines do not coincide, therefore, is due to *either* the inaccuracies of the measured water temperatures, *or* the difference of the errors in the two apparent input powers, or both. If all measured water temperatures are known to be accurate, it can be deduced whether the errors in both apparent input powers can be acceptable, or whether at least one is unacceptable. Of course, the same principle holds if there is a common water flow through the condensers. In the following case study, it was proved in this way that the apparent input power of at least one machine was unacceptably in error.

5.2.6 Case Study C: Two Machines in Lead-Lag Configuration

This case study concerned two machines in an underground installation, and had been described previously (Bailey-McEwan, 1991). The use of the enhanced Thorp method was reported later (Bailey-McEwan, 1995a). As shown in Figure 5.12, the machines were connected in the "counterflow lead-lag" configuration of Figure 3.20; the water being chilled

first entered the evaporator of Machine 1, and the heat-removing water first entered the condenser of Machine 2. These .nachines were of 3,5 MW(R) capacity, possessed three-stage centrifugal compressors and two interstage economisers (as in Figure A7.1, Appendix 7), and employed Refrigerant 12.

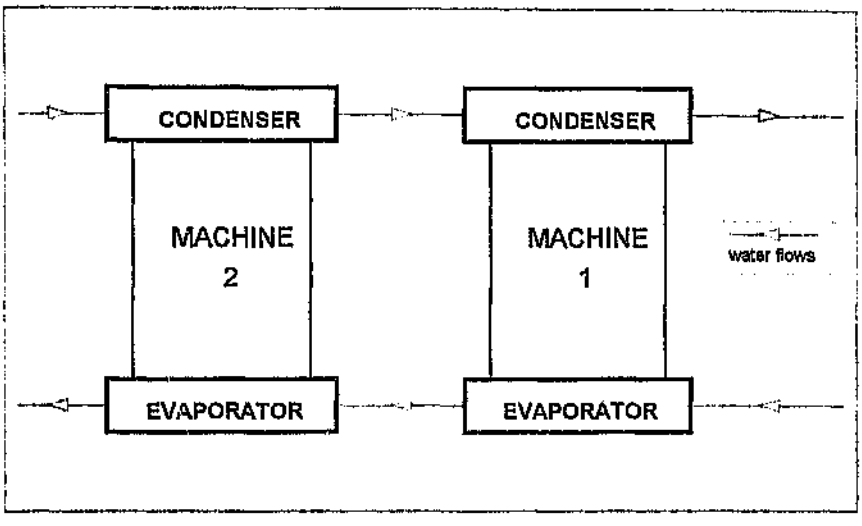

Figure 5.12 Case Study C: Two Machines in Lead-Lag Configuration

The only measurements known to be reliable in this survey were the water and refrigerant temperatures. Use of the enhanced Thorp method yielded Table 5.4 below.

The heat imbalances of both machines were unacceptable, being +27,6% and +23,2% respectively. As both of these were higher than the upper unacceptability confirmation limit of +13%, at least one unacceptable error was present in the measurements on both machines. The acceptability plot for the lead machine was drawn as in Figure 5.13 below. Again, the uncertainties, estimated as for Case Study A, in the corrected refrigerant-

circuit COPs were ±1,45% and ±1,88% respectively,[11] so the conclusions from the acceptability plots were not affected.

Table 5.4 Case Study C: Verification of Principal Measurements by Enhanced Thorp Method

QUANTITY	UNIT	MACHINE 1 (Lead)	MACHINE 2 (Lag)
Apparent Evaporator Load	kW(R)	3 001	2 745
Apparent Input Power	kW(M)	998	914
Apparent Rejection Load	kW(R)	-5 521	-4 768
Heat Imbalance ε	%	+27,6	+23,2
Apparent $COP_{[EE]p}$		3,01	3,01
Apparent $COP_{[JB]p}$		4,53	4,22
Refrigerant-Circuit COP		3,306 ± 0,047	3,811 ± 0,071
Corrected Refrigerant-Circuit COP		3,266 ± 0,047	3,761 ± 0,071

In Figure 5.13, because of the large heat imbalance, the load error lines were far apart, passing through the load acceptability band for widely separate, non-overlapping ranges of error in apparent input power. Hence, *whatever the error in apparent input power, it was impossible for both apparent loads to be acceptable;* apparent evaporator load, rejection load or both were unacceptably in error.

A similar conclusion was drawn from the acceptability plot for the lag machine. However, when the two plots were superimposed - that is, the load error lines for both machines were drawn on the same plot, as in

---

[11] Again, these uncertainties were lower than in Case Study A because the refrigerant liquid entering the expansion valves was saturated, whereas the liquid entering the expansion valve in Case Study A was subcooled. These uncertainties did depend on the uncertainty in *evaporating* refrigerant pressures here, because the refrigerant vapour leaving both evaporators was slightly superheated, so the enthalpy thereof depended on pressure as well as temperature.

Figure 5.14 - it also emerged that the apparent input power of one or both machines was unacceptably in error!

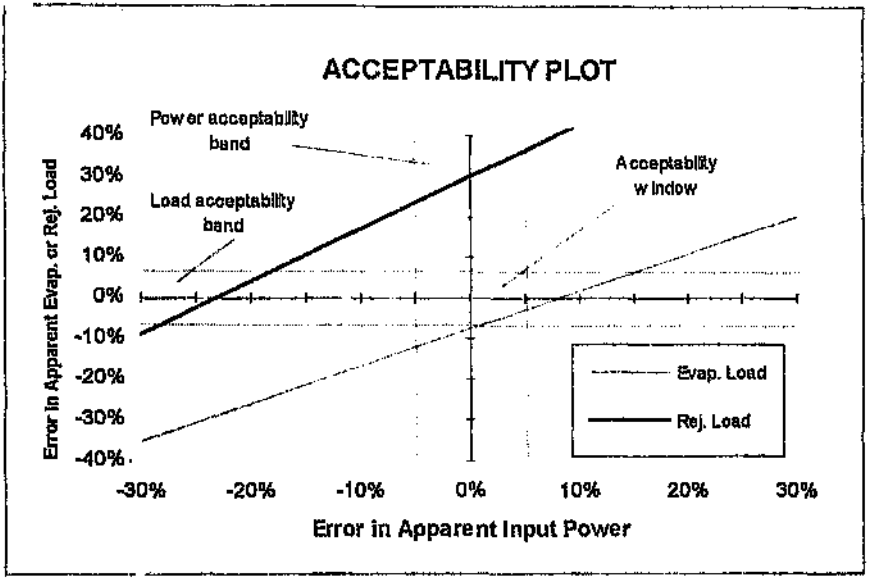

Figure 5.13 Case Study C: Acceptability Plot (Lead Machine)

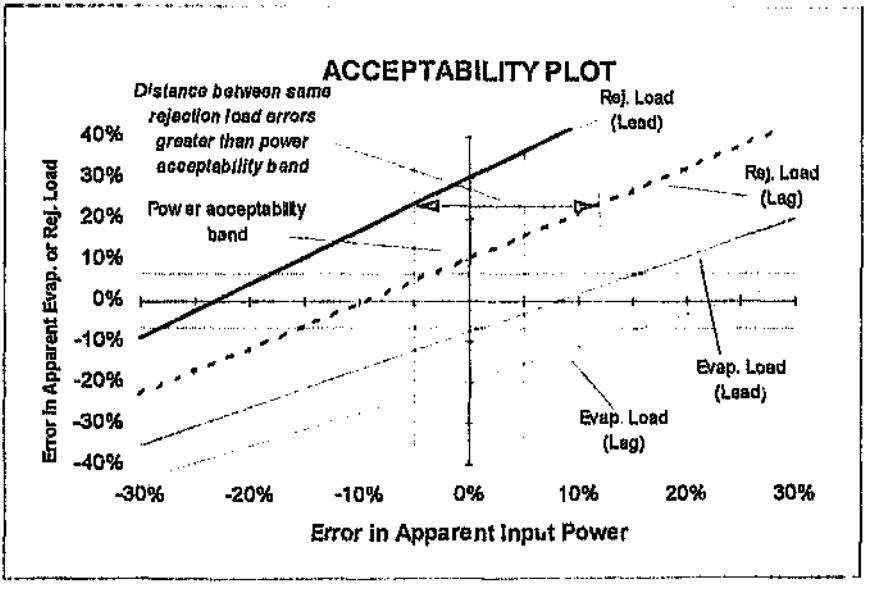

Figure 5.14 Case Study C: Acceptability Plot (Lead and Lag Machines)

This was deduced as follows. The condensers shared a common water flow, and water temperatures had been measured as simultaneously as possible and were known to be accurate. Consequently, the errors in apparent rejection loads of the two machines had to be approximately equal. *For equal errors in apparent rejection load, the horizontal distance between the two rejection load error lines was always greater than the width of the power acceptability band* (as shown by example in the figure). It was thus impossible for the errors in both apparent input powers to be inside this acceptability band at once. Therefore, at least one of these errors was unacceptable. (As the evaporators also shared a common water flow, the same conclusion could have been drawn by examining the horizontal distance between the two evaporator load error lines.)

This was as much as could be deduced through the enhanced Thorp method, and confirmed the initial analysis of this case (Bailey-McEwan, 1991). It is shown by machine modelling in Section 5.4.2 below that the apparent evaporator water flow was in fact accurate. Knowing this, it is readily seen from Figure 5.14 that the apparent rejection loads (and hence the apparent condenser water flow) were at least +37 per cent in error, and the errors in apparent input powers were both unacceptable - approximately +9% and +25% respectively.

5.2.7 Limitations of Enhanced Thorp Method

The enhanced Thorp method, although powerful, has its limitations. If it is to verify apparent machine performance (and hence verify the principal measurements), the refrigerant-circuit COP must be possible to determine precisely, and at least one constituent of the heat balance must be independently known to be acceptably accurate. There are many cases where one or both of these requirements are not met.

Refrigerant-Circuit COP Impossible to Determine Precisely

If the refrigerant-circuit COP is to be determined precisely, all confirming measurements required for this must be obtainable. For conventional machines operating normally (that is, with no auxiliary devices introducing additional refrigerant flows), the only confirming measurements necessary are easily obtainable, key refrigerant pressures and temperatures. Hitherto, therefore, in the South African mining industry, the Thorp method has been used only with conventional machines operating normally, as noted in Chapter 4.

There are two reasons why all confirming measurements required to precisely determine refrigerant-circuit COP may not be obtainable. First, as also noted in Chapter 4, when auxiliary devices (such as hot gas bypass valves) are operating in conventional machines and so do introduce additional refrigerant flows, extra confirming measurements of these additional flows *and the main flow entering the evaporator* are required. The same applies in general to non-conventional, custom-built machines employing screw compressors, which generally possess such auxiliary devices. The difficulty here is that these measurements are almost never obtainable, as refrigerant flow meters are almost never installed.[12]

Second, extra confirming measurements - difficult or impossible to obtain - may suddenly become necessary if the refrigerant circuit is not in good order, due to undesirable values of some process parameters or state variables. For example, an overcharge of refrigerant may cause refrigerant flows from evaporators to compressors - normally single-phase vapour flows - to entrain considerable fractions of liquid. Determining the enthalpy of such a two-phase flow requires an extra confirming

---

[12] It is difficult to install such meters in the tightly confined, curved piping of conventional, packaged machines. With non-conventional, custom-built machines, such installation is easier, particularly if requested at the time of ordering.

measurement: the mass fraction of liquid therein. Alternatively, the refrigerant may be contaminated with sufficient oil, water or non-condensable gas to become a poorly understood mixture with thermodynamic and thermophysical properties differing significantly from those of pure refrigerant. Determining the enthalpy of such a mixture requires extra confirming measurements of the mass fractions of each contaminant (as well as information, not necessarily available, enabling reliable determination of the enthalpy of the mixture once these mass fractions are known). Even if such extra confirming measurements were simple to obtain, machines are not fitted with facilities for obtaining them, as they are not necessary if the refrigerant circuit is in good order.

It is shown in Section 5.3 following that the enhanced Thorp method can be extended to cases where the refrigerant-circuit COP cannot be determined precisely for either of these reasons. However, on its own, this extension, termed the *inexact Thorp method,* is no longer capable of fully verifying the apparent performance. It can only indicate, on a balance of probabilities, which apparent constituents of the heat balance are likely to be unacceptably erroneous. Additional information is necessary to prove the *absence* of such errors, or to unambiguously determine the identities and magnitudes of those that exist. Fortunately, knowledge of machine specifications and design performance yields the required additional information in many such cases. To fully and unequivocally verify apparent performance, though, it is necessary to resort to machine modelling, discussed in Section 5.4 below.

All Apparent Constituents of Heat Balance Uncertain

As in Case Study C above, examples do occur where the refrigerant-circuit COP can be precisely determined, but *no* apparent constituent of the heat balance is independently known to be acceptably accurate. From principle E.2, page 188, no precise conclusion can then be drawn from the acceptability plot, so the enhanced Thorp method cannot verify

apparent performance. In such cases it is again necessary to resort to machine modelling for this purpose, as was done in Case Study C and as described in Section 5.4 below.

5.3 Verifying Apparent Performance by Inexact Thorp Method

It is now shown that the enhanced Thorp method can be extended to cases where the refrigerant-circuit COP cannot be determined precisely. The absence of unacceptable errors from the apparent performance cannot be verified, but a modification of the acceptability plot, known as the *acceptability band plot*, can still indicate the relative likelihood of all apparent constituents of the heat balance being acceptably accurate, or whether one or more must be unacceptably erroneous. Moreover, even though actual COP cannot be precisely estimated, it may be feasible to determine a range in which it must lie. Finally, in many cases, knowledge of machine specifications and design performance supplies the balance of the information necessary to identify some unacceptably erroneous measurements, or at least to yield valuable implications in this regard. A procedure for this appropriately termed *inexact Thorp method* is now given, following which it is demonstrated through three case studies. This inexact method and the three case studies have been reported (Bailey-McEwan, 1995b).

5.3.1 The Inexact Thorp Method: Procedure

As for the enhanced Thorp method, the apparent evaporator block load $\sum Q_{EBp}$, rejection load $\sum Q_{JBp}$ and input power $\sum W_{VCBp}$ are calculated from the performance survey. Then, the relative heat imbalance ε is calculated per (5-7), and the apparent evaporator-load COP, $COP_{[EB]p}$, and rejection-load COP, $COP_{[JB]p}$, are calculated per (5-9c).

The Acceptability Band Plot

As for the enhanced Thorp method, the limits of accuracy of ISO R916 (ISO, 1968) for the apparent evaporator block load, rejection load and input power are adopted. The bands between these limits are termed the *acceptability bands* for the apparent loads and input power.

In the *acceptability band plot*, the framework of which is illustrated in Figure 5.15, the horizontal axis represents the actual COP, and the vertical axis the relative error n_{VCBp} in apparent input power. The power acceptability band of ±5% is indicated on this vertical axis.

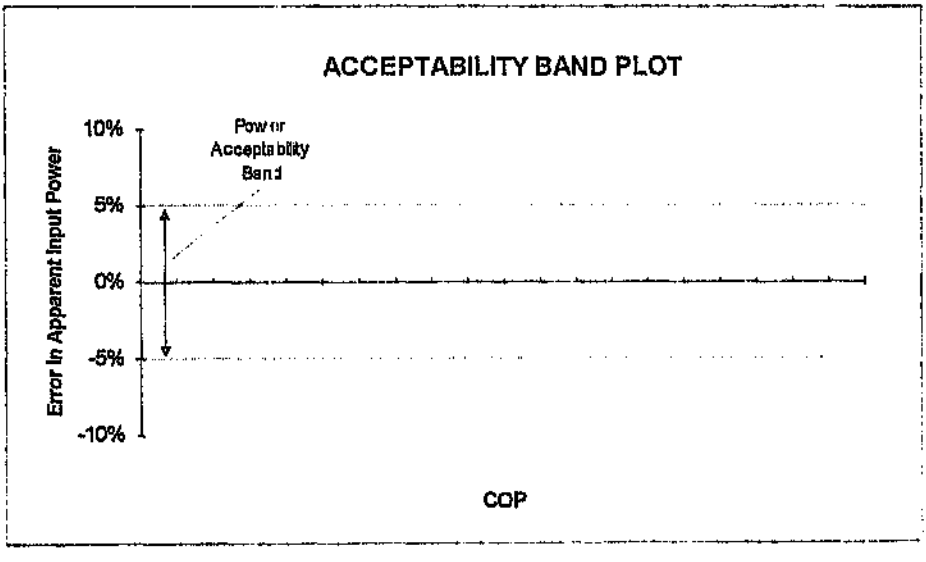

Figure 5.15 Framework for Acceptability Band Plot

The acceptability limits of ±7% for the two apparent loads are then plotted graphically on this plot. For the apparent evaporator block load, it is shown in Appendix 13 that the lower (-7%) and upper (+7%) limits of acceptability are given by the following relations between actual COP and error n_{VCBp}:

Lower limit (-7%): $$COP = \frac{COP_{[EB]p}\left(1+n_{VCBp}\right)}{0{,}93}$$

Upper limit (+7%): $$COP = \frac{COP_{[EB]p}\left(1+n_{VCBp}\right)}{1{,}07} \qquad (5\text{-}13a)$$

Similarly, the corresponding limits of acceptability for the apparent rejection load are shown in Appendix 13 to be given by

Lower limit (-7%): $$COP = \frac{\left(1+COP_{[JB]p}\right)\left(1+n_{VCBp}\right)}{0{,}93} - 1$$

Upper limit (+7%): $$COP = \frac{\left(1+COP_{[JB]p}\right)\left(1+n_{VCBp}\right)}{1{,}07} - 1 \qquad (5\text{-}13b)$$

The pairs (5-13a) and (5-13b) of relations are linear relationships, and thus particularly easy to plot on the acceptability band plot. How this is done, and the information which the acceptability band plot then yields, is best illustrated by the case studies following.

The COP Range Plot

Next, if feasible, the *range* in which actual COP must lie is estimated from the obtainable confirming measurements in the refrigerant circuit. The procedure for doing this depends on the particular machine and its operating circumstances, and so is also best illustrated in the case studies below. This range is then plotted on an appropriately termed *COP range plot.*

Interpretation of Plots in Light of Machine Specifications and Design Performance

Finally, the manufacturer's specifications and quoted design performance are consulted in interpreting the information yielded by the acceptability band plot and the COP range plot. It may hence be possible to identify one or more unacceptably erroneous measurements, especially where the

acceptability band plot and possible range of actual COP definitely indicate that such erroneous measurements exist.

5.3.2 Case Study D: Acceptable Heat Imbalance: Machine Bypassing Hot Gas

When conventional machines operate under severe part-duty conditions, hot gas may have to be bypassed from condenser to evaporator in order to keep the centrifugal compressor stable. Here, such a machine of 3,5 MW(R) rated capacity, with a two-stage centrifugal compressor and employing Refrigerant 12, was operating with the hot gas bypass valve open. This machine, situated in an underground installation, is illustrated schematically in Figure 5.16 below.

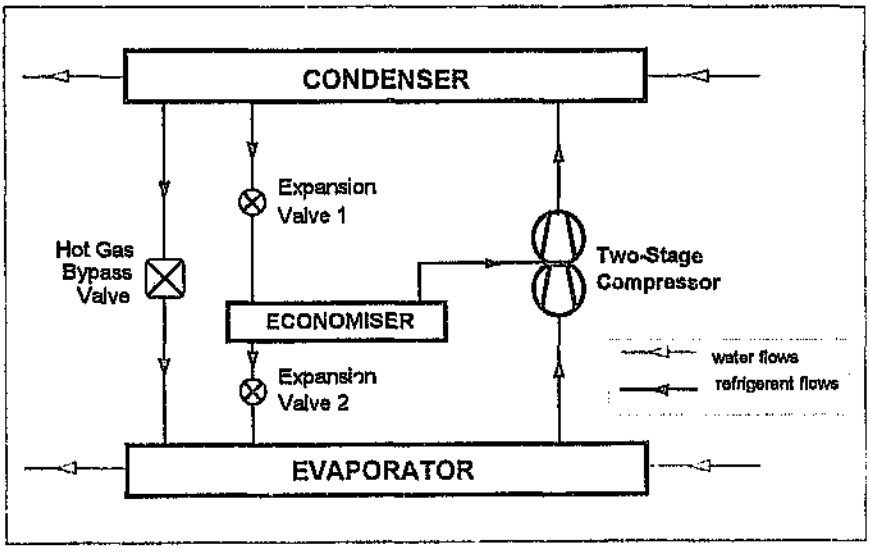

Figure 5.16 Case Study D: Two-Stage Centrifugal Machine Bypassing Hot Gas

The heat imbalance and the apparent evaporator-load and rejection-load COPs could be determined in the same way as before, and are given in Table 5.5 below. The heat imbalance evaluated to +7,9%, which was between the unacceptability confirmation limits of -15% and +13%. It was

possible, therefore, that all principal measurements were acceptably accurate.

Table 5.5 Case Study D: Calculated Heat Imbalance and Apparent COPs

QUANTITY	UNIT	VALUE
Apparent Evaporator Load	kW(R)	2 600
Apparent Input Power	kW	796
Apparent Rejection Load	kW(R)	-3 686
Heat Imbalance ε	%	+7,89
Apparent $COP_{[EB]p}$		3,27
Apparent $COP_{[JB]p}$		3,63

Acceptability Band Plot

The acceptability band plot was then constructed as follows. Plotting the acceptability limits of ±7% for apparent evaporator load, given by (5-13a), on the framework of Figure 5.15 yielded the evaporator load acceptability band as shown in Figure 5.17. (By way of example, Appendix 14 details how this was done.) The intersection of the evaporator load acceptability band with the power acceptability band is the *area of joint acceptability* of apparent evaporator load and input power, shown with a shaded border in the figure.

A brief observation on this area of joint acceptability is in order. It began at corner A in the figure, where the COP was 2,90. Thus, had the actual COP been less than or equal to 2,90, the likelihood of apparent evaporator load and input power *both* being acceptably accurate would have been zero. For larger values of COP, this likelihood initially increased rapidly. It reached a maximum at corner B, corresponding to a higher COP of 3,21 (vertical line BB'B" in the figure). Here, the error in apparent input power could lie anywhere in the power acceptability band

of ±5% (portion BB' of that line) *and still be within the area of joint acceptability.* Thus, had the actual COP been 3,21, apparent evaporator load would certainly have been acceptably accurate if apparent input power had been so. Between this COP and a COP of 3,34 (corner D; vertical line DD'D" in the figure), this condition held. For still higher values of COP, the likelihood of apparent evaporator load and input power both being acceptably accurate decreased rapidly, reaching zero again at corner C, where the COP was 3,69.

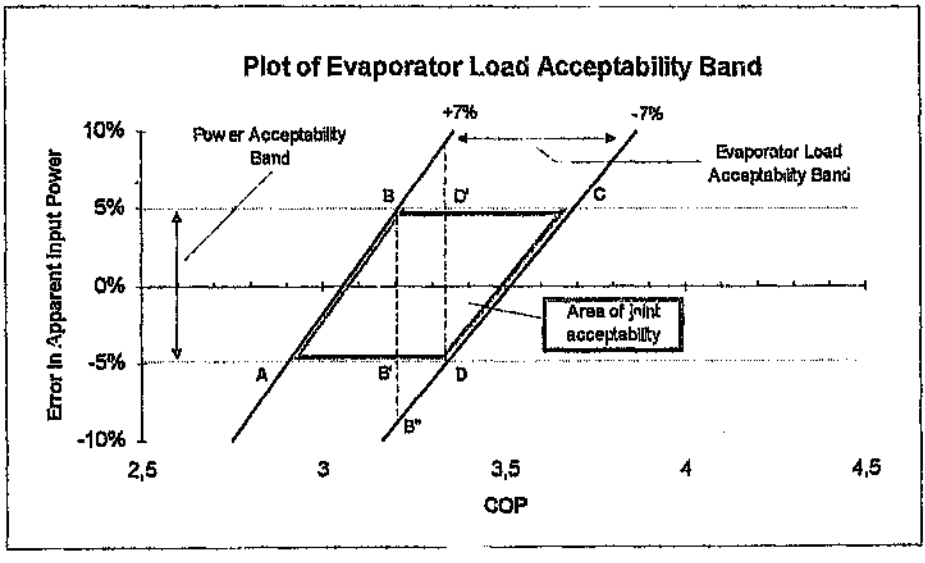

Figure 5.17 Case Study D: Plot of Evaporator Load Acceptability Band

Next, the similar acceptability limits for apparent rejection load, given by (5-13b), were also plotted on Figure 5.17. (Appendix 14 again shows how this was done.) This yielded the complete acceptability band plot for this case, shown in Figure 5.18. Here, the area of joint acceptability of apparent evaporator load and input power (shown in Figure 5.17) overlapped with the similar area of joint acceptability of apparent rejection load and input power. The area of overlap EFCD, shaded in Figure 5.18, was where *both* apparent loads and input power - that is, all three

apparent constituents of the heat balance - would have been acceptably accurate, and is hence termed the *area of complete acceptability*.

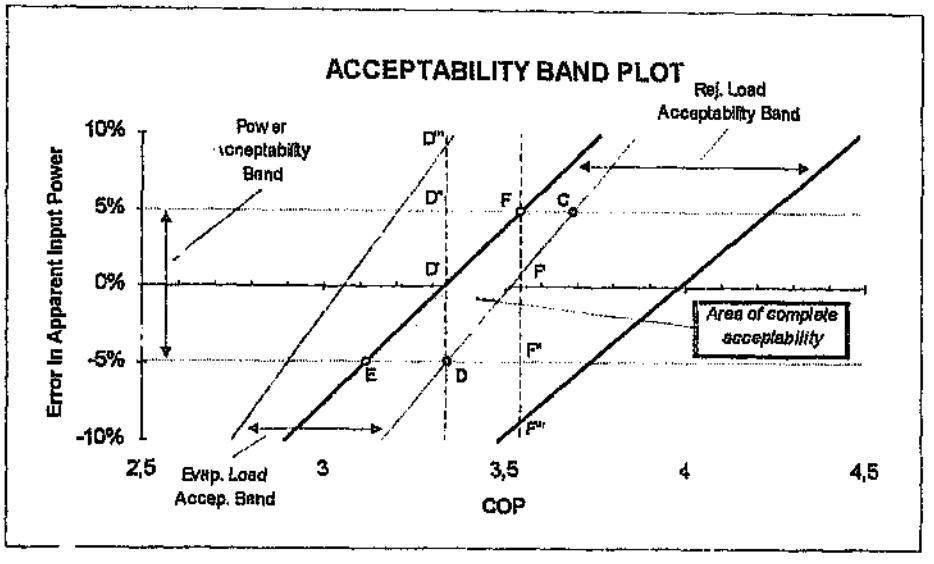

Figure 5.18 Case Study D: Acceptability Band Plot

Upon careful examination of this area of complete acceptability, the relative likelihood of all three apparent constituents of the heat balance being acceptably accurate was small. First, the width of this area was less than half the widths of the evaporator and rejection load acceptability bands. Hence, whatever the actual error in apparent input power was, the likelihood of the actual COP being inside this area had to be regarded as relatively small.

Second, whatever the actual COP was, the likelihood of the actual error in apparent input power being within this area was also small. This likelihood was initially zero at corner E, where the COP was 3,11. At corner D, where the COP was 3,34, denoted by the vertical line DD'D"D"', this likelihood was at a maximum, represented by the portion DD' of this line within the area of complete acceptability. Even here, however, this portion DD' just exceeded half the width DD'D" of the power acceptability

band; thus, even if it had been independently known that apparent input power was acceptably accurate, the likelihood of all three apparent constituents being acceptably accurate could only just have exceeded 50 per cent. Between corners D and F, this likelihood decreased slightly. At corner F, where the COP was 3,55, represented by the vertical line FF'F"F'", the portion FF' within the area of complete acceptability was less than half the width of the power acceptability band. Thereafter, this likelihood decreased rapidly to zero again at corner C, where the COP was 3,69.

The acceptability band plot thus indicated that whereas it was possible for all apparent constituents of the heat balance to be acceptable, it was more likely that at least one was unacceptably in error.

COP Range Plot

Next, the COP range plot was constructed. The only obtainable confirming measurements in the refrigerant circuit were of key pressures and temperatures. These are listed in Table 5.6, together with the full-duty design values for comparison.

It was not possible to precisely determine refrigerant-circuit COP from these measurements, and hence to correct this to estimate actual COP. This was because the refrigerant-circuit COP of this type of machine is given by (3-22b), reproduced below:

$$COP_{(r)} = \frac{(h_{Eo} - h_{ECto}) - \dfrac{m_{(r)HG}}{m_{(r)EX2}} \cdot (h_{HGi} - h_{Eo})}{(h_{Po} - h_{Eo}) \cdot \left(1 + \dfrac{m_{(r)HG}}{m_{(r)EX2}}\right) + A(h_{Po} - h_{ECvo})} \qquad (5\text{-}14)$$

where $$A = \frac{h_{EX1i} - h_{ECto}}{h_{ECvo} - h_{EX1i}}$$

and the ratio $m_{(r)HG}/m_{(r)EX2}$ is of refrigerant mass flow through the hot gas bypass valve of Figure 5.16 to that through Expansion Valve 2 (the one feeding the evaporator) in that figure. This mass flow ratio, termed *hot gas bypass ratio* for convenience, could not be determined, as no refrigerant flow meters were fitted to the machine. However, as all enthalpies h in (5-14) could be determined from the confirming measurements of refrigerant pressures and temperatures in Table 5.6, it was quite possible to plot actual COP[13] for a range of possible values of this ratio. The resulting plot, shown in Figure 5.19, constituted the *COP range plot* for this case; it is seen that COP strongly depended upon hot gas bypass ratio.

Table 5.6 Case Study D: Obtainable Confirming Measurements in Refrigerant Circuit

QUANTITY	UNIT	VALUE	*Design full-duty value for comparison*
EVAPORATOR			
Refrigerant pressure	kPaa	341,2	*342,4*
Refrigerant temperature	°C	-	*3,22*
ECONOMISER			
Refrigerant temperature	°C	19,7	*28,07*
COMPRESSOR			
Vane opening	%	50	*100*
Suction temperature	°C	3,5	*2,22*
Discharge temperature	°C	53,0	*60,61*
HOT GAS BYPASS VALVE			
Opening	%	50	*closed*
CONDENSER			
Refrigerant pressure	kPaa	1 067	*1 315*
Outlet refrigerant temperature	°C	42,5	*53,33*

[13] Given by the corrected refrigerant-circuit COP; (5-14) was corrected, per (5-10c), for the effect of the compressor oil cooler.

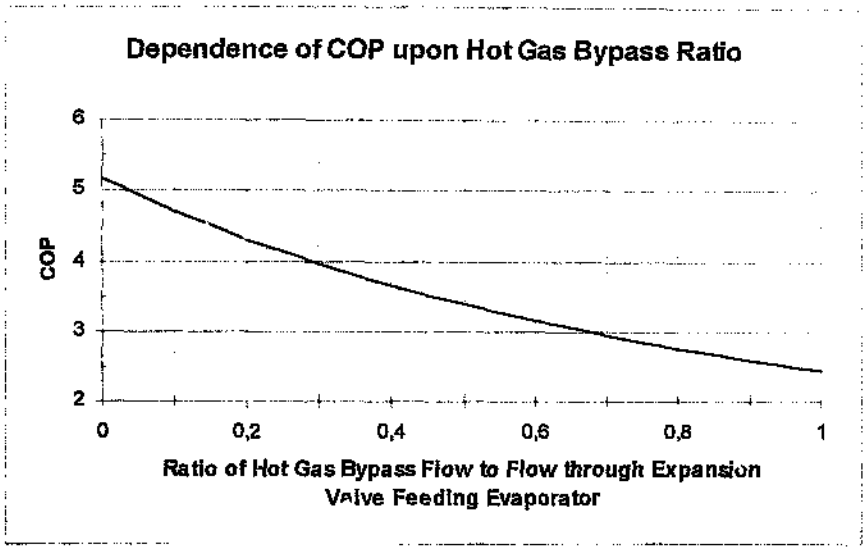

Figure 5.19 Case Study D: COP Range Plot

Interpretation of Acceptability Band Plot and COP Range Plot in Light of Design Performance

Finally, on comparing the confirming measurements and corresponding full-duty design values in Table 5.6, the following was noted.

(1) Not only was hot gas being bypassed, but the compressor was operating at part-capacity (its vane opening was 50 per cent), and thus at reduced efficiency. Both these factors would have acted to reduce COP below the full-duty design value.

(2) On the other hand, while evaporating pressure was almost equal to design value, condensing pressure was 19 per cent below design value. The pressure rise which the compressor had to develop was thus 25 per cent lower than design value; the required lift was thus reduced, which would have acted to *increase* the COP.

Because of these counteracting factors, all that could be concluded was that the actual COP, whatever it was, was unlikely to be greater than the full-duty design value of 3,43 quoted by the machine manufacturer. It was

almost certainly at least somewhat lower. From Figure 5.19, this meant that the hot gas bypass ratio was at least 0,5! More importantly, though, if actual COP had been lower than the full-duty design value of 3,43, it was most unlikely to have been within the area of complete acceptability in Figure 5.18. At a COP of 3,11 (91 per cent of 3,43), it would have been outside this area. Therefore, it was most likely that apparent rejection load (and hence condenser water flow[14]) was unacceptably, erroneously high. There was no guarantee, though, that apparent evaporator load was acceptably accurate; so it was certainly justifiable, as a precautionary measure, to check the evaporator water flow meter too when the opportunity presented itself.

5.3.3 Case Study E: Unacceptable Heat Imbalance: Overcharge of Refrigerant

A case study is now presented where the heat imbalance was unacceptable and the refrigerant-circuit COP was uncertain. This involved a two-stage centrifugal machine - identical to that in Figure 5.16 above - which was clearly overcharged with refrigerant. The heat imbalance and the two apparent COPs could be determined in the same way as before, and are given in Table 5.7 below.

In contrast to the previous case studies, there was a large heat imbalance. This evaluated to -29,2%, which was well below the unacceptability confirmation limit of -15%. Clearly, therefore, at least one principal measurement was unacceptably in error. The acceptability band plot for this case is shown in Figure 5.20 below.

Here, the two areas of joint acceptability did not overlap. Hence, as the unacceptably large heat imbalance of 29,2% showed anyway, it was impossible for all three apparent constituents of the heat balance to be

---

[14] Because all water temperatures, including condenser inlet and outlet water temperatures, had been measured with accurate thermometers.

acceptably accurate. However, the acceptability band plot yielded more information; as the two areas did not overlap, *it was impossible for both apparent evaporator load and rejection load to be acceptably accurate.* One or both of these loads were unacceptably erroneous.

Table 5.7 Case Study E: Calculated Heat Imbalance and Apparent COPs

QUANTITY	UNIT	VALUE
Apparent Evaporator Load	kW(R)	2 070
Apparent Input Power	kW	871
Apparent Rejection Load	kW(R)	-2 277
Heat Imbalance ε	%	-29,2
Apparent $COP_{[EB]p}$		2,37
Apparent $COP_{[JB]p}$		1,6

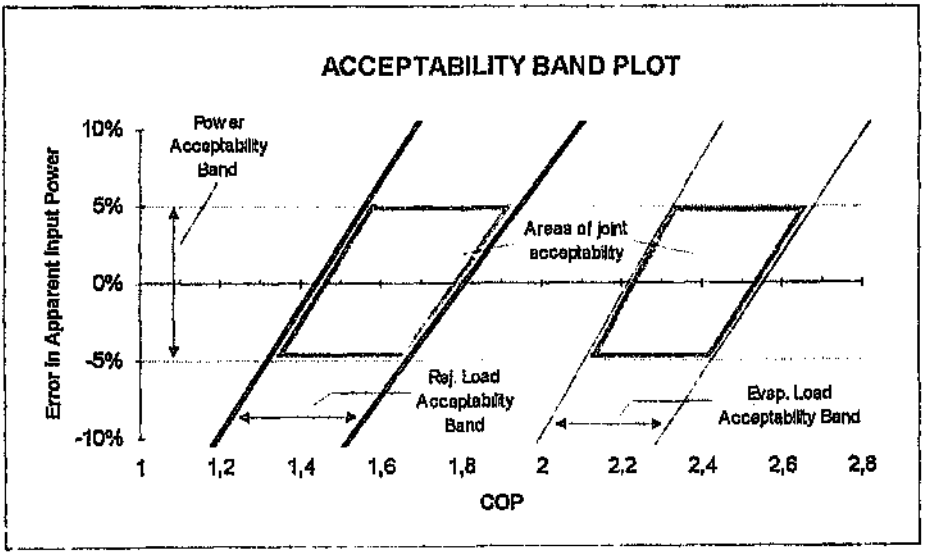

Figure 5.20 Case Study E: Acceptability Band Plot

In this case, the apparent input power was presumed to be acceptably accurate, as it had been calculated from readings from the kilowatt-hour meter measuring electrical energy input to the compressor drive motor. However, the apparent input power could have been substantially uncertain (such as if it had to be estimated from compressor motor current readings and incomplete motor specifications). Even if it had been so, the acceptability band plot would have nevertheless proved that at least one of the apparent loads was unacceptably in error, *whatever the actual error in apparent input power.*

The COP range plot was next constructed. The obtainable confirming measurements in the refrigerant circuit are listed in Table 5.8, together with the full-duty design values for comparison.

Table 5.8 Case Study E: Obtainable Confirming Measurements in Refrigerant Circuit

QUANTITY	UNIT	VALUE	*Design full-duty value for comparison*
EVAPORATOR			
Refrigerant pressure	kPaa	316,1	*342,4*
Refrigerant temperature	°C	-	*3,22*
Refrigerant level		normal	*normal*
ECONOMISER			
Refrigerant temperature	°C	26,50	*28,07*
COMPRESSOR			
Vane opening	%	50	*100*
Suction temperature	°C	2,82	*2,22*
Discharge temperature	°C	56,20	*60,61*
HOT GAS BYPASS VALVE			
Opening	%	closed	*closed*
CONDENSER			
Refrigerant pressure	kPaa	1 302	*1 315*
Outlet refrigerant temp.	°C	51,57	*53,33*

Here, refrigerant-circuit COP could not be precisely estimated because the compressor discharge temperature was low, being only 4,6°C above

refrigerant condensing temperature. This indicated an overcharge of refrigerant, causing liquid droplets to be entrained in the vapour leaving the evaporator. For this situation, the enthalpy h_{Eo} of the refrigerant leaving the evaporator is given by

$$h_{Eo} = x h_{(f)Eo} + (1-x) h_{(g)Eo} \tag{5-15}$$

where x is the fraction of liquid entrained in the refrigerant, and $h_{(f)Eo}$ and $h_{(g)Eo}$ are the enthalpies of saturated refrigerant liquid and vapour, respectively, at the evaporator outlet. These enthalpies could be determined from pressure and temperature measurements, but the liquid fraction x was unknown and impossible to measure. However, (5-15) could be substituted for h_{Eo} in formula (3-22c), reproduced below, for the refrigerant-circuit COP of this type of machine when bypassing no hot gas:

$$COP_{(r)} = \frac{h_{Eo} - h_{ECIo}}{(h_{Po} - h_{Eo}) + A(h_{Po} - h_{ECVo})} \tag{5-16}$$

where $$A = \frac{h_{EX1l} - h_{ECIo}}{h_{ECVo} - h_{EX1l}}$$

As all enthalpies in (5-15) and (5-16) could be deduced from the confirming measurements of refrigerant pressures and temperatures, it was possible to plot actual COP[15] for a range of possible liquid fractions in the refrigerant leaving the evaporator. The resulting COP range plot is shown in Figure 5.21 below. As seen, the COP depended strongly upon this liquid fraction.

Finally, the plots of Figures 5.20 and 5.21 were interpreted in the light of the manufacturer's quoted design performance in Table 5.8. Not only

---

[15] As in the previous case study, to reflect actual COP, (5-16) was corrected, per (5-10c), for the effect of the compressor oil cooler.

were there liquid droplets in the refrigerant leaving the evaporator and thus entering the compressor, but the compressor was operating at part-capacity (its vane opening was 50 per cent), and thus at reduced efficiency. Both these factors would have combined to reduce COP below the full-duty design value. Unlike the previous case study, there was no counteracting factor; the pressure rise which the compressor had to develop was virtually equal to the design value. Therefore, it could safely be concluded that the actual COP, whatever it was, was significantly below the full-duty design COP of 3,43. From Figure 5.21, this meant that liquid fraction in the refrigerant leaving the evaporator was above 7 per cent - a value high enough to raise concern about possible damage to the compressor.

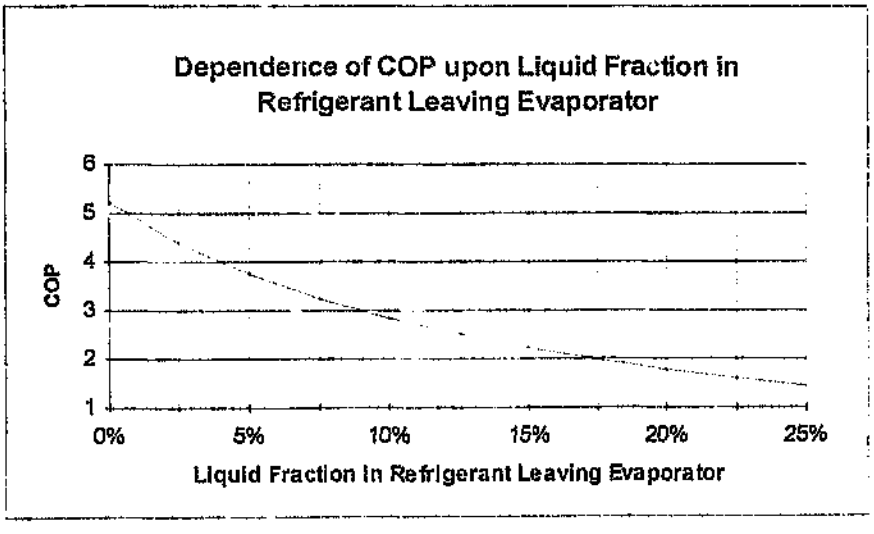

Figure 5.21 Case Study E: COP Range Plot

While actual COP was certainly lower than the full-duty design value of 3,43, both areas of joint acceptability in Figure 5.20 lay in ranges of COP which were considerably lower. The COPs at the centres of these two areas were the two apparent COPs in Table 5.7 above: 2,37 and 1,61. From Figure 5.21, the corresponding liquid fractions in the refrigerant

leaving the evaporator were 13% and 23% respectively. It seemed unlikely that the actual liquid fraction was of the order of the latter percentage; swift damage to the compressor would surely have resulted. From Figure 5.20, therefore, it appeared most likely that apparent rejection load (and hence condenser water flow) was unacceptably, erroneously low. What could definitely be concluded, though, was:

- either one or both apparent loads were unacceptably in error, so both evaporator and condenser water flow meters required checking;
- the liquid fraction in the refrigerant leaving the evaporator and entering the compressor was above 7 per cent; so in order to prevent damage to the compressor, the refrigerant charge had to be reduced to specification at the earliest opportunity.

5.3.4 Case Study F: Unacceptable Heat Imbalance; Custom-Built Machine with Two Screw Compressors

In principle, there is nothing limiting the use of the Thorp method to conventional machines. A case study is now presented of the use of the inexact Thorp method with a non-conventional, custom-built machine of 8,4 MW(R) capacity. This machine possessed two banks of open plate-type evaporators (as in Figure 3.29), two shell-and-tube condensers connected in parallel, and two screw compressors. The refrigerant employed was ammonia. As is common in modern practice, the screw compressors were equipped with liquid-injection oil cooling systems. This is the machine of Figure 3.22.

The apparent constituents of the heat balance, the heat imbalance, and the two apparent COPs could be determined in the same way as before, and are given in Table 5.9 below. The heat imbalance evaluated to +29,7%, which was well above the upper unacceptability confirmation limit of +13%. Obviously, at least one apparent constituent of the heat balance

was unacceptably in error. Constructing the acceptability band plot yielded Figure 5.22 below.

Table 5.9 Case Study F: Calculated Heat Imbalance and Apparent COPs

QUANTITY	UNIT	VALUE
Apparent Evaporator Load	kW(R)	7 868
Apparent Input Power	kW(M)	1 718
Apparent Rejection Load	kW(R)	-13 629
Heat Imbalance ε	%	+29,7
Apparent $COP_{[EB]p}$		4,58
Apparent $COP_{[JB]p}$		6,94

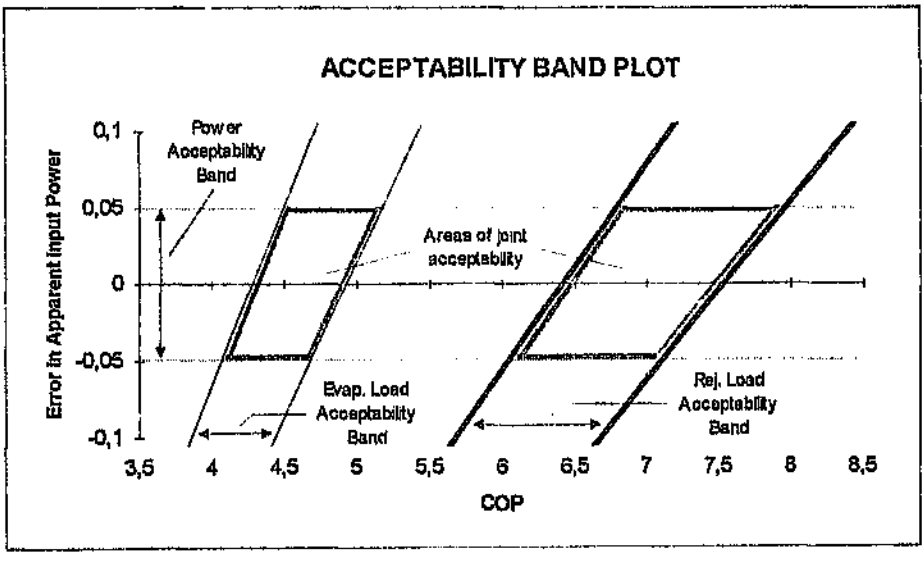

Figure 5.22 Case Study F: Acceptability Band Plot

As for the previous case study, the two areas of joint acceptability did not overlap, again showing that it was impossible for both apparent loads to

be acceptably accurate. One or both of these loads were unacceptably in error, *whatever the actual error in apparent input power.*

Next, the COP range plot was constructed. Obtainable confirming measurements in the refrigerant circuit are listed in Table 5.10, together with full-duty design values for comparison.

Table 5.10 Case Study F: Obtainable Confirming Measurements in Refrigerant Circuit

QUANTITY	UNIT	VALUE	*Design full-duty value for comparison*
EVAPORATORS			
Refrigerant temperature	°C	-2,71	*-2,78*
COMPRESSORS			
Slide valve opening	%	100	*100*
Suction pressure	kPaa	352	*374*
Suction temperature	°C	-	*-3,33*
Discharge pressure	kPaa	1 230	*~1 260*
Discharge temperature	°C	108,5	*90,0*
CONDENSERS			
Outlet refrigerant temp.	°C	29,57	*32,2*

From (3-24), the refrigerant-circuit COP of the machine in Figure 3.22 was:

$$COP_{(r)} = \frac{h_{SDo} - h_{LRo}}{\left(h_{(P1+P2)o} - h_{SDo}\right) + \dfrac{m_{(r)U1} + m_{(r)U2}}{m_{(r)EX}}\left(h_{(P1+P2)o} - h_{LRo}\right)} \qquad (5\text{-}17)$$

The ratio of total liquid-injection flow to the main refrigerant flow $\left(m_{(r)U1} + m_{(r)U2}\right)/m_{(r)EX}$, termed the *liquid injection ratio*, was unobtainable, as no refrigerant mass flow meters were installed. However, as all enthalpies in (5-17) could be determined from the confirming

measurements of refrigerant pressures and temperatures, it was possible to plot actual COP[16] for a range of possible values of this ratio. The resulting COP range plot is shown in Figure 5.23 below, where it is seen that COP depended fairly strongly upon this ratio.

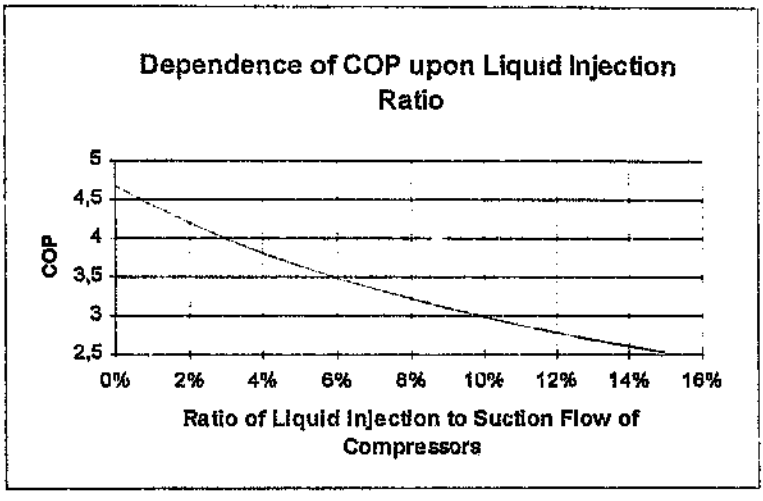

Figure 5.23 Case Study F: COP Range Plot

Under specified full-duty design conditions, the manufacturer's quoted COP was 5,20. It was hence deduced, using (5-17), that the design liquid injection ratio was 1,6 per cent. From Table 5.10, conditions in the refrigerant circuit were close to full-duty design values; it was therefore almost certain that the actual liquid injection ratio was of a similar order.

Figure 5.23 thus showed that actual COP was almost certain to be above 4. However, *it had to be lower than 4,67,* the value for zero liquid injection ratio! Referring to Figure 5.22, it was thus very likely that actual COP was within the area of joint acceptability of apparent evaporator block load and

---

[16] Here, simply refrigerant-circuit COP. No water flows passed through the vapour-compression block, and all refrigerant flows passing between blocks were included in (5-17), which thus needed no correction (see (5-10a)) for it to reflect actual COP.

input power - *and it was impossible for actual COP to lie in the area of joint acceptability of apparent rejection load and input power.*

It was therefore certain that apparent rejection load was erroneously high to an unacceptable extent. As all temperatures had been measured with calibrated thermometers, the apparent water flows through the two condensers of the machine were far higher than the true values. Figures 5.22 and 5.23 strongly implied that apparent evaporator load was acceptably accurate; this implication, though, did not amount to definite proof. As for Case Study D, it was therefore advisable, as a precautionary measure, to check the evaporator water flow meter when the opportunity presented itself.

5.3.5 The Inexact Thorp Method Without the COP Range Plot

In some cases, it may be impracticable to determine the range in which actual COP must lie, and hence to construct the COP range plot. An example is when the refrigerant is significantly contaminated with dissolved compressor oil; as explained on page 210, determining the enthalpy of the resulting mixture requires extra measurements and information which are not obtainable. However, *regardless of whether the COP range plot can be obtained, the acceptability band plot can always be constructed,* because this latter plot involves no refrigerant-circuit measurements. Interpreting just this plot with the aid of the manufacturer's specifications and quoted design performance may still yield valuable conclusions or implications.

Such a case, shown in Figure 5.24, is briefly cited. Here, the heat imbalance, -4,7%, was small, so the areas of joint acceptability in the plot overlapped considerably. The area of complete acceptability was thus more than half of either area of joint acceptability. The COP range plot

was constructed, but was difficult to interpret.[17] However, the machine was operating at full compressor capacity, with water flows and temperatures close to design values. Moreover, full-duty design COP was 6,48. In the region of this value of COP, it is seen from Figure 5.24 that provided that the error in apparent input power was within the power acceptability band, it was almost certain that apparent rejection load was acceptably accurate, and most likely that apparent evaporator load was so. Therefore, the implication (which did not amount to definite proof, though) was that all principal measurements were acceptably accurate.

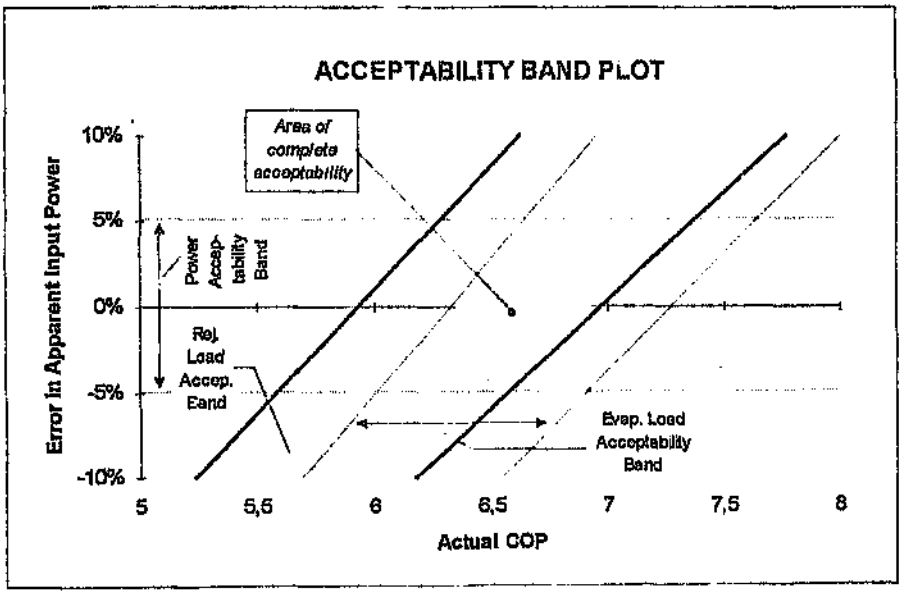

Figure 5.24 Example of Acceptability Band Plot for Small Heat Imbalance

[17] This machine was equipped with an unusual system injecting a small fraction of the condensed refrigerant liquid into the side inlet of the compressor to quieten it. Unfortunately, so much liquid was being injected that the vapour at the compressor discharge had negligible superheat. Almost certainly, therefore, this refrigerant was not entirely vapour (as it should have been), but a mixture of liquid droplets and vapour. An extra variable - the liquid content in this vapour - was thus introduced into the refrigerant-circuit COP, making the range plot difficult to interpret.

One further remark on Figure 5.24 is in order. If the possible range of actual COP had been available, it could have corresponded well, poorly or not at all with the range of COP spanned by the area of complete acceptability. Good correspondence between these ranges would have strengthened the implication that all apparent constituents of the heat balance were acceptably accurate. On the other hand, if there had been poor or no correspondence between these ranges, *one or more apparent constituents of the heat balance would have been unacceptably erroneous,* despite the small heat imbalance. As for the acceptability plots of Figures 5.4 and 5.11, the most probable conclusions would have been that either both apparent loads were unacceptably and similarly erroneous, or apparent input power was unacceptably erroneous. Thus the acceptability band plot, like the acceptability plot of the enhanced Thorp method, *can detect the presence of similarly erroneous constituents masked by a small heat imbalance* if the range of COP spanned by the area of complete acceptability corresponds poorly or not at all to the range of actual COP (provided that this latter range is known).

5.3.6 Limitation of Inexact Thorp Method

The major limitation of the inexact Thorp method is that without a precise estimate of actual COP, it cannot ascertain the *actual* performance of a machine. Thus it cannot prove that unacceptable errors are *absent* from the apparent performance, and so it cannot conclusively verify it. Where this inexact method is used, therefore, it is desirable, wherever practicable, to resort to fundamental or empirical machine modelling to finally ascertain actual performance. As explained more fully below, knowledge of just all water temperatures, and all refrigerant pressures and temperatures, may be sufficient for machine modelling to verify the apparent performance and hence the principal measurements. Here, the enhanced or inexact Thorp methods can provide valuable initial estimates of the measurements to be verified (for example, the water flows). Machine modelling is in any case necessary to be able to predict

corresponding normal or optimal performance, and hence assess the actual performance once this is ascertained. In addition, modelling of at least some machine components is necessary in order to estimate important, non-measurable process parameters (such as water-side fouling factors) or state variables to see which of these may have undesirable values contributing to unsatisfactory performance.

5.4 Verifying Apparent Performance by Machine Modelling

Wherever, then, either the refrigerant-circuit COP cannot be determined precisely, or no apparent constituent of the heat balance is independently known to be acceptably accurate, the apparent performance should, if possible, be verified by machine modelling. As will be seen, though, this is sometimes deceptively complicated, as any significant abnormalities - some of which may be faults - present have to be modelled as well. The presence of such abnormalities, due to the extra unknown quantities thereby introduced, can make machine modelling very complex, or even sometimes impracticable.

As stated in Chapter 4, if a water chilling machine is modelled on a fundamental level, its specifications and the well-known principles of thermodynamics, fluid mechanics, and heat transfer provide enough information to calculate its predicted performance for any given set of operating conditions - the inputs, process parameters and state variables. The predicted measures of quality and effectiveness of performance consist of both directly measurable outputs and derived, characteristic quantities.

When checking the performance of an actual water chilling machine, the process parameters (apart from the known machine specifications) are generally unknown. Suppose as well that some directly measurable inputs and outputs have not been measured accurately, and hence are also unknown. *Provided that the known specifications, fluid properties and inputs and outputs permit the set of equations constituting the*

fundamental model to be solved for the unknown inputs, outputs, process parameters and state variables, the same fundamental model of a water chilling machine can be used to calculate *backwards* and estimate these unknown quantities, and hence the performance of the machine.

For example, in a conventional machine, suppose that water flow-rates through evaporator and condenser *(inputs)* and electrical power drawn by the compressor motor *(a measurable output)* are unknown. It is then not possible to determine any apparent constituent of the heat balance, so the Thorp method cannot be used. The water-side fouling factors *(process parameters)* are unknown too. Suppose further, though, that inlet water temperatures and the setting of the compressor capacity-regulating device *(the other inputs)* and refrigerant pressures and temperatures at all key points in the refrigerant circuit *(measurable outputs)* are known. Then there is one and only one set of water flow-rates and water-side fouling factors which will cause the water chilling machine - operating with the known inlet water temperatures and setting of the compressor capacity-regulating device - to yield the set of known outlet water temperatures and refrigerant pressures and temperatures. This set of water flow-rates and water-side fouling factors can be found by solving a sufficiently comprehensive fundamental model of the machine, if its specifications are known sufficiently well.

In general, the specifications of the evaporator and condenser are known in detail. The required specifications of the centrifugal compressor are detailed characteristic performance curves of each compressor stage; however, as noted in Chapter 3, manufacturers generally do not release such information. What can be done, though, is to use artificial curves, and match these as closely as possible to the limited amount of performance data furnished by the manufacturer. This facility is afforded in the CHILLER computer program (Bailey-McEwan and Penman, 1987), described in Appendix 16, which was used in the first two case studies now presented.

A useful check on the accuracy of such machine modelling is how closely the COP thereby predicted agrees with actual COP as verified by the enhanced Thorp method (in cases where the refrigerant-circuit COP can be determined precisely).

5.4.1 Case Study G: All Water Flow Meters Out of Order

Machine modelling verified actual performance, as now described, with another conventional machine of the type of Figure 5.16. This case has been reported by Bailey-McEwan and Roman (1992).

Here, *all* water flow meters were out of order, so the apparent evaporator and rejection loads could not be determined. The only available measurements were inlet and outlet water temperatures, pressures and temperatures at key points in the refrigerant circuit, and compressor vane opening and motor current. However, the refrigerant circuit appeared to be in good order, and the hot gas bypass valve was closed, so the refrigerant-circuit COP could be precisely determined and then corrected to reflect actual COP. No kilowatt-hour meter was fitted to measure motor input power; all that was available was the reading of motor current. Fortunately, as this was virtually identical to the full-load value on the motor nameplate, it was a simple matter to estimate motor input power, and hence apparent input power W_{VCBp}. Then apparent evaporator and rejection loads could be estimated as follows from (5-9b):

$$Q_{EBp} = COP \cdot W_{VCBp} \qquad Q_{JBp} = -(1+COP) \cdot W_{VCBp}$$

Evaporator and condenser water flows could hence be estimated, as all water temperatures had been measured with accurate thermometers. These estimated flows are included in the third column of Table 5.11.

Table 5.11 Case Study G: Apparent and Predicted Performance

QUANTITY	UNIT	Apparent Performance (water flows est. by Thorp Method)	Predicted Performance (CHILLER Program)	*Design Full-Duty Performance for Comparison*
EVAPORATOR				
Water flow-rate	l/s	7/,9	79,8	*64,78*
Inlet water temperature	°C	19,4	19,4	*19,00*
Outlet water temperature	°C	8,4	8,4	*6,00*
Water chilling load	kW(R)	3 586	3 673	*3 526*
Fouling factor	m²°C/W		0,00026	*0,000088*
Refrigerant pressure	kPaa	no meas. point	364,8	*361,0*
Refrigerant temperature	°C	5,2[18]	5,2	*4,88*
ECONOMISER				
Refrigerant pressure	kPaa		698,6	*704,6*
Refrigerant temperature	°C	26,9	27,6	*27,90*
CONDENSER				
Water flow-rate	l/s	338,5	341,4	*199,88*
Inlet water temperature	°C	39,1	39,1	*40,00*
Outlet water temperature	°C	42,3	42,3	*45,26*
Water heating load	kW(R)	4 468	4 577	*4 417*
Fouling factor	m²°C/W		0,00035	*0,000352*
Refrigerant pressure	kPaa	no meas. point	1 163,2	*1 211,9*
Outlet refrigerant temperature	°C	48,0	48,0	*49,71*
COMPRESSOR				
Vane opening	%	100	100	*100*
Input power	kW	882	903	*874*
Suction temperature	°C	5,2	5,2	*4,55*
Discharge temperature	°C	64,3	62,8	*65,60*
Measures of performance				
Coefficient of performance (COP)		4,07	4,07	*3,96*

As the ammeter indicating motor current had not been calibrated, though, it was not independently known to be acceptably accurate, and so neither was apparent input power W_{VCBp}. The CHILLER computer program was therefore resorted to in order to independently verify apparent machine performance. All machine specifications were available for this purpose, except the detailed isentropic head and efficiency curves for both stages

[18] No point was available to measure this temperature; as the refrigerant charge was normal, it was assumed equal to compressor suction temperature.

of the centrifugal compressor. The artificial compressor stage curves of CHILLER that yielded closest agreement with the design full-duty performance data furnished by the manufacturer were therefore used.[19]

The fundamental model within CHILLER was solved for the unknown water flow-rates and water-side fouling factors. Appendix 17 describes how CHILLER was used to do this. The performance accordingly predicted by CHILLER is given in the fourth column of Table 5.11.

As seen, apparent and predicted performance agreed very closely. Particularly striking was the close agreement of the input power predicted by CHILLER (903 kW) with the apparent input power of 882 kW estimated from motor current and motor and gearbox specifications. Moreover, *the COP predicted by CHILLER agreed with the actual COP yielded by the Thorp method.* Therefore, in this case, CHILLER could verify, purely from machine specifications and known temperatures, that apparent input power was likely to be acceptably accurate.

The practical value of both the Thorp method and CHILLER is strikingly illustrated here; they revealed that one of the unknown inputs was dangerously high in this machine. Compared to the design value in Table 5.11, the apparent condenser water temperature rise was too low, suggesting (which the Thorp method and CHILLER confirmed) that the condenser water flow-rate was almost 71 per cent too high. A simple calculation showed that the corresponding water velocity in the condenser tubes was 3,8 metres per second. Velocities higher than 3 metres per second tend to erode cupro-nickel tubes, and, of course, considerable water pumping power was being wasted. Because the condenser water flow meter was out of order, *this dangerously high flow-rate would otherwise have gone undetected,* and could well have resulted in a costly breakdown.

---

[19] These artificial curves are described in Section A15.4 of Appendix 15.

5.4.2 Case Study C: Two Machines in Lead-Lag Configuration

The case study of Section 5.2.6 and Figure 5.12 is now revisited. The machine modelling here has been reported by Bailey-McEwan (1991). In this case the only measured quantities known to be reliable were the water and refrigerant temperatures. CHILLER was thus again used to verify the apparent performance of both lead and lag machines. Again, the set of artificial compressor curves that yielded closest agreement with the limited amount of performance data furnished by the manufacturer was used. However, as the available version of CHILLER could only model two-stage centrifugal compressors, the real three-stage compressors had to be modelled as virtual two-stage ones; Appendix 18 describes how this was done. The unknown inputs (the common evaporator and condenser water flow-rates, and the vane openings of the first stages of each compressor) and the unknown process parameters (the four water-side fouling factors of the two evaporators and two condensers) were adjusted, again by the method of Appendix 17, to reproduce measured outlet refrigerant and water temperatures in the evaporators and condensers. The results are presented in Table 5.12.

The predicted water flow-rates through the *evaporators* were strikingly close to the apparent values, thus showing that these were acceptably accurate. Also, the predicted COP of 3,32 for the lead machine was very close to the actual COP of 3,27[20] yielded by the Thorp method. The predicted COP of 3,37 for the lag machine, though, was 10 per cent less than the actual COP of 3,72.[20] Thus modelling by CHILLER was not as accurate for the lag machine, most probably because CHILLER's own artificial characteristic curves were unlikely to have perfectly matched the real compressor curves, and because of additional inaccuracies due to modelling the real three-stage compressor as a virtual two-stage one.

---

[20] That is, the corrected refrigerant-circuit COP in Table 5.4.

Table 5.12 Case Study C: Apparent and Predicted Performances

QUANTITY	UNIT	Lead Machine		Lag Machine	
		Predicted (virtual 2-stage compr.)	Apparent	*Predicted (virtual 2-stage compr.)*	Apparent
EVAPORATOR					
Water flow-rate	l/s	*118,1*	117,6	*115,4*	116,9
Inlet water temperature	°C	*17,7*	17,7	*11,64*	11,64
Outlet water temperature	°C	*11,62*	11,61	*6,04*	6,03
Water chilling load	kW(R)	*3 006*	3 001	*2 707*	2 747
Fouling factor	m²°C/W	*0,00044*	0,00044	*0,00012*	0,00012
Refrigerant pressure	kPaa	*375,6*	366,4	*347,1*	332,8
Refrigerant temperature	°C	*6,14*	6,15	*3,64*	3,65
ECONOMISER					
Refrigerant temp. (1st stage)	°C	-	39,64	-	34,01
Refrigerant temp. (2nd stage)	°C	*20,05*	22,84	*16,01*	17,38
CONDENSER					
Water flow-rate	l/s	*149,8*	211,5	*156,0*	211,5
Inlet water temperature	°C	*48,25*	48,25	*43,54*	43,54
Outlet water temperature	°C	*54,49*	54,48	*48,92*	48,92
Water heating load	kW(R)	*3 912*	5 521	*3 511*	4 768
Fouling factor	m²°C/W	*0,00022*	0,00018	*0,00027*	0,00023
Refrigerant pressure	kPaa	*1 437*	1 525	*1 274*	1 274
Outlet refrigerant temperature	°C	*57,29*	57,29	*51,94*	51,95
COMPRESSOR					
Vane opening	%	*78*	50	*66*	50
Input power	kW	*905*	998	*803*	914
Suction temperature	°C	*6,14*	10,55	*3,64*	4,90
Discharge temperature	°C	*72,44*	78,03	*69,04*	67,43
Measures of performence					
Coefficient of performance (COP)		3,32	3,01	3,37	3,01

Objective conclusions about faulty instruments as well as about water chilling machine performance could therefore be drawn from Table 5.12. The condenser water flow meter was indicating about 39 per cent erroneously high, *and* both motor kW meters were indicating too high (the lead one by +9 per cent and the lag one by +24 per cent; the size of this latter error strongly suggesting erroneous electrical connections). Regarding water chilling machine performance, the high water-side fouling factor of the lead water chilling machine's evaporator seemed to

indicate that its tubes required cleaning: however, this might have been of no benefit unless the control philosophy was altered, as Chapter 6 will show.

In this case study and the preceding one, the refrigerant-circuit COP could be precisely determined, but apparent performance was verified by machine modelling because no apparent constituent of the heat balance was known to be acceptably accurate. As stated above, machine modelling should also be used to verify apparent performance where the refrigerant-circuit COP cannot be determined precisely. An example of this is Case Study D above, where the degree of opening of the hot gas bypass valve had been observed, and its characteristics were available. Therefore, a machine model incorporating the effect of hot gas bypass could have been used to precisely ascertain this machine's actual performance. Unfortunately, the available version of CHILLER did not model the effect of hot gas bypass, so this was not done.

The next case study illustrates the use of machine modelling not to verify apparent performance, but to verify an abnormal internal condition.

5.4.3 Case Study A (Refrigerant Circuit Not in Good Order)

Even though the acceptability plot may suggest that all principal measurements are acceptable, and this is confirmed through one apparent constituent of the heat balance being independently known to be acceptably accurate, all this proves is that the performance survey was acceptably accurate - that is, that apparent performance accurately reflects actual performance. *It does not prove that the machine is necessarily in good order;* this is only proved if actual performance, upon assessment, is satisfactory according to the definition of Chapter 4.

If a machine is not in good order, some of its process parameters or state variables have abnormal, undesirable values. Difficulties may therefore be encountered in verifying its apparent performance by machine

modelling, *as the effects due to these undesirable values of process parameters or state variables have to be modelled as well.* Not only are some such abnormalities very difficult to model, but the model can become very complex and almost impracticable to use. Moreover, there is always the possibility that an unanticipated abnormality might occur. If, however, anticipated abnormalities can practicably be incorporated into the machine model, valuable indications of whether process parameters or state variables have undesirable values constituting faults can be gained.

Case Study A is returned to for an example. The refrigerant and water circuits of this machine, depicted in Figure 5.8, are reproduced in Figure 5.25 below.

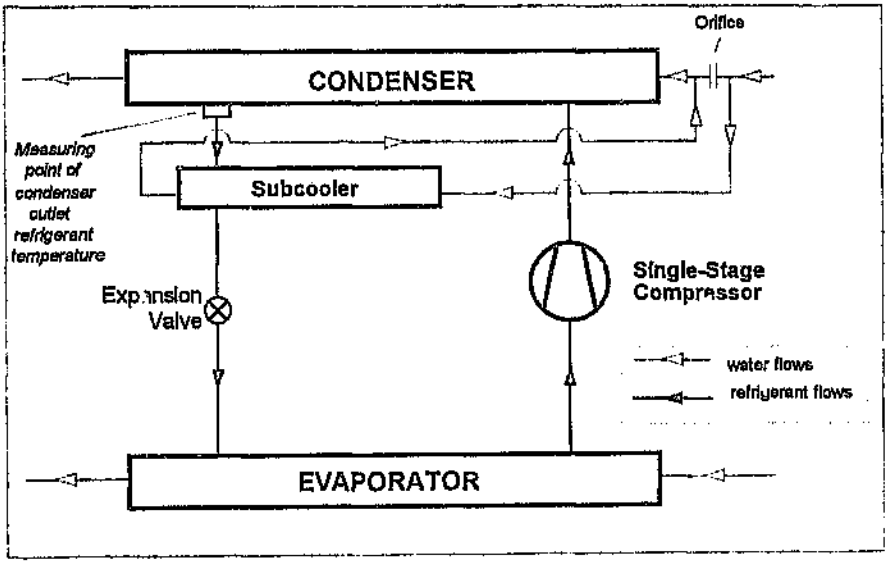

Figure 5.25 Machine of Case Study A

The incentive for modelling this machine arose out of an earlier survey not conducted by the author. In this earlier survey, the measured refrigerant pressure in the condenser, and the outlet refrigerant temperature (measured at the point shown), indicated that the refrigerant liquid leaving

the condenser was subcooled by approximately 7 degrees. As noted in Section 3.2.5 of Chapter 3, though, a shell-and-tube condenser normally subcools condensed refrigerant liquid negligibly in the absence of special arrangements. No such arrangements existed in the condenser of this machine. Therefore, the only way for this amount of subcooling to occur was for the bottom rows of condenser tubes to be submerged in liquid refrigerant.[21] It was not known whether such submergence had actually occurred, though, so the veracity of this earlier survey was thus placed in doubt. The author therefore decided to confirm, by experiment, whether it was possible to submerge the bottom rows of tubes by deliberately maladjusting the setpoint of the liquid level controller of the condenser.

It proved indeed possible to do this. Fortunately, the condenser was equipped with a liquid level glass gauge, and the setpoint of its liquid level controller was adjusted so as to submerge its first two or three bottom rows of tubes (thus submerging 59 or 93 of the 2 340 tubes). The actual performance, as verified by the enhanced Thorp method, is tabulated in the third column of Table 5.14. The liquid leaving the condenser was considerably subcooled, by just over 4 degrees.[22]

It was next attempted to reproduce this abnormal effect, termed a "flooded condenser", (the effect of a state variable, the refrigerant liquid content in the condenser, having an undesirable value significantly above zero) in accurate modelling of this machine. The machine model thus had to be expanded to cater for submergence of the bottom rows of condenser tubes in liquid refrigerant. This proved unexpectedly difficult. As

---

[21] Two other possible explanations were non-condensable gas in the condenser, or erroneously high measured condensing pressure. However, the measured outlet refrigerant temperature was lower than the outlet water temperature. This would have confirmed actual subcooling in the condenser if the temperature measurements had been known to be accurate.

[22] Subcooling was now proved here by the condenser outlet refrigerant temperature being lower than its outlet water temperature, both temperatures being measured with accurate thermometers.

described in Appendix 19 and illustrated in Figure 5.26, the real two-pass condenser had to be modelled as three interconnected heat exchangers. On the water side, the bottom pass of tubes now comprised "Condenser 1" (the non-submerged portion of these tubes) and "Subcooler 1" (the submerged or flooded portion of these tubes) connected in parallel. The top pass of tubes comprised "Condenser 2" (connected in series with "Condenser 1" and "Subcooler 1"). The entering refrigerant vapour was condensed by both "Condenser 1" and "Condenser 2"; *all* condensed refrigerant liquid then passed through "Subcooler 1" before leaving the condenser.

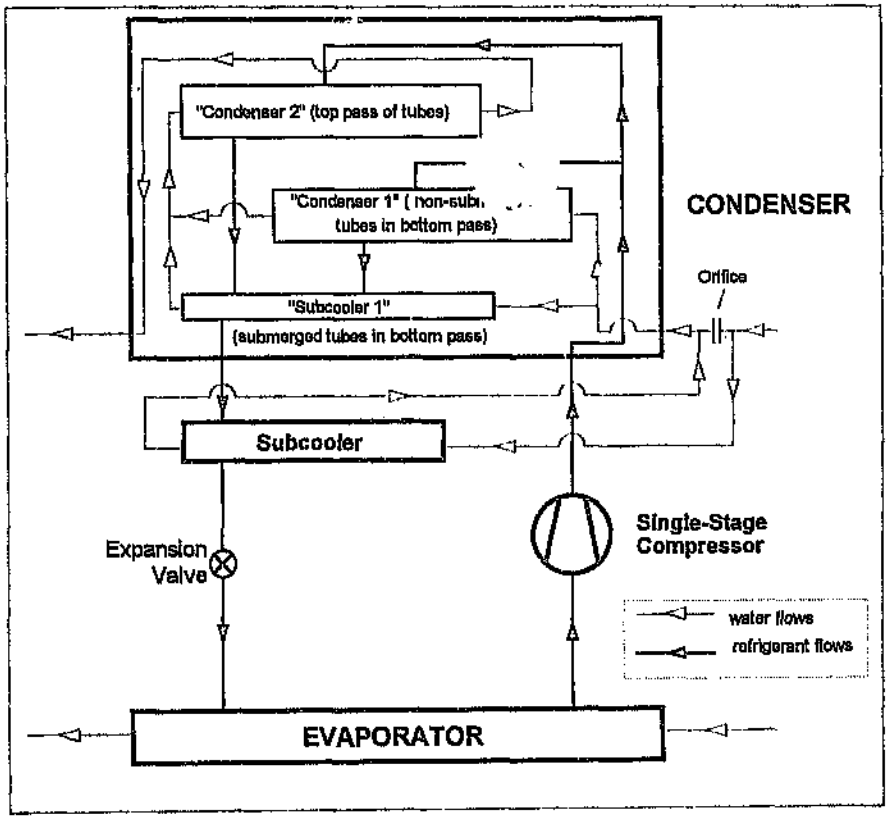

Figure 5.26 Expanded Model of Condenser in Machine of Case Study A

This machine was not modelled using CHILLER, as the version then available could not simulate subcooling of refrigerant liquid in a condenser or subcooler. A spreadsheet program with numerical equation-solving capability, Microsoft Excel 4.0, was therefore used to simulate this machine, using the same component models as in CHILLER (modified where necessary as described in Appendix 19). The compressor characteristic curves employed w[illegible] "typical" ones furnished by the manufacturer; however, it was not known whether these were identical to those of the actual compressor at its actual running speed.

Known inputs were inlet water temperatures of condenser and evaporator, and compressor vane opening. Known outputs were refrigerant pressures in evaporator and condenser, outlet refrigerant temperatures of condenser and subcooler, and outlet water temperatures of evaporator, condenser and subcooler. Accordingly, this expanded model was solved for the unknown inputs (water flow-rates) and unknown process parameters (water-side fouling factors) for various values of the unknown state variable, the mass of liquid refrigerant in the condenser (expressed more conveniently as the amount of flooded tubes therein). This state variable could only have discrete values, corresponding to the amount of submerged tube rows, as in Table 5.13 below.

Table 5.13 Machine of Case Study A: Amounts of Submerged Tube Rows and Tubes in Condenser

Amount of Tube Rows Submerged	Amount of Tubes thus Submerged
1	28
2	59
3	93
4	129
5	167

The best correspondence to actual performance was obtained for the value of this state variable being *five* rows of submerged tubes (167 such tubes, comprising 7 per cent of the 2 340 tubes in the condenser).

Table 5.14 lists the performance predicted for this condition, together with actual performance and full-duty design performance for comparison.

Table 5.14 Machine of Case Study A with Flooded Condenser: Actual and Predicted Performance

QUANTITY	UNIT	Actual Performance (verified by enhanced Thorp Method)	Predicted Performance (Machine Model)	*Design Full-Duty Performance for Comparison*
EVAPORATOR				
Water flow-rate	l/s	150	155,8	*168*
Inlet water temperature	°C	15,25	15,25	*15,0*
Outlet water temperature	°C	5,12	5,12	*4,5*
Water chilling load	kW(R)	6 362	6 608	*7 386*
Fouling factor	$m^2°C/W$	-	0,0003[22]	*0,0003*
Refrigerant pressure	kPaa	335	335	*339*
Refrigerant temperature	°C	no meas. point	2,54	*2,7*
CONDENSER				
Water flow-rate	l/s	384,4	381,3	*377*
Inlet water temperature	°C	no meas. point	22,55	*22,2*
Outlet water temperature	°C	27,21	27,21	*27,3*
Water heating load	kW(R)	7 665[23]	7 442	*8 050*
Fouling factor	$m^2°C/W$	-	0,00023	*0,0003*
Refrigerant pressure	kPaa	761	761	*759*
Amount of tubes submerged		93 (3 rows)[24]	167 (5 rows)	*nil*
Outlet refrigerant temperature	°C	26,8	26,80	*30,4*
SUBCOOLER				
Water flow-rate	l/s	no meas. point	94,1	*125*
Inlet water temperature	°C	22,45	22,45	*22,2*
Outlet water temperature	°C	22,85	22,85	*22,6*
Water heating load	kW(R)	-	158,6	*209,3*
Fouling factor	$m^2°C/W$	-	0,00041	*0,0003*
Outlet refrigerant temperature	°C	23,6	23,56	*24,9*
COMPRESSOR				
Vane opening	degr.	38,9	36,4	*not given*
Input power	kW	925	991	*1 048*
Isentropic efficiency	%	-	78,2	*82,9*
Suction temperature	°C	4,29[25]	2,36	*3,0*
Discharge temperature	°C	40,85	42,43	*41,0*
Coefficient of performance (COP)		7,19[26]	6,67	*7,05*

[23] This is the combined water heating load of the condenser *and* subcooler.

[24] Established from the liquid level in the sight glass of the condenser, and from drawings of the tube arrangement therein.

[25] This corresponded to superheating of the suction vapour by about 1,7°C. The reason was that the mass of refrigerant in the evaporator lessened as that in the condenser (to force flooding of the bottom rows of tubes) increased.

[26] Corrected refrigerant-circuit COP as in Table 5.2.

Here, the model could reproduce all measured water and refrigerant temperatures,[27] as well as measured refrigerant pressures in the evaporator and condenser. The compressor vanes, though, were predicted to be slightly less open than in reality, and predicted input power and COP were 7 per cent higher and lower respectively.

The model over-predicted the amount of tubes that were submerged, but this was to be expected, as the modelling assumed that heat was transferred solely by natural convection in the flooded zone.[28] This, of course, was not true; there was significant forced movement of liquid within this zone, due to both its surface being disturbed by the "rain" of condensed liquid onto it from above, and also due to its flow out of the condenser through a single outlet. Thus there were significant forced-convection effects, which augmented heat transfer.

Second, a low water flow of 94,7 l/s through the subcooler was predicted; but no reliance could be placed on this value, because of the uncertainty in the very low rise in water temperature (0,4°C). As this was computed from the indications of two separate thermometers, it was subject to considerable uncertainty.[29] An error of just ±0,1°C in this temperature rise caused the computed water flow to vary from 79 to 129 l/s (-17 per cent to +36 per cent of the predicted value of 94,7 l/s). However, this was not the case with the computed fouling factor, which varied from 0,00039 to 0,00042. Indications thus were that the subcooler fouling factor was definitely above design value. As will be seen in Chapter 6, this model predicted further that a significant amount of input power would be saved if the tubes of all heat exchangers were kept as clean as possible.

---

[27] Except compressor suction temperature; as noted in Table 5.14, the vapour at this point was slightly superheated. The evaporator was not modelled in sufficient detail to allow for superheating at its outlet.

[28] See Appendix 19, Section A19.4.

[29] Of course, if this small temperature difference was measured directly, it would be possible to estimate this water flow-rate accurately.

Here, therefore, in verifying actual performance, machine modelling could confirm that that flooding of a small fraction of condenser tubes was the cause of the refrigerant liquid subcooling at the condenser outlet. This would have been valuable to mine maintenance staff had the condenser *not* been equipped with a liquid level glass gauge enabling direct verification of this flooding (and most condensers of conventional machines are not so equipped). However, the increase in model complexity required to account for this possible abnormality is considerable, as may be gauged by comparing Figures 5.25 and 5.26. Furthermore, if more accurate prediction of the amount of flooded tubes had been desired, it would have been necessary to account for forced-convection effects in the flooded zone, further increasing model complexity. This relatively simple case thus illustrates that expanding a fundamentally-based machine model to account for all possible abnormalities may increase its complexity by orders of magnitude to the point of unwieldiness. This approach is thus not necessarily the most effective way of detecting faults, as will be elaborated upon in Chapter 7.

5.4.4 Appraisal of Verifying Apparent Performance by Machine Modelling

Machine modelling, then, either by a program such as CHILLER or by other computer-based means, enables information otherwise impracticable to use - the specifications of the water chilling machines - to be used in verifying apparent performance. Modelling of at least some machine components is in any case necessary to estimate unknown process parameters and state variables. Two considerations must be borne in mind, though. First, the more accurately water chilling machine specifications, particularly compressor characteristic curves, are known, the more accurate is the modelling; this is a further incentive for co-operation between manufacturers and mines. Second, if abnormalities in process parameters or state variables are present, the machine model must account for these to correctly verify apparent performance. Thus in

Case Study A, for example, a model *not* accounting for flooding in the condenser would have yielded incorrect results, inconsistent with actual performance. Similarly, using CHILLER to verify the apparent performance of Case Study E would have been invalid, because the model of a conventional machine in the version of CHILLER then available did not account for possible refrigerant overcharge, and thus for possible entrainment of liquid droplets in the vapour flow entering the compressor. *It thus remains essential to note all indications of possible abnormalities at the time of a performance survey,* so that it may be evaluated beforehand whether the available computer-based machine models are comprehensive enough to be validly used in verifying apparent performance.

5.5 Review

This chapter has attempted to provide the first desirable improvement to current practice identified at the close of Chapter 4 - that of a confirming check in routine performance surveys which positively verifies apparent performance by independently ascertaining actual performance. Three ways of performing such a confirming check have been presented and demonstrated. The enhanced Thorp method suffices wherever the refrigerant-circuit COP can be precisely determined and at least one apparent constituent of the heat balance is known to be acceptably accurate.

Where the refrigerant-circuit COP cannot be precisely determined, the inexact Thorp method indicates the relative likelihood of all apparent constituents of the heat balance being acceptably accurate. It is likely to yield more definite conclusions if the range of actual COP can be determined and machine specifications and design performance are known. However, the inexact Thorp method cannot precisely ascertain actual performance, and so cannot positively verify apparent performance, as it cannot prove that unacceptable errors are absent therefrom.

The third way of performing a confirming check is by machine modelling. Wherever the enhanced Thorp method cannot be used to verify apparent performance, machine modelling should be used if a fundamental, computer-based model is available and machine specifications, particularly compressor characteristic curves, are known sufficiently well. Such machine models must be sufficiently comprehensive to account for suspected abnormalities, in which case they can confirm the extent or absence of such.

In parenthesis, ascertaining actual performance through the enhanced Thorp method or machine modelling is a quick way of confirming, at least coarsely, the accuracy of certain site-fitted instruments such as water flow meters, as suggested by Kourelos (1995). Of course, this should never replace more precise on-site calibration.

It is finally recalled that the accuracy of any confirming check is directly dependent upon the accuracies of its confirming measurements. Accuracy in measurement of all fluid properties, particularly refrigerant pressures and temperatures, thus remains essential. An added reason for this is to ensure that any symptoms of possible abnormalities, such as flooding of the condenser in Case Study A or refrigerant overcharge in Case Study E, are not false.

In Chapter 6, machine modelling will be used to provide the second desirable improvement to current practice, identified in Chapter 4, for proper assessment of actual performance - rapid, accurate prediction of corresponding normal performance, and of optimal performance under the same or an alternative operating regime.

6. ASSESSING PERFORMANCE OF WATER CHILLING MACHINES

Once actual machine performance has been ascertained by the methods of the previous chapter, proper assessment of this actual performance, as stated in Chapter 4, requires comparison with at least the normal performance for the same operating regime - and possibly the optimal performance for the same or an alternative operating regime. Only by comparing actual performance with this corresponding normal or optimal performance can the extent of unsatisfactory performance be established, and hence the causes - within the machine or elsewhere - reliably pinpointed and appropriate remedial action justified.

Chapter 4 concluded that fundamental mathematical modelling, if practicable, was the most reliab'e and versatile method of obtaining corresponding normal and even optimal performance. The present chapter illustrates, through some case studies of Chapter 5, the use of such modelling in predicting corresponding normal and optimal performance. Actual performance is then assessed, and the questions of whether modifying important, estimated process parameters or state variables will improve or optimise performance are investigated. Some unanticipated findings emerge for two case studies involving pre-1980 conventional machines with a multi-stage centrifugal compressor. These are that at part-duty, normal performance may be worse than actual performance, and that to attain optimal performance and thus maximum utilisation of a machine from the mine's viewpoint, altering the control philosophy to maximise the load may be more important than maintaining normal values of process parameters or state variables.

6.1 Computer Program Selected to Predict Normal or Optimal Performance

As noted in Chapter 4, the calculations involved in fundamentally modelling the performance of a water chilling mac ine are impractica'le

without the aid of a computer. Moreover, as will be shown, it is often necessary to predict the *simultaneous* behaviour of the machine and other installation components if their performance is interdependent. The CHILLER computer program, developed by the Chamber of Mines of South Africa for the South African mining industry (Bailey-McEwan and Penman, 1987), is ideally suited to such work, because it can predict the performance of complete water chilling installations, consisting of multiple conventional water chilling machines, cooling towers, and reservoirs interconnected in any user-specified configuration. It was accordingly used to predict machine performance in the case studies below, except in Case Study A, where the same Microsoft Excel spreadsheet program as before was used. CHILLER is described in detail in Appendix 16.

It is worthwhile noting that predicting *normal* or *optimal* performance by machine modelling is easier than the task in Chapter 5 of verifying *actual* performance thereby, because no abnormalities and their resulting complexities have to be modelled.

6.2 Case Studies of Assessment of Machine Performance

6.2.1 Case Study A: Flooded Condenser

When it is suspected that an undesirable value of an internal process parameter or state variable, like flooding in a condenser, may constitute a fault, the most direct way of verifying this is to predict performance under identical operating conditions except for that undesirability. Accordingly, the same Microsoft Excel spreadsheet model as before was used to predict the performance of the machine of Case Study A, with *no* flooding in its condenser. The operating regime was the same: identical inputs and the compressor vane opening being controlled to maintain the specified outlet chilled water temperature of 5°C. Corresponding normal performance for this same operating regime, with water-side fouling factors of evaporator, condenser and subcooler set to the design value of

0,0003 m²°C/W, was also predicted. Table 6.1 lists these predicted performances, together with actual and predicted performance with the *flooded* condenser, for comparison.

Table 6.1 Case Study A: Predicted Performances with Flooded and Unflooded Condenser

QUANTITY	UNIT	Actual Performance with Flooded Condenser[1]	Predicted Performance with Flooded Condenser	Predicted Performance with Unflooded Condenser	Predicted Performance Normal
EVAPORATOR					
Water flow-rate	l/s	150	155,8	155,8	155,8
Inlet water temperature	°C	15,25	15,25	15,25	15,25
Outlet water temperature	°C	5,12	5,12	5,12	5,12
Water chilling load	kW(R)	6 362	6 608	6 608	6 608
Fouling factor	m²°C/W	-	0,00038	0,00038	0,0003
Refrigerant pressure	kPaa	335	335	335	342
Refrigerant temperature	°C	no meas. point	2,54	2,53	3,15
CONDENSER					
Water flow-rate	l/s	384,4	381,3	381,3	381,3
Inlet water temperature	°C	no meas. point	22,55	22,63	22,67
Outlet water temperature	°C	27,21	27,21	27,20	27,22
Water heating load	kW(R)	7 360	7 442	7 294	7 260
Fouling factor	m²°C/W	-	0,00023	0,00023	0,0003
Amount of submerged tubes		93 (3 rows)	167 (5 rows)	nil	nil
Refrigerant pressure	kPaa	761	761	753	778
Refrigerant *condensing* load	kW(R)	-	7 244	7 294	7 260
Refrigerant *subcooling* load	kW(R)	-	198	nil	nil
Outlet refrigerant temperature	°C	26,8	26,80	30,42	31,7
SUBCOOLER					
Water flow-rate	l/s	no meas. point	94,1	94,1	94,1
Inlet water temperature	°C	22,45	22,45	22,45	22,45
Outlet water temperature	°C	22,85	22,85	23,18	23,35
Water heating load	kW(R,	-	158	290	355
Fouling factor	m²°C/W	-	0,00041	0,00041	0,0003
Inlet refrigerant temperature	°C	26,8	26,80	30,42	31,64
Outlet refrigerant temperature	°C	23,6	23,56	24,51	24,43
COMPRESSOR					
Vane opening	degrees	38,9	36,4	36,2	35,9
Refrigerant mass flow-rate	kg/s	-	50,8	51,1	51,0
Inlet volumetric flow-rate	m³/s	-	2,65	2,67	2,61
Pressure ratio		-	2,38	2,36	2,38
Isentropic efficiency	%	-	78,2	79,1	77,5
Input power	kW	925	992	976	1 006
Suction temperature	°C	4,29	2,36	2,35	2,97
Discharge temperature	°C	40,85	42,43	41,68	43,4
Coefficient of perf. (COP)		7,19	6,67	6,77	6,57

[1] As in the third column of Table 5.14.

Predicted Performance with Unflooded Condenser

With the condenser merely unflooded, no significantly better quality of performance was predicted. Predicted compressor input power decreased by 1,5 per cent. The 167 tubes previously predicted as flooded, and thus unavailable for condensing the refrigerant vapour, were now available for this purpose, representing a 7 per cent increase in area available for such condensation. This decreased the necessary log-mean temperature difference (LMTD), so the predicted condensing temperature fell slightly from 30,8°C to 30,4°C, with a corresponding fall in condensing pressure from 760 to 753 kPaa. The pressure ratio across the compressor accordingly dropped by approximately 1 per cent, and isentropic efficiency rose by the same percentage. The enthalpy rise through the compressor thus dropped by 2,2 per cent. However, the refrigerant mass flow-rate increased by approximately 0,7 per cent; this was why the abovementioned decrease in input power was only 1,5 per cent.[2] These rises in isentropic efficiency and refrigerant mass flow-rate, which had opposite effects on input power, are now explained.

The reason for the rise in isentropic efficiency is illustrated in Figure 6.1. As documented in Appendix 19, the compressor characteristic curves for isentropic efficiency were conveniently expressed in terms of vane opening and pressure ratio. Figure 6.1 depicts the curve for the predicted compressor vane opening with and without flooding in the condenser.[3]

As seen in this figure, the operating point with the flooded condenser was at a pressure ratio higher than that for peak isentropic efficiency. Therefore, the 1 per cent *fall* in pressure ratio with the condenser unflooded resulted in a 1 per cent *rise* in isentropic efficiency. The

[2] It will be recalled that compressor input power (neglecting mechanical inefficiencies) is the product of refrigerant mass flow-rate and enthalpy rise through the compressor.

[3] These predicted vane openings of 36,4° and 36,2° differed so little that their corresponding curves virtually coincided, and are represented as one curve in Figure 6.1.

refrigerant mass flow-rate increased because the total subcooling load decreased by 19 per cent from 356 kW(R) - 198 kW(R) in the condenser itself plus 158 kW(R) in the subcooler - to 290 kW(R), all in the subcooler. The outlet refrigerant temperature of the subcooler, which was no longer assisted by subcooling from flooded condenser tubes, therefore rose by about 1°C. The correspondingly higher enthalpy of this subcooled refrigerant, which passed through the expansion valve and then into the evaporator, resulted in a 0,7 per cent decrease in refrigerating effect (the enthalpy rise through the evaporator). As the water chilling load was identical, the refrigerant mass flow-rate rose by 0,7 per cent to compensate for this reduced refrigerating effect.

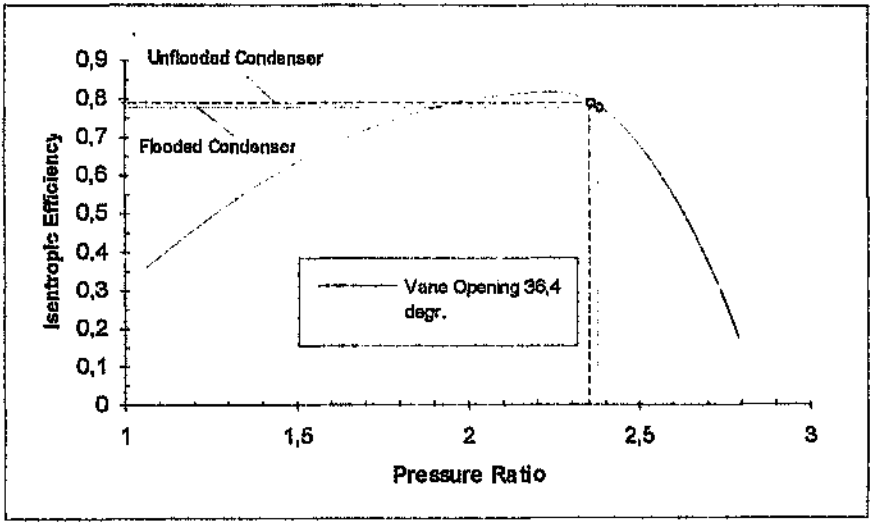

Figure 6.1 Case Study A: Predicted Isentropic Efficiencies of Compressor with Flooded and Unflooded Condenser

For identical evaporator water-side performance - identical inlet and outlet water temperatures and water chilling load - there are thus three factors, two of which counteract, affecting compressor input power when condenser tubes are flooded. The two counteracting factors are increased pressure ratio due to the loss of heat-transferring area for

condensing the refrigerant vapour; and decreased refrigerant mass flow-rate owing to the increased refrigerating effect arising from the extra subcooling provided by the flooded tubes. These factors increase and decrease input power respectively. The third factor is change in compressor isentropic efficiency. If compressor vane opening does not change significantly, as in Figure 6.1, this efficiency increases if the pressure ratio approaches nearer to the point of peak efficiency; otherwise, it decreases. (Changes in vane opening also strongly affect efficiency, but this is illustrated in the subsequent case studies.)

Because of the first two counteracting factors, and because the predicted changes in pressure ratio and thus isentropic efficiency were small, it was concluded that for identical water chilling load, quality of performance would not significantly worsen merely because the first few rows of condenser tubes were flooded. This conclusion offered a benefit in an unexpected way. As noted in Chapter 5, the flooding in the condenser was deliberately caused by maladjusting the setpoint of the condenser liquid level controller. When this setpoint was restored to normal, maintaining the liquid level well below the bottom rows of tubes, the liquid which had flooded these tubes reverted to the evaporator, whence it had come. It was thereupon noticed that compressor discharge temperature had dropped to only one degree above refrigerant condensing temperature, and that input power had increased by 7 per cent! Clearly, therefore, liquid droplets were being entrained in the vapour entering the compressor, so there was excessive liquid refrigerant in the evaporator. Ordinarily, maintenance personnel would have withdrawn the excessive refrigerant from the machine to prevent damage to the compressor bearings. The alternative recommended to the mine, however, was to move the excess liquid back into the condenser by sufficiently raising the setpoint of its liquid level controller. This offered a more convenient way, with an insignificant penalty in input power, of precisely adjusting the

amount of liquid refrigerant in the evaporator to ensure proper performance, yet eliminate the threat of compressor damage.

Predicted Normal Performance

The predicted normal performance, in the rightmost column of Table 6.1, yielded an input power slightly higher than that for the condenser merely unflooded. The reason was that the design condenser fouling factor of 0,0003 m²°C/W was 30 per cent higher than the estimated actual value of 0,00023 (in the fourth and fifth columns of Table 6.1). A higher condensing pressure resulted. In the compressor, this led to a higher pressure ratio and (by Figure 6.1) a lower isentropic efficiency, combining to raise input power by 3 per cent. This slight rise was not significant.

Predicted Optimal Performance (Minimum Input Power)

However, in the light of Figure 6.1, the question thus naturally arose of whether input power could be significantly decreased by *reducing* evaporator and condenser fouling factors to minimum practicable values. Performance for the same inputs and water chilling load was thus re-predicted, assuming that all heat exchangers were "fairly clean" and thus had a water-side fouling factor of 0,00015 m²°C/W, half the design value.

Predicted compressor input power fell significantly to 862 kW - 88 per cent of that predicted with the condenser merely unflooded. The decreased resistance to heat transfer in condenser and evaporator led to a decrease of 9 per cent in the required pressure ratio in the compressor. This also resulted in a 1 per cent increase in refrigerating effect, and hence a 1 per cent decrease in required refrigerant mass flow-rate. Owing to all these factors, the compressor vane opening reduced from 36,4 to 30,4 degrees. Isentropic efficiency remained unchanged at 79 per cent, because the increase owing to decreased pressure ratio counteracted the decrease due to decreased vane opening, as seen in Figure 6.2 below. The enthalpy rise through the compressor decreased

by 11 per cent. This decrease and that of 1 per cent in refrigerant mass flow-rate combined to yield the 12 per cent decrease in input power.

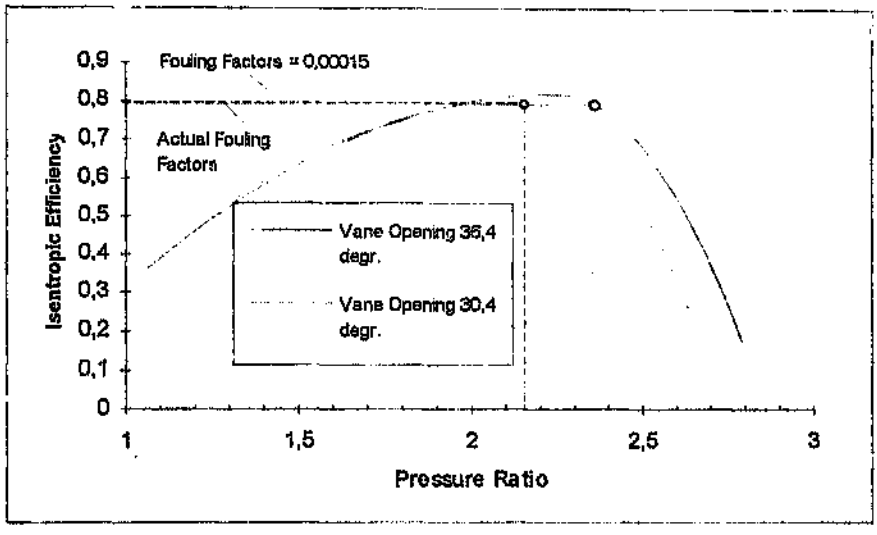

Figure 6.2 Case Study A (Unflooded Condenser): Predicted Isentropic Efficiencies of Compressor for Actual Fouling Factors and Fouling Factors of 0,00015 m²°C/W

Finally, performance for the same inputs and water chilling load was predicted with "almost clean" heat exchangers - that is, with all water-side fouling factors set to 0,00005 m²°C/W. For the same reasons as before, predicted input power fell further to 807 kW - 82 per cent of that with the condenser simply unflooded.[4] For the machine under its actual operating regime, which was close to design specification,[5] the model therefore predicted that maintaining the tubes of all heat exchangers as clean as possible would yield optimal performance, that is, minimal input power.

---

[4] Isentropic efficiency decreased by only 1 per cent because of the same counteracting effects of decreased vane opening and decreased pressure ratio.

[5] See Table 5.14: the actual inputs - water flows and inlet water temperatures of evaporator, condenser and subcooler - were in the neighbourhood of their design values.

Assessment of Performance

The predictions of the model indicated that for identical inputs and water chilling load, remedying the slight flooding in the condenser would not save a significant amount of input power. This abnormality therefore did not constitute a fault. On the contrary, as mentioned above, it offered a more convenient way of accommodating a small refrigerant overcharge, by simply permitting the excess refrigerant liquid to reside in the condenser, with an insignificant power penalty.

The actual pressure ratio of the compressor was past the point of peak isentropic efficiency. Therefore, a significant power saving of the order of 10 per cent was predicted if the tubes of all heat exchangers were kept as clean as practicable by effective water filtering and conditioning. This was because predicted isentropic efficiency hardly decreased; the decrease due to the lower vane opening was almost cancelled by the increase owing to the lower pressure ratio. Here, therefore, cleaning the heat exchangers and so improving their performance was predicted to optimise the performance of the whole machine for no disadvantage to its mine.

It had to be remembered, though, that the accuracy of all these predictions was directly dependent upon the accuracy of modelling, and in particular on the accuracy of compressor modelling, where limited information is normally available from manufacturers. Here, as noted in Chapter 5, the manufacturer did provide more information than usual, in the form of "typical" compressor characteristic performance curves; however, whether these corresponded exactly to those of the actual compressor at its actual speed was unknown. For example, if - contrary to the model - actual pressure ratio had *not* been past the point of peak isentropic efficiency, no worthwhile power saving might have accrued from cleaning the tubes of the heat exchangers. Clearly, therefore, accurate compressor characteristic performance specifications must be to hand if accurate models are desired from which valid conclusions can be drawn.

It is fair to expect, though, that such information will only be released if manufacturers as well as mines perceive sufficient advantage therein.

6.2.2 Case Study G: All Water Flow Meters Out of Order

The actual performance of this machine, as verified by the CHILLER program, is listed in the fourth column of Table 5.11. Assessing the performance of this machine was particularly important because the actual evaporator and condenser water flows - which were unknown until ascertained by the Thorp method and verified by the CHILLER program - were 23 and 71 per cent above their design values.

Predicted Normal Performance

First, corresponding normal performance was predicted. In this regard, it was important to recall that the compressor was operating at full capacity, with the inlet guide vanes of the regulated first stage fully open; but also that the measured evaporator outlet water temperature of 8,4°C was considerably above the design value of 6,0°C. So, in contrast to Case Study A, the machine had not lowered its chilled water delivery temperature to the design value,[8] and was operating at full capacity in a sustained attempt to do this. Normal performance was predicted for the same operating regime: identical evaporator and condenser water flows and inlet water temperatures, and the machine attempting to deliver chilled water at 6,0°C. The process parameters - the water-side fouling factors of the evaporator and condenser - were decreased from their estimated actual values of 0,000260 and 0,000354 m²°C/W to their design values of 0,000088 and 0,000352 m²°C/W respectively. Thus while the

---

[8] Of course, the reason for this was an off-design operating regime: the actual evaporator water flow-rate, 79,8 l/s, was 23 per cent above its design value! The decision whether a higher-than-design chilled water delivery rate at a higher-than-design temperature of over 8°C better suited the prevailing working conditions, and was hence acceptable, rested with the mine.

evaporator fouling factor was reduced threefold, there was no distinguishable reduction in the condenser fouling factor.

Table 6.2 Case Study G: Predictions of Normal Performance

	UNIT	Performance predicted by CHILLER			
		Actual	Normal	Normal (at design condenser water flow-rate)	*Design full-duty values for comparison*
EVAPORATOR					
Water flow-rate	l/s	79,8	79,8	79,8	*64,78*
Inlet water temperature	°C	19,40	19,40	19,40	*19,00*
Outlet water temperature	°C	8,40	7,97	8,11	*6,00*
Water chilling load	kW(R)	3 673	3 816	3 771	*3 526*
Water-side fouling factor	m²°C/W	0,000260	0,000088	0,000088	*0,000088*
Refrigerant pressure	kPaa	365	378	380	*361,0*
Refrigerant temperature	°C	5,21	6,35	6,49	*4,88*
ECONOMISER					
Refrigerant pressure	kPaa	699	717	730	*704,6*
Refrigerant temperature	°C	27,60	28,55	29,26	*27,90*
CONDENSER					
Water flow-rate	l/s	341,4	341,4	199,9	*199,88*
Inlet water temperature	°C	39,10	39,10	39,10	*40,00*
Outlet water temperature	°C	42,30	42,43	44,73	*45,26*
Water heating load	kW(R)	4 577	4 761	4 710	*4 417*
Water-side fouling factor	m²°C/W	0,000354	0 000352	0,000352	*0,000352*
Refrigerant pressure	kPaa	1 163	1 173	1 221	*1 211,9*
Outlet refrigerant temp.	°C	48,00	48,34	50,08	*49,71*
COMPRESSOR					
Vane opening	%	100	100	100	*100*
1st stage mass flow-rate	kg/s	28,8	30,0	29,8	*27,8*
1st stg. inlet vol. flow-rate	m³/s	1,36	1,37	1,36	*1,33*
1st stage isentropic head	kJ/kg	11,42	11,24	11,50	*11,84*
1st stg. isentr. efficiency	%	72,5	71,4	73,0	*73,75*
2nd stage mass flow-rate	kg/s	33,9	35,2	35,4	*33,1*
2nd stg. inlet vol. flow-rate	m³/s	0,89	0,90	0,89	*0,86*
2nd stage isentropic head	kJ/kg	9,39	9,08	9,46	*9,96*
2nd stg. isentr. efficiency	%	70,8	67,8	71,4	*73,75*
Input power	kW	903	945	938	*874*
Suction temperature	°C	5,21	6,35	6,49	*4,55*
Discharge temperature	°C	62,78	63,75	64,53	*65,60*
Coefficient of perf. (COP)		4,07	4,04	4,02	*3,96*

Normal performance predicted by CHILLER is tabulated in the fourth column of Table 6.2, and as expected, was not a significant improvement. Compressor vane opening remained at 100 per cent, because the machine could still not attain a chilled water delivery temperature of

6,0°C. Predicted chilled water delivery temperature dropped to 7,97°C, still well above this value. Water chilling load rose by 3,9 per cent, and input power rose by 4,6 per cent. Thus the COP dropped slightly and insignificantly from 4,07 to 4,04.

It is of value to show why the rise of 4,6 per cent in input power was greater than that in water chilling load. This was because inlet volumetric flow-rate in both compressor stages increased by the order of 1 per cent.[7] Therefore, because the inlet volumetric flow-rates at actual performance were past the points of peak isentropic efficiency, the predicted isentropic efficiencies of the first and second stages decreased from 72,5 to 71,4 per cent, and from 70,8 to 67,8 per cent, respectively. This is illustrated in the lower plot, in Figure 6.3, of the artificial compressor characteristic curves used in the CHILLER program to model the real compressor.

Again, it had to be remembered that the accuracy of these predictions was directly dependent on the accuracy of compressor modelling. Here, in contrast to Case Study A, the usual situation prevailed where the manufacturer had supplied only limited, full-duty performance data. CHILLER's artificial compressor stage curves, used to model the real compressor, had therefore been selected to reproduce the specified full-duty performance at design conditions, and thus to coincide with the real full-capacity curves, whatever these were, at the design operating points. Therefore, in the *neighbourhood* of these design operating points, it was reasonable to expect good correspondence between the artificial and real full-capacity curves.

In this case, for both predicted actual and normal performance, both compressor stages were operating on their full-capacity curves, because

---

[7] Refrigerant mass flow-rate through both stages increased by the order of 4 per cent, but this was almost cancelled by a 3 per cent decrease in refrigerant specific volumes at both stage inlets, owing to the higher pressures in the evaporator and economiser.

the vanes of the first compressor stage were fully open and the second stage was unregulated. Moreover, the predicted operating points on CHILLER's artificial full-capacity curves, shown in the plots of Figure 6.3, were close to the design (full-duty) operating points, also shown there.

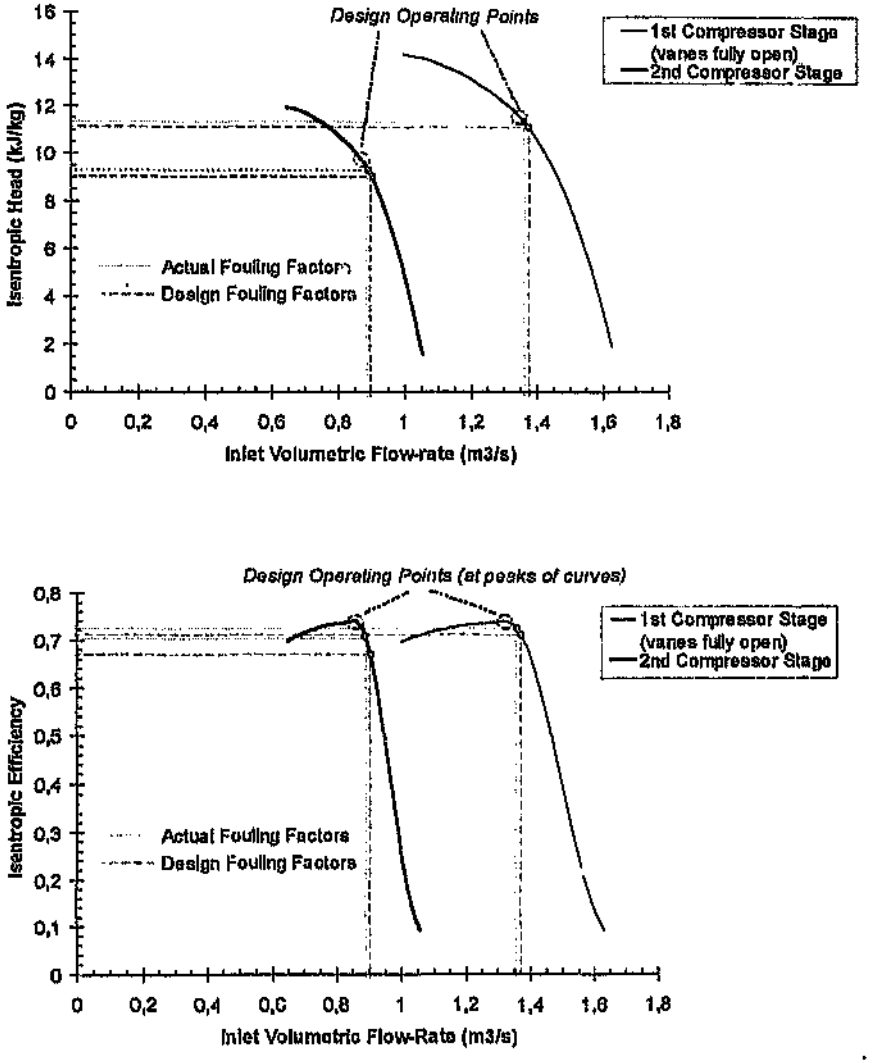

Figure 6.3 Case Study G: Predicted Isentropic Heads and Efficiencies of Compressor Stages at Actual and Normal Fouling Factors

Therefore, reasonable confidence could be placed in CHILLER's predictions of actual and corresponding normal performance. It was unwise, however, to place complete confidence therein, because there was no guarantee that the *peaks* of isentropic efficiency were at the design operating points, as assumed by CHILLER's artificial curves[8] and so depicted in the lower plot of Figure 6.3. Hence it was prudent to merely conclude that predicted normal performance, owing to the greatly reduced evaporator fouling factor, would yield about 4 per cent increase in water chilling load for no significant change in COP. Moreover, the machine would still not attain its design chilled water delivery temperature of 6°C unless the evaporator water flow-rate was reduced to the neighbourhood of its design value.

Normal Performance at Design Condenser Water Flow-Rate

It will be recalled from Section 5.4.1, Chapter 5 that the actual condenser water flow-rate was dangerously high, being 71 per cent above the design value of 199,9 l/s. It was thus natural to ask whether there was any benefit in the condenser water flow-rate being so high. CHILLER could also be used to answer this question, simulating the machine under identical inputs except for the condenser water flow-rate being reduced to its design value, and evaporator and condenser fouling factors remaining at their design values. Predicted performance under these conditions is tabulated in the fifth column of Table 6.2.

Predicted chilled water delivery temperature rose from 7,97°C to 8,11°C, water chilling load dropped by 1,2 per cent, and compressor shaft power dropped by 0,7 per cent. Thus the COP dropped slightly further, from

---

[8] This was assumed in the version of CHILLER then available. However, as stated by Cahill (1974), "... each manufacturer of centrifugal refrigeration compressors must limit himself to a finite range of impellers, each with its own characteristics". Thus it is unlikely that in every machine, the peak efficiencies of one or all compressor stages will occur at the *machine's* specified full-duty design conditions.

4,04 to 4,02. This would be insignificant in reality. Predicted condensing temperature rose to 50,08°C (which was not excessive, as design condensing temperature was 49,71°C), and the compressor did not go into surge. Thus the indication was that the actual, excessive condenser water flow-rate yielded no benefit whatsoever for the mine.

Predicted condenser outlet water temperature naturally rose from 42,43°C to 44,73°C, because of the much-reduced water flow-rate. A further question thus arose. Would the temperature of the water at the condenser inlet (i.e. the water returning from the heat rejection plant, consisting of a single cooling tower) remain at 39,10°C under these conditions, and if not, how would this affect performance? Furthermore, what would the influence of the two other machines in the water chilling plant be?

It is thus seen that, as soon as it is attempted to predict the effect of any substantial change in the operating conditions of one machine, it is necessary to consider its whole water chilling installation, due to the inevitable interacting effects between the water chilling plant (and between every machine in this plant) and the heat rejection plant. As noted previously, CHILLER has been designed for just such a task.

Normal Performance of Two Machines Connected to their Heat Rejection Cooling Tower

Accordingly, using CHILLER, the normal performance of the two usually operating machines (that of Case Study G and its neighbour) in the water chilling plant was predicted, with their evaporators connected in parallel, as they actually were. The water flow-rate through the evaporator of the neighbouring machine was assumed to be 75 l/s;[9] that of the machine of Case Study G, from Table 6.2, was 79,8 l/s. The condensers, also in

---

[9] As for the machine of Case Study G, the water flow meters of its neighbour were out of order. It was therefore assumed that its evaporator water flow-rate was roughly similar.

parallel, were connected in a closed circuit to the heat rejection cooling tower. Water flow-rate through each condenser was set at the design value, 199,9 l/s; the flow-rate through the tower was thus 399,8 l/s. The predictions are given in Table 6.3 below.

Table 6.3 Case Study G: Normal Performance of Machine and Neighbour Connected to Heat Rejection Cooling Tower

	UNIT	Normal performance predicted by CHILLER		
		Machine of Case Study G	Neigh-bouring machine	*Design full-duty values for comparison*
EVAPORATOR				
Water flow-rate	l/s	79,8	75,0	*64,78*
Inlet water temperature	°C	19,40	20,30	*19,00*
Outlet water temperature	°C	8,20	8,31	*6,00*
Water chilling load	kW(R)	3 740	3 764	*3 526*
Water-side fouling factor	m²°C/W	0,000088	0,000088	*0,000088*
Overall conductance (UA)	kW/°C	692,5	681,6	*689,22*
Refrigerant pressure	kPaa	381	383	*361,0*
Refrigerant temperature	°C	6,59	6,77	*4,88*
ECONOMISER				
Refrigerant pressure	kPaa	739	742	*704,6*
Refrigerant temperature	°C	29,72	29,87	*27,90*
CONDENSER				
Water flow-rate	l/s	199,9	199,9	*199,88*
Inlet water temperature	°C	40,26	40,26	*40,00*
Outlet water temperature	°C	45,85	45,88	*45,26*
Water heating load	kW(R)	4 679	4 708	*4 417*
Water-side fouling factor	m²°C/W	0,000352	0,000352	*0,000352*
Overall conductance (UA)	kW/°C	602,8	602,6	*655,22*
Refrigerant pressure	kPaa	1 251	1 254	*1 211,9*
Outlet refrigerant temperature	°C	51,15	51,22	*49,71*
COMPRESSOR				
Vane opening	%	100	100	*100*
1st stage isentropic head	kJ/kg	11,66	11,63	*11,84*
1st stage isentropic efficiency	%	73,7	73,6	*73,75*
2nd stage isentropic head	kJ/kg	9,68	9,64	*9,96*
2nd stage isentropic efficiency	%	73,0	72,7	*73,75*
Input power	kW	939	945	*874*
Suction temperature	°C	6,59	6,77	*4,55*
Discharge temperature	°C	65,22	65,32	*65,60*
Coefficient of performance (COP)		3,98	3,98	*3,96*

Predicted inlet condenser water temperature of both machines rose by one degree to 40,26°C; chilled water delivery temperatures were 8,2 and

8,3°C respectively; and COPs dropped slightly and insignificantly further to 3,98. Thus the predicted influence of the neighbouring machine and the heat rejection cooling tower were not significant. The dominating factor was that the compressors of both machines continued to operate at full capacity in vainly attempting to reduce the temperatures of the higher-than-design evaporator water flows to 6,0°C. Because the operating points on the full-capacity stage curves of both compressors were close to the design points and safely away from the surge points, they were insignificantly affected by the rise of one degree in inlet condenser water temperature.

Assessment of Performance

The performance of the machine of Case Study G was thus assessed as follows. There was no benefit in the actual condenser water flow-rate being 71 per cent above design value; this was the worst aspect of a badly off-design operating regime,[10] and had to be remedied urgently in order to avoid tube erosion. The benefit to be gained by maintaining the fouling factors at design values was negligible, being a reduction in chilled water delivery temperature of 0,2°C to 8,2°C, representing a 1,8 per cent increase in water chilling load for no improvement in COP. Therefore it was not necessary to clean the evaporator tubes for this reason. Only if the evaporator water flow-rate was reduced to approximately its design value would the machine attain the desired chilled water delivery temperature of 6°C.

As noted in Chapter 5, the water flow meters of this machine were entirely out of order, so the excessively high condenser water flow-rate would have gone undetected had the Thorp method not been used to ascertain actual performance (which machine modelling then verified). Premature

---

[10] The other aspect being the evaporator water flow-rate of 23 per cent above design value.

tube failure in the condenser would most probably have occurred, resulting in costly repairs and downtime.

6.2.3 Case Study C: Two Machines in Lead-Lag Configuration

The actual performances of both machines here, as ascertained by the Thorp method on the basis of the apparent evaporator water flow-rate being verified by the CHILLER program, are given in Table 5.12. It will be recalled from Chapter 5, though, that the version of CHILLER available at the time could model only two-stage centrifugal compressors, so in using CHILLER to verify apparent performance, the real three-stage compressors were modelled as virtual two-stage ones. In further use of CHILLER here to assess actual performance, therefore, comparisons were always made with the *pseudo*-actual performance - hereafter termed "2-stage actual" performance - predicted with the virtual two-stage compressors, rather than with the actual performance obtaining with the real three-stage compressors. This was done so that the comparisons would be internally consistent and thus of maximal validity.

The machines were attaining their desired chilled water delivery temperatures, and corresponding normal performances for the same operating regimes were first predicted for each machine in isolation. Each machine was simulated under the same evaporator and condenser water flows and inlet water temperatures. The vane openings of the regulated, first compressor stages were set to maintain the actual evaporator outlet water temperatures of 11,62°C and 6,03°C respectively. The process parameters - the evaporator and condenser water-side fouling factors - were set to their design values of 0,000088 and 0,000176 m²°C/W respectively. Predicted normal performances - and "2-stage actual" performances from Table 5.12 - are tabulated comparatively in Table 6.4.

Table 6.4 Case Study C: Predictions of Normal Performance of Machines

		Performance predicted by CHILLER			
		Lead Machine		Lag Machine	
	UNIT	"2-stage actual"	Normal	"2-stage actual"	Normal
EVAPORATOR					
Water flow-rate	l/s	118,1	118,1	115,4	115,4
Inlet water temperature	°C	17,70	17,70	11,64	11,64
Outlet water temperature	°C	11,62	11,62	6,04	6,03
Water chilling load	kW(R)	3 006	3 006	2 707	2 709
Water-side fouling factor	m²°C/W	0,000439	0,000088	0,000122	0,000088
Overall conductance (UA)	kW/°C	369,3	664,1	582,5	625,0
Refrigerant pressure	kPaa	376	416	347	350
Refrigerant temperature	°C	6,14	9,47	3,64	3,91
ECONOMISER					
Refrigerant pressure	kPaa	568	575	506	500
Refrigerant temperature	°C	20,05	20,50	16,01	15,59
CONDENSER					
Water flow-rate	l/s	149,8	149 .	156	156
Inlet water temperature	°C	48,25	48,25	43,54	43,54
Outlet water temperature	°C	54,49	54,56	48,92	48,93
Water heating load	kW(R)	3 912	3 961	3 511	3 520
Water-side fouling factor	m²°C/W	0,000219	0,000176	0,000267	0,000176
Overall conductance (UA)	kW/°C	733,5	809,2	666,8	814,2
Refrigerant pressure	kPaa	1 437	1 427	1 275	1 250
Outlet refrigerant temp.	°C	57,29	56,96	51,94	51,10
COMPRESSOR					
Vane opening	%	78,4	54,2	65,6	61,3
1st stage mass flow-rate	kg/s	22,24	22,08	19,61	19,56
1st stg. inlet vol. flow-rate	m³/s	1,02	0,92	0,97	0,96
1st stage isentropic head	kJ/kg	7,22	5,65	6,56	6,19
1st stage isentr. efficiency	%	70,2	43,5	60,1	53,0
1st stage input power	kW	229	286	214	228
2nd stage mass flow-rate	kg/s	30,40	29,97	26,19	25,98
2nd stg. inlet vol. flow-rate	m³/s	0,96	0,95	0,93	0,94
2nd stage isentropic head	kJ/kg	16,87	16,88	16,94	16,92
2nd stage isentr. efficiency	%	75,9	75,7	75,3	75,5
2nd stage input power	kW	676	668	589	582
Input power	kW	905	954	803	811
Suction temperature	°C	6,14	9,47	3,64	3,91
Discharge temperature	°C	72,44	76,08	69,04	69,31
Coefficient of perf. (COP)		3,32	3,15	3,37	3,34

For the lead machine - where the evaporator fouling factor was reduced fivefold from its estimated actual value of 0,000439 to 0,000088 m²°C/W - input power at predicted normal performance *rose* by 5,5 per cent! Yet a *decrease* in input power was expected, because evaporator conductance (UA) increased by 80 per cent, as seen in Table 6.4. This increase in

evaporator conductance, though, caused evaporating refrigerant temperature to rise by 2,4 degrees to 9,5°C, and at this higher temperature, the specific volume of refrigerant vapour leaving the evaporator decreased by 9 per cent. Consequently, even though the refrigerant mass flow-rate through the first virtual compressor stage hardly decreased, the inlet volumetric flow-rate decreased by 10 per cent. The head demanded of the first stage also decreased significantly, so the vanes closed to 54 per cent opening, where the isentropic efficiency was far lower at 43,5 per cent. This is shown in Figure 6.4 below. Power input to this first stage therefore climbed by 25 per cent! Isentropic head and efficiency of the unregulated second virtual stage were virtually unchanged; power input to this stage dropped insignificantly by 1 per cent.

In this case, therefore, the predicted benefit of cleaning the heavily fouled evaporator tubes of the lead machine was negative - there was actually a notable power penalty! This was because the vanes of the first virtual compressor stage, in closing to maintain the same chilled water delivery temperature, materially reduced the efficiency of this stage.[11]

For the lag machine, predicted input power rose for the same reasons, but by only 1 per cent, because the difference between estimated actual evaporator fouling factor and its design value was much less. Power input to the first virtual stage rose by 7 per cent, and that to the second virtual stage dropped by 1 per cent. Isentropic head and efficiency of the latter stage again remained virtually unchanged.

---

[11] To check if input power reached a minimum somewhere between actual and design values of evaporator fouling factor, performance was predicted for a range of evaporator fouling factors between these values. Minimum input power was almost at the actual evaporator fouling factor of 0,000439 m²°C/W. Thus even moderate cleaning of the tubes would have increased input power.